International Journal of Emerging Technologies in Sciences and Engineering

ISSN 1923-9181

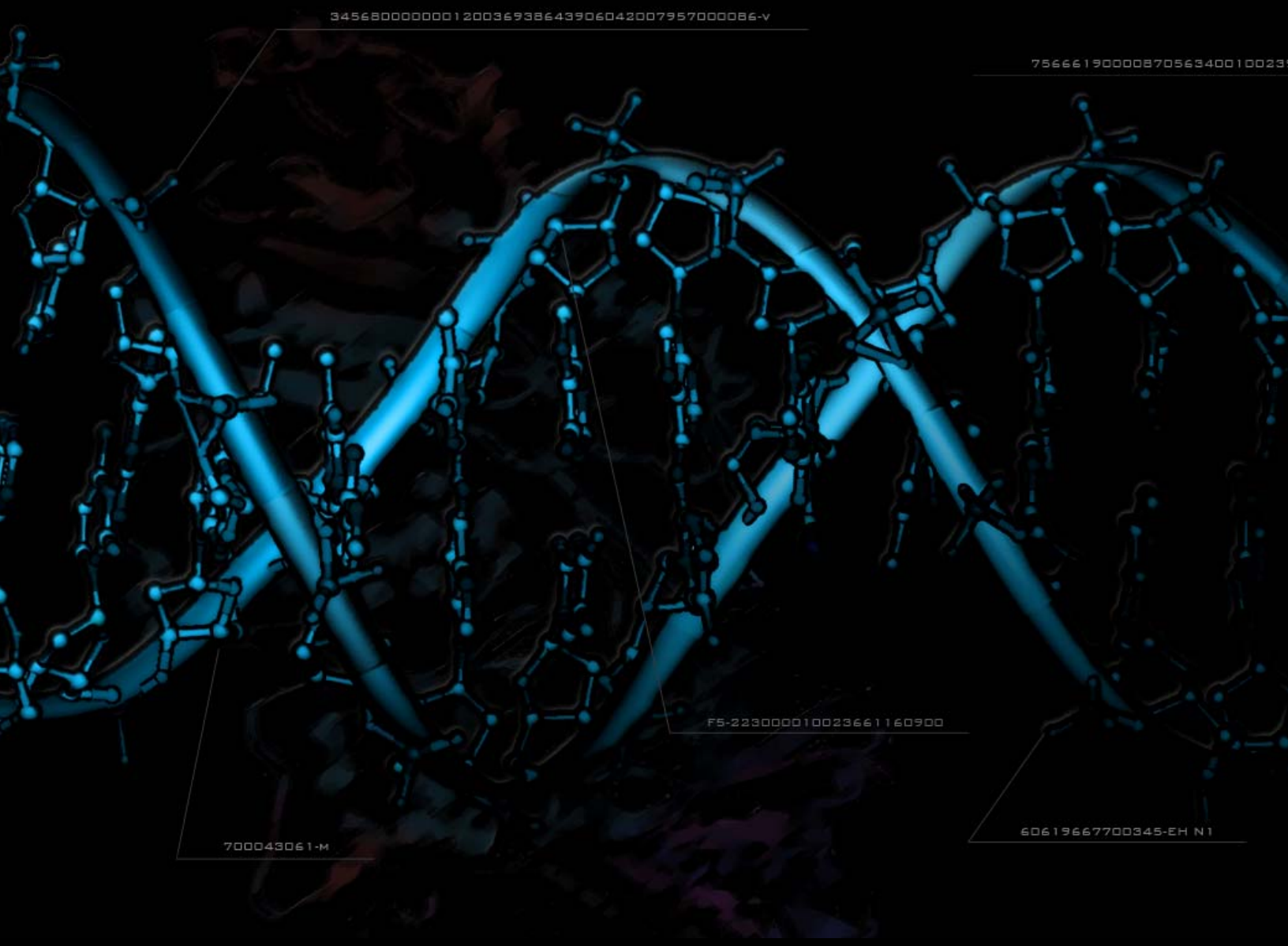

Volume 4 Number 1
April, 2011

www.ijetse.com

International Journal of Emerging Technologies in Sciences and Engineering (IJETSE)
Volume 4, Issue 1

Performance Analysis of QPSK System With Different BER Tools

T.P. surekha [1] , T. Ananthapadmanabha [2] , C. Puttamadappa [3] , A.P.Suma[4]

[1] Research Scholar and Assistant Professor, Department of Electronics and Communication Engineering, Vidyavardhaka College of Engineering, Mysore, India. e-mail: tpsuriramesh@gmail.com.

[2] Professor and Head, Department of Electrical and Electronics Engineering, National Institute of Engineering, Mysore, India. and Honorary secretary of IEI, Mysore local center, Mysore , India. E-mail:drapn2008@yahoo.co.in

[3] Professor and Head, Department of Electronics and Communication Engineering, S.J.B. Institute of Technology, Bangalore, India.
E-mail: puttamadappa@gmail.com

[4] Persuing her masters at SJCE, Department of Instrumentation and Technology, Mysore, India

Abstract - **The most appropriate modulation for a VSAT system is QPSK. QPSK has been widely used, Because of its ease of implementation and VSATs are very cost – sensitive.. In this paper, a Simulink based simulation system is designed and the details of the simulation model are provided. Simulation study helps to visualize eye-diagram and RRC Filter with scatter plot at the transmitter and at the receiver and also to observe Spectrum scope. Characteristic performance analysis is done by comparing the simulated BER with theoretical simulation using different BER tools. The BER curve for a Communication system illustrates the relationship between power in the transmitted signal in terms of SNR and the resulting BER for the system. In ideal QPSK condition with ideal RRC filter, with- out coding, a value of E_b / N_o of 10.6 db is used to achieve a BER of 1e-6.**

***Key words:** AWGN, BER, E_b / No, GUI, QPSK, SNR, VSAT*

1.INTRODUCTION

Digital modulation is the obvious choice for satellite transmission of signals that originate in digital form and that are used by digital devices. All digital links are designed using specific symbol rate, and specific filters that minimize Inter symbol interferences (ISI). A symbol in a baseband link is a pulse of current or voltage. VSAT stands for Very Small aperture Terminal, used in comm ercial satellite communication system.In a Satellite link, Modulation is an important key consideration in determining the efficient and error-free transfer of information over a communication channel. In choosing the most appropriate modulation for a VSAT system, ease of implementation is a major factor, since VSATs are very cost-sensitive. The most common forms of modulation used in VSAT system are Quadrature Phase Shift Keying. (QPSK). The purpose of this paper is to illustrate some important aspects on analysis and simulations of QPSK system operating over an Additive White Gaussian Noise (AWGN) channel. All the modeling and simulation is carried out using Simulink. In the simulation model, Error rates of QPSK systems versus the SNR are used to evaluate the system performance analysis.

The basic description of QPSK system is as shown in Fig. 1. It consists of Information source, Transmitter, Channel, Receiver and sink.

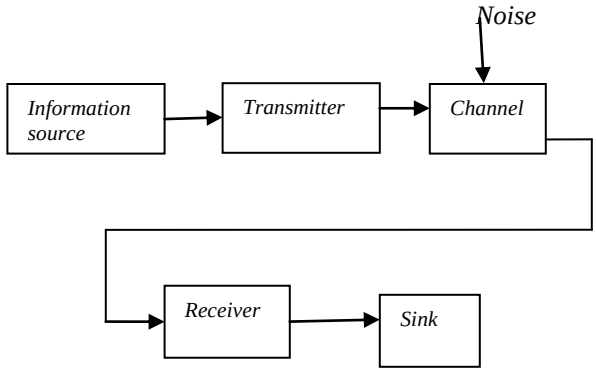

Fig. 1 The basic QPSK system.

1.1 Information source

The source generates a stream of information bits to be transmitted by the transmitter. In QPSK system, input signal is frame-based signal representation, by formatting data as an M-by-1 column vector, where M represents the number of samples per frame and element of the vector corresponds to values at the sample time. Thus information source is a Bernoulli Binary Generator, will generate an output bit sequence. In an M-ary signaling scheme, two or more bits are grouped to form symbols and one of M possible signals is transmitted during each symbol period. Usually, the number of possible signals is $M= 2^n$, where n is an integer.

1.2 Transmitter

The transmitter converts the bits into QPSK symbols and applies optional pulse shaping and up-conversion. As with many digital modulation techniques, the constellation diagram is a useful representation. Complex modulation schemes are best viewed using a scatter diagram. The scatter diagram allows us to visualize the real and the imaginary (in-phase and quadrature) component of the complex signal. Pulse shaping is an important consideration in the design of a system. The pulse shape filter must make efficient use of bandwidth and also have limited duration in time. A pulse too wide in time will overlap into adjacent symbol periods and cause inter symbol interference(ISI). This filtering can be performed by using Root-Raised cosine (RRC) filters. The eye diagram allows us to understand the time domain characteristic of a signal and its susceptibility to symbol timing error.

1.3 Channel

Communication channels introduce noise, fading, interference, and other distortions to the transmitted signals. Simulating a communication system involves modeling a channel based on mathematical descriptions of the channel. Several different channels are possible, the one being used here is AWGN channel. It is assumed that while passing electromagnetic waves through air or other mediums, there is an additive noise introduced to the transmission. Thus channel simply adds white Gaussian noise to the signals as shown in Fig. 2.

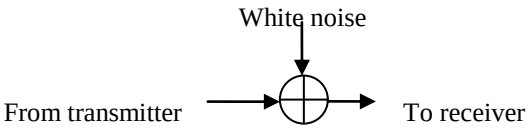

Fig. 2 An AWGN channel

1.4 Receiver

The receiver is the most complex part in the system. It performs the reverse process of the transmitter. Receiver block takes the output from the channel, estimates timing and phase offset, and demodulates the received QPSK symbols into information bits, which are fed to the bit sink. In a simulation condition, the bit sink counts the number of errors that occurred to-gather statistics used for investigating the performance of the system.

.

1.5 Sink

The Error Rate Calculation block compares a transmitted data stream with a receive data stream to calculate the Bit error rate of a system. It also outputs the number of error events that have occurred, and the total number of bits or symbols compared.

II IMPLEMENTATION

2.1 Methodology

Modeling and simulating of QPSK system is implemented in this paper. The bits are mapped onto corresponding QPSK symbols using Gray coding, as shown in Fig. 3.

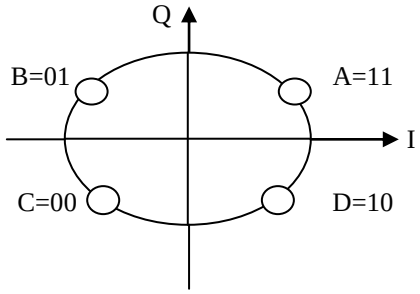

Fig. 3 Constellation diagram for QPSK

The implementation of QPSK is of higher order PSK. Writing the symbols in the constellation diagram in terms of the sine and cosine waves used to transmit them are

$$Si(t) = \sqrt{\frac{2Es}{Ts}} Cos\,[2\pi f_c t + (2i-1)\pi/4] \quad 0 \le t \le Ts$$

Where i = 1,2,3,4 (1)

This yields the four phases $\frac{\pi}{4}, \frac{3\pi}{4}, \frac{5\pi}{4}, \frac{7\pi}{4}$ as needed.

For the QPSK signal set, the four signals in the set can be expressed in terms of the basis signals as

$$Sqpsk(t) = \left\{\sqrt{Es}\ Cos\ \left[(2i-1)\frac{\pi}{4}\right]\phi_1(t) - \sqrt{Es}\ Sin\ \left[(2i-1)\frac{\pi}{4}\right]\phi_2(t)\right\}$$

Where i = 1,2,3,4 (2)

$\dot{\phi}_1$ (t) and $\dot{\phi}_2$ (t) are the basis functions defined by

$$\dot{\phi}_1(t) = \sqrt{\frac{2}{Ts}}\ Cos\,(2\pi fct) \qquad 0 \leq t \leq Ts \qquad (3)$$

$$\dot{\phi}_2(t) = \sqrt{\frac{2}{Ts}}\ Sin\ (2\pi fct) \qquad 0 \leq t \leq Ts \qquad (4)$$

The first basis function is used as the in-phase component of the signal and the second as the quadrature component of the signal.

The average probability of bit error in the additive white Gaussian noise (AWGN) channel is obtained as

$$Pe, QPSK = Q\left(\sqrt{\frac{2E_b}{N_o}}\right) \qquad (5)$$

Where Es is the energy of the signal given by
$Es = 2E_b$, and N_o is the noise.

2.2: Simulation model

Simulink, developed by the Mathworks, is an tool for multi-domain simulation and Model-based Design for dynamic and Communication systems. Communication Blockset of Simulink is helpful in simulating the modeling. The simulation model of QPSK system is as shown in Fig. 4.

QPSK Specifications:
Upsample Factor =8, Pulse shaping Filter α = .25
Group Delay = 4

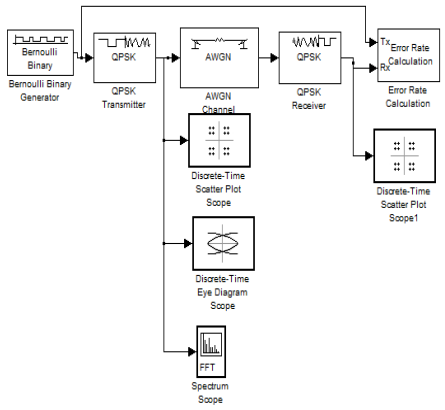

Fig. 4 The QPSK simulation model

All signal sources in the signal processing and communication 's can generate frame based data. In this work, the signal is frame based and samples are propagated through a model and multiple samples are processed in batches. Frame – based processing takes advantage of Simulink matrix processing capabilities to reduce overhead. Complex modulation scheme are best viewed using a scatter diagram. The scatter diagram allows us to visualize the real and imaginary (in-phase and quadrature) component of the complex signal. Thus Fig. 5 and shows the Scatter plot of QPSK system in the transmitter and Fig. 6 shows the Scatter plot of QPSK system in the receiver. Fig. 7 shows the Spectrum scope. i.e (PSD) The power spectral density embodies the frequency- domain properties of a process. Plot of power density spectrum with root raised cosine pulse is chosen for QPSK system to study the better results compared to Rectangular pulse shape.

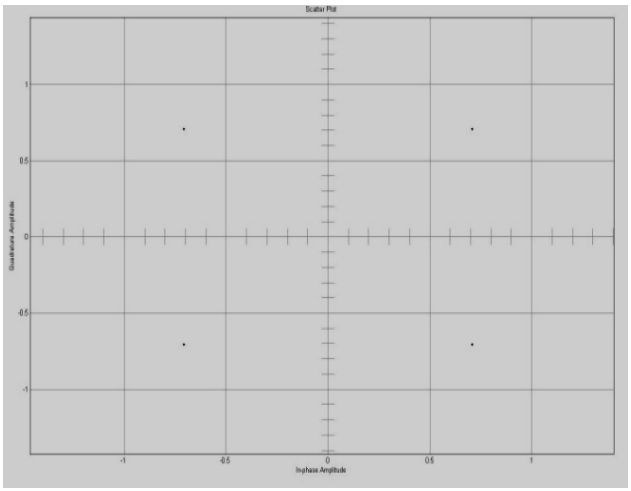

Fig. 5 Scatter plot of QPSK system in the transmitter.

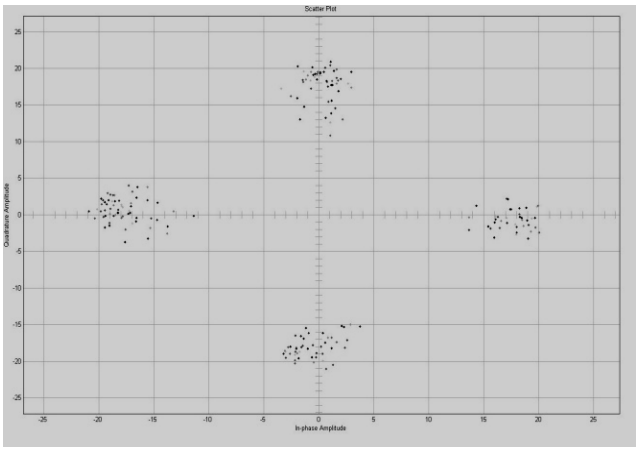

Fig. 6 Scatter plot of QPSK system at the receiver.

Since the Raised-Cosine Nyquist filter is considered at the transmitter and the receiver, a slight amount of phase and magnitude distortion can be seen at the output of the filter. Introducing a time-varying phase shift in the channel and investigating the performance for a phase shift by $\frac{\pi}{4}$ during the transmission of one data block. Certainly there is a change in the scatter plot as shown in Fig. 6. The best way

to visualize the effects of frequency and phase offset is by using the scatter plot scope. Therefore correcting such offsets can be performed by using phase/frequency offset block.

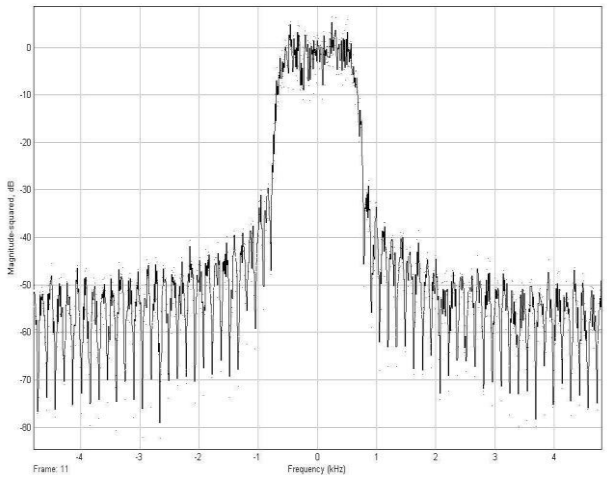

Fig. 7 Spectrum scope of QPSK system at the transmitter.

An Eye diagram is a convenient way to visualize a shaped signal in the time domain, which indicates that the 'eye' is most widely opened, and use that point as the decision point when de-mapping a demodulated signal to recover a digital message as shown in Fig. 8.

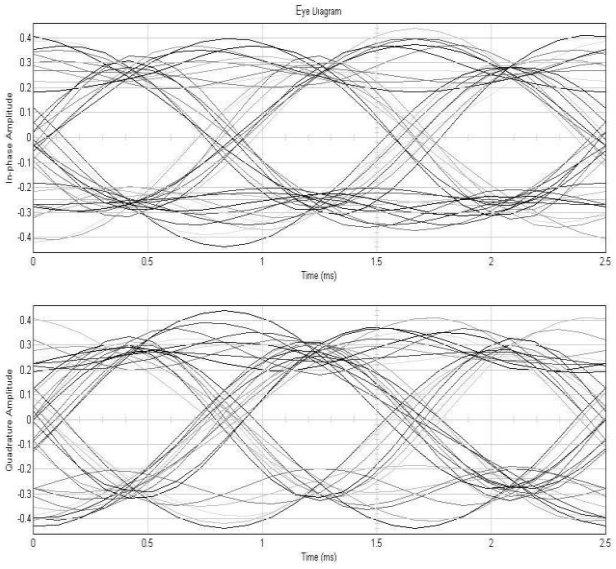

Fig. 8 Eye diagram of QPSK system

Using the Root-raised Cosine (RRC) filters at the transmitter and the receiver, a slight amount of phase and magnitude distortion can be seen at the output of the transmitting filter. To verify that the model was built properly, Error rate Calculation block compares a transmitted data stream with a receive data stream to calculate the error rate of a system. It also outputs the number of error events that have occurred, and the total number of bits or symbols compared. The block can output the error statistics as a variable in the displayed port.

2.3 System analysis

Characterizing the performance of a communication system under noisy conditions is an important part of the design process. Noise, interference, fading, and other types of distortion affecting the transmitted signal can cause incorrect decisions to be made by the receiver, resulting in bit errors. The ratio of bit errors to received bits is called the bit error rate (BER). The BER curve illustrates the relationship between power in the transmitted signal in terms of signal-to-noise ratio (SNR) and the resulting BER for the system. By analyzing the BER curve for a given system, we can find the minimum SNR that is required to achieve a particular BER. Thus bit error rate is computed by simulating the QPSK system and comparing the input with the resulting output sequence without coding. Performing such simulation for a range of SNR value results in the BER curve as shown in Fig. 9.

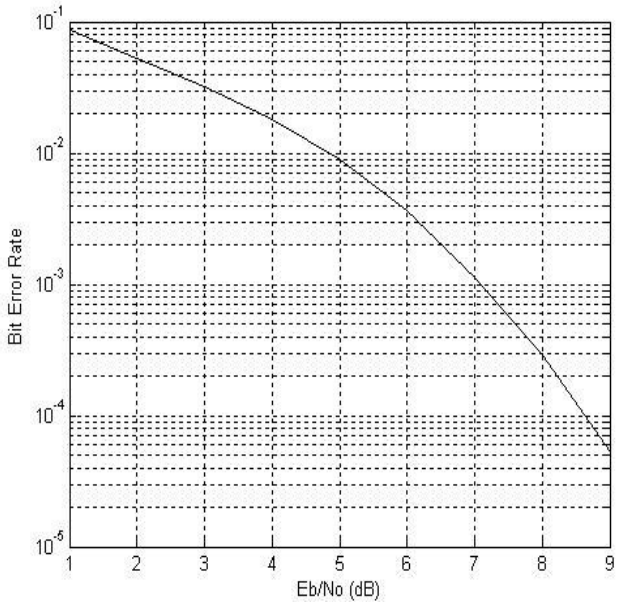

Fig. 9 Bit error rate as a function of E_b /No for un-coded QPSK curve.

III RESULTS AND CONCLUSION

BER curve with Monte-carlo simulation as shown in Fig. 9 is compared with BER Tool curves to display theoretical

BER curve and semi-analytic curve as shown in Fig.10. BER Tool is a Graphical User Interface (GUI) for analyzing bit error - error - rate statistics of a communication model. BER Tool helps us generate and analyze the BER data for a given system using different methods.

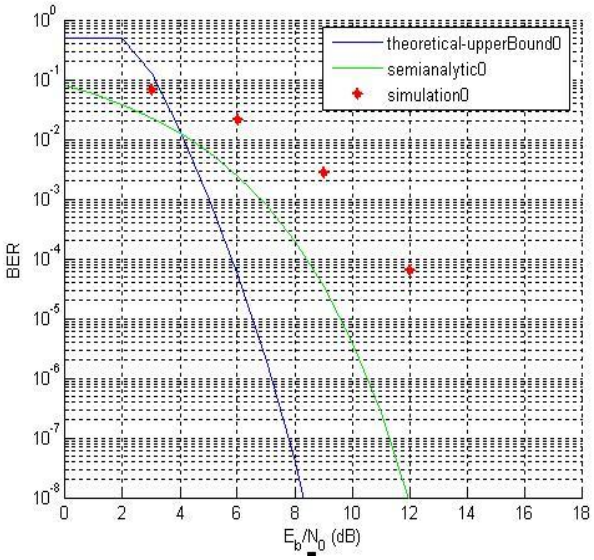

Fig. 10 Bit error rate as a function of E_b /No Compared with theoretical results.

The first method being used here is theoretical simulation, which invokes the simulation for E_b /N_o values that is specified, collects the BER data from the simulation and creates a plot. The second method is semianalytic technique, which computes the bit error rate communication system by using a combination of analysis and simulation. Thus by using 2different methods of BER Tool, Fig.10 gives a final comparison of all three plots. The first plot is theoretical simulation and second plot is semi-analytic plot and these two plots are compared with simulated un-coded QPSK system. The first two BER plots provides closer results to ideal values of E_b/N_o compared to simulated result. Thus BER tool plays an important role in Characteristic performance analysis of QPSK system.

IV ACKNOWLEDGEMENT

The authors are very grateful to the Management of Vidya vardhaka College of Engineering, Mysore, Karnataka, India. The National Institute of Engineering, Mysore ,Karnataka India. S J B I T, Kengeri, Bangalore, Karnataka, India. for their constant encouragement, and Motivation during their work.

REFERENCES

[1] XiaolongLi," Simulink – based Simulation of quadrature Amplitude Modulation (QAM) System" , Proceedings of the 2008 IAJC – IJME International Conference

[2] Tenna Sakla, Divya Jain, Sandhya Gautham, "Implementation of Digital QPSK modulator by using VHDL/MATLAB", @ International Journal of Engineering and Technology.,Vol 2(9).

[3] T. Pratt, C . Bostian , J.Allnutt, "Satellite Communication" John Wiley and Sons, 2nd Edition.

[4] Theodore S. Rappaport, "Wireless Communications" , Principles and Practice, Prentice – Hall of India Private Limited, 2nd Edition.

[5] Sanjay Sharma "Wireless and Cellular Communications",S.K. Kataria and Sons.

[6] M.C.Jeruchim, Philip Balaban and K.Sam shanmugan, "Simulation of Communication System" Modeling, Methodology and Techniques, Kluwer Academic Publishers, 2nd Edition, 2000.

[7] www.mathworks.com, online project assignment,EQ2310 Digital Communications, "Analysis and Simulation of a QPSK system".

V. BIOGRAPHIES

T.P. Surekha, received the B.E degree from Mangalore University, Mangalore. And M.Tech degree from Visvesvaraya Technological University, Belgaum. Presently she is working as Asst professor in the department of Electronics and Communication Engineering, Vidyavardhaka College of Engineering, Mysore. Her research interest include Power-line communication System, Automation and Simulation of Communication System in Power System.

. T. Ananthapadmanabha received the B.E. degree, M.Tech degree and Ph.D. degree from the University of Mysore, Mysore. Presently, he is working as Professor and Head in the Department of Electrical Engineering, The National Institute of Engineering, Mysore. He is also Honorary Secretary of Institute of Engineers, (India), Mysore Local Centre, Mysore. His research interest include voltage stability, distribution automation and AI applications in power system. Simulation of Power and Communication System.

C Puttamadappa, received the B.E degree from Mysore University, Mysore. And M. E degree from Bangalore University, Bangalore. Ph.D degree from Jadvapur University, Kolkatta. Presently he is working as professor and Head in the department of Electronics and Communication Engineering, S J B institute of Technology, Kengeri, Bangalore, His research interest include Power Electronics, Simulation of communication systems, and Mobile Wireless Networks.

A.P. Suma, received the B.E. degree from Visvesvaraya Technological University, Belguam. She is pursuing her Masters degree at SJCE, Mysore. Her area of Interest include Power system Communications, Embedded systems and Automation and Simulation of communication system.

New Multiband Microstrip Patch Antenna On Rt Duroid 5870 Substrate For Pervasive Wireless Communication (X & Ku Band)

Dr T K Bandoupadhya [1] Dr Anubhuti khare[2] Rajesh Nema[3] and Puran Gour [3]
[1] BIST, [2] UIT RGPV, [3]NIIST
Bhopal, India

Abstract - An overview of work done in the area of micro strip antennas is presented and several recent developments in the fields are highlighted. In addition, new antenna configurations that improve electrical performance and manufacturability are described. We have analyzed multiband micro strip antenna in IE3D by finite moment of method. The proposed antenna design on 125 mil RT DUROID 5870 substrate and analyzed results between 1GHz to 15GHz, the proposed antenna design on a 125 mil RT DUROID 5870 substrate from Rogers-Corp with dielectric constant of 2.33 and loss tangent of .0005. At 14GHz (Ku band) the verify and tested result on IE3D SIMULATOR are Return loss = -33.4dB, VSWR=1.044, Directivity=8dbi, Characteristic impedance Z_O=49.13Ω, 53% bandwidth. The optimum 125mil RT DUROID 5870 substrate multiband micro strip patch antenna implement very effectively between 8GHz to 15GHz(X Band and Ku Band) in wireless communication. All results shown in Simulation results.

Key words: *Micro strip antenna, IE3D SIMULATOR, Dielectric, Patch width, Patch Length, Characteristic Impedance, Losses, strip width, strip length***.**

INTRODUCTION TO MICROSTRIP ANTENNA

A A Deshmukh and G Kumar [9] proposed compact L Shape patch broadband Microstrip antenna experimentally increase bandwidth up to 13.7%. Z M Chen [14] further increase bandwidth of this antenna up to 23.7% - 24.4%. J George [3] proposed optimal angle between feed line and patch for enhancing bandwidth. K F Lee [14] proposed U Shape slot shorting post small size Microstrip Antenna and increase bandwidth up to 42%. Z M chen Tsai K F Lee [14] [13] used low permittivity in proposed design for enhancing Bandwidth. R Garg P Bharti [10] significant increasing in bandwidth by increasing height of dielectric material. Latif S I Shafai [2] enhances gain and bandwidth by novel technique form ring by depositing multiple conductor layer separated by laminating dielectric. S C Gao [8] used uniplanar photonic band gap structure for enhancing band width and gain. M Khodier[11] New wideband stacked microstrip antennas for enhancing band width. W. S. Yun, Wideband microstrip antennas for PCS/IMT-2000 services. Major issue for microstrip antenna is narrow Bandwidth. The results of proposed Multiband microstrip patch antenna verified in IE3D Simulator .All results shown in simulation result.We find mathematical analysis of micro strip given below

EFFECTIVE PARAMETERS

The electric field radiated from a micro strip antenna meets a boundary between two different dielectrics: air and the substrate material. Because of the slight distortion of the field at the boundary, the patch can appear longer in an electrical sense. Thus we have an effective patch length. There is also an effective relative permittivity when performing micro strip antenna analysis. The

effective relative permittivity can be calculated by this formula used widely in

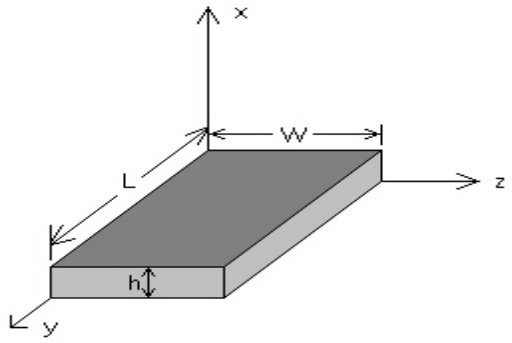

Figure 1

E-plane pattern

$$E_{\Phi} = \frac{kV_0 w}{2\pi r} e^{-jkr} \left[\sin\theta \left(\frac{\sin\left(\frac{kw}{2}\cos\theta\right)}{\frac{kw}{2}\cos\theta} \right) \right]$$

H-plane pattern

$H_{\theta} = E_{\Phi}/\eta$

Characteristic impedance of microstrip line feed

for $w/h \leq 1$

$$Z_0 = \frac{60}{\sqrt{\varepsilon_{reff}}} \ln\left[\frac{8h}{w} + \frac{w}{4h}\right]$$

For $w/h \geq 1$

$$Z_0 = \frac{120\pi}{\sqrt{\varepsilon_{reff}}\left[\frac{w}{h} + 1.393 + .667\ln\left(\frac{w}{h} + 1.44\right)\right]}$$

Beam widths E-plane

$$\theta_E \cong 2\cos^{-1}\sqrt{\frac{7.03\lambda 0^2}{4\left(3Le^2 + h^2\right)\pi^2}}$$

H-plane

$$\theta_H \cong 2\cos^{-1}\sqrt{\frac{1}{2+kw}}$$

Transmission line method is the easiest method as compared to the rest of the methods. This method represents the rectangular micro strip antenna as an array of two radiating slots, separated by a low impedance transmission line of certain length.

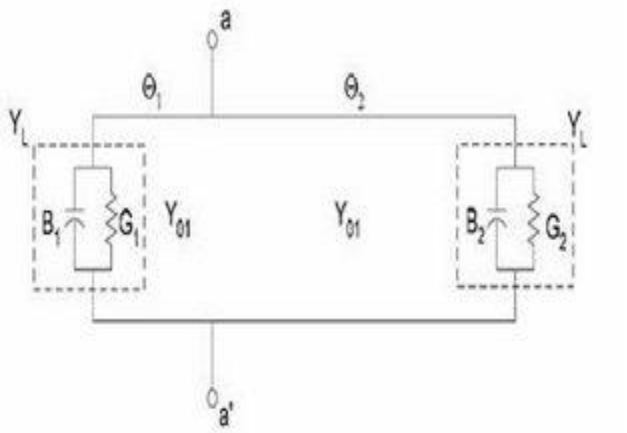

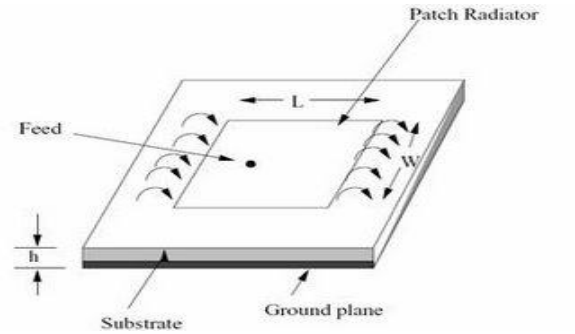

Figure 2

The above Figure 3 shows a patch antenna from the Transmission Line Model perspective. We can observe the

fringing at the edges increasing the effective length.

$$\varepsilon_{reff} = \frac{(\varepsilon r - 1)}{2} + \frac{(\varepsilon r + 1)}{2}\left(1 + 10\frac{h}{w}\right)^{-1/2}$$

$$w = \frac{c}{2 f r}\sqrt{\frac{2}{\varepsilon_r + 1}}$$

PROPOSED ANTENNA DESIGN FOR X BAND AND KU BAND ON 125 mil RT DUROID 5870 substrate

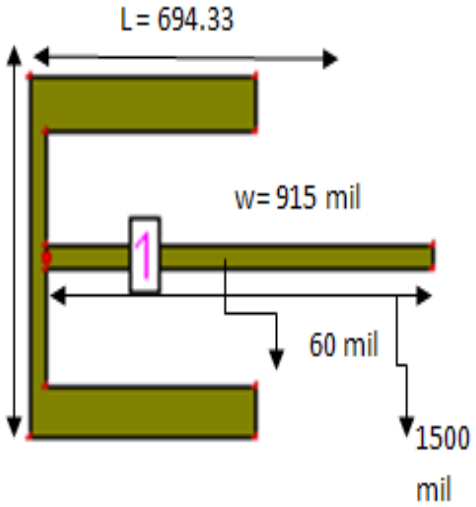

The Proposed antenna has:-

Proposed Patch length = 694.33mil

Proposed Patch Width = 915

Strip Path Length= 1500miles

Strip Path Width= 60miles

Cut width =650miles

Cut depth = 650 miles

SIMULATED PROPOSED ANTENNA IN IE3D SIMULATOR

1 *VSWR VS FREQUENCY (IN GHz)*

VSWR VS FREQUENCY (IN GHz)

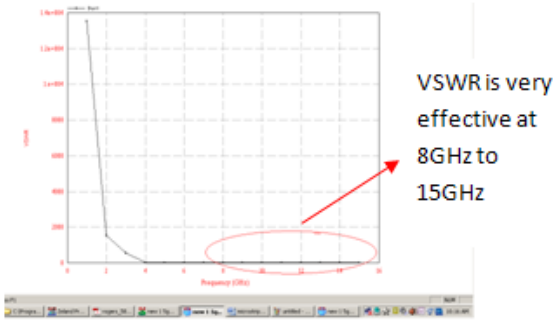

For proposed design **VSWR** is effective between **8GHz to 15GHz** (shown in table), for this range return loss is minimum. At **14GHz return loss** : -33.4dB and **VSWR** : 1.044, At **15GHz return loss** is -18.03dB and **VSWR** is 1.287, At **13GHz VSWR** is 1.49715GHz and **return loss** is -14.03dB,

2 Directivity VS FREQUENCY

Directivity vs frequency

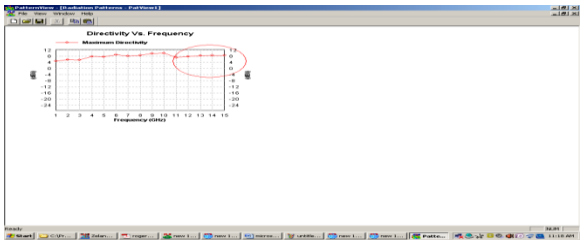

At 14 GHz Directivity **is** 8dBi**,** and for

11—15GHz Directivity **is** 8dBi**.**

3 Return loss VS Frequency (in GHz)

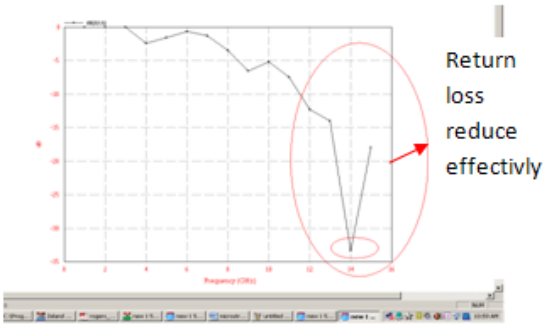

The frequency at **9GHz return losses** : -6.552, at **11GHz return losses** : -7.518, at **14GHz return losses** reduce very effectively :- 33.4, at **12GHz return loss** : -12.34, at **13 GHz return loss** :-14.03, **15GHz return loss** : -18.03, return losses are reduce very effectively between **12GHz to 15GHz,**

4 S Parameter (magnitude in db and phase) VS Frequency in GHz

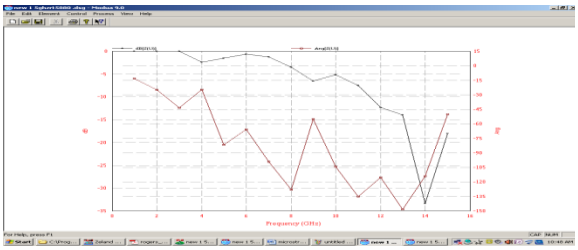

5 SIMTH CHART FOR DIFFERENT MEASURMENT

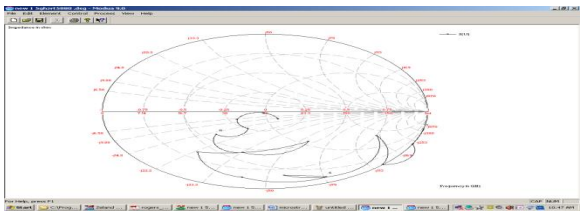

(6) Radiation Pattern:-

Analyzed radiation characteristic of antenna at 14 GHz in IE3D shown in figure

(a) Elevation Pattern

Elevation Pattern of E maximum,

Elevation Pattern of E Total at phi =90(deg)

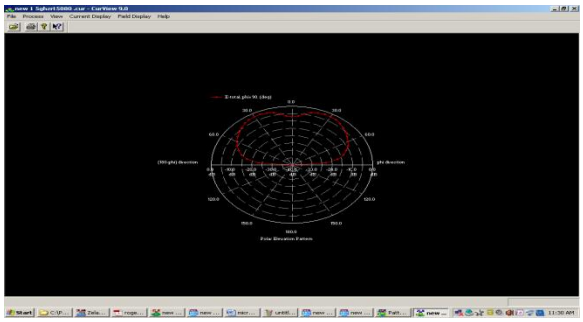

Elevation Pattern of E Total, E Right, E left, E theta, E Phi at phi=90 (deg)

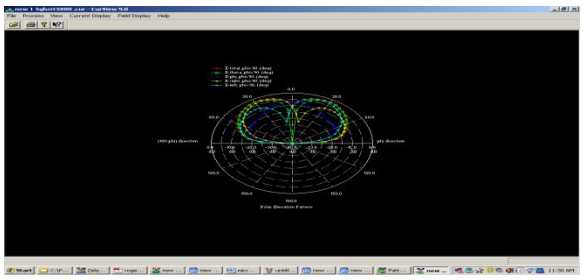

(b) Azimuth Pattern

Azimuth Pattern of E Total at theta=45(deg)

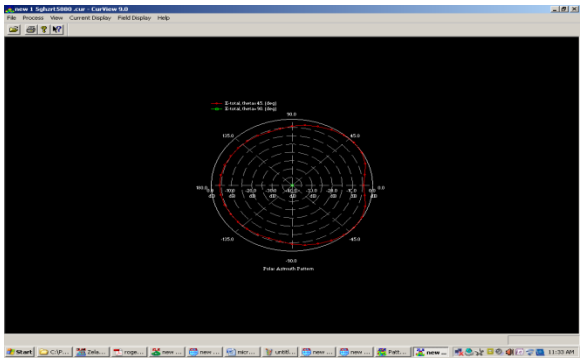

Azimuth Pattern of E Total, E Right, E left, E theta, E Phi at theta=90(deg)

AXIAL RATIO PATTERN

(A)FOR AZIMUTH PATTERN

Axial Pattern at theta=45(deg)

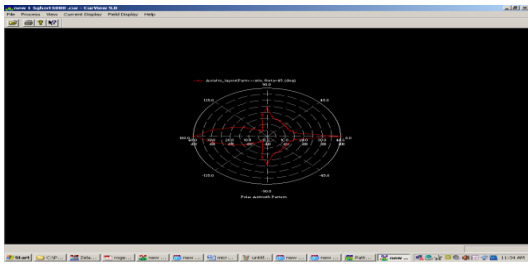

(B)FOR ELEVATION PATTERN

Axial Pattern at Phi =40(deg)

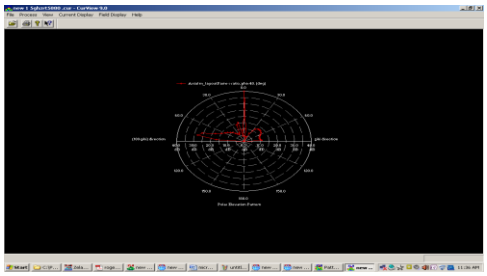

Axial Pattern at Phi =90(deg) & 40(deg)

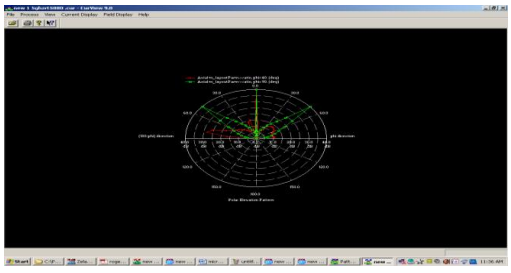

3D Pattern of radiation pattern

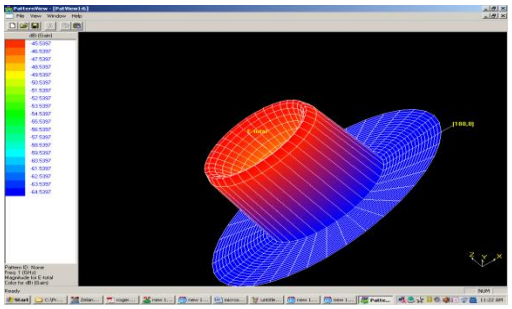

3D Current density Animation for proposed design

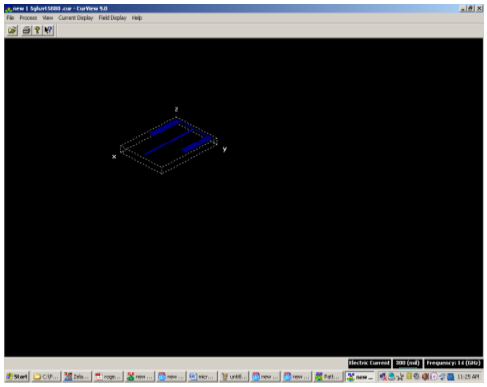

Table -1 dB [S (i j)] in dB and Ang[S (i j)] in Deg

Freq [Ghz]	dB[S(1,1)] 31 mil RT DUROID 5880 substrate
1	-1.285e^{-003}
2	-1.134e^{-002}
3	-3.203e^{-002}
4	-2.449
5	-1.569
6	-0.6582

7	-1.281
8	-3.525
9	-6.552
10	-5.223
11	-7.518
12	-12.34
13	-14.03
14	-33.4
15	-18.03

10	3.425
11	2.453
12	1.637
13	1.497
14	1.044
15	1.287

Table -2 Frequency (GHz) vs. VSWR (MEASUREMENT BY IE3D SIMULATOR)

Frequency [GHz]	**VSWR 125 mil RT DUROID 5870 substrate**
1	1.3 e^{+004}
2	1532
3	542.3
4	7.14
5	11.1
6	26.41
7	13.58
8	4.996
9	2.776

CONCLUSION: Most notably communication systems where many frequency ranges could be accommodated by a single antenna. The design antenna will be multiband and used in wireless communication for X Band and Ku band. By using transmission line model demonstrating the bandwidth effects by changing the various parameters. The proposed antenna design on a 125mil RT DUROID 5870 substrate from Rogers-Corp with dielectric constant of 2.33and loss tangent of .0005 has 694.33 mil patch length, 915mil patch width and more feed line length. The results of proposed designing are very effective between 8GHz - 15GHz (X Band and Ku Band). The bandwidth of design antenna is 53%. The optimum results of proposed antenna verify and tested in IE3D SIMULATOR. The simulated results of IE3D at 14GHz is **Return loss** = -33.4db, **VSWR**=1.044,**Directivity**=8dbi.**bandwidth** is 53%, the proposed antenna is multiband and implement very effectively for wireless communication in X Band and Ku band.

REFERENCES:

[1] Design considerations for rectangular rmicrostrip patch antenna on electromagnetic crystal substrate at terahertz frequency Infrared *Physics & Technology, Volume 53, Issue 1, January 2010, Pages 17-22* G. Singh

[2] Latif, S.I. Shafai, L. Shafai, C. Dept. of Electr. & Comput. Eng., Univ. of Manitoba, Winnipeg, MB "Ohmic loss reduction and gain enhancement of microstrip antennas using laminated conductors "Antenna Technology and Applied Electromagnetics and the Canadian Radio Science Meeting, 2009. ANTEM/URSI2009. 13th International Symposium on Toronto,

[3] 2009 WRI International Conference on Communications and Mobile Computing Improved Microstrip Fractal Patch Antenna Using Uni-planar Compact Photonic Bandgap Structure (UC-PBG) January 06-January 08 Gao Wei Deng Hui

[4] Progress in Electromagnetics Research Symposium Proceedings, Moscow, Russia, August 18{21, 2009 1087 Annular Ring Micro strip Patch Antenna on a Double Dielectric Anisotropic Substrate C. F. L. Vasconcelos1, S. G. Silva1, M. R. M. L.Albuquerque1, J. R. S. Oliveira2, and A. G. d'Assun»c~ao1

[5] Abbaspour,M. and H. R. Hassani, Wideband star-sharped microstrip patch antenna,"Progress In Electromagnetic Research Letters, Vol. 1, 61{68, 2008.

[6] Sabri, H. and Z. Atlasbaf, \Two novel compact triple-band micro strip annular-ring slot antenna for PCS-1900 and WLAN applications," *Progress In Electromagnetics Research Letters*, Vol. 5, 87{98, 2008

[7] A.Shackelford, K. F. Lee, D. Chatterjee, Y. X. Guo, K. M. Luk, and R. Chair,"Small size wide bandwidth microstrip patch antennas," in IEEE Antennas and Propagation International Symposium, vol. 1, (Boston, Massachusetts), pp. 86–89,IEEE, July 2001.

[8] S. C. Gao, L. W. Li, M. S. Leong, and T. S. Yeo, "Design and analysis of a novel wideband microstrip antenna," in IEEE Antennas and Propagation International Symposium,vol. 1, (Boston, Massachusetts), pp. 90–93, IEEE, July 2001.

[9] A.A.Deshmukh and G. Kumar, "Compact broadband gap-coupled shorted L-shaped microstrip antennas," in IEEE Antennas and Propagation International Symposium, vol 1, (Baltimore, Maryland), pp. 106–109, IEEE, July 2001.

[10] R. Garg, P. Bhartia, I. Bahl, and A. Ittipiboon, Microstrip Antenna Design Handbook.London: Artech House, 2001.

[11] M. Khodier and C. Christodoulou, "A technique to further increase the bandwidth Of stacked microstrip antennas," in IEEE Antennas and Propagation International Symposium, vol. 3, (Salt Lake City, Utah), pp. 1394–1397, IEEE, July 2000.

[12] K. Wong and W. Hsu, "A broadband patch antenna with wide slits," in IEEE Antennas and Propagation International Symposium, vol. 3, (Salt Lake City, Utah),pp. 1414– 1417, IEEE, July 2000.

[13] K. F. Lee, K. M. Luk, K. F. Tong, Y. L. Yung, and T. Huynh, "Experimental study of the rectangular patch with a U-shaped slot," in IEEE Antennas and Propagation International Symposium, vol. 1, (Baltimore, Maryland), pp. 10–13, IEEE, July 1996.

[14] Z. M.Chen and Y.W.M. Chial, "Broadband probe-fed L-shaped plate antenna," Microwave and Optical Technology Letters, vol. 26, pp. 204–206, 1985.

[15]A.Shackelford, K. F. Lee, D. Chatterjee, Y. X. Guo, K. M. Luk, and R. Chair, "Smallsize wide bandwidth microstrip patch antennas," in IEEE Antennas and Propagation International Symposium,vol. 1, (Boston, Massachusetts), pp. 86–89, IEEE, July 2001.

[16] C. Balanis, Antenna Theory: Analysis and Design. Toronto: John Wiley and Sons, 2nd ed., 1997.

Performance Analysis of an Multiple input/Multiple output Free-space Optical System with Q-ary Pulse-Position Modulation

Bobby Barua[#1] and Dalia Barua[#2]

[#1] *Assistant Professor, Department of EEE, Ahsanullah University of Science and Technology, Dhaka, Bangladesh*

[#2] *Student, Institute of ICT, Bangladesh University of Engineering and Technology, Dhaka, Bangladesh*

bobby@aust.edu

***Abstract*— Free Space Optical (FSO) communication is a telecommunication technology that uses light propagating in free space to transmit data between two points. FSO communication technology became popular due to its large bandwidth potential, unlicensed spectrum, excellent security and quick and inexpensive setup. . However, optical wave propagation through the air experiences fluctuation in amplitude and phase due to atmospheric turbulence. The use of multiple laser transmitters combined with multiple photo detectors has the potential for combating fading effects on turbulent optical channels. . In this paper, the modulation format is Q-ary PPM across lasers, with intensity modulation. Ideal photodetectors are assumed, with and without background radiation. It is found that MIMO system provides significant performance not only under weak turbulence but also strong turbulence. The performance results are evaluated in terms of symbol error probability for several system parameters.**

Keywords*— *Free space optics (FSO), multiple input/multiple output(MIMO) , pulse position modulation (PPM), probability of density function (PDF) , symbol error probability (SEP)

1. Introduction

Free-space optical (FSO) communication is an attractive and cost-effective solution for high-rate image, voice, and data transmission [1-6]. It has received significant attention recently, as a possible alternative to solve the bottleneck connectivity problem, and as a supplement to more conventional RF/microwave links. However, optical wave propagation through the air experiences fluctuation in amplitude and phase due to atmospheric turbulence. This intensity fluctuation, also known as scintillation is one of the most important factors that degrade the performance of an FSO communication link even under the clear sky condition [3]. Two primary challenges are attached to free-space optical communication. First, the narrow beam-width implies the need for careful pointing, and perhaps a need for active pointing and tracking mechanisms to combat building sway, etc. Second, the need to combat link fading due to scattering and scintillation. To enable the transmission under the atmospheric turbulence the use of the multi-laser multi-detector (MLMD) concept has been reported in Ref. [4, 5]. Specifically, we envision separate lasers, assumed to be intensity-modulated only, together with photodetectors (PDs), assumed to be ideal noncoherent (direct-detection) receivers. The sources and detectors are physically situated so that the fading experienced between source–detector pairs is statistically independent, and thus, diversity benefits can accrue from the multiple-input multiple-output (MIMO) channel [6]. Though we assume an LOS path exists between the transmitter and receiver array, the transmitted field from a single laser will propagate through an atmosphere and may experience several effects [3]. First, electromagnetic scattering from water vapor and other molecules causes a redirection of the optical energy, with corresponding loss of signal power at the receiver. Normally, this is only a significant effect if the water vapor content (and drop size) becomes large, or if substantial haze conditions exist.

A second phenomenon is refraction on a more macroscopic scale. Here, small regions of density in homogeneity in the atmosphere, due to pressure and/or temperature gradients, create a non uniform index of refraction throughout the medium. This is especially prominent on optical links parallel to and near the ground. Even though these regions can be treated as lossless, the aggregate field received at some point in the plane of the PDs becomes a random variable. This field strength is a function of space and also time, due to assumed turbulence of the medium.Obviously, the assumption of independence may not be valid, depending upon the spacing of the devices, and on the nature of the fading [7]. For example, a cloud or fog bank that fills most of the link will obviously induce large fades on all source–detector pairs. Alternative means of operation in such environments must be considered.

In this paper, we develop an analytical approach to evaluate the performance for both weak and strong turbulence with Q-ary PPM. The developed scheme allows aggregation of RF/microwave signals and a conversion to the optical domain in a very natural way and may be a good candidate for hybrid RF/microwave-FSO systems. The symbol error probability (SEP) are evaluated with and without fading in the presence of background radiation. In the determination of SEP it is also assumed that p.i.n. photodiodes are used, and the channel is modeled using Lognormal distribution for weak turbulence and Gamma-Gamma distribution for strong turbulence.

Manuscript received
Manuscript revised

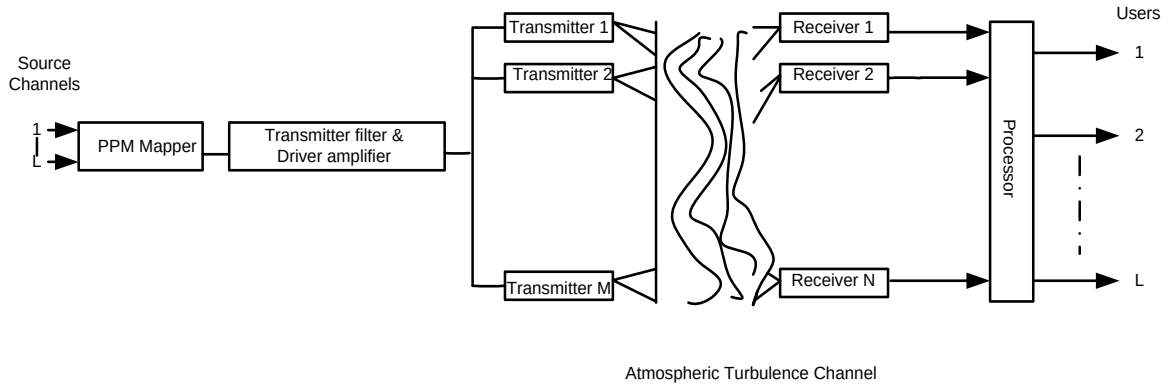

Fig. 1. Atmospheric optical MIMO system with Q-ary PPM

2. System Model

Fig. 1 depicts a block diagram of the physical system under study. ***M*** laser sources, all pointed toward a distant array of ***N*** PDs, are intensity-modulated by an information source. The laser beam-widths are narrow, but sufficiently wide to illuminate the entire PD array. For example, if the half-
power beam-width is 10 mrads, the half-power spot size at distance 1 km has diameter 10 m. The ***MN*** optical path pairs may experience fading, and we designate $\mathbf{A_{nm}}$ as the amplitude of the path gain (field strength multiplier) from **m** source to detector. A Q-ary PPM scheme transmits ***L=log2Q*** bits per symbol, providing high power efficiency. In the transmitter, the signals are described by the waveforms

$$\begin{aligned} s_0(t) &= A=\sqrt{2}P, \quad 0 \le t \le T_s/4 && \text{'00'} \\ s_1(t) &= A=\sqrt{2}P, \quad T_s/4 \le t \le T_s/2 && \text{'01'} \\ s_2(t) &= A=\sqrt{2}P, \quad T_s/2 \le t \le 3T_s/4 && \text{'10'} \\ s_3(t) &= A=\sqrt{2}P, \quad 3T_s/4 \le t \le T_s/4 && \text{'11'} \end{aligned} \qquad \textbf{(1)}$$

At the receiver the received signal *r(t)* after optical/electrical conversion is:

$$r(t) = \eta h(t) I_0 + n(t) \qquad \textbf{(2)}$$

where I_0 =the average transmitted light intensity and
$I = hI0$ =the corresponding received intensity in an ON PPM slot.
h =the channel fading coefficient
n =receiver noise.

The aggregate optical field is detected by each PD, assuming an ideal photon counting model with typical quantum efficiency. Also a single-channel link analysis is included to suggest typical link parameters. Though the transmission rate is rather flexible, we have in mind systems sending in the range of 100 Mb/s. Here we consider the chosen parameters rate 100 Mb/s, the expected number of detected photoelectrons per slot is on the order of 300 in either binary or quaternary PPM. Though this is more than adequate for the desired performance with the ideal photon-counting model, fading and other parameter choices could make this number much smaller.

3. Channel Modeling

To characterize the FSO channel from a communication theory perspective, it is useful to give a statistical representation of the scintillation. The reliability of the communication link can be determined if we use a good probabilistic model for the turbulence. Several models exist for the aggregate amplitude distribution, though none is universally accepted, since the atmospheric conditions obviously matter. Most prominent among the models are the log-normal , Rayleigh and gamma-gamma model.

Log-normal and Rayleigh Model

For propagation distances less than a few kilometers, variations of the log-amplitude are typically much smaller than variations of the phase. Over longer propagation distances, where turbulence becomes more severe, the variation of the log amplitude can become comparable to that of the phase. Based on the atmosphere turbulence model adopted here and assuming weak turbulence, we can obtain the approximate analytic expression for the covariance of the log-amplitude fluctuation of plane and spherical waves which is also known as Rytov variance, given by[1],

$$\sigma_R^2 = 1.23 C_n^2 k^{7/6} L^{11/6} \qquad \textbf{(3)}$$

where C_n^2 is the wave number spectrum structure parameter and depends on the altitude. Due to the turbulence of the atmosphere, the field strength received at the detector becomes a random field. We adopt both log-normal and Rayleigh models - which are the most

accurate among them. In the log-normal model, the amplitude of the random path gain **A** can be written as $\mathbf{A}=\mathbf{e}^{\mathbf{X}}$, where **X** is normal with mean $\boldsymbol{\mu}_{\mathbf{x}}$ and variance $\boldsymbol{\sigma}^2_{\mathbf{x}}$. By definition, the logarithm of *A* follows a normal distribution. The p.d.f. of *A* is given by [4],

$$f_A(a)=\frac{1}{(2\pi\sigma_x^2)^{\frac{1}{2}}a}\exp\left(-\frac{(\log_e a-\mu_x)^2}{2\sigma_x^2}\right),a>0 \qquad \textbf{(4)}$$

Thus, the logarithm of the field amplitude-scale factor is normally distributed. (This also means that the optical intensity, proportional to $\mathbf{A}^2$is log-normally distributed.) Since the mean path intensity is unity, i.e. $\mathbf{E[A^2]=1}$, we require $\boldsymbol{\mu}_{\mathbf{x}}=-\boldsymbol{\sigma}^2_{\mathbf{x}}$. The scintillation index (S.I.), a measure of the strength of atmospheric fading, known to information theorists as the "amount of fading", is defined as

$$S.I.=\frac{E\left[A^4\right]}{E^2\left[A^2\right]}-1 \qquad \textbf{(5)}$$

which, for lognormal distribution, can be shown to equal $S.I.=4e^{\sigma_x^2}-1$**.** Typical values appearing in the literature are S.I. in the range of 0.4–1.0.

Rayleigh fading emerges from a scattering model that views the composite field as produced by a large number of non dominating scatterers, each contributing random optical phase upon arrival at the detector. Furthermore, with Rayleigh fading, the diversity order which means the number of independently fading propagation paths - of the MIMO system becomes apparent by analyzing the slopes of the symbol error probability curves . The p.d.f of *A* under the Rayleigh distribution is

$$f_A(a)=2ae^{-a^2},a>0 \qquad \textbf{(6)}$$

The central limit theorem then gives a complex Gaussian field, whose amplitude is Rayleigh.

Gamma-gamma Model

Under weak fluctuation conditions, the scintillation index [Eq. (5)] increases with increasing values of the Rytov variance [Eq. (3)]. The scintillation index continues to increase beyond the weak fluctuation regime and reaches a maximum value greater than unity (sometimes as large as 5 or 6) in the regime characterized by random focusing. With increasing path length or in homogeneity strength, the focusing effect is weakened by multiple self-interference and the fluctuations slowly begin to decrease, saturating at a level for which the scintillation index approaches unity from above.

The reliability of the communication link can be determined if we use a good probabilistic model for the turbulence. Several probability density functions (p.d.fs) have been proposed for the intensity variations at the receiver of an optical link. Al-Habash et al. [7] proposed a statistical model that factorizes the irradiance as the product of two independent random processes each with a Gamma p.d.f. The p.d.f of the intensity fluctuation is given by [7],

$$f(I)=\frac{2(\alpha\beta)^{(\alpha+\beta)/2}}{\Gamma(\alpha)\Gamma(\beta)}I^{\frac{(\alpha+\beta)}{2}-1}K_{(\alpha-\beta)}(2\sqrt{\alpha\beta}I),I>0 \qquad \textbf{(7)}$$

I is the signal intensity, $\Gamma(.)$ is the gamma function, and $\boldsymbol{K}_{\boldsymbol{\alpha\beta}}$ is the modified Bessel function of the second kind and order. **αβ. α** and **β** are PDF parameters describing the scintillation experienced by plane waves, and in the case of zero-inner scale are given by [7]

$$\alpha=\frac{1}{\exp\left[\frac{0.49\sigma_R^2}{(1+1.11\sigma_R^{12/5})^{7/6}}\right]-1} \qquad \textbf{(8)}$$

$$\beta=\frac{1}{\exp\left[\frac{0.51\sigma_R^2}{(1+0.69\sigma_R^{12/5})^{5/6}}\right]-1} \qquad \textbf{(9)}$$

4. Theoretical Analysis

Symbol error probability (SEP) analysis of the system

We consider four cases: without or with background radiation, and non-fading or fading links. We discuss a general theory, and illustrate with specific results for the most interesting cases. The situation without background radiation and non-fading links is the easiest and is treated first. All these cases are discussed for both Lognormal and Gamma-gamma model.

Case:1 No Fading, No Background Radiation

With no loss of generality, we assume the symbol with the first *w* of total *Q* slots 'on' is sent. At the receiver end, we receive a matrix **Z** with elements [$\boldsymbol{Z_{nq}}$, $n = 1,\ldots\ldots N$; $q = 1,\ldots\ldots ,Q$] where *n* indicates the receiver number and ***q*** indicates the slot number. Since there is no background radiation, then $\lambda_b = 0$. If slot $\boldsymbol{q \in Qo_{ff}}$ $\boldsymbol{Z_{nq}}$ will be zero. The channel gain is the same for all paths with $\boldsymbol{a_{nm}} = 1$. The maximum likelihood detector becomes

$$\begin{aligned}\hat{\boldsymbol{x}} &= \arg\max_{x\in X}\sum_{n=1}^{N}\sum_{q\in Q_{on}}Z_{nq}\log\frac{\left(\frac{\lambda_s}{M}\sum_{m=1}^{M}a_{nm}^2+\lambda_b\right)}{\lambda_b}\\ &= \arg\max_{x\in X}\sum_{n=1}^{N}\sum_{q\in Q_{on}}Z_{nq}\log\left(\frac{\lambda_s+\lambda_b}{\lambda_b}\right)\\ &= \arg\max_{x\in X}\sum_{q\in Q_{on}}\sum_{n=1}^{N}Z_{nq}\end{aligned} \qquad \textbf{(10)}$$

In this case, an error will only occur when one or more of the ***w*** 'on' slots register zero counts at *all N* detector outputs and likelihood ties represents the only mechanism for decision error. When ***Q* = 2** and ***w* = 1** this is equivalent to a binary erasure channel. Specifically, suppose ***i*** of the ***w*** 'on' slots **(*i* ≤ *w*)** produce a column of zeros in the Z matrix where non-zero counts are expected. Then, a likelihood tie occurs among ***Q-w+i*** candidates and tie-breaking errors have probability

$$P\left[making\ an\ error\right]=\frac{\binom{Q-w+i}{i}-1}{\binom{Q-w+i}{i}}=t\left(Q,w,i\right) \quad \textbf{(11)}$$

By the Poisson property and independence we have that the probability of exactly ***i*** of ***w*** columns registering zero counts is

$$P\left[i\ of\ w\ columns=0\right]=\binom{w}{i}p^{i}\left(1-p\right)^{w-i} \quad \textbf{(12)}$$

where $p = e^{-\lambda s}$, and $\lambda_s = \acute{}P_rT_Q/hf = \eta P_rT_s/hfQ$.

Putting this altogether we can derive the symbol error probability in no background radiation, for a non-fading channel

$$P_s=\sum_{i=1}^{w}\binom{w}{l}t\left(Q,w,i\right)p^{i}\left(1-p\right)^{w-i} \quad \textbf{(13)}$$

By expanding the last term using a binomial expansion, i.e.

$$\left(1-p\right)^{w-i}=\sum_{l=0}^{w-i}\left(-1\right)^{l}\binom{w-i}{l}p^{l} \quad \textbf{(14)}$$

we can combine terms to get a finite series expansion for symbol error probability:

$$P_s=\sum_{i=1}^{w}\sum_{l=0}^{w-i}(-1)^{l}\binom{w}{i}\binom{w-i}{i}t(Q,w,i)p^{i}(1-p)^{w-i}e^{-\lambda_s N(i+l)} \quad \textbf{(15)}$$

From the equation it is found that, for a fixed total transmitter energy, the probability of symbol error is independent of ***M***, i.e., there is no phased-array gain attached to the multiple sources, since these are non-coherent sources. The effective received power does increase linearly with ***N***, the effect of increasing receiving aperture size.

By the Poisson property and independence, the SEP for both lognormal and gamma-gamma model is given by [4],

$$P_s=\frac{Q-1}{Q}\left[e^{-\frac{M\eta(\frac{P_r}{M})T_s}{hfQ}}\right]^{N}=\frac{Q-1}{Q}e^{-\frac{\eta E_s N}{hf}} \quad \textbf{(16)}$$

Case II: Fading Channel, No Background Radiation

First, we assume the channel gain of every laser-detector pair is fixed over a symbol duration. Letting $\boldsymbol{a_{mn}}$ denote the amplitude fading on the path from laser ***m*** to photodetector ***n***, we define the channel gain matrix as A with element $[a_{nm},\ n = 1,\ldots\ldots,N,\ m = 1,\ \ldots\ldots M]$. The probability of symbol error conditioned on the fading variables is

$$P_{s|A}=\sum_{i=1}^{w}\sum_{l=0}^{w-i}(-1)^{l}\binom{w}{i}\binom{w-i}{i}t(Q,w,i)e^{-\frac{\lambda_s}{M}\sum_n\sum_m a_{nm}^2(i+l)} \quad \textbf{(17)}$$

To extend the analysis of non-fading link and no background radiation case to the case of link fading, we can simply average the (conditional) symbol error probability of (17), with respect to the joint fading distribution of the $\boldsymbol{A_{nm}}$ variables. We emphasize that this produces the symbol error probability averaged over fades. Formally, we find $\boldsymbol{P_s}$ by evaluating

$$P_S=\int P_{s|A}\,f_A(a)da \quad \textbf{(18)}$$

where the integral is interpreted as an ***MN***-dimensional integral. Since the $\boldsymbol{A_{nm}}$ variables are assumed independent, the above averaging leads to

$$P_s=\sum_{i=1}^{w}\sum_{l=0}^{w-i}(-1)^{l}\binom{w}{i}\binom{w-i}{i}t(Q,w,i)\left(\int_0^{\infty}e^{-\frac{\lambda_s}{M}(i+l)a^2}f_A(a)da\right)^{MN} \quad \textbf{(19)}$$

If the channel is under log-normal fading, the probability of zero count in slot 1 at detector n is given by [1],

$$P\left[allZ_{n1}=0\,|\,slot1,A\right]=e^{-\sum_{m=1}^{M}\sum_{n=1}^{n}a_{nm}^2\left(\frac{\eta P_r}{Mhf}\right)\left(\frac{T_s}{Q}\right)} \quad \textbf{(20)}$$

If the path gains are independently distributed and identical, the average symbol error is given by [4],

$$P_s=\int P_{s|A}\,f_A(a)da=\frac{Q-1}{Q}\left\{\left[\int e^{-\frac{a^2\eta\left(\frac{E_S}{M}\right)}{hf}}f_A(a)da\right]^{N}\right\}^{M} \quad \textbf{(21)}$$

In case of gamma-gamma fading, the probability of zero count in slot 1 at detector n is

$$P\left[allZ_{n1}=0\,|\,slot1,A\right]=e^{-\sum_{m=1}^{M}\sum_{n=1}^{n}a_{nm}^2\left(\frac{\eta P_r}{Mhf}\right)\left(\frac{T_s}{Q}\right)} \quad \textbf{(22)}$$

If the path gains are independently distributed and identical, the average symbol error becomes

$$P_s=\int P_{s|A}\,f(I)dI=\frac{Q-1}{Q}\left\{\left[\int e^{-\frac{a^2\eta\left(\frac{E_S}{M}\right)}{hf}}f(I)dI\right]^{N}\right\}^{M} \quad \textbf{(23)}$$

Case III: No Channel Fading, with Background Radiation

At the receiver end, it received a matrix **Z** with elements $[Z_{nq}, n = 1,\ldots\ldots\ldots,N, q = 1,\ldots\ldots\ldots,Q]$. $\boldsymbol{\lambda_b}$ is the Poisson count random variable parameter due to the background radiation, and if slot $\boldsymbol{q}$ is an 'off' slot, $\boldsymbol{Z_{nq}}$ will be also a Poisson distributed random variable with parameter λ_b. For signal 'on' slot, the Poisson count random variable parameter is $\lambda_s+\lambda_b$. The channel gain is the same for all paths with $\boldsymbol{a_{nm}} = 1$.
Again, we assume without lose of generality that the symbol with the first $\boldsymbol{w}$ slot 'on' is send. The maximum likelihood detector becomes

$$\hat{x} = \arg \max_{x\in X} \sum_{n=1}^{N} \sum_{q\in Q_{on}} Z_{nq} \log\left(\frac{\lambda_s}{M}\sum_{m=1}^{M} a^2 + \lambda_b\right) = \arg \max_{x\in X} \sum_{q\in Q_{on}} \sum_{n=1}^{N} Z_{nq} \quad (24)$$

where $\boldsymbol{Q_{on}} = [1,\ldots\ldots\ldots,w]$ is the set of all 'on' slot that pulses are sent and $\boldsymbol{Q_{off}} = [w + 1, \ldots\ldots\ldots,Q]$ is the set of all 'off' slot that only background noise is received. Detection is correct only if all of the noise slot counts $\boldsymbol{Z_{nq}}$ are less than all the signal slot counts. Thus the symbol error probability is given by

$$P_s \le 1\text{-}P(\text{all signal slot counts greater than noise slot counts}) \quad (25)$$

Adding the tie-break part, we can get the exact error probability.

$$P_s \le P\left[\min(Z_{on}) < \max(Z_{off})\right] = 1 - \sum_{i=1}^{\infty}\left(poisson\ \ pmf\ \ (N(\lambda_s+\lambda_b), i+1)\right) X\left(1-\left(poisson\ \ cmf\ \ (N(\lambda_s+\lambda_b), i)\right)\right)^{w-1} X\left(poisson\ \ cmf\ \ (N(\lambda_b), i)\right)^{Q-w-1} \quad (26)$$

where *Poisson pmf*(*x*,*y*) represent the Poisson p.d.f at value $\boldsymbol{y}$ using the corresponding parameter $\boldsymbol{x}$ and *Poisson cmf*(*x*,*y*) represent the Poisson probability cumulative function at value $\boldsymbol{y}$ using the corresponding parameter $\boldsymbol{x}$.
For the exact error probability

$$P_s = P\left[\min(Z_{on}) < \max(Z_{off})\right] + \sum_{k=1}^{w}\sum_{s=1}^{Q-w}\binom{k+s}{s} P\left[\min(\underline{Z_{on}}) = \max(\underline{Z_{off}})\right] \quad (27)$$

we can get a precise form

$$P_s = P\left[\min(Z_{on}) < \max(Z_{off})\right] + \sum_{k=1}^{w}\sum_{s=1}^{Q-w}\binom{k+s}{s} P\left[\min(\underline{Z_{on}}) = \max(\underline{Z_{off}})\right] \quad (28)$$

where $\boldsymbol{s}$ minimal signal slots have the same counts as $\boldsymbol{k}$ maximum noise slots.

Then the exact error probability can be written for both lognormal and Gamma-gamma channel as

$$P_s \cong w(Q-w)P[dis\tan ce - 2error] \quad (29)$$

A union bound on symbol error probability will be dominated by error events with symbol Hamming distance 2, of which there are $\boldsymbol{w(Q- w)}$ occurrences.

$$P_s \le 1 - P\left[all\ Z_q < Z_1\right] = 1 - \left(P\left[Z_2 < Z_1\right]\right)^{Q=1} = 1 - \left[\sum_{i=1}^{\infty}\sum_{j=0}^{i-1} P\left(Z_1 = i, Z_2 = j\right)\right]^{Q-1} \quad (30)$$

The latter two-signal probability can be bounded, using the appropriate Poisson distributions, by a Chernoff bound

$$P[dis\tan ce - 2error] \le \frac{\exp\left(2\lambda_b\left(\left(1+\mu\right)^{\frac{1}{2}} - 1\right) - \lambda_s\right)}{2} \quad (31)$$

where $\mu = \frac{n_s}{n_b}$. Expanding the exponent with a Taylor series in μ for small μ gives

$$P_S \cong \frac{w(Q-w)}{2}\exp\left(-\frac{\lambda_S^2}{4\lambda_B}\right) \quad (32)$$

Case IV: Fading Channel, with Background Radiation

This case is the most general in practice, and there is no simple expression for the symbol error probability. Here some incorrect symbol can have higher likelihood (an incorrect set of $\boldsymbol{w}$ slots have larger weighted column sums) same as in Case III. By using equal-gain-combiner, the upper bound on $\boldsymbol{P_s}$ conditioned on fading path gain matrix A is

$$P_s \le 1 - \sum_{i=1}^{\infty}\left(poisson\ \ pmf\ \ \left(\sum_{n=1}^{N}\sum_{m=1}^{M} a_{nm}^2\frac{\lambda_s}{M} + N\lambda_b, i+1\right)\right) X\left(1-\left(poisson\ \ cmf\ \ \left(\sum_{n=1}^{N}\sum_{m=1}^{M} a_{nm}^2\frac{\lambda_s}{M} + N\lambda_b, i+1\right)\right)\right)^{w-1} X\left(poisson\ \ cmf\ \ \left(N(\lambda_b), i-1\right)\right)^{Q-w-1} \quad (33)$$

We can get the overall symbol error probability by averaging the conditional symbol error probability. Numerical integration is a prohibitively slow process due to the large number of fading variables combined with the infinite summation. In this case, using numerical integration is not an efficient way to calculate the symbol error probability. We use simulation instead to analyze the performance of the MIMO system.

For both log-normal and gamma-gamma case, the optimal detector is as described by the following equation. We propose instead a more realistic design of simply summing over the received PD counts for each time slot as was optimal for the cases presented above. Channel estimation

at the receiver is thereby avoided in exchange for a small performance penalty.

$$P_{S/X} = 1 - \left[\sum_{i=1}^{\infty} \sum_{j=0}^{i-1} \frac{\left(N(\lambda_s + \lambda_b)\right)^i e^{-N(\lambda_s+\lambda_b)}}{i!} X \frac{\left(N\lambda_b\right) j e^{-N\lambda_b}}{j!} \right]^{Q-1} \quad \textbf{(34)}$$

The average symbol error becomes

$$P_s = \int P_{S|X} \, f(z) dz \quad \textbf{(35)}$$

where f(z)= lognormal or gamma-gamma p.d.fs.

5. Results and Discussion

Following the analytical approach presented in section IV, we evaluate the symbol error probability result of a MIMO FSO link with Q-ary PPM and direct detection scheme under various turbulence conditions. For the convenience of the readers the parameters used for computation in this paper are shown in table 1.

Table1: System Parameters used for computation

Parameter Name	**Value**
Bit Rate, B_r	100 Mbps
Modulation	Q-PPM
Order of PPM, Q	2, 4, 8, ……..
Channel Type	Log-normal, Gamma-gamma
Scintillation Index, S.I.	0.2-3.0
Symbol energy with background noise	-170dBJ
Rytov Variance, σ_x	0.1-0.8
Symbol Energy, E_s	10^{-16} Joules
Quantum efficiency, η	0.5

In Fig 2 it is found that due to the turbulence of the atmosphere, the field strength received at the detector becomes a random field. where C_n^2 is the wave number spectrum structure parameter and depends on the altitude.

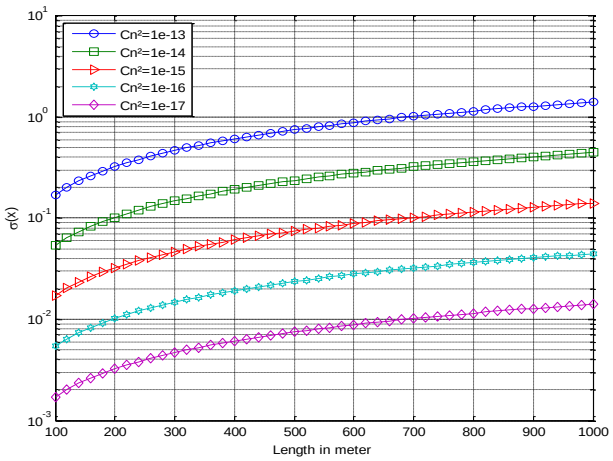

Fig.2: Standard deviation of the log-amplitude fluctuation versus propagation distance for a plane wave

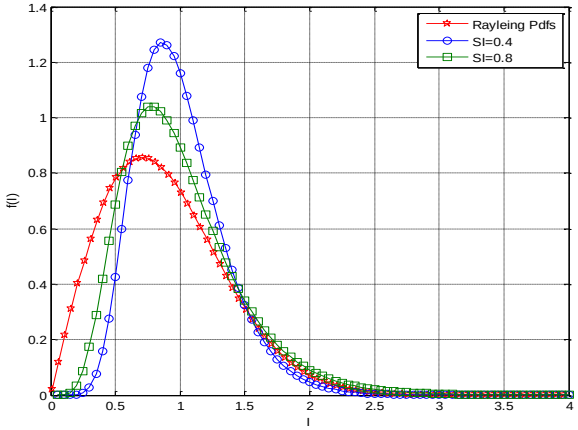

Fig.3: Lognormal and Rayleigh p.d.fs

The simulations are performed using matlab, the influence of scintillation is modeled assuming both Lognormal and Gamma-Gamma distribution, and an ideal photon counting receiver is employed. The plots of the probability density function in Fig. 3 for lognormal cases and in Fig 4 for gamma gamma cases with several typical values of scintillation index (S.I) and turbulence strength.

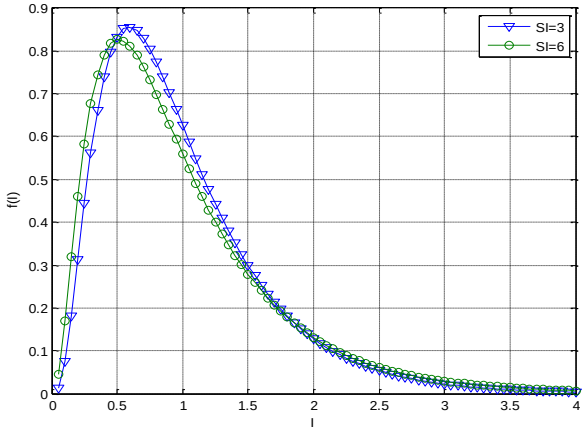

Fig4: Probability of Distribution Function for Gamma-Gamma.

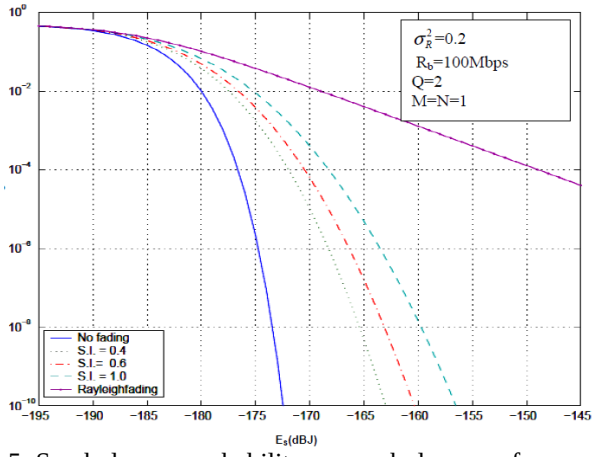

Fig-5: Symbol-error probability vs. symbol energy for Q=2, M=N=1 and no background noise, for lognormal channel with different S.I

Fig 5 shows the plots of symbol-error probability vs. symbol energy for Rayleigh fading and log-normal fading with varying the values of scintillation index by using a single laser and photodetector. Keeping the others parameters are constant, we compare the performance of the system for Rayleigh fading and log-normal fading.

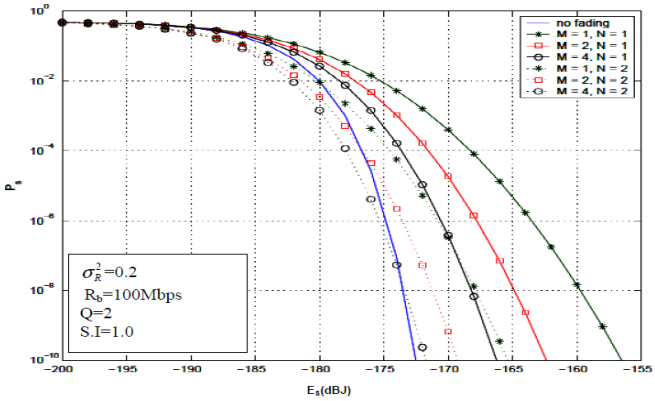

Fig-6: Symbol error probability vs. symbol energy for log-normal fading (S.I = 1.0), no background radiation, $Q = 2$; $M \in (1; 2; 4)$; $N \in (1; 2)$

Fig. 6 shows the plots of symbol-error probability vs. symbol energy for log-normal fading with varying the no. of transmitting and receiving antennas. From the plots it is found that, the performance will improve if the no. of corresponding transmitter and receiver increases.

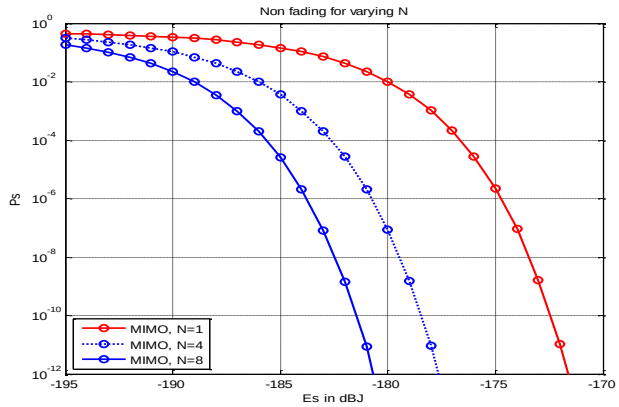

Fig7: SEP with varying N, for gamma-gamma non- fading with *S.I. = 3*, *Q= 2*. M=1 and no background noise

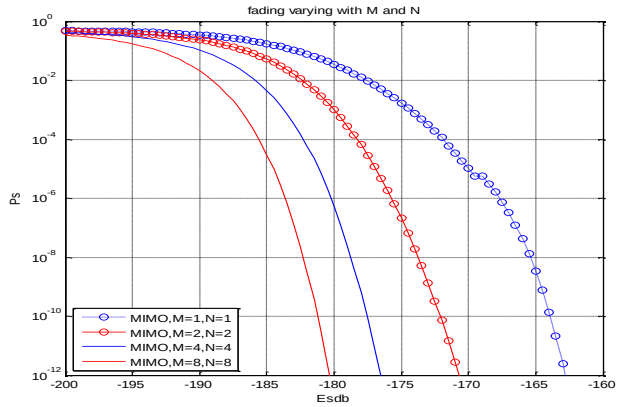

Fig.8 :SEP with varying both M and N, for gamma-gamma fading with *S.I. =3*. *Q= 2* and no background noise.

In particular, notice the gamma-gamma model has a much higher density in the high amplitude region, leading to a more severe impact on system performance. Fig. 7 shows the SEP under strong turbulence for non faded system with Q-ary scheme. The SEP are shown in Fig. 8 for several combinations of transmitting and receiving antennas under faded condition.. The symbol energy due to background light is set to -170 dBJ for both system It is noticed that, SEP improves as the numbers of lasers and photodetectors are increased and in the presence of background light the SEP decreases as the order of the Q-ary PPM scheme increases.

6. Conclusions

We have analyzed an optical MIMO system employing QPPM across sources, together with direct detection. Lognormal and Gamma gamma model has been treated, assuming independent fading on source–detector pairs. The analysis shows the beneficial effects from a diversity standpoint of multiple sources and detectors, and transmit diversity is achieved here without additional special coding. Some aspects of the optical MIMO system here mimic those of the microwave MIMO systems. Full transmit diversity can be shown analytically for the no-background-noise case. Even for the case of normal background radiation, QPPM is still able to approach the performance of the unfaded case by increasing the number of transmitter. The proposed MIMO scheme provides excellent gains for different atmospheric turbulence conditions, ranging from the weak to the strong turbulence regimes.

References

[1] Cvijetic N., Wilson S.G., and Brandt- Pearce M., *"Receiver optimization in turbulent free-space optical MIMO Channels with APDs and Q-ary PPM,"IEEE photon tehnol.Lett.18, 1491-1493 (2006)*

[2] J. Strohbehn, Ed. "*Laser Beam Propagation in the Atmosphere*" New York: Springer, 1978.

[3] L. C. Andrews, R. L. Phillips, C. Y. Hopen, M. A. Al-Habash, "*Theory of optical scintillation*," J. Opt. Soc. Am. A 16, 1417–1429 (1999).

[4] Wilson S.G., Brands-Pearce M., Cao Q., and Leveque J.J.H.,III, "*Free-Space optical MIMO transmission with Q-ary PPM*," *IEEE Trans. Commun.53,1402-1412(2005)*

[5] G. Ochse, *Optical Detection Theory for Laser Applications*. NewYork: Wiley- Interscience, 2002.

[6] B. Saleh, *Photoelectron Statistics*. Berlin, Germany: Springer- Verlag,1978.

[7] M.A. Al-Habash, L.C. Andrews, and R. L. Phillips, *Optical Engineering 40*,pp.1554- 1562 (2001).

Detection and Removal of Lead from the Local Industrial Waste Water.

[1]Muhammad Zahid Qureshi, [1]Shazia Khurshid, [1]Gugan Jabeen, [2]Mukhtar ul Hassan and [1] Jalil Tariq

1. Department of Chemistry, G.C. University Lahore, Pakistam
2. University of the Punjab, Lahore. Pakistan

Abstract:

The lead is well known pollutant in the world. It causes many nervous disorders, kidney failure and memory loss that is why it is under intensive investigation for its removal from the industrial waste waters by different techniques. The search for more efficient methods for its removal is also under inquiry. The work reported in this article was carried out to remove lead from the samples of effluents collected from a local industrial cluster by its adsorption *on Nymphaea alba* (nilofar flower) .The estimation of lead in industrial effluents before and after adsorption was accomplished applying atomic absorption spectrometry. It proved a remarkable technique in a sense that there was no use of any expensive chemicals. The results suggested that the method of removal of lead from the effluent is cheap, efficient and very effective.

Key words: *lead, adsorbent, Nymphaea alba (Nilofar flower) industrial, waste water.*

Introduction

Different toxic elements are being produced by many chemical industries. These industries are releasing these poisonous metals and other chemical waste as effluents that are being drained without treatment to the nearest water bodies: rivers, streams, canals, ponds, etc. Among other chemicals one poisoning metal is lead. Poisoning is a pattern of symptoms from mid to high level of exposure. Both organic and in-organic compounds of lead are present as

industrial effluents. But exposure to organic lead is more toxic than in-organic lead compounds. Lead poisoning is different in adults and children. In adults main symptoms are memory loss, abdominal pain, kidney failure and headache. Classic sign and symptoms in children are loss of appetite, vomiting, weight loss, constipation, anemia, and kidney failure and behavior problems. These symptoms in children and adults starts appearing at round 50-60 ug/dl. Chronic poisoning is associated with three types of systems. Gastrointestinal, neuromuscular and neurological. People exposed to working industries like radiation shields, plumbing, jet engines, ceramic, glaze, lead miners and smelters, manufacturing of glass, battery manufacturing and paint are at risk of lead exposure. Lead store in blood, soft tissues and bones. Lead not only poisoning the humans but also marine life. Lead can be stored in fish and indirectly to humans as these fish is used by humans. So exposure to lead decrease the life span and effects health in long terms.

Removal of lead from industrial waste water like other toxic metals is need of today Number of methods have been utilized for the removal of toxic metals from waste water like mercury copper chromium and lead etc,. Sea nodules (Bhattacharjee, S. et al., 2003) .Aluminium-red mud(Gupta,V.K. et al., 2001). Activated tea waste (Mondal, M.K. 2009) and granulated blast furnace slag (Dimitrova, S.V. et al., 1998) have been used for removal of these metal ions and they proved to be best sorbent for the adsorption of thee heavy metals due to availability, low cost and effectiveness.

Nymphaea alba (Nilofar) flower is easily available in Pakistan. It is present in ponds and lakes. It was used as an adsorbent for the removal of lead from industrial waste effluents. It is highly economic, naturally occurring and effective adsorbent. It can be used not only for lead but for other heavy metals like chromium. While performing this experiment other factors like temperature, pH, amount of adsorbent contact time etc, were also studied. Influence of each parameter was positive for removal of high concentration of lead from industrial waste water.

Materials and Methods:

Chemical used for this experimental work were of analytical grade and

made by Merck/BDH, Germany. For preparation and dilution of solutions doubly distilled Atomic absorption spectrometer, AA-100 Perkin Elmer was used for the determination of lead contents. Fuel was acetylene and oxidant was air with the ratio of 1:3. Eutech instrument pH meter 510 was used to check the different pH ranges of solutions. For continuous shaking Technico 10S-207 incubator shaker was used and for heating purposes Gallenkamp incubator size one was used. Electric balance was used for weighing of different chemicals.

Adsorbent

Nymphaea_alba was used to remove the Lead. It was collected from different ponds. It was washed with doubly distilled water and dried properly in sun then it was dried in oven at 50 ^{0}C for one hour. . After its complete drying it was powdered using grinder moulinex . It was sieved and stored to save it from moisture and contamination.

Detection of metal:

Waste water samples were collected from five different industries located on Sheikupura road near Lahore. Industries are listed below

Siddique Leather Works.

Hassan Dying .

Mandialli Paper Mills.

Big one Carpets Centre.

Al- Ghazi Plastic industry.

Samples were collected in the plastic bottles and refrigerated.

Before the treatment samples were doubly filtered off. 10ml of each sample was diluted to 100ml.After that 50ml of these effluents were transferred to different flasks. Detection of these samples were done by using atomic absorption spectrophotometer. Burners provided the heat energy to ionize the chemical compounds to free analyte forms. Spectrometer measured the absorbance at specific wavelength. Various toxic metals were reported in all these industrial effluents. Lead was present in a maximum amount.

Removal of lead

Calibration curve for lead

Estimation of lead was done against standard lead acetate solutions. 2.8309 g of lead acetate was dissolved in 1L of distilled water. Other standard solutions of required concentrations were prepared from stock solution. 50ml of different ppm solutions were transferred to conical flasks.

Absorbance was measured at 283.3nm. by atomic absorption spectrometer, AA-100 Perkin Elmer . Fuel was acetylene and oxidant was air with the ratio of 1:3. Calibration curve was made between absorbance and concentration of known standards. A correlation coefficient of 0.9584 was obtained for the calibration curve as represented in the table 1.

Adsorption Experiment

Adsorption experiment was done at room temperature after taking 50ml of known concentration of lead solutions in different flasks. Different amount of adsorbent were added in each flasks and were shaken at 100rpm for half an hour. All samples were treated in the same manner after that solution were doubly filtered off. Analysis of solutions was done by atomic absorption spectrometer at 283.3nm.The % removal efficiency was shown in the table 2.

Various other parameters and their effect on adsorption were also studied.

Effect of contact time on adsorption

50 ml of 50 ppm concentration solutions were transferred in different flasks. Then 0.6g of adsorbent was added to every flask and were shaken at 100rpm for different time intervals like 10, 20, 30, 40 …….100 minutes. After that solutions were doubly filtered off. These solutions were analyzed by atomic absorption spectrometer. The graph was drawn between % removal efficiency and time in minutes as shown in table 3 .

Effect of thermal treatment on adsorption

Removal of lead from solution was also studied at different temperatures.50ml of 50ppm solution was taken in different flasks. 0.6 grams of adsorbent was added to each flask. These flasks were shaken in an incubator shaker at 100rpm for 100 minutes at different temperature ranges like 20, 25, 30,35,40,45,50,55,60 and 65^0 C etc, .After the treatment solutions were finally filtered off. Analysis was done by atomic absorption spectrometer at 283.3nm. Results were drawn between % removal efficiency and temperature. Table 4.

Determination of Effect of pH on adsorption

Elimination of lead from solution was also studied by varying pH of the solutions. Standard Solutions were taken in different flasks. Then 0.6 g of adsorbent in each flask were added after that different pH ranges like 2, 3, 4……11 were adjusted with the help of 0.1M NaOH and HCl solutions.

These flasks were shaken in shaker at 100rpm for 100 minutes at 60 °C. These solutions were doubly filtered off. Analysis was done by atomic absorption spectrometer at 283.3nm. Results were drawn between % removal efficiency and pH.Table 5.

Effect of agitation speed on adsorption

To the standard solutions 0.6 g of adsorbent was added and pH was adjusted 8.These flasks were shaken in an incubator shaker at 60 ^{0} C for 100 minutes at different agitation speeds like 25, 50, 75,100……250rpm. These solutions were doubly filtered off. Analysis was done by atomic absorption spectrometer at 283.3nm. Results were drawn between % removal efficiency and agitation speed. Table 6.

Removal of lead from dying industry

Waste effluent collected from Hassan Dying industry near Sheikhpura was treated by using same method as used above for lead standard solutions.

50 ppm of diluted waste water was doubly filtered off. Its absorbance was measured by atomic absorption spectrometer at 283.3nm.

Maximum absorbance of waste sample = 1.653 nm.

Concentration of lead = 48.90 ppm.

50 ppm of sample solutions were transferred to flasks after filtration. Different amount of adsorbent were added to waste water samples. Solutions were shaken at 175rpm for 100 minutes at 60^{0}C. Samples were analyzed by atomic absorption spectrometer. The percent removal efficiency is shown in the table 7.

Results and discussions

The experimental work was based on the detection and removal of toxic elements. It was done by atomic absorption spectrometer. Method adopted was to find the initial concentration of the solutions and then calculating the concentration after treatment. The difference calculated was showing the removal of lead metal from waste water. The data collected has been reported in form of tables and figures.

For calibration curve standard solutions of different concentrations were prepared and then treated by adsorbent. Analysis was done by atomic absorption spectrometer. Different other factors were also studied and their results were represented by different tables and respective figures.

Effect of amount of adsorbent:

The effect of amount of adsorbent was studied from 0.2 g to 2.0g in different standard solutions. As the amount of

adsorbent was varied, with that maximum adsorption of 89% was achieved with 0.6 g of adsorbent. Results are verified from calculations in figure and table 2.

Effect of contact time:

Effect of contact time between the adsorbent and solution was studied by keeping other parameter constant like amount of adsorbent 0.6g .Time duration varied from10, 20 30,…..100 minutes. Results revealed that more contact time proved better removal of metal from solution. When contact time was 100 minutes the maximum removal of 93% was observed as revealed in figure and table 3.

Influence of temperature:

Influence of temperature was studied by varying temperature from 20, 25, 30, 35…….65 ^{o}C keeping other parameters constant. Removal of metal from effluents was more efficient at high temperature like 60^{0}C than low temperature. The maximum removal of 95% was observed at 60^{0}C shown in figure and table 4.

Effect of pH:

Samples were treated at different pH ranges like 2,3,4…….to 11. Maximum absorbance of 92% was observed at pH 8. Table and figure reveals the further confirmation. Table 5.

Effect of agitation speed:

As waste samples were shaken in an incubator shaker at different speeds. Maximum removal was observed at maximum shaking. With maximum shaking adsorbent and metal get more surface area to come in contact and react fastly. So solution at agitation speed of 175 rpm gave best adsorption of 93% than at low speed along with other parameters constant. Table 6.

SN.	Concentration in ppm.	Absorbance nm
1	5ppm	0.187
2	10ppm	0.294
3	15ppm	0.449
4	20ppm	0.691
5	25ppm	0.681
6	30ppm	0.98
7	35ppm	1.19
8	40ppm	1.24
9	45ppm	1.78
10	50ppm	1.67

Calibration curve for lead.Table 1.

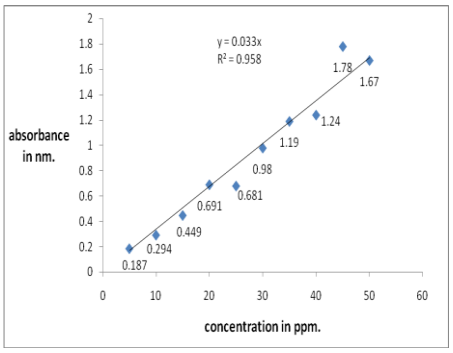

Calibration curve for lead.

Effect of the amount of adsorbent.

Table 2.Effect of adsorbent on % removal of lead**.**

S/ N	Initial conc. of 50ml of solution ppm.	Mass of adsorbent g.	Absorbance after removal Nm	Conc. after removal ppm.	%removal efficiency
1	50ppm	0.2	0.69	20.40	59.17%
2	50ppm	0.4	0.58	17.15	65.68%
3	50ppm	0.6	0.181	5.35	89.28%
4	50ppm	0.8	0.201	5.94	88.10%
5	50ppm	1.0	0.20	5.917	88.16%
6	50ppm	1.2	0.230	6.804	86.39%
7	50ppm	1.4	0.263	7.781	84.43%
8	50ppm	1.6	0.264	7.81	84.37%
9	50ppm	1.8	0.259	7.662	84.67%
10	50ppm	2.0	0.250	7.396	85.20%

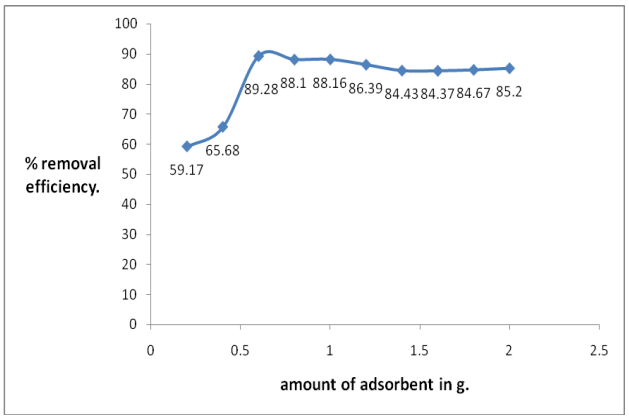

Effect of the amount of adsorbent

Effect of contact time on adsorption

Table 3. Effect of contact time on %removal of lead.

SN	Initial concentration of 50ml of solution ppm.	Contact time min	Absorbance after removal nm	Concentration after removal ppm.	%removal efficiency
1	50ppm	10	0.821	24.284	51.42%
2	50ppm	20	0.709	20.97	58.04%
3	50ppm	30	0.580	17.15	65.68%
4	50ppm	40	0.571	16.89	66.21%
5	50ppm	50	0.358	10.59	78.81%
6	50ppm	60	0.351	10.38	79.23%
7	50ppm	70	0.201	5.94	88.10%
8	50ppm	80	0.117	3.46	93.07%
9	50ppm	90	0.119	3.52	92.95%
10	50ppm	100	0.109	3.22	93.55%

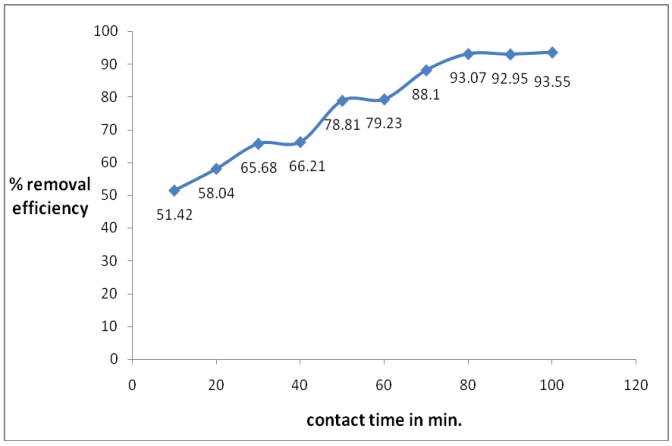

Effect of contact time

Effect of thermal treatment on adsorption

Table 4. Effect of temperature on %removal of lead.

SN	Initial concentration of 50ml of solution ppm.	Temperature ^0C	Absorbance after removal nm	Concentration after removal ppm.	%removal efficiency
1	50ppm	20	0.699	20.68	58.63%
2	50ppm	25	0.69	20.41	59.17%
3	50ppm	30	0.591	17.48	65.02%
4	50ppm	35	0.339	10.02	79.94%
5	50ppm	40	0.229	6.775	86.44%
6	50ppm	45	0.117	3.46	93.07%
7	50ppm	50	0.116	3.43	93.13%
8	50ppm	55	0.109	3.22	93.55%
9	50ppm	60	0.082	2.42	95.14%
10	50ppm	65	0.083	2.45	95.08%

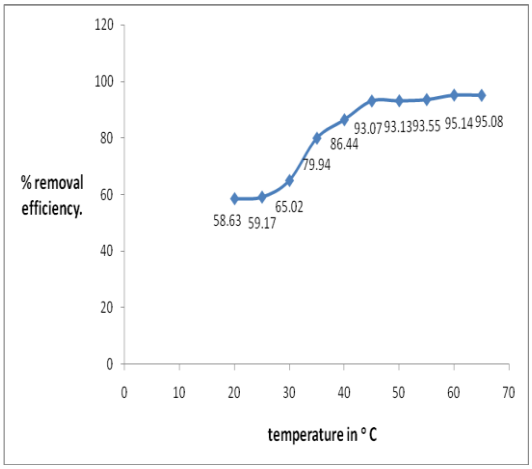

Effect of temperature

Effect of pH on adsorption.

Table 5. Effect of PH on %removal of lead.

SN	Initial concentration of 50ml of solution ppm.	pH	Absorbance after removal nm	Concentration after removal ppm.	%removal efficiency
1	50ppm	2	0.781	23.10	53.78%
2	50ppm	3	0.732	21.65	56.68%
3	50ppm	4	0.609	18.01	63.96%
4	50ppm	5	0.598	17.69	64.61%
5	50ppm	6	0.368	10.88	78.22%
6	50ppm	7	0.271	8.01	83.96%
7	50ppm	8	0.128	3.78	92.42%
8	50ppm	9	0.259	7.66	84.67%
9	50ppm	10	0.43	12.72	74.55%
10	50ppm	11	0.572	16.92	66.15%

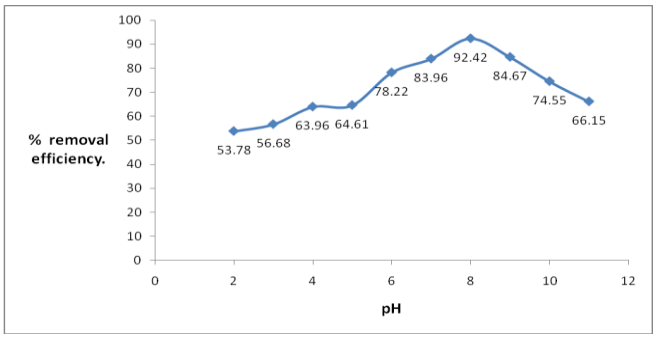

Effect of pH

Effect of agitation speed.

Table 6. Effect of agitation speed on %removal of lead.

SN	Initial concentration of 50ml of solution ppm.	Agitation speed rpm.	Absorbance after removal nm	Concentration after removal ppm.	%removal efficiency
1	50ppm	25	0.821	24.28	51.42%
2	50ppm	50	0.732	21.65	56.68%
3	50ppm	75	0.499	14.76	70.47%
4	50ppm	100	0.127	3.75	92.48%
5	50ppm	125	0.128	3.78	92.42%
6	50ppm	150	0.135	3.99	92.01%
7	50ppm	175	0.133	3.42	93.14%
8	50ppm	200	0.140	4.14	91.71%
9	50ppm	225	0.149	4.40	91.18%
10	50ppm	250	0.145	4.28	91.42%

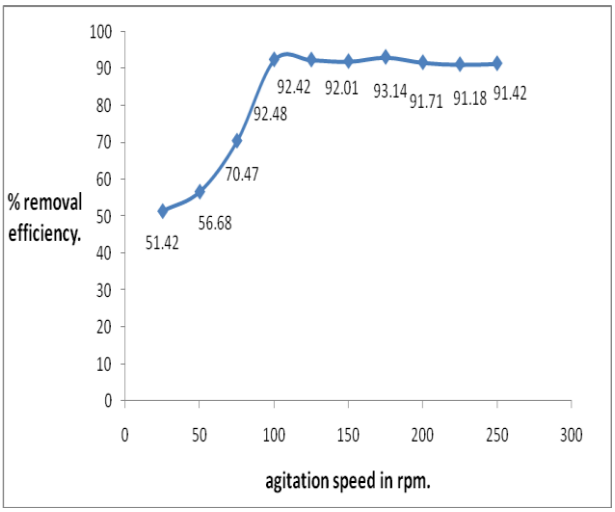

Effect of agitation speed

Table 7. Removal of lead from dying industry

Industry	Initial concentration of 50ml of solution ppm	Mass of adsorbent g.	Absorbance after removal nm	Concentration after removal ppm.	%removal efficiency
Hassan Dying Industry	48.90	0.2	0.711	21.03	56.98%
	48.90	0.6	0.163	4.822	90.13%
	48.90	1.0	0.286	8.46	82.69%
	48.90	1.6	0.216	6.39	86.93%
	48.90	2.0	0.408	12.07	75.31%

Conclusion:

Method used above for removal of heavy metal like lead from various industrial effluents is quite easy, cheap, adoptable and efficient method. It is economical because Nelofar flower is easily available in Pakistan. Experimental technique is also simple and easy because no complicated methodology is used, no chemicals are required. This technique was applied on standard solutions of known concentrations and to industrial waste effluents. The experimental methodology at normal temperature of 60^0C, pH 8 and less amount of adsorbent 0.6 g proved to be 100% efficient. As more contact time was provided more removal was observed .This technique is not only for the removal of lead but it is applicable for removal of other toxic elements like chromium. So different industrialist should apply this method for removal of toxic elements from industrial waste without any cost.

References:

1. B.M.W.P.K. Amarasinghe, and R.K. Williams. Tea waste as a low cost adsorbent for the removal of Cu and Pb from wastewater. Chemical Engineering Journal. 132. (1-3). 299-309. 2007

2. H. Benhima, M. Chiban, F.Sinan, P. Seta, M.Persin. Removal of lead and cadmium ions from aqueous solution by adsorption onto micro-particles of dry plants . Colloids and Surfaces B: Biointerfaces.61. (1).10-16. 2008

3. S. Bhattacharjee, S. Chakrabarty , S. Maity , S. Kar, P.Thakur, G. Bhattacharyya . Removal of lead from contaminated water bodies using sea nodule as an adsorbent . Water Research. 37. (16). 3954- 3966. 2003.

4. S. V. Dimitrova , D.R .Mehandgiev. Lead removal from aqueous solutions by granulated blast-furnace slag . Water Research. 32(11). 3289-3292. 1998.

5. O.J. Esalah, E.M. WeberVera, . Removal of lead from aqueous solutions by precipitation with sodium di-(n-octyl) phosphinate. Separation and Purification Technology. 18. (1).25-36. 2000.

6. V. K. Gupta, M. Gupta, S. Sharma . Process development for the removal of lead and chromium from aqueous solutions using red mud—an aluminium industry waste . Water Research. 35. (5).1125-1134. 2001.

7. A. S.H. Halim, A.M.A .Shehata, M.F. El-Shahat. Removal of lead ions from industrial waste water by different types of natural materials . Water Research. 37.(7).1678-1683. 2003.

8. E. Hautala , J. Randall, A. Goodban, A. Waiss Jr. Calcium carbonate in the removal of iron and lead from dilute waste water . Water Research. 11(2).243-245. 1977.

9. F. Hammy, G. Mercier, J.F. Blais . Removal of lead in APCR leachates from municipal solid waste incinerator using peat moss in a batch counter-current sorption process. Hydrometallurgy. 80. (4).232-240. 2005.

10. T. A. Ioannidis , A.I. Zouboulis . Selective removal of lead and bromide from a hazardous industrial solid waste using Limited Acid Demand and Separation Factor at ambient conditions . Journal of Hazardous Materials. 131. (1-3). 46-58. 2006.

11. F. Kaczala, M. Marques, W. Hogland. Lead and vanadium removal from a real industrial wastewater by gravitational settling/sedimentation and sorption onto Pinus sylvestris sawdust . Bioresource Technology.100(1). 235-243. 2009.

12. M. K. Mondal, Removal of Pb (II) ions from aqueous solution using activated tea waste: Adsorption on a fixed-bed column.. Journal of Environmental Management.90. (11).3266-3271. 2009.

13. A. S. Özcan, S. Tunali, T. Akar, A. Özcan. Biosorption of lead(II) ions onto waste biomass of Phaseolus vulgaris L.: estimation of the equilibrium, kinetic and thermodynamic parameters . Desalination. 244.(1-3). 188-198. 2009.

14. Y. Seida, Y. Nakano, Y. Nakamura . Rapid removal of dilute lead from water by Pyroaurite-like compound . Water Research. 35(10). 2341-2346. 2001.

15. s. K. R. Yadanaparthi, D. Graybill, R. Wandruszka. Adsorbents for the removal of arsenic, cadmium, and lead from contaminated waters. Journal of Hazardous Materials. 171. (1-3). 1-15. 2009.

Experimental study of bearing failure analysis at higher speed by simulating local defect on its races.

Abhay Utpat[1], R. B. Ingle[2], M. R. Nandgaonkar[3]
[1]SVERI's CO Engineering, Pandharpur (MH), India.
[2]Vishvakarma Institute. of Information Technology, Pune (MH),India.
[3]College of Engineering, Shivajinagar, Pune (MH) India.

Abstract – One of the most important causes of disastrous failure of machinery is failure of bearing because bearing is fundamental part of any rotary machine. Vibration signature analysis is one of the most effective tools for monitoring the condition of ball bearings. Best method to study the failure analysis of ball bearing is by creation of artificial cracks of different sizes on various elements and noting down its signatures. It takes long time for life test where healthy bearings are rotated till initialization of crack. Most of the techniques work satisfactorily in case of moderate operating speed. But at higher speed, problem arises. This paper highlights the study of crack detection technique at comparatively higher speed. Increase in amplitudes of vibration is observed with speed but with load, it almost remains same. A noticeable increase in the vibration amplitude is also observed with increase in defect size. However, outer ring defected bearings give better response than inner ring defected bearings at all the speeds. The effort has also been taken in measuring the vibrations of test bearings with defective support bearings. The effect of vibrations generated by defective support bearings is clearly observed in the spectra of test bearings.

Keywords: *Ball Bearing, Condition Monitoring, Vibration analysis, Defect frequency.*

1. Introduction

Single row deep groove ball bearings find wide applications in industrial sector. As bearing is very crucial part, its failure can cause huge failure of machinery. Life of the bearing depends upon construction variables like design, material and application variables like speed, load and lubrication. The construction of any antifriction bearing consists of many vital elements such as outer ring, inner ring and rolling element like ball or roller. Each element of bearing develops a unique characteristic vibration signature during rotation. Surface irregularity or defect in any of these elements can be detected in vibration spectra of bearing. These surface irregularities are either local or dispersed. Pits, cracks, voids are local defects and waviness, deformation are commonly observed dispersed defects in the bearing. By calculating typical characteristic defect frequencies associated with bearing elements, prediction of the defect is possible whether it is on outer ring, inner ring or on the ball. These defect frequencies depend upon the fundamental running speed of the shaft and bearing dimensions. To calculate these frequencies typical formulas has been developed by few researchers [1],[2]. These fundamental frequencies are excited when defect on one element strikes its mating element which results vibration of rotor bearing system. Measurements of these vibrations are either with time domain or frequency domain approach. The advantage of frequency domain approach is that it gives severity as well as location of the defect. The frequency domain approach is widely used for bearing defect detection. Choudhury and Tandon [2] carried out experimental work for co-relating vibration amplitudes with extent of defect on bearing elements. Variation in vibration amplitude with change in defect position and severity of the defect was observed during their study. In further study, Tandon et al [3] have measured the vibration amplitudes of bearing with contaminated grease. They found that the particles in the lubricant induce mechanical vibration and noise.

Vibration based technique for bearing fault detection was demonstrated theoretically by several researchers. McFadden and Smith [4],[5] have developed a theoretical model for simulating vibrations produced by a single point defect and multi point defect in rolling element bearings. Model incorporates the effect of bearing geometry, shaft speed, bearing load distribution, transfer function and the exponential decay of vibration. A comparison of predicted and measured demodulated vibration spectra confirms satisfactory performance of the model. Few other studies by Patil et al [6] have also confirmed the theoretical results after experimental verification. The model yields both frequency and the acceleration of vibration components of bearing. Igarashi and Hamada [7] have also developed bearing fault detection methodology based on vibration signals. Emphasis was also given on bearing fault diagnosis by application of sound technique and it was concluded that vibration analysis is best technique of diagnosis. Detailed literature on vibration based condition monitoring is given in a review paper by Tandon et al [8]. It was concluded that the distributed defects also has drawn the attention of few number of researchers.

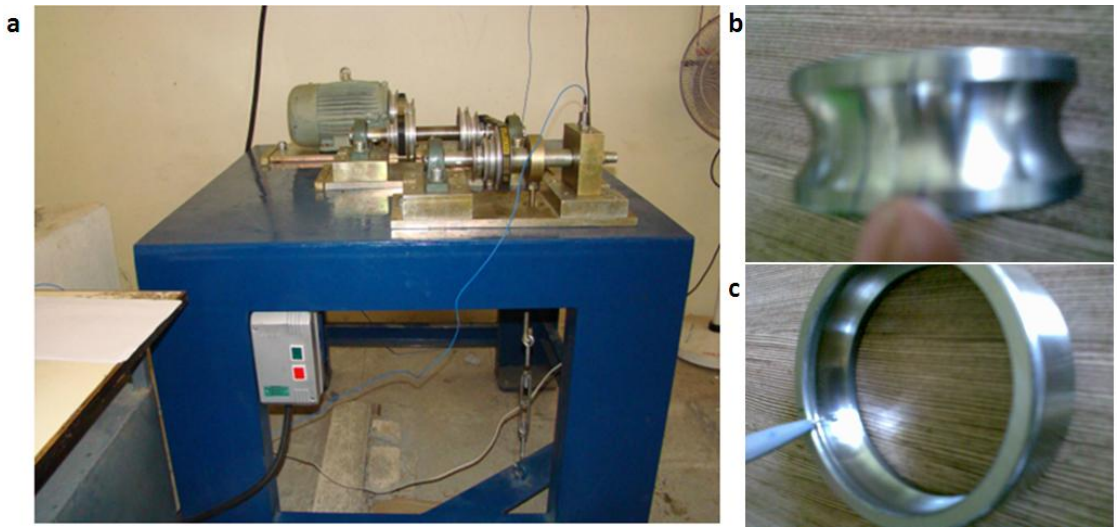

Fig 1-Experimental Setup a) A photograph of bearing test rig b)Defected inner ring c)Defected outer ring

Most of the work on bearing fault diagnosis was carried out by considering normal speed range of about 500 rpm to 1500 rpm. At this speed range and moderate bearing faults, most of the techniques work satisfactorily. However there are few applications where bearing operates at higher speed, typically above 5000 rpm and at low speed typically below 50 rpm. Few authors have considered these applications and discussed the problems during working. Kim et al [9] demonstrated Acoustic Emission (AE) based condition monitoring system at low speed of about 10 rpm. From various tests carried out for seeded faults, it was observed that RMS and entropy were best parameters for condition monitoring. However, in case of some faults, results were conflicting. Smith [10] has recorded some experimental observations of slightly damaged bearing at low to medium operating speed and compared the acceleration, shock pulse, acoustic emission and jerk measurements. In his study, inconsistent results were found with AE transducer at low speed. Apart from the study at low speed, the efforts have also been carried out by Sawalhi et al [11] by analyzing signals taken from a high-speed test rig, which contained a bearing with a spalled inner race. Authors present an algorithm to enhance diagnostic capability of spectral kurtosis as an analysis tool for rolling element bearings.

It is found from above review that there is a scope for study of bearing signature analysis at higher speed. The objective of present work is to undertake condition monitoring approach for ball bearings at higher speed. Vibration amplitudes of healthy bearings at characteristics defect frequencies are measured and used for comparison with vibration amplitudes of faulty bearings. The effect of vibrations of defective support bearings on the spectra of test bearing has also been studied during the present work.

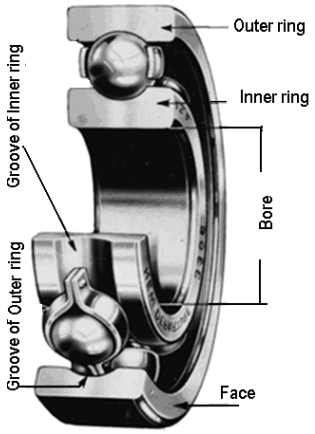

Fig 2:- Section of Ball bearing

2. Rotor Bearing System

For measuring the amplitudes of vibration at various speeds, the Test Rig designed is as shown in Fig-1. It consists of a shaft mounted on the support bearings. As explained in few literatures, the test bearing was mounted at free end of shaft with cantilever position. Such arrangement is rarely observed in actual working conditions. Hence to serve the actual working conditions, test bearings are mounted at simply supported position in the present work. A split type bearing housing is designed for mounting and dismounting ease of test bearing. Load is applied by tension rod through load cell. A 2000 N capacity load cell is used for load measurements.

Load applied on test bearing varies from 50N to 300N as per requirement. A special purpose bearing DFM 85 is used as test bearing which is single row deep groove ball bearing with contact angle zero and normally used in four wheeler engines. These are supplied by

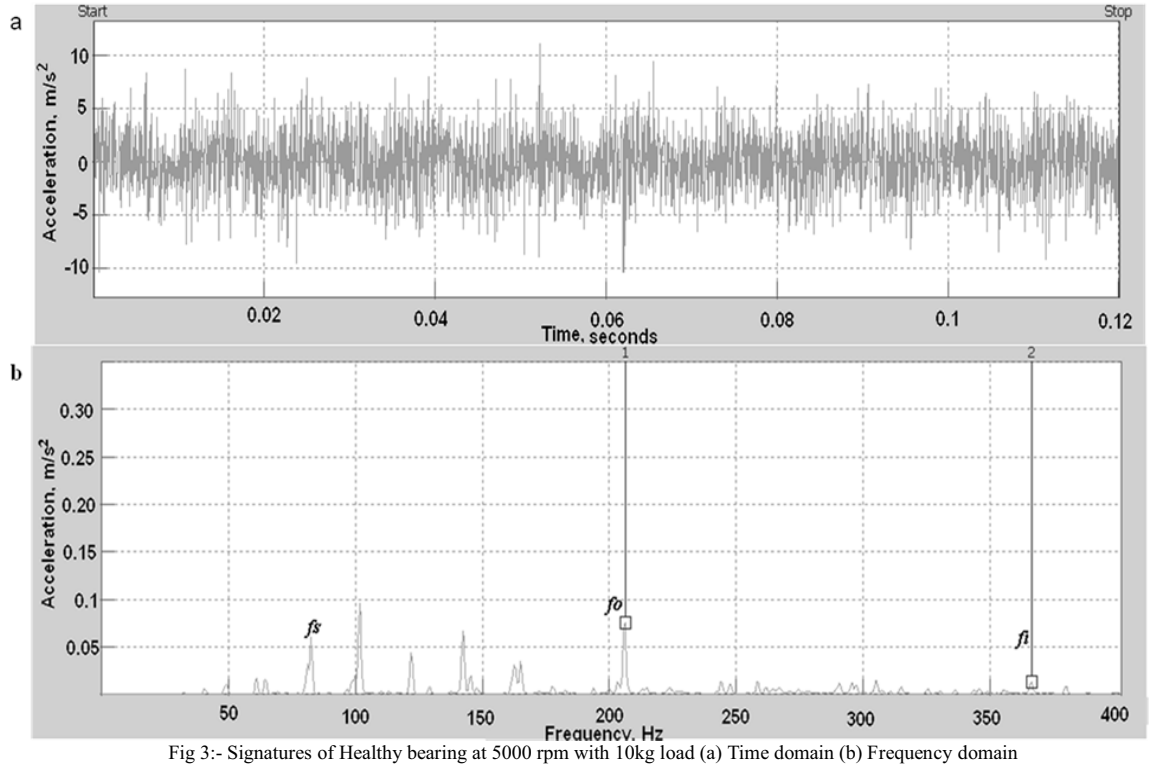

Fig 3:- Signatures of Healthy bearing at 5000 rpm with 10kg load (a) Time domain (b) Frequency domain

Research and Development center of DJR Deluxe Bearings Ltd, Pune. Ten test bearings are used in the same two are without defect (Healthy) and eight are defective with dent on various bearing elements. The test bearings have been prepared by creating an artificial defect of width 250 micron to 2000 micron on the outer ring and inner ring respectively.

During the experiments, outer ring of bearing is rigidly fixed in the housing and inner ring is revolving with shaft rotation frequency of f_s. With this frequency, the ball revolution frequency, f_b and cage rotation frequency ,f_c are calculated. If there is a defect on inner ring, it strikes the balls which are revolving at speed of f_c. But inner ring itself is revolving with shaft speed f_s. During the time bearing makes one complete revolution, the defect comes in to contact with certain number (Z) of balls. In case of defect on the outer ring, Z number of balls strikes the defect with cage speed of f_c. Hence the outer ring defect frequency is Z times the cage frequency. In case of defect on ball, both outer ring and inner ring comes in contact with the defect when ball completes one revolution.

Typical dimensions of the DFM-85 bearing have been measured for knowing the characteristic defect frequencies. These are; 30mm bore with 85 mm outer diameter, 61mm pitch circle diameter and seven balls with 17.463mm diameter each. Formulas for defect frequencies are as given in Appendix 1. Fig-2 shows cross section of ball bearing. For bearing geometry and different spindle speeds, important frequency components are f_s, f_o, f_i, f_c, f_b, & f_{bd}. The values for these defect frequencies at different spindle speeds are calculated by using the formulas given in appendix-1. All test bearings are mounted on the test rig one after other by applying equal amount of grease. Proper cleaning was carried out before application of grease to make them free from contaminants, if any. High frequency range accelerometer of 10 kHz capacity and sensitivity 97.5mV/g is mounted on the outer ring of test bearing which is connected to the monitor through FFT analyzer to record the signals.

3. Experimental Procedure

Measurements of amplitudes of vibration are carried out on the test rig which consists of shaft powered by 3-phase AC motor and gives output speed in the range of 1000 rpm to 5000 rpm. Single row deep groove ball bearing DFM 85 with 30mm bore is selected as test bearing for experimentation. Well lubricated deep groove ball bearings are used as support bearings. The effort has also been carried out in measuring the amplitudes of test bearing when support bearings are defective. A sampling rate of 25.6 kilo samples per second has been used during the measurements. The amplitudes of vibration are confirmed after measuring it for 3 to 5 times for the same speed and load. At every time, error of only 0.2 to 0.6 % was observed in amplitude levels. Sensor is mounted at the maximum position in the load zone that is at the top of bearing. The signals captured by accelerometer are then processed through data processing unit which is OROS made 4 channel FFT analyzer and converts time domain signals in to frequency domain.

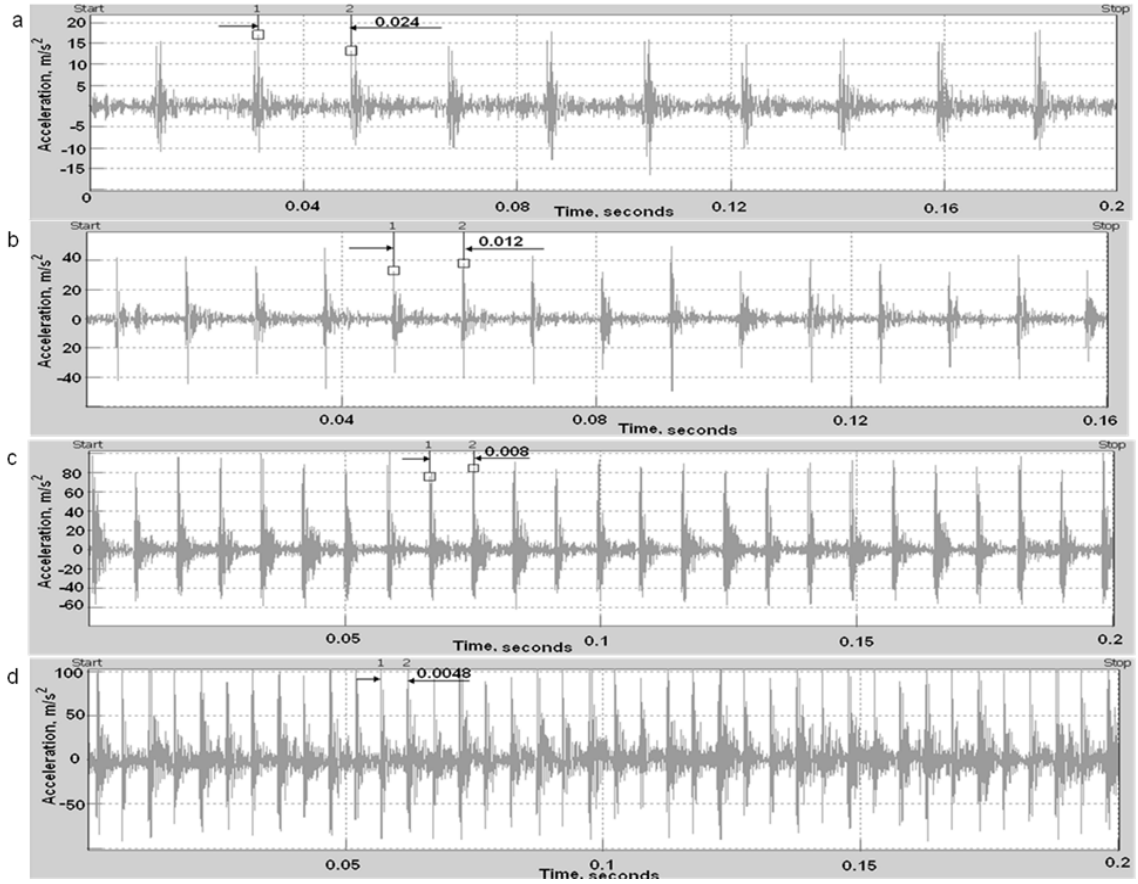

Fig.4 Acceleration vs Time for bearing with 1 mm defect on outer ring at 10 Kg load and speeds (a)1000rpm (b)2000rpm (c)3000rpm (d)5000rpm

3.1 Detection of fault in test bearings

Equal amount of grease is applied to all the test bearings before mounting them on the test rig. Signatures of healthy bearings are first recorded at different conditions of speed and load. Defect is stationary with respect to shaft in case of outer ring defected bearings and hence they are mounted in such a way that the location of defect remains always at maximum position in the load zone. Variation in amplitudes of vibration is observed by shifting the defect location in the load zone. Impulses are obtained at ball pass frequency of outer race (BPFO) which is also called as outer ring defect frequency. In case of inner ring defected bearings, defect rotates with the shaft and impulses are observed at ball pass frequency of inner race (BPFI) that is inner ring defect frequency.

Vibration signature spectra of defected bearings show number of peaks. The peaks at interested frequencies are marked and used for the comparison.

4. Results and discussion

Acceleration amplitudes of DFM 85 bearings recorded at various speeds and loads are plotted and results are discussed. Signatures of healthy bearings are recorded at different speeds and results are then used for comparison with defected bearings. Typical time and frequency plot for healthy bearing at 5000rpm with 10 Kg load is as depicted in Fig 3. Corresponding characteristic defect frequencies for outer ring (*fo*) and inner ring (*fi*) are located at 208Hz and 365Hz respectively. At these frequencies, vibration amplitudes are very less and used for comparison with defective bearings. Typical amplitude versus time graph at various speeds for 1mm defect size on outer ring is as shown in Fig 4. The amplitudes of vibration increases with speed for healthy as well as defected bearings. Impulses are obtained at interval of 1/*fo* for all the speeds as shown in Fig 4. Fig 5 depicts amplitude versus frequency curve for one of the outer ring defected bearings at 3000 rpm with 10 kg load. Strong peaks at ball pass frequency of outer ring (*fo*) that is 124.915 Hz

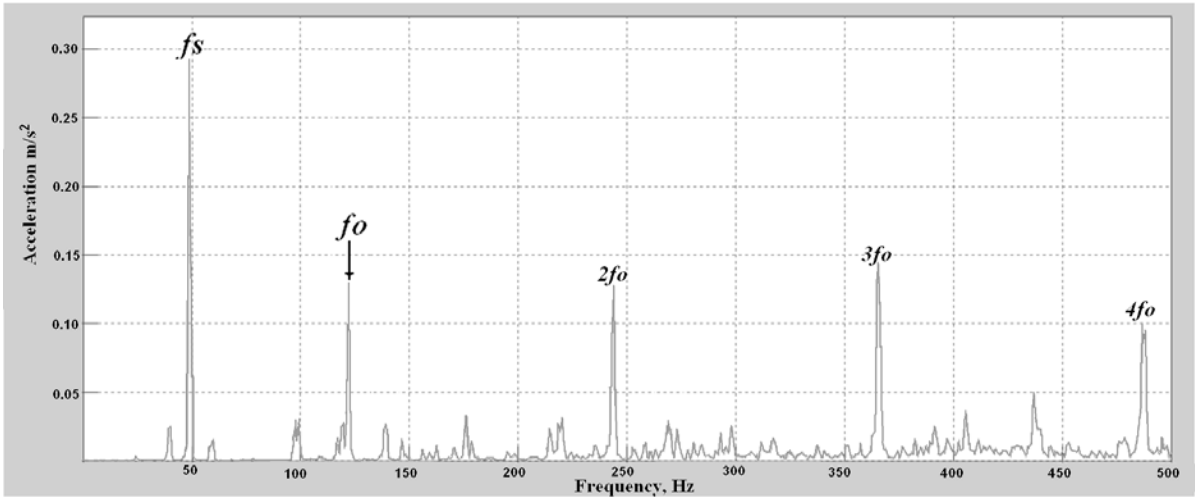

Fig5:- Signatures of bearing with defect of 1mm on outer ring at 3000 rpm and 10kg load

and its harmonics (*2fo, 3fo* and *4fo*) are clearly observed. At the same time number peaks are also observed corresponding to *fo+fs, fo-fs, 2fo+fs, 3fo+fs* etc at 5000 rpm which is explained in the last part of experimentation as shown in Fig 11a. Noise level at higher speed is slightly more than at lower speed. The signatures of outer ring defected bearings for all defect sizes are obtained at all the speeds.

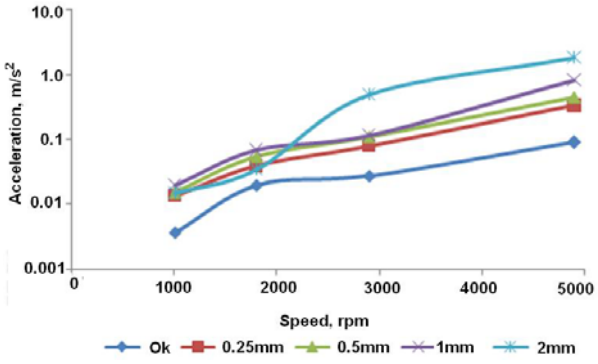

Fig 6:- Acceleration amplitudes of outer ring defected bearings with respect to Speed and at 10kg load.

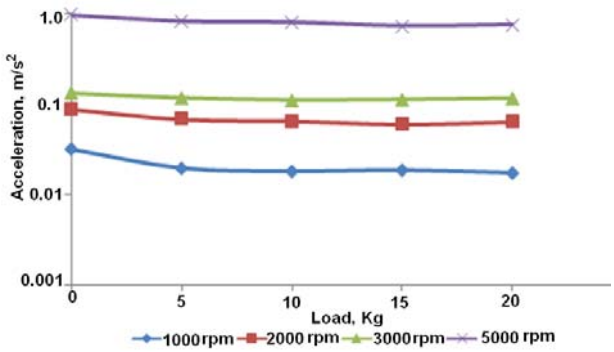

Fig 7:- Acceleration amplitudes of outer ring defected bearings with respect to Load at defect size of 1mm on outer race.

Fig 6a gives amplitude versus speed graph for different defect sizes on outer ring. Increase in amplitudes of vibration with defect size is clearly noted. Bearing with maximum defect size gives good response at higher speed than at lower speed.

Fig 6b depicts amplitude versus load plot for various speeds and at constant defect size. Very small variations in vibration amplitude are observed with increase in load for all the speeds. This is because load damps the vibrations.

Signatures of bearing with various defect sizes on inner ring are also noted at different speeds and different loads. Amplitude versus frequency response for one of such bearings with 1mm defect on inner ring is as shown in Fig 7a and 7b at 3000 rpm and 5000 rpm respectively. Inner ring defected bearings also show the harmonic peaks. Fig 7a shows peaks at shaft rotation frequency (*fs*), BPFI (*fi*) and other frequencies such as *fi + fs, fi –fs, fi- 2fs, 2fi* etc. Whereas Fig 7b shows two strong peaks one at shaft rotation frequency (*fs*) and other at BPFI (*fi*).

Fig 8 is plotted by recording the signatures of inner ring defected bearings at speed range of 1000rpm to 5000rpm. After comparing the frequency response curves it is noted that outer ring defected bearings give better response than inner ring defected bearings for the same speed and defect size. Amplitude versus frequency plot for the bearings with 1mm defect on outer and inner ring is as depicted in Fig 9. In this case 'ok*fo*' and 'ok*fi*' curves are obtained by noting the amplitudes at defect frequencies (BPFO and BPFI) from the signatures of healthy (ok) bearing (Fig 3b). It is observed that amplitude of vibrations for outer ring defected bearing (od_3) and inner ring defected bearing (id_3) is almost same at low speed. But at higher speed, higher level of amplitude is observed for outer ring defected bearing. It can also be cleared from Fig 10 that in both the cases vibration amplitude increases with the defect size.

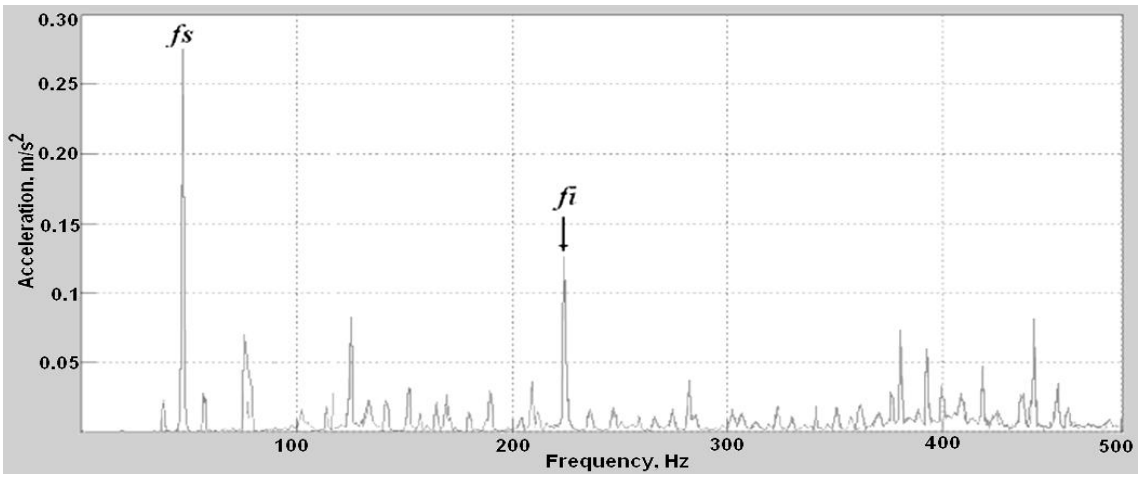

Fig 8:- Signatures of bearing with defect of 1mm on inner ring with 10 kg load at 3000 rpm.

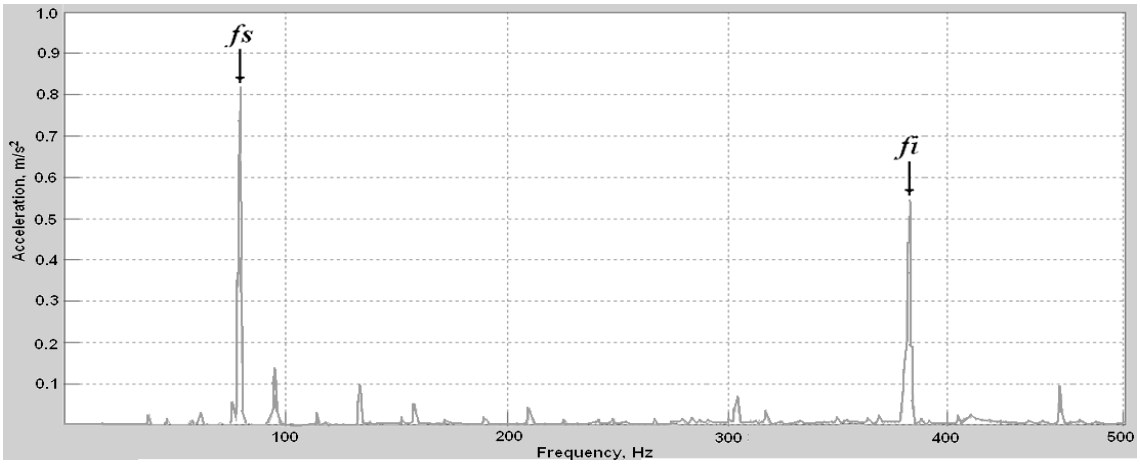

Fig 9:-Signatures of bearing with defect of 1mm on inner ring with 10 kg load at 5000 rpm

In the first phase of experimentation, all the test bearings have been tested when support bearings are working smoothly without generating vibrations. In later part of experimentation, one of the support bearing is replaced by defective bearing and signatures are noted. Slight increase in the noise level is observed in the spectrum of test bearing when support bearings are generating the vibrations. This effect is observed in the spectra of outer ring defected bearing at different conditions as shown in Fig 11. It is clear that there is negligible change in the peak amplitude at characteristic defect frequency (208 Hz in this case) of test bearing. But due to defective support bearings, effect on amplitudes at shaft rotation frequency is noted. Some other peaks are also pointed out in figure which shows increase in the noise level. This is because defective support bearings cause some misalignment in the output shaft and hence show peaks around shaft rotation frequency.

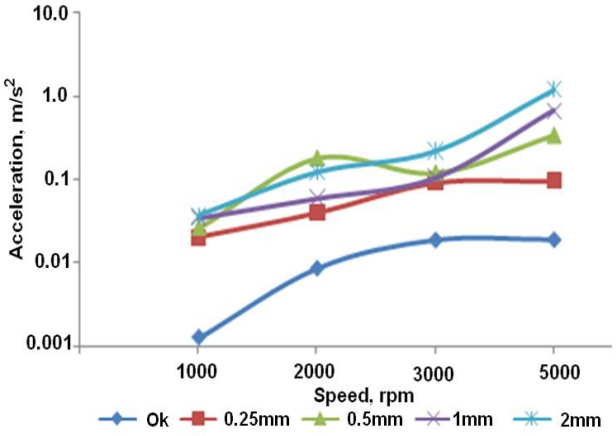

Fig 10:- Amplitudes of inner ring defected bearings With respect to Speed at 10kg load.

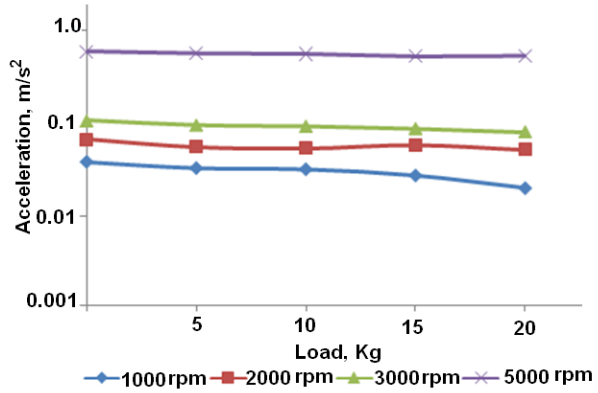

Fig 11:- Amplitudes of inner ring defected bearings with respect to Load at defect size of 1mm on inner race.

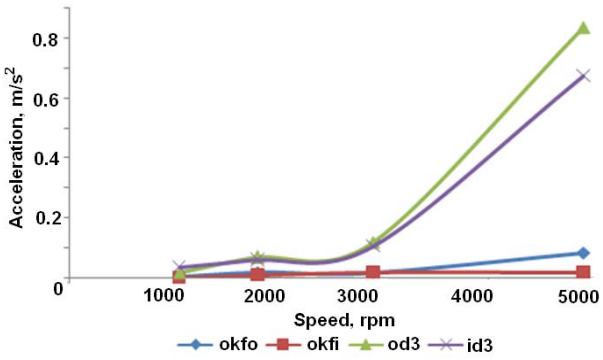

Fig 12:- Amplitude vs speed at constant defect size (1mm) and 10kg load.

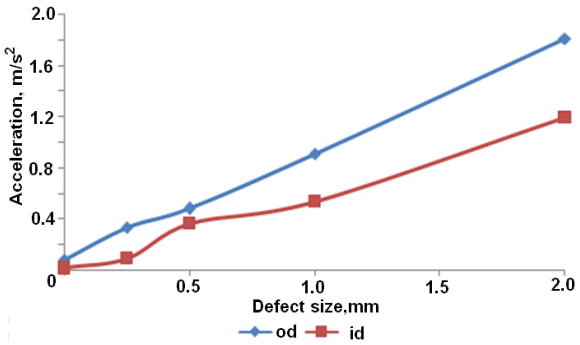

Fig 13:-Amplitude vs defect size at 5000rpm speed and 10kg load.

5. Conclusion

Attempt has been made in the present work to monitor the vibration response characteristics of ball bearing working at higher speed. Vibration acceleration signals have been measured in the frequency range 25Hz to 1 kHz. Failure is predicted by correlating peaks at characteristic defect frequencies with corresponding defects. Vibration measurement can be made by time as well as frequency domain, but the advantage of frequency domain is that it can detect the location of defect. Following conclusions are made from the present work;

a) Amplitudes of vibration in healthy as well as defective bearings increase with increase in speed whereas amplitude levels are not showing far variation with increase in load at the same speed.

b) Bearing with outer ring defect gives good response at all the speeds and for all the defect sizes than that of inner ring defected bearing. At the same time bearing with large defect size gives good response at higher speed than lower speed.

c) For the same defect size, outer ring defected bearing gives higher vibration amplitudes than inner ring defected bearing at constant speed and load.

d) In case of inner ring defected bearing, as defect is rotating, the peaks are not observed at exact values of defect frequencies. They are deviating by 5Hz to 8 Hz because actual speed of rotation is slightly varying than theoretical speed at which defect frequencies are calculated.

e) When support bearings are defective or generating the vibrations, spectra of test bearing shows number of peaks around the shaft rotation frequency. This is because of increase in the level of noise due to jerk produced by defective support bearing on output shaft.

The scope of this work is limited only up to response of vibrations due to local defects on bearing races. Study of response of vibrations due to defect on ball is not covered in the present work. Rolling element such as ball not only rotates about races but also spins about its own axis. Hence defect on the ball may not always in between ball and races. Thus it is difficult to record the signatures at higher speed. However, it may be possible to record the signals of ball defected bearings at comparatively lower speed.

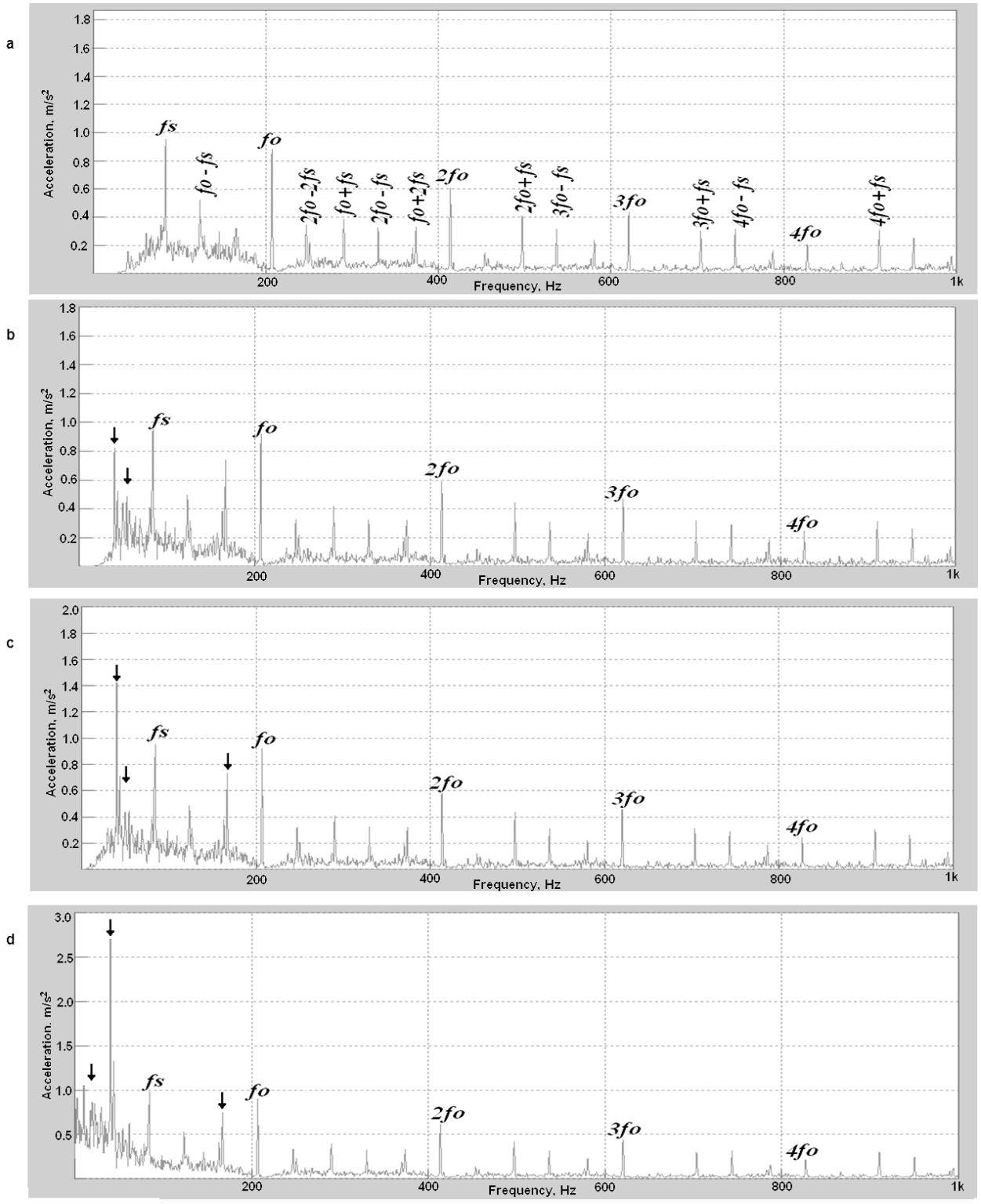

Fig 14:- Bearing with defect of 1mm on outer ring at 5000 rpm and 10 kg load when,
a) Support bearings are Healthy b) Left support bearing defective c) Right support bearing defective d) Both bearings defective.

Appendix-1

TABLE I
BEARING CHARACTERISTICS DEFECT FREQUENCIES [2]

Bearing Defect Frequency	*Equations*
Ball Revolution Frequency	$f_b = \frac{Df_s}{2d}\left[1-\frac{d^2}{D^2}\cos^2\alpha\right]$
Cage Rotation Frequency	$f_c = \frac{f_s}{2}\left[1-\frac{d}{D}\cos\alpha\right]$
Outer ring Defect Frequency	$f_o = \frac{Zf_s}{2}\left[1-\frac{d}{D}\cos\alpha\right]$
Inner ring Defect Frequency	$f_i = \frac{Zf_s}{2}\left[1+\frac{d}{D}\cos\alpha\right]$
Ball Defect frequency	$f_{bd} = \frac{Df_s}{d}\left[1-\frac{d^2}{D^2}\cos\alpha\right]$

Acknowledgements

The authors would like to acknowledge the DJR Deluxe Bearings Ltd, Pune (India) for providing the test bearing samples required for the experimentation. The gratitude is also extended to Dr. S. G Joshi, Sangli (India) for his valuable guidance during this work.

References

[1] Harris T.A., **Rolling Bearing Analysis** ,4th Edition, John Wiley pub ltd, New York, 2001.

[2] A Choudhury, N.Tandon, Vibration Response of Rolling Element Bearings in a Rotor Bearing System to a Local Defect Under Radial Load, **Jr of Tribology***, 128,* 253-258, 2006.

[3] N. Tandon, K.M. Ramakrishna, G.S. Yadav, Condition Monitoring of Electric Motor Ball Bearing For the Detection of Grease Contaminants, **Tribology International,***40,*29–36,2007.

[4] P. D. Mcfadden , J. D. Smith, Model for the Vibration Produced by a Single Point Defect in a rolling Element Bearing, **Jr of Sound and Vibration**, 96-1 69-82,1984.

[5] P D. Mcfadden, J. D. Smith, The Vibration Produced By Multiple Point Defects in a Rolling Element Bearing, **Journal of Sound And Vibration,** *98-2,* 263-273,1985.

[6] M.S. Patil , Jose Mathew , P.K.Rajendrakumar , Sandeep Desai ,A theoretical model to predict the effect of localized defect on vibrations associated with ball bearing, **Journal of mechanical Science** *(In press).*

[7] Igarashi, H Hamada, Studies on the vibration and sound of defective rolling bearings ,first report vibration of ball bearings with one defect, **Bulletin of the Japan Soc. of Mech. Engg**.*25*, 994- 1001, 1982.

[8] N. Tandon , A. Choudhury, A review of vibration and acoustic measurement methods for the detection of defects in rolling element bearings**, Tribology International** *32,* 469–480,1999.

[9] Eric Y. Kim, Andy C. C. Tan , Bo-Suk Yang, Vladis kosse1, Experimental Study on Condition Monitoring of Low Speed Bearings: Time Domain Analysis**, 5th Australasian Congress on Applied Mechanics, ACAM, Brisbane,** Australia, Dec- 2007.

[10] J D Smith, Vibration monitoring of bearings at low speeds, **Tribology International.** 139-144, 1982.

[11] N. Sawalhi, R.B. Randall, H. Endo, The enhancement of fault detection and diagnosis in rolling element bearings using minimum entropy deconvolution combined with spectral kurtosis, **Mechanical Systems and Signal Processing** , *21*,2616–2633, 2007.

Assessment Instrument for Software Process Improvement (AISPI): A CASE Tool

Altaf Hussain[1] and Rashid Ahmad[2]
Department of Computer Engineering, EME, NUST, Pakistan

Abstract - To compete in the international market, there is a need to improve both the quality of our software products and our ability to deliver the product within time and budget. These improvements depend strongly on process as well as on technology. Software Process Improvement (SPI) is an ongoing effort as process keeps evolving over time. The current problem with SPI is not a lack of standard or model, but rather a lack of an effective strategy to implement these standards or models. SPI implementation being a complex process in its own right and so the organizations should determine their SPI implementation maturity through an organized set of activities. Niazi et al suggested SPI implementation maturity model that has the potential to help companies assess and improve their SPI implementation processes. This paper introduces an assessment instrument in the shape of a Computer-Aided Software Engineering (CASE) tool to the software industry so that the organizations can evaluate their SPI status.

Key words: Software Process Improvement (SPI), Capability Maturity Model Integration (CMMI), Critical Success Factor (CSF), Critical Barrier, Assessment Instrument, CASE Tool

1. Introduction

Problems associated with software quality are widely acknowledged to affect the development cost and time [1]. The Standish Group's just-released report, "CHAOS Summary 2009," which reported that this year's results showed a marked decrease in project success rates, with 32% of all projects succeeding which are delivered on time, on budget, with required features and functions. Further it said 44% were challenged which are late, over budget, and/or with less than the required features and functions and 24% failed which were cancelled prior to completion or delivered and never used. These numbers show a downward trend in the success rates from the previous study, as well as a significant increase in the number of failures, says Jim Crear, chairman of Standish Group. These results show the highest failure rate in over a decade [2].

A study, conducted at Royal Academy of Engineering and British Computer Society, shows that despite spending 22.6 billion pounds on IT projects in UK during 2003-2004, significant numbers of projects still fail to deliver key benefits on time and to target cost and specification [3].
There have been increasing calls for the software industry to find solutions to software quality problems [4]. Software organizations are realizing that one of their fundamental problems is to have an effective software development process [5]. In order to have an effective software development process in place different methods have been developed, of which Software Process Improvement (SPI) is the one, mostly used.

Surviving in the increasingly competitive software business requires more than hiring smart, knowledgeable software engineers and buying the latest development tools. Effective software development processes are also needed, so that skilled workforce can use the best technical and managerial practices to successfully complete their projects within allotted time and budget. More organizations are looking at software process improvement as a mean to improve the quality, productivity, and predictability of their software development, acquisition, and maintenance efforts [6].

Different models and standards have been developed in order to improve software processes. The Capability Maturity Model (CMM) is developed by Software Engineering Institute (SEI) at Carnegie Mellon University, USA to improve organizations' software processes. The Capability Maturity Model Integration (CMMI) [7] is the latest SPI model from the SEI. SPICE is a set of international standards for software process assessment [8]. SPICE is intended to harmonize different approaches to software process assessment and provides an approach that encourages self-assessment. The ISO 9000 series of standards [9] were developed with the intent of creating a set of common standards for quality management and quality assurance.

Different advances have been made in the development of software process improvement (SPI) standards and models,

e.g. capability maturity model (CMM), more recently CMMI, and ISO's SPICE. However, these advances have not been matched by similar advances in the adoption of these standards and models in software development which has limited success for many SPI efforts. The current problem with SPI is not a lack of standard or model, but rather a lack of an effective strategy to successfully implement these standards or models. Another problem with SPI is that researchers do suggest solutions but most of these solutions remain in theoretical form and the industry can not benefit from these solutions.

In [10] authors have proposed a maturity model for SPI implementation that has the potential to help companies assess and improve their SPI implementation processes. Specifically, they have adopted CMMI approach and developed a maturity model to guide organizations in assessing and improving their SPI implementation processes. Our work is influenced by their work and in fact we have physically implemented their work by developing a software tool for this model.

2. Maturity Model Implemented by AISPI CASE Tool

The CASE tool presented in this paper uses the assessment dimension of maturity model for SPI presented in [10]. This model is extracted from Capability Maturity Model Integration (CMMI) and is based on critical success factors (CSFs) and critical barriers identified through literature and an empirical study. This model has three dimensions; Stage Dimension, Critical Success Factor (CSF) Dimension, and Assessment Dimension. Stage dimension comprises of four maturity levels; initial, aware, defined and optimizing. CMMI consists of process areas (PAs) categorized across five maturity levels but authors in [10] believe that successful SPI implementation process should be viewed in terms of CSFs rather than PAs. For this reason a set of CSFs and critical barriers for all these levels has been defined in CSF dimension. The PAs of CMMI are split into four categories [7]. In this model, CSFs and critical barriers are categorized into three i.e. Awareness, Organizational and Support. This distribution is show in table 01 (adapted from [10]).

These factors are not necessarily mutually exclusive and there may be a certain degree of overlap among them. The awareness category is directly linked to Maturity Level-2 i.e. Aware of the maturity model. While organizational is directly linked to maturity level-03 i.e. defined where the focus is on the systematic definition of SPI implementation process. Similarly support is linked to maturity level-04 i.e. optimizing where focus is completely on continuous improvement. To achieve a specific maturity level its factor category as well as its earlier maturity level category must be implemented in the practice of considerable organization. So the current factor category for implementation is called "Front-End-Category" and the previously implemented category is called "Back-End-Category". This factor categorization is shows in table 02 (adapted from [10]):

Table 1: Factors Categorization

Category	***CSFs & Critical Barriers***
Awareness	SPI Awareness, Staff involvement, Training and monitoring, Senior management commitment
Organizational	Time pressure, Lack of support, Experienced staff, Formal methodology, Organizational politics, Staff time and resources, Creating process action team
Support	Review

Table 2: CSFs Dimension

Maturity	***Front End Category***	***Back End Category***
4 – Optimizing	Support	Organizational, Awareness
3 – Defined	Organizational	Awareness
2 – Aware	Awareness	
1 – Initial		

In assessment dimension each of the CSF and critical barrier is measured in order to assess how well the factor has been implemented in practice of that organization. In order to resolve the conflict of different stakeholder's evaluation standards of same factor, an already tested instrument at Motorola [11] i.e. the Motorola instrument has been used in assessment dimension. For each CSF and critical barrier five practices has been identified through literature review and empirical study [10]. These practices of each CSF and critical barriers are measured using following three dimensions of Motorola instrument shown in Appendix-A.

1. Approach: Organization commitment and management support for the practice as well as the organization's ability to implement the practice.
2. Deployment: The breadth and consistency of practice implementation across project areas.
3. Results: The breadth and consistency of positive results over time across project areas.

In addition, following are the steps adopted for the assessment of SPI implementation through maturity model [10].

Step-01: All the CSF and critical barriers are being assigned to the concerned stakeholder within the company.
Step-02: For each practice of CSF and critical barriers, the concerned stakeholder will calculate the above three dimensions scores of Motorola instrument shown in Appendix-A.
Step-03: Three dimensional score is averaged to find the score of specified practice of a CSF or critical barrier.
Step-04: At length the score of each CSF or critical barrier is being found by averaging the score of its all practices.
Step-05: Repeat this procedure for each CSF and critical barriers. Add together the score of each practice and average it to gain an overall score for each CSF and critical barrier.
Step-06: For achieving a maturity level, all the CSFs and critical barriers of that maturity level must have average score equal to 7 or above [10, 11]. For example to achieve level-02-Aware of maturity model for SPI, all CSFs and critical barriers of this level must have score equal or higher than 7. Any CSF or critical barrier average score that falls below 7 is considered a weakness [10, 11].
Keeping in view this assessment procedure using Motorola instrument, we developed this AISPI CASE tool to guide the software companies about their weaknesses in SPI implementation.

3. AISPI Design and Architecture

UML diagrams describe the various aspects and uses of an application before starting coding, to ensure that everything is covered. Millions of programmers in all languages have found UML to be an invaluable asset to their craft [12]. Figure 1 shows the use case diagram for AISPI representing the all behaviors of this instrument and interacting actors. This use case diagram shows two different actors of AISPI; one is project manager of the company and other is the stakeholders of that company. Activity diagram is designed to be a simplified look at what happens during an operation or a process of a system. It's like a flowchart that shows steps (called activities) as well as decision points and branches [12]. It is an integral part of system analysis. Figure 2 shows the activity diagram of AISPI that shows the sequence of all activities being executed by this instrument.

Similarly, figure 3 shows the relational data model of AISPI showing all tables and relationships among them for maintaining data requirement of this instrument.

4. CASE Tool Demonstration

AISPI is a CASE Tool that has a web based GUI that is very simple and easy to use. The user of this instrument may be the project manager of a software company who wants to assess the practices and software processes of his/her own company. Initially, project manager has to register his/her company using interface shown in Figure 4. Similarly using Figure 4, project manger has to define some stakeholders involved in those software processes that are to be evaluated using AISPI CASE Tool. Therefore, project manager has to assign the factors of maturity model for SPI to these concerned stakeholders using interface shown in Figure 5. This provides an interface to project manager to assign factors to stakeholders or revoke an already assigned factor to stakeholder. In this interface there is a combo-box that contains all the defined stakeholders and two list-boxes to display the unassigned factors and assigned factors to the stakeholder selected in the combo-box. If project manger needs to define a new stakeholder or wants to drop an existing one, then he/she can do it using interface shown in Figure 6. In case of dropping a stakeholder, all assigned factors to him/her will be free and these can be assigned to another stakeholder by project manger.

Each stakeholder is required to evaluate their assigned factors using their login. Being login to instrument user can evaluate all the practices of their assigned factors regarding three dimensions of Motorola instrument using the interface shows like Figure 8. Figure 8 provides a simple and user friendly interface to stakeholders to evaluate their factors without having any knowledge of maturity model for SPI or its assessment process. It contains three combo-boxes at the top; first on top-left for displaying his/her assigned factors by project manager, second on top-right for displaying three dimensions (Approach, Deployment, Results) of Motorola instrument, and third below these two combo-boxes for displaying all practices of his/her assigned factor selected in top-left combo-box. Below these combo-boxes there is series of TRUE/FALSE questions from Motorola instrument depending upon the dimension (Approach, Deployment, Results) selected in top-right combo-box. All these questions are the key activities shown in Motorola instrument shown in Appendix-A. These key activities are divided in three dimensions in Motorola instrument and each key activity is given a score between 1 and 10. In the evaluation of a CSF or critical barrier, stakeholder will have to reply in TRUE/FALSE to all questions (key activities of Motorola instrument) of these three dimensions for all of its practices. Simply, stakeholder has to do the following for each practice:

- Select "Approach" dimension in top-right combo-box. By this all true/false questions of this dimension along-with true/false combo-box will be displayed.
- Select the desired practice of CSF or critical barrier and reply all these questions by simply selecting TRUE or FALSE from concerned combo-box and click on button at bottom with title EVALUATE.
- Repeat this procedure twice for the same practice; one for answering TRUE/FALSE questions of "Deployment" dimension and other for that of "Result" dimension.
- Following these three steps, this practice is evaluated completely.

Stakeholder must have to evaluate all of his/her assigned CSF or critical barriers by repeating the above procedure for all of its practices. Moreover, stakeholder can get guidance for evaluation process using a link "Guidance for Company Evaluation" on the same interface in Figure 8. Stakeholder can check the score of each practice of the assessed factors as shown in figure 7. This interface has a combo-box and grid, combo-box for factors and grid for its related practices, to show the evaluated score of selected factor and its all practices. This interface shows the weak areas of concerned company as respective practices have low score.

After evaluating all assigned factors by concerned stakeholders, this instrument will automatically determine the maturity level of this company in the form of a complete assessment report. This assessment report comprises of company maturity level, maturity level description, all factors and its practices' score that clearly show the weaknesses and strengths of the company. Figure 9 shows this assessment report.

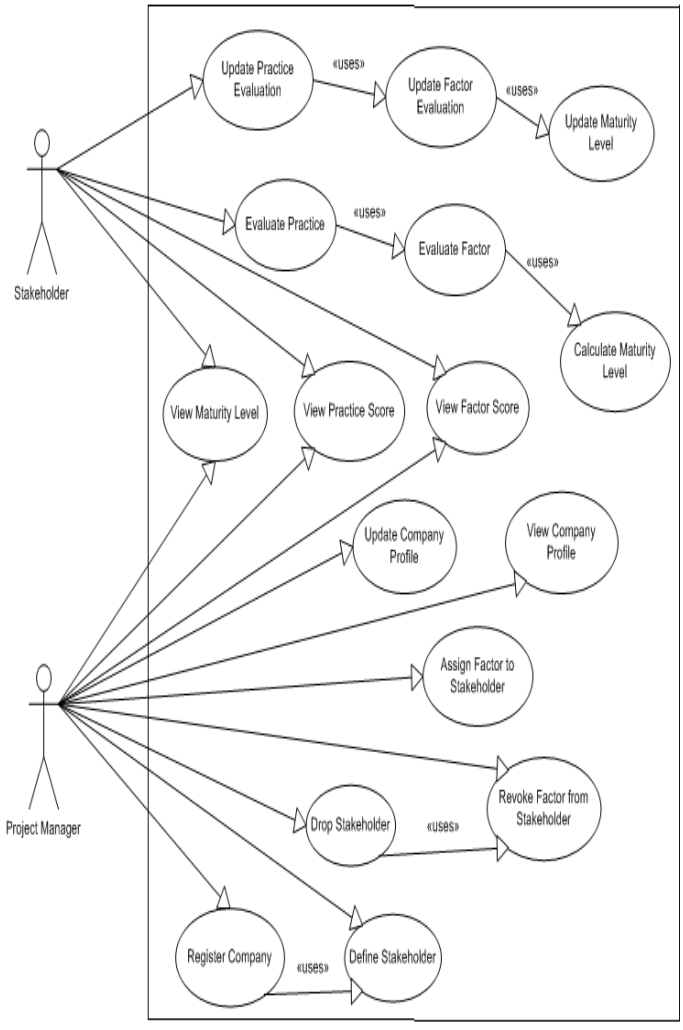

Figure 1: Use Case Diagram

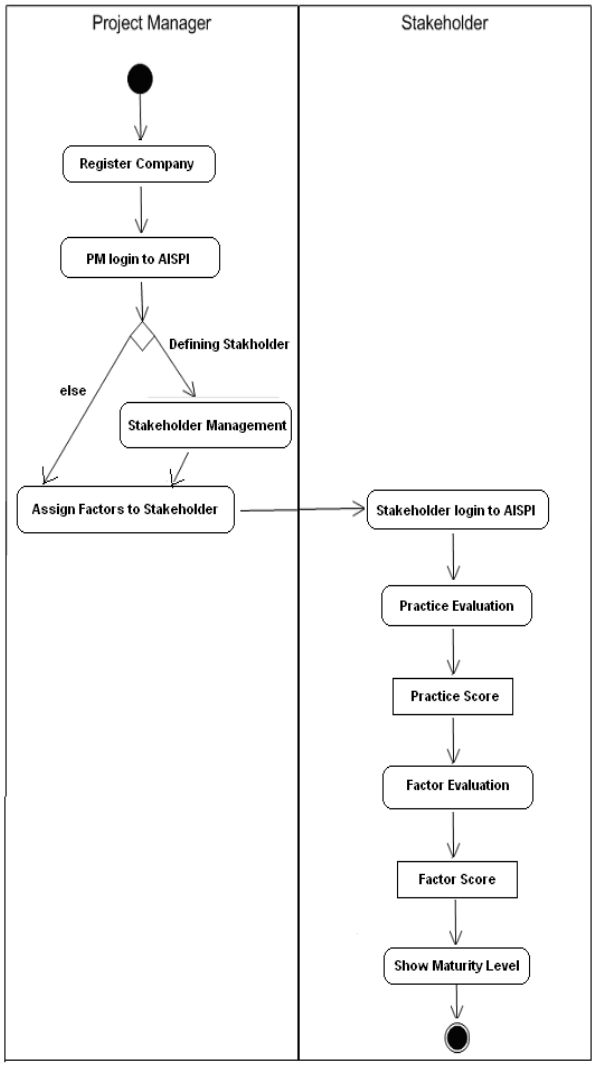

Figure 2: Activity Diagram

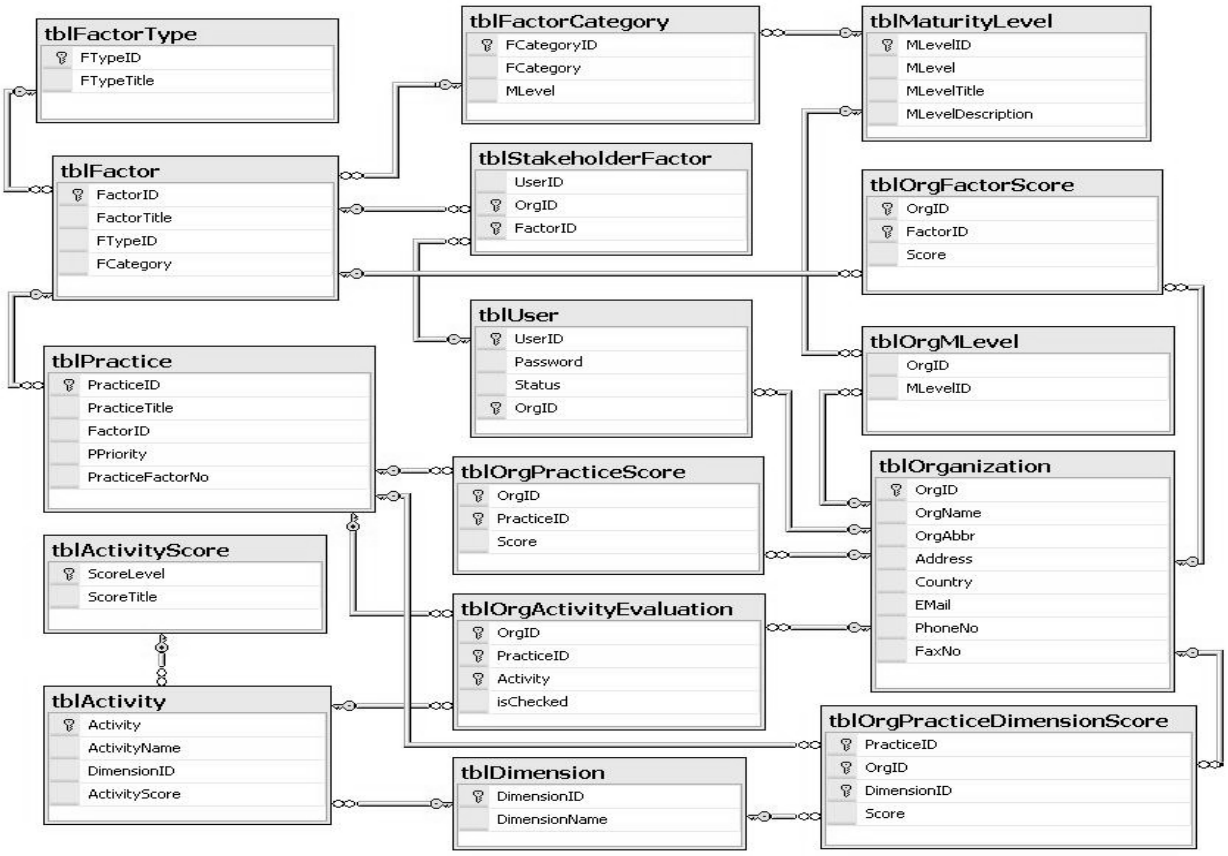

Figure 3: AISPI Relational Data Model

Figure 4: Company Registration

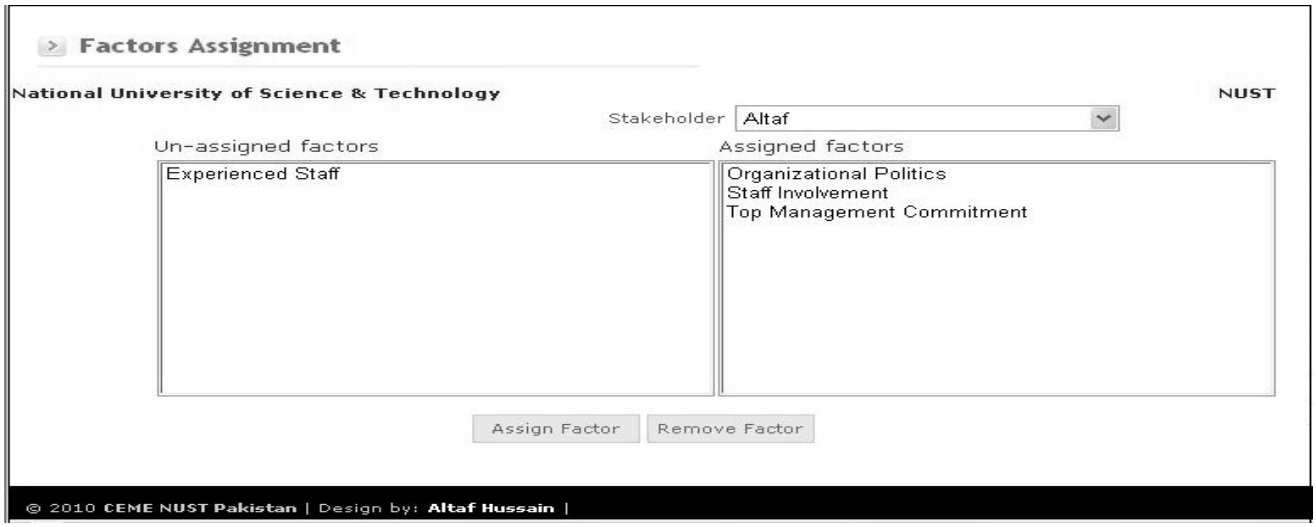

Figure 5: Factors Assignment to Stakeholders

Figure 6: Stakeholder Management

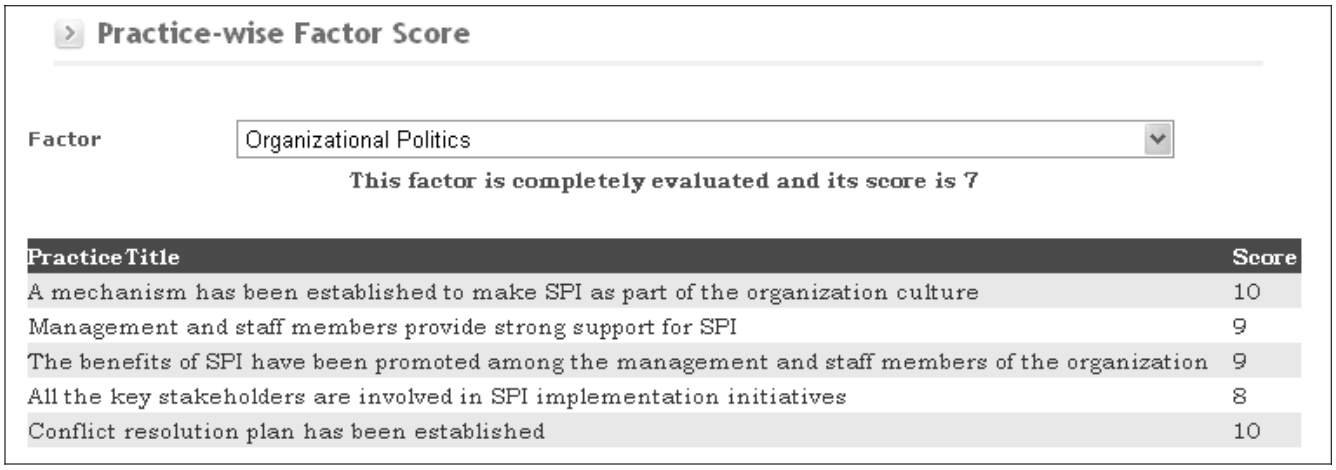

Practice Title	Score
A mechanism has been established to make SPI as part of the organization culture	10
Management and staff members provide strong support for SPI	9
The benefits of SPI have been promoted among the management and staff members of the organization	9
All the key stakeholders are involved in SPI implementation initiatives	8
Conflict resolution plan has been established	10

Figure 7: Practice-wise score of each factor

Figure 8: Factors evaluation

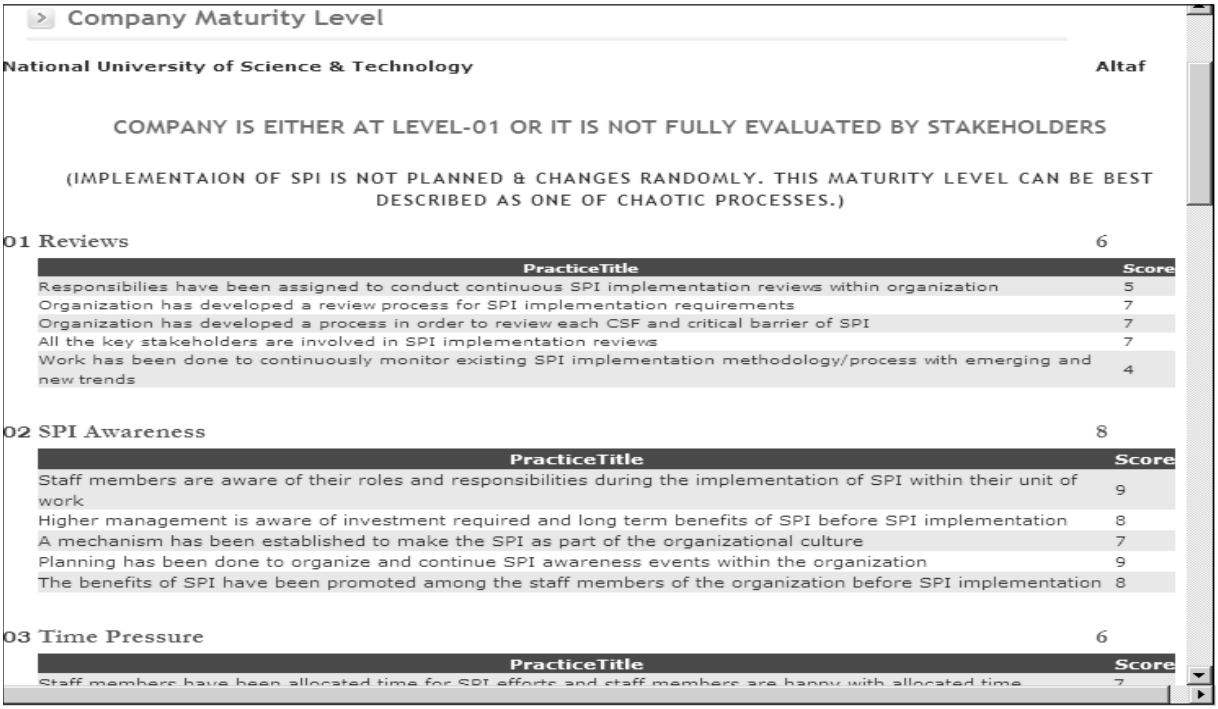

Figure 9: Company evaluation report (comprising of 12 factors and related practices)

5. Conclusion

In this paper, the assessment dimension of maturity model [10] is used to develop AISPI CASE tool. This tool uses a simple and user friendly web based interface. This tool is very useful for the software companies and enables its project manager to first register his/her company and initially define about four stakeholders keeping in view the factors being mentioned in maturity model for the assessment of their company processes. Then, project manager has to assign the concerned factors to these stakeholders and they have to evaluate all practices of their assigned factors using Motorola Instrument. After evaluating all factors, CASE tool provides the stakeholders with current SPI status of their company and suggests them improvements in the form of mentioning factors faintly implemented in practice of their organization. This tool provides the final assessment report to stakeholder showing the maturity level of their company and status of all factors along with their defined practices. As exactly five practices are suggested in this model [10] for achieving a specific CSF, so the score of each of these practices evaluated by stakeholders shows that how well that practice is implemented and either need any improvement or not. Therefore, considering this report, the practitioners involved in the weakly implemented processes in the company, highlighted by assessment instrument, can be guided accordingly by the project manager.

Acknowledgments

The authors would like to give deep appreciation to Dr. Mehmood Niazi, lecturer in SE at Keele University UK, for providing assistance and sharing his knowledge and experiences about designing maturity model. It helped us in the implementation of presented AISPI CASE tool.

References

[1] Sommerville, I.: Software Engineering Fifth Edition. Addison-Wesley.(1996).

[2] The Standish Group's Report, "CHAOS Summary 2009".

[3] "The Challenges of Complex IT Projects", A report by a working group from The Royal Academy of Engineering and The British Computer Society. ISBN 1-903496-15-2 (2004)

[4] Crosby, P.: Philip Crosby's reflections on quality. McGraw-Hill.(1996)

[5] Pitterman, B.: Telcordia Technologies: The journey to high maturity, IEEE Software (July/August). (2000) 89-96.

[6] Karl E. Weigers, Software Process Improvement: Ten Traps to Avoid, Software Development Magzine. May, 1996

[7] SEI: Capability Maturity Model® Integration (CMMISM), Version 1.1. SEI, CMU/SEI-2002-TR-029 (2002).

[8] ISO/IEC-15504: Information technology - Software process assessment. Technical report - Type 2 (1998).

[9] ISO-9000: International Standard Organization, http://www.iso.ch/iso/en/iso9000-14000/iso9000/iso9000index.html,

Site visited 23-02-2004 (2004)

[10] Niazi, M., Wilson, D. and Zowghi, D.: A Maturity Model for the Implementation of Software Process Improvement: An empirical study, Journal of Systems and Software 74 (2). (2005) 155-172

[11] Daskalantonakis, M.K., 1994. Achieving higher SEI levels. IEEE Software 11 (4)

[12] Joseph Schmuller, Sams Teach Yourself UML in 24 Hours, Third Edition. (March 15, 2004)

Appendix-A Motorola Instrument [Source 10]

Score	Key Activity evaluation dimensions		
	Approach	Deployment	Results
Poor (0)	▪ No management recognition of need ▪ No organizational ability ▪ No organizational commitment ▪ Practice not evident	▪ No part of the organization uses the practice ▪ No part of the organization shows interest	▪ Ineffective
Weak (2)	▪ Management begins to recognize need ▪ Support items for the practice start to be created ▪ A few parts of organization are able to implement the practice	▪ Fragmented use ▪ Inconsistent use ▪ Deployed in some parts of the organization ▪ Limited to monitoring/verification of use	▪ Spotty results ▪ Inconsistent results ▪ Some evidence of effectiveness for some parts of the organization
Fair (4)	▪ Wide but not complete commitment by management ▪ Road map for practice implementation defined ▪ Several supporting items for the practice in place	▪ Less fragmented use ▪ Some consistency in use ▪ Deployed in some major parts of the organization ▪ Monitoring/verification of use for several parts of the organization	▪ Consistent and positive results for several parts of the organization ▪ Inconsistent results for other parts of the organization
Marginally qualified (6)	▪ Some management commitment; some management becomes proactive ▪ Practice implementation well under way across parts of the organization ▪ Supporting items in place	▪ Deployed in some parts of the organization ▪ Mostly consistent use across many parts of the organization ▪ Monitoring/verification of use for many parts of the organization	▪ Positive measurable results in most parts of the organization ▪ Consistently positive results over time across many parts of the organization
Qualified (8)	▪ Total management commitment ▪ Majority of management is proactive ▪ Practice established as an integral part of the process ▪ Supporting items encourage and facilitate the use of practice	▪ Deployed in almost all parts of the organization ▪ Consistent use across almost all parts of the organization ▪ Monitoring/verification of use for almost all parts of the organization	▪ Positive measurable results in almost all parts of the organization ▪ Consistently positive results over time across almost all parts of the organization
Outstanding (10)	▪ Management provides zealous leadership and commitment ▪ Organizational excellence in the practice recognized even outside the company	▪ Pervasive and consistent deployed across all parts of the organization ▪ Consistent use over time across all parts of the organization ▪ Monitoring/verification for all parts of the organization	▪ Requirements exceeded ▪ Consistently world-class results ▪ Counsel sought by others

Minimizing Power Distribution System Active Power Loss Using Heuristic Network Reconfiguration Technique

Adejumobi I.A[1,a] and Opeodu F.A[2,b]
[1,2]Department of Electrical and Electronics Engineering,
University of Agriculture,
Abeokuta, Nigeria

ABSTRACT - In the light of the inadequacies in electricity generation, it becomes imperative that efforts be made to use the available electrical energy to greatest advantage by reducing the losses incurred when distributing this electrical energy. The uneven load distribution on primary distribution feeders has been identified as one of a major source of power loss power distribution system. Hence, a step by step approach of network reconfiguration technique will go a long way to solve this problem. In this paper, heuristic network reconfiguration method for radial distribution system was adopted. Applying appropriate power equations, the choices of the switches to be opened were based on each feeder's prior calculations of voltage at the buses, active and reactive powers flowing through feeders , active power losses and voltage deviations. In order to obtain fast and reliable results, two different algorithms were developed using Visual Basic.Net. the first algorithm was used for the power flow analysis on the feeders to determine the power losses and voltage profiles on the feeders, while the second one for the reconfiguration of the network by transferring loads between possible closed feeders based on results from the former. The validity of the developed algorithms was ascertained using three pairs of suspected critical loaded feeders within the Ilorin distribution network. The results from the analyses showed that power losses are reduced considerably and voltage profiles of the selected feeders improved. The adoption of heuristic network reconfiguration on distribution will go a long way in saving the economics of Distribution utilities and release spare electric energy for the competing consumers.

Key Words: *Distribution system, power loss, reconfiguration, algorithms, primary feeders, consumers.*

Introduction

Electricity remains one of the primary needs for socio-economic development in our society. Without it, the present social infra-structures would not be feasible. In the electricity supply systems, the distribution system is the most visible part of the supply chain that has direct link with consumers, hence, its proper and effective functioning is always desired. The insufficient electricity generation in Nigeria has devastating effect on the distribution system, in addition to problems due to poor management and maintenance. About 30 to 40 % of total investments in the electrical energy sector go to distribution systems, but nevertheless, they have not received the technological impact in the same manner as the generation and transmission systems especially in the developing nations [1]. The effectiveness with which a distribution system fulfills its function is measured in terms voltage regulation, power loss reduction, reliability and cost. Average power transmission loss of power utilities figures around 5-6% of total power demand whereas 60-70% of the loss is estimated to be lost in distribution system [2]. Electrical power distribution system suffers unbalanced feeder structure and unbalanced loading which affects system power loss, quality and electricity prices.

The distribution systems deliver power to the customers through a set of distribution substations, and these are normally configured radially for effective and easy co-ordination of their protective systems. There are two types of switches used in primary distribution systems; sectionalizing switches (normally closed) and tie switches (normally open). They are designed for both protection and configuration management in the system. Under normal operating conditions, feeders are frequently reconfigured by changing the open/closed state of each switch in order to reduce line losses or to avoid the overloading network branches [3].

In distribution system various configurations or switching combinations are possible. However, effective and efficient switching that guarantees minimum power loss is achieved only when a functional computational tool is available to calculate power loss and voltage drop at each switching. Due to radial system constraint and the discrete nature of the switches, the use of classical techniques to solve the reconfiguration problem should be avoided because of long computational time. In this work, a heuristic configuration technique is adopted so as to have a very minimum power loss on a radial distribution system. The proposed technique starts with initial (base) configuration with all tie switches are in open position. A set of simplified feeder-line flow formulations is employed to determine the power losses in each section of the system as well as the total power loss of the system, which is the objective function to be minimized by using branch exchange.

Losses in Distribution System

In electricity supply system, losses refer to the amounts of electricity injected into the transmission and distribution grids

that are not paid for by users [4]. Various factors contributes to power distribution losses. These include uneven distribution of loads among various feeders, lengthy distribution feeders, overloading of distribution transformers, inactive reactive compensation, inappropriate conductor sizing etc.. Total losses being experienced in distribution have two components: technical and non-technical [5].. Many utilities suffer both the technical and non-technical energy losses, which sometimes account for about 40 percent of the total energy generated or imported. Report has shown that the optimal total power losses in the distribution network (primary distribution and secondary distribution) ranges from between 6 percent and 12 percent [5].

Power Loss Minimization Using Heuristic Network Reconfiguration

The technique applied in the implementation of proposed feeder reconfiguration approach is divided into four phases. These are[6]:

- Formulation of optimization model for loss minimization.
- Load flow analysis of the distribution network.
- Proposed Heuristic approach to feeder reconfiguration.
- Program implementation.

Optimization Model for Loss Minimization: In the radial distribution system, each radial feeder is divided into load sections with sectionalizing switches (normally-closed switches) and is connected to other feeders via tie switches (normally-open switches). The network reconfiguration problem in a distribution system is to find the configuration with minimum distribution loss while satisfying the operating constraints under a certain load pattern. The operating constraints are voltage drop, current capacity and radial operating structure of the system.

The mathematical formulation for the minimization of power loss reconfiguration problems are presented in the literatures in different ways. In this work, the problem formulation is presented as given in equations 1 and 2 [3]:

Minimize (1)

(2)

Subject to the following constraints [7]:

- Radial network constraints:
  The network must remain radial after reconfiguration
- Power source limit constraint:
  The total loads of a certain partial network cannot exceed the capacity limit of the corresponding power source.
- Voltage constraint:
  Voltage magnitude at each bus must lie with their permissible ranges to maintain power quality.
  (3)
- Current constraint:
  Current magnitude of each branch must lie within their permissible range of the conductor used.
  (4)

Where

i specifies nodes (buses) on the feeders;
j specifies branches between two nodes on the feeders;
$P_{T,Loss}$ is the total real power loss of the system;
$P_{Loss}(j)$ is the real power loss in the branch *j;*
V_i is Voltage magnitude of bus *i;*
V_{min} is the bus minimum voltage;
V_{max} is bus maximum voltage;
I_j is the magnitude of the current in branch *j;*
$I_{j,max}$ is the maximum current limit of branch *j;*
N is the total number of nodes on the feeder and the laterals

Load Flow Analysis of The Distribution Network: The load flow analysis provides a systemic mathematical approach for determining the bus voltages, branch currents, active and reactive power flow through the branches of the distribution network[8,9]. In the load flow analysis, a single line diagram of the given system is used. A suitable mathematical derivation of the system, that adequately describes the relationship between voltages and powers in the interconnected system, is solved with the appropriate constraints to obtain the various bus voltages, active and reactive power in the branches, as well as the power loss in each branch of the feeder [9].

Forward-Backward Sweep Load Flow Method: There are several power flow methods based on forward/backward sweep technique. They may be classified as power summation methods and current summation methods. Current summation method is used in this paper as it is more convenient and fast than power summation method because it uses the values of the voltage 'V' at the nodes (buses) and the current 'I' in each branch, instead of the real and reactive power flow in each branch.

Backward Sweep: The purpose of the backward sweep is to update branch currents in each section, by considering the previous iteration voltages at each node. During backward propagation voltage values are held constant at the values obtained in the forward path and updated branch currents are transmitted backward along the feeder using backward path.

Backward sweep starts from extreme end branch and proceeds along the forward path [10]:

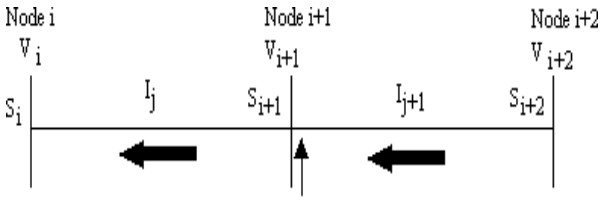

Figure 1. Bacward Sweep

The current taken by a load at node *i*is given by [9]

(5)

The value of current flowing in branch *j* (as shown in figure1) is obtained as the sum of current flowing in branch (*j+1*) and the current taken by load at node (*i+1*)

(6)

(7)

If a lateral is attached to the main feeder at the node (*i+1*) as shown in figure 2, then, the current in the branch *j* is the sum of current in branch (*j+1*), load current at node *i* and the current flowing in the first branch (nn) of the lateral. This is expressed in equation (8) .

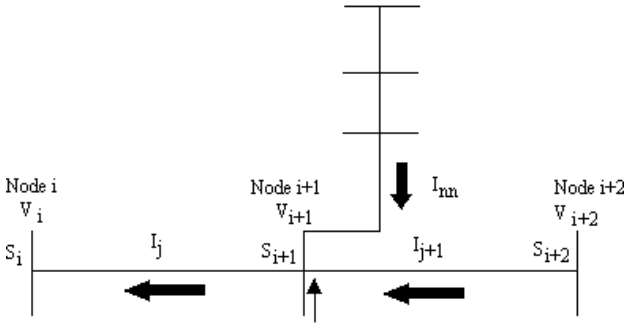

Figure 2 Backward Sweep for a feeder with lateral

(8)

Where,

* specifies the conjugate of a vector.

I_i^k is the current sink at node *i* in *k*th iteration (backward path).

S_i^k is the power injected into node *i* in the *k*th iteration (backward path).

V_i^{k-1} is the voltage at the *i*th node obtained during the (*k-1)*th iteration (forward path).

I_j^k is the current in branch *j* in the *k*th iteration.

I_{j+1}^k is the current in branch (*j+1*) in the *k*th iteration.

I_{nn}^k is the current in the branch 'nn' joining the first node of a lateral to the common node on a feeder.

Forward Sweep: The purpose of the forward sweep is to calculate the voltages at each node starting from the source node.

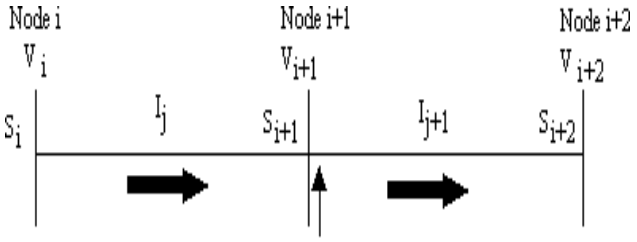

Figure 3: Forward Sweep

The source node voltage is set as 1.0 per unit (11.0kV) and other node voltages are calculated as [11]:

(9)

Where,

is the voltage at the *i*th node obtained during the *k*th iteration (forward path).

Z_j^k is the impedance of the *j*th branch (between the *i*th and (*i+1)*th node).

I_j^k is the current in the jth branch (between the *i*th and (*i+1)*th node) in the *k*th iteration.

These calculations will be carried out till the voltage at each bus is within the specified limits. At this point the voltages at each node, and the currents flowing in all line segments are known, which are used to find the power losses in each line segment.

Assumptions: It is assumed that three-phase radial distribution networks are balanced and represented by their single-line diagrams. Because of the complexity of the large scale distribution system, network reconfiguration problem is normally assumed as symmetrical system and constant loads [3]. Therefore, the distribution lines are represented as series impedances of the value

$Z_j = R_j + jX_j$. (10)

R_j is the resistance of the *j*th branch of the line.

X_j is the reactance of the *j*th branch of the line.

The load demand at each node (bus) is represented as constant and balanced power sinks with a power factor of 0.7 [9].

$S_L = P_L + jQ_L$. (10a)

P_{Li} is the real power demand at the *i*th bus.

Q_{Li} is the reactive power demand at the *i*th bus.

Derivations: The figure 1 above shows two consecutive nodes (buses) *i* and (*i+1*) on a feeder,

Where,

V_{i+1} is the voltage at the $(i+1)$th node;

V_i is the voltage at the ith node;

j specifies the branch connecting node i and $(i+1)$;

I_j is the current flowing in branch j;

Z_j is the impedance of branch j;

S_{i+1} is the power injected into node $(i+1)$, that is, power flowing in the branch j.

(11)

(1 2)

13)

— —— (14)

(15)

Where, ∅ is the power factor.

Real power loss in branch j is given by:

(16)

Reactive power loss in branch j is given by:

(17)

Proposed Heuristic Approach to Feeder Reconfiguration

Generally, in feeder reconfiguration, many tie or sectionalize switches are to be closed or opened to obtain the feasible network reconfiguration. If the reconfigured network leaves any branches unconnected or forms a closed loop it will lead to an infeasible switching combination for network reconfiguration. Hence, to avoid the infeasible switching combinations, the connectivity from the source to all the nodes and radial structure of the network must be checked. [3].

Feeder reconfiguration is performed by opening/closing two types of switches; tie and sectionalizing switches. The tie switches are normally open to separate two feeders, while the sectionalizing switches are normally closed to connect the nodes (buses) on the feeder. A whole feeder or part of a feeder may be served from another feeder by closing a tie switch linking the two while an appropriate sectionalizing switch must be opened to maintain radial structure [7]. In the context of loss reduction, the problem to be addressed in this work is to identify tie and sectionalizing switches that should be closed and opened, respectively, to achieve minimum system losses.

The change in the losses can easily be computed from the results of two load flow studies of the system configurations before and after the feeder reconfiguration. The details of the proposed algorithm with heuristic rules are below:

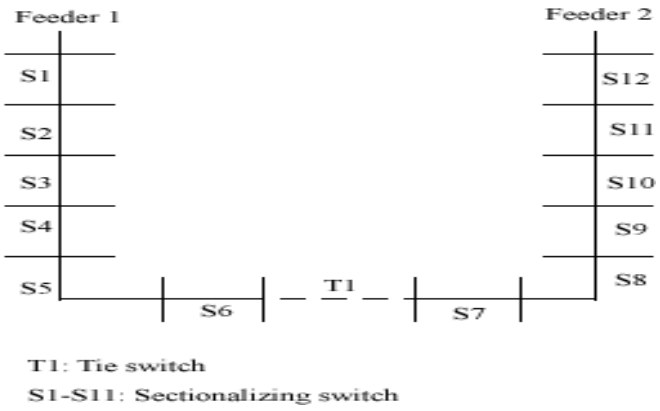

Figure. 4: Two radial feeders (networks) joined by a tie switch

shown in figure 4, by running the load flow, the voltage at the nodes and the real power losses for the radial networks are obtained. The losses of the two networks are compared to determine the network with lower loss. This is selected as the destination network, where loads will be transferred to from the other network. A branch-exchange method is used achieve the transfer of loads for the overloaded network (having higher loss) to the one with less load (having lower loss). Then, the open tie switch connecting the two networks (feeders) is closed while the adjacent sectionalizing switch on the overloaded network is opened to implement a transfer of load (or the exchange of branch). The load-flow program is run to determine the state of losses after the first load transfer. The step by step algorithm to execute optimum reconfiguration of the exchange of load between two feeders is given below

Algorithm for switching operation: The proposed technique involves the following steps:

- Read the system input data;
- Run the load flow program for the radial distribution networks;
- Initialize number of load transfer operation, k = 1.
- Compute the Power loss and voltage at various nodes and the sum of the real power loss of the two-network system, and store it in $P_{Loss}(k)$;
- Identify the network with the lower real power loss
- Increase the value of k by 1
- Identify the open switch between the two networks and the adjacent sectionalizing switch to be opened.
- Close the tie switch to form the loop and open the adjacent sectionalizing switch (to retain radiality of each network).

- Calculate the real power loss of the two-network system and store it in $P_{Loss}(k+1)$;
- If $P_{Loss}(k) \leq P_{Loss}(k+1)$, then the branch opening in the *k*th operation is the optimal configuration, go to step 11; Otherwise go to step 10;
- Implement next load transfer for the next iteration: go to step 5
- Run the load flow and the print the results;
- Stop.

Program Development: The proposed method (the load flow analysis and the switching operation) is programmed and coded in Visual Basic.NET on a Personal Computer Windows 7, 1.67-GHz processing speed, with 2.5GB RAM.

Visual Basic.NET was chosen basically because it an object-oriented programming languages and can be used to achieve a rapid application development with the Microsoft Visual Studio Integrated Development Environment. It's easy to use, understand, learn and very fast to code with. The program contains three major interfaces: variable interface, input interface and output interface. The variable interface is used to set the values of the system variable and constraints; while the input and output interface used for inputting network data and displaying obtained results.

The flow chart for the developed algorithm is shown in figure 5, with sample of output interface showing in figure 6 when the program was running.

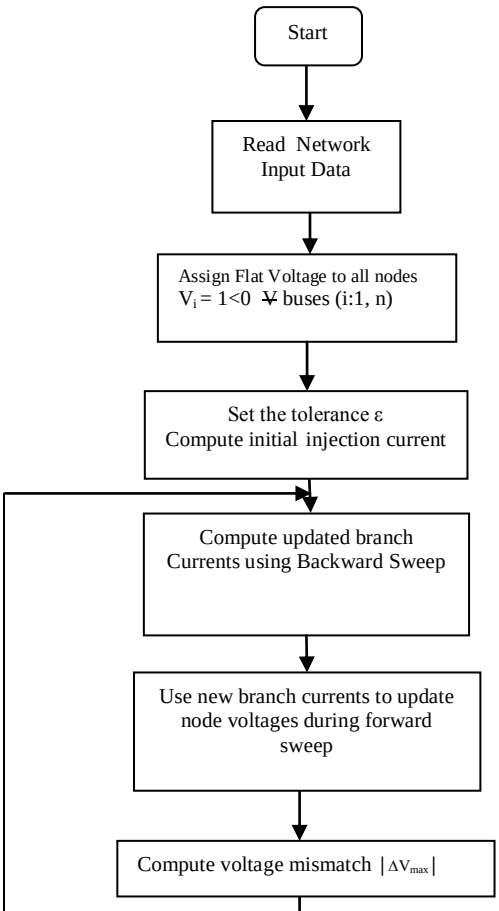

Results and Discussion

The networks used for the implementation of this work are extracted from a previous work carried by [12] on a section of Ilorin distribution system . The proposed reconfiguration technique is tested on three pairs of feeders by performing load flow analysis and branch exchange on each pair of the feeders. The networks used are 11kV distribution feeders of the Primary distribution system of Ilorin district. The Ilorin district center has two undertakings: GRA urban centre and Baboko Urban service centre. Two more undertakings are also fed from Ilorin 132kV/33kV injection substation through 33kV overhead lines. These are: Ogbomosho/Otte and Kishi/Igbeti undertakings. The primary feeders used in this project are: Offa Road and Airport feeders, Township I and Township II feeders, and Adewole and Township II feeders; all assumed with the conductor area of $150mm^2$ and maximum load demand. Using the developed algorithms from the mathematical equations 1 to 21, total active power losses and percentage voltage drops on the selected feeders were determined for both pre-reconfiguration and after reconfiguration. The obtained results are presented in tables 1 to 4.

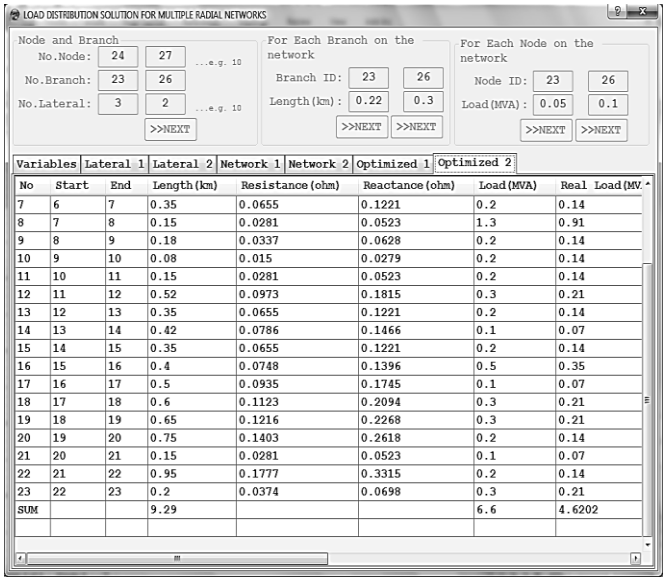

Figure 6: Output interface of program (for laterals)

\Table 1: summary of active power losses before and after for the selected feeders

Feeder	Total active power loss before reconfiguration (MW)	Total active power loss after reconfiguration (MW)	Reduction in active power loss (MW)	Percentage reduction in active power loss
Airport	**0.3414**	**0.2242**	**0.1172**	**34%**
Offa-Road	**0.8233**	**0.2097**	**0.6136**	**74.5%**
Township I	**1.7061**	**0.5629**	**1.1432**	**67%**
Adewole	**1.061**	**0.5097**	**0.4640**	**43.7%**
Township II feeders	**0.8037**	**0.7746**	**0.0291**	**3.6%**

Table2: summary of active power losses before and after reconfiguration for pairs of feeders.

Feeder Pair	Total active power loss before reconfiguration (MW)	Total active power loss after reconfiguration (MW)	Reduction in active power loss (MW)	Percentage reduction in active power loss
Airport and Offa-Road feeders	**1.0475**	**0.5511**	**0.4964**	**47.4%**
Township I and Township II feeders	**2.4807**	**1.3306**	**1.1501**	**46.4%**
Adewole and Township II feeders	**1.8356**	**1.4057**	**0.4299**	**23.4%**

Table 3: Summary of the voltage drop and the percentage voltage on the individual feeders

	Before reconfiguration		After reconfiguration	
Feeders	**Voltage drop (kV)**	**Percentage Voltage drop**	**Voltage drop (kV)**	**Percentage Voltage drop**
Airport	1.0165	9.24%	1.4434	13.12%
Offa-road	2.6083	23.71%	0.9944	9.04%
Township I	4.2264	38.42%	1.9363	17.60%
Township II	2.5491	23.17%	1.9867	18.06%
Adewole	3.7833	34.39%	2.1307	19.37%
Township II	2.5491	23.17%	2.7874	25.34%

Table 4: Summary of the voltage drop and the percentage voltage on the selected pair feeders.

	Before reconfiguration		After reconfiguration	
Feeder pair	**Total Voltage drop (kV)**	**Percentage Voltage drop**	**Total Voltage drop (kV)**	**Percentage Voltage drop**
Airport and Offa-road	3.6248	16.48%	2.4378	11.08%
Township I and Township II	6.7755	30.80%	3.923	17.83%
Adewole and Township II	6.3324	28.78%	4.9181	22.36%

From the tables 1 to 4 it is shown that, with the developed reconfiguration algorithms, the voltage drops and the active power losses on the selected individual and pair of feeders were reduced after reconfiguration exercise.

Conclusion

Power loss reduction was achieved by network reconfiguration, the concept of restructuring the topology of the distribution network to minimize losses was immediately be recognized as being cost efficient. The heuristic solution algorithm was based on the method of "branch exchange". The feasibility of a branch exchange was determined through the calculation of the electrical condition of the network. Once the electrical condition of the network was known for a given branch exchange, the objective function was quantified and the operational constraints of the system was verified. From the analysis, it is shown that reconfiguration methods are useful in both reducing the power losses in the primary distribution system and improving the voltage condition of the feeders.

The developed program can be used in any power distributions systems with or without automation.

References:

[1] L. Ramesh," Minimization of Power Loss in Distribution Networks by Different Techniques". **International Journal of Electrical Power and Energy Systems Engineering** Vol,2, No1,2009.pp..123-,

[2] H. Hamdoui,. et al,. "A New Constructive Method for Electric Power System Reconfiguration Using Ant Colony". **Leonardo Electronic Journal of Practice and Technologies**. Vol. 12,2008,pp. 49-60.

[3] R. SrinivasaRao and S. V. L, Narasimham. "A New Heuristic Approach for Optimal Network Reconfiguration in Distribution Systems". **International Journal of Applied Science, Engineering and Technology.** Vol.5,No.,2009, pp.15-20..

[4] **World Bank Group Energy Strategy**, Reducing Technical and Non-Technical Losses in the Power Sector",2009

[5] **PB Network Issue 48**: Loss Reduction in Distribution Networks. retrieved from http://www.PBNetwork.com, 48:58pp

[6] T. Taylor, and D. Lukeman,. ."Implementation of heuristic search strategies for distribution feeder reconfiguration", **IEEE Trans. on Power Delivery**,.Vol. 5. No. 1,1990, pp. 239 – 246.

[7] Hadi Sadat. **Power System Analysis**" McGraw-Hill Publishing Company Limited, New York, 2006 pp.189-237.

[8] M. E. Baran,. and F. F. Wu, "Network reconfiguration in distribution systems for loss reduction and load balancing**," IEEE Trans. Power Del.,** Vol. 4, No.2,1989, pp.1401–1407.

[9] A. S. Pabla, .**Electric Power Distribution**" McGrawHills Limited, New Delhi.,2004

[10] J.D. Glover,. and , M Sarma. **Power System Analysis and Design**, 2nd ed., PWS,1994, Publishing Company, Boston.

[11]D. Shirmohammadi and H. W. Hong , Reconfiguration of electric distribution networks for resistive line loss reduction**", IEEE Trans. Power Del**. Vol.4, No.2,pp 1998, 1492–1498.

[12] I. A. Adejumobi, ,"Distribution System Load Growth Prediction: Least Square Regression Approach", **Nigerian Journal of Pure and Applied Science.** 2003, Vol.18,pp.1506 – 1515.

An EOQ Model with Quantity Discount and Permissible Delay in Payments

Alok Kumar[1], K K Kaanodiya[2] and R R Pachauri[2*]
[1] Institute of Engineering and Technology, Agra (India), [2]B.S.A. College, Mathura (India)
Dr B R Ambedkar University, Agra (India)
dralokumar@gmail.com[1], kkkaanodiya@yahoo.in[2] and rrpachauri@gmail.com[2*]

Abstract - This paper considers a mathematical model for retailers optimal order quantity under the conditions of permissible delay in payments and quantity discount scheme offered by the supplier. It is assumed that the supplier provides to his/her customer two periods of permissible delay period to settle the account of purchasing goods and quantity discount to promote his product. If the retailer pays before the first permissible delay period, the supplier does not charge any interest. If the retailer pays after first permissible delay period but before second permissible delay period, then the supplier charges the retailer a low interest rate on unpaid balance. If the retailer pays after second permissible delay period then the supplier charges the retailer a higher interest rate on unpaid balance. In this paper, we determine retailer's optimal order quantity with minimize the total cost of inventory systems for the retailer under the conditions of permissible delay in payments and quantity discount scheme. Computational algorithm is given easy and rapidly determines ordering policies for retailer and finally, a numerical example is given to show validity of propose problem.

***Key words:** Permissible delay period, Quantity discount, Finance, Inventory, EOQ.*

1. Introduction

Development in global competition, advanced in technology environment, where the survival of the companies is become more difficult day by day. Hence, there is needed to be agile and fast in this globalised world. In common industrial practice, the supplier usually adopts some business strategies by offering quantity discount and permissible delay in payment to settle the account of his/her customer to stimulate his demand of product, to reduce per unit setup cost and to meet competition. In permissible delay policy, the supplier does not charge any interest if the payment is made before credit period. However, if the payment is paid beyond the predefined period, a high interest rate is charged.

Goyal (1985) is believed to be the first who developed the economic order quantity (EOQ) model under the conditions of permissible delay in payments. Davis and Gaither (1985) presented EOQ model when supplier offers one time opportunity to delay the payments of order in case an order for additional units is placed. Chand and Ward (1987) investigated Goyal (1985) model under the assumptions of classical economic order quantity model. Shah *et al.*(1988) studied the same model incorporating shortages. Mondal and Phaujdar (1989c) extended this issue by considering the interest earned from the sales revenue. Shah (1993a, b) also developed EOQ models for perishable items where delay in payment is permissible. Aggarwal and Jaggi (1995) developed Goyal's (1985) model to the case of exponential deterioration, Shah and Sreehari (1996) presented an extended issue of EOQ model where the delay in payment is permitted and the capacity of own warehouse is limited. Liao *et al.* (2000) and Sarker *et al.*(2000a) deal this problem with inflation. Chu *et al.*(1998),Chung (2000) and Chang and Dye (2001) examined this issue with allowable shortage. Chang *et al.* (2001) investigated this topic in the case of linear trend demand. Mondal and Phaujdar (1989b), Hwang and Shinn (1997), Jamal *et al.* (1997) and Sarker *et al.* (2001) extended this issue with deteriorating items. Teng (2002) modified Goyal's (1985) model by assuming the selling price is not necessary equal to purchase price. Other papers related to this area are Chang and Dye (2002), Chang *el al.* (2001), Chen and Chung (1999), Chung (1998a, b) Jamal *et al.* (2000), Salameh *et al.* (2003), Huang and Chung (2003), Arcelus *et al.* (2003), Abad and Jaggi (2003), Shinn and Huang (2003), Chung and Huang (2003), Chung and Liao (2004), Chung *et al.* (2005), Chung and Liao (2006), Huang (2007) and Liao and Chung (2009).

In above models, the supplier adopts a business strategy of permissible delay period in paying the purchasing cost to attract more customers. The retailer takes the benefit of trade credit and sells the product and earns the interest by putting generated revenue in an interest bearing account. They implicitly assumed that the buyer would pay the supplier as soon as he/she receives the items. As mentioned earlier, supplier only offers a trade credit to the retailer but retailer does not provide any trade credit to his/her customer which means we deal with one level of trade credit. However, in many real-world cases, this condition will not hold. Recently, Huang (2003) modified this assumption by assuming that the retailer will also adopt the trade credit policy to stimulate his/her customer

Manuscript received May 25, 2010.
Manuscript revised July 15 , 2010.

demand to develop retailer replenishment model and this method is called two level of trade credit policy.

In quantity discount philosophy, the supplier reduced the price of goods to attract the customer, generally a reduce price encourage the customer to buy more. In this viewpoint, Abad (1988), Kim and Hwang (1988), Goyal and Gupta (1990), Hwang *et al* (1990) and Burwell *et al* (1991) developed the traditional quantity discount model. Mohanan (1984) show that the application of all-units discounts contributes to reducing the buyer's inventory cost and improving the supplier's profit simultaneously (Rubin and Benton 2003, Yano and Gilbert 2004). Mohanan's approach generalized by Rosenblatt and Lee (1985), Lee and Roseblatt (1986), Kim and Huang (1989), Weng and Wong (1993), Weng (1995), Klastorin *et al* (2002) and Shin and Benton (2004). Recently, Shin and Benton (2007) developed a quantity discount model with uncertain demand in supply chain coordination.

This paper extends Goyal *et al.* (2007) model in light of quantity discount scheme. In this paper, the supplier provided not only a quantity discount but also a permissible delay in payments when retailer settles the outstanding amount by *M* (first PDP), the supplier does not charge any interest, if the retailer pays after *M* (first PDP) but before *N* (Second PDP) offered by the supplier, then the supplier charges the retailer on the un-paid balance at the rate Ic_1 , if the retailer settles the account after *N* (Second PDP), then he will have to pay at interest rate Ic_2 on the un-paid balance $(Ic_2 > Ic_1)$. The paper, however, considers only one break point (one quantity discount) in the permissible delay in payments. With aforesaid conditions, we model the retailer's inventory system as a cost minimization problem to determine the retailer's optimal order quantity, optimal inventory cycle time, optimal total relevant cost. Computational algorithm is given easy and rapidly determines ordering policies for retailer and finally, a numerical example is given to show validity of propose problem.

2. Assumption and Notation:

For convenience, most Assumption and Notations similar to Goyal *et al.* (2007) will be used in the present paper.

2.1 Assumptions

1) The inventory system deals with single items and demand is constant.
2) Lead time zero and Shortages are not allowed.
3) Replenishment rate is infinite.
4) Time horizon is infinite.
5) Single price break
6) Trade credit between supplier and retailer as follows:
   - If the retailer pays by M, then supplier does not charge the retailer any interest.
   - If the retailer pays after M but before N, he keeps his/her profit and sells revenue is utilized to earn interest with annual rate Ie. Then the supplier charges the retailer an interest rate of Ic_1on the balance amount.
   - If the retailer pays after second permissible delay period N, then supplier charges the retailer an interest rate of Ic_2 on the balance amount, with $Ic_2 > Ic_1$.

2.2 Notation

1) D The demand rate per year
2) h The stock- holding cost/unit/year excluding interest charges.
3) P The selling price per year
4) c The unit purchasing cost, with $c < P$
5) S The ordering cost per order
6) T The replenishment cycle
7) M The first permissible delay period for settling account without extra charge
8) N The second permissible delay period for settling account with an interest charge of Ic_1 on balance amount and $N > M$.
9) Ic_1 The interest charged per $ in stock per year by the supplier when the retailer pays after M before N
10) Ic_2 The interest charged per $ in stocks per year by the supplier when the retailer pays after N
11) Ie The interest earned per $ per year
12) Q The order quantity
13) $I(t)$ The level of inventory at time $t, 0 \leq t \leq \frac{Q}{D}$
14) TC The total cost of an inventory system/unit time

3. Mathematical Formulation

The level of inventory $I(t)$ gradually decreases mainly to meet the demands. Hence, the change of inventory level

with respect to time can be describes by the following equation

$$\frac{dI(t)}{dt} = -D,\ 0 \le t \le Q/D, \quad (1)$$

With the initial conditions $I\left(\frac{Q}{D}\right) = 0$, consequently, the solution of Eq. (1) is given by

$$I(t) = D(\tfrac{Q}{D} - t) \quad , \quad 0 \le t \le Q/D \quad (2)$$

And order quantity is

$I(0) = Q$

The total cost of inventory system consists following elements

(a) Cost of placing orders $= \frac{AD}{Q}$ (3)

(b) Cost of carrying inventory

$$= \frac{hD}{Q}\int_0^{Q/D} I(t)\,dt = \frac{hQ}{2} \quad (4)$$

(c) Cost of purchasing goods $= \frac{cQ}{Q/D} = cD$ (5)

Regarding interests charged and earned based on the length of the replenishment cycle Q/D, three cases may arise:

(1) $\frac{Q}{D} \le M$ (2) $M \le \frac{Q}{D} \le N$ (3) $\frac{Q}{D} \ge N$

Case 1 $Q/D \le M$

Here, the retailer sells Q units during $[0, Q/D]$ and paying for cQ units in full to the supplier at time $M \ge Q/D$ with zero interest charged i.e.

$$IC_1 = 0 \quad (6)$$

Retailers sell Q units and deposit the revenue into an account for the period $[0,\ M]$. Therefore, sales revenue is accumulated from period $[0, Q/D]$ to $[Q/D, M]$ and interest earned in this period is PIe. The annual interest earned is as follows.

$$IE_1 = \frac{PDI_e}{Q}\left[\int_0^{Q/D} Dtdt + Q(M - Q/D)\right]$$

$$= PIeD\left(M - \frac{Q}{2D}\right) \quad (7)$$

Using eq 3, 4, 5, 6 and 7 we have total relevant cost per year is

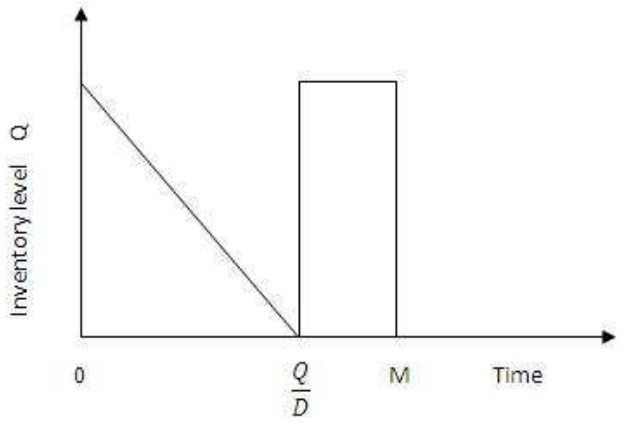

Fig. 1 $Q/D \le M$

$$TC_1(Q) = cD + \frac{SD}{Q} + \frac{hQ}{2} - PI_eD\left(M - \frac{Q}{2D}\right) \quad (8)$$

The optimum values of $Q = Q_1$ is the solution of equation

$$\frac{dTC_1(Q)}{dQ} = -\frac{SD}{Q^2} + \frac{h}{2} + \frac{PI_e}{2}$$

$$Q_1 = \sqrt{\frac{2SD}{h + PI_e}} \quad (9)$$

$Q = Q_1$ Minimizes total cost; $TC_1(Q)$ provided by the following

$$\frac{d^2Tc_1(Q)}{dQ^2} = \frac{2SD}{Q^3} > 0, \text{ for all } Q \quad (10)$$

Case 2 $M < \frac{Q}{D} < N$

The retailer sells products and earned interest I_e/\$/year by deposits the revenue into an interest earning account during the period $[0, M]$. Hence interest earned, IE_2 is as follows

$$IE_2 = PI_e\int_0^M Dtdt = PI_e\frac{DM^2}{2} \quad (11)$$

Retailer purchases Q-units at time $t = 0$ and pays at the rate of c \$/unit to the supplier during $[0, M]$. The retailer sells DM-units at sell price $\$P$/unit. So he has generated revenue of PDM plus the interest earned, IE_2 during $[0, M]$ which arises two cases:

Sub-Case 2.1 $PDM + PIeD\frac{M^2}{2} \ge cQ$

In this case, the retailer has sufficient balance in his/her account to pay off full purchasing cost of items at time M. So, there is no interest charge. The interest earned per years is as follows

$$IE_{2.1} = \frac{PDI_e}{Q}\int_0^M Dtdt = PI_eD^2M^2/2Q \quad (12)$$

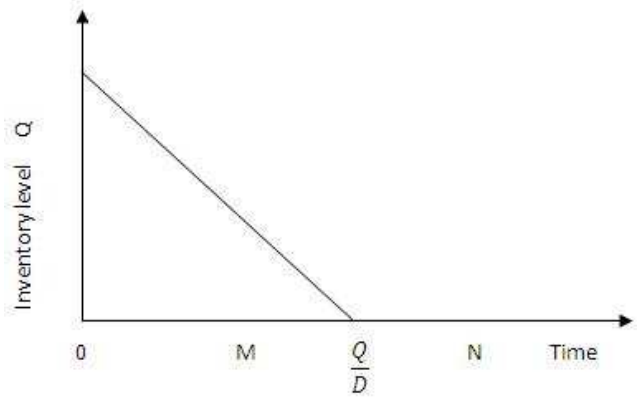

Fig. 2 $M \le Q/D \le N$

Using eq $3, 4, 5$ and 12 therefore, the total relevant cost per year is as follows

$$TC_{2.1}(Q) = cD + \frac{SD}{Q} + \frac{hQ}{2} - \frac{pI_eD^2M^2}{2Q} \quad (13)$$

The optimal value of $Q = Q_{2.1}$ is the solution of equation

$$\frac{TC_{2.1}(Q)}{dQ} = -\frac{SD}{Q^2} + \frac{h}{2} + \frac{pI_eD^2M^2}{2Q^2}$$

$$Q_{2.1} = \sqrt{\frac{D(2S - pI_eDM^2)}{h}} \quad (14)$$

$Q = Q_{2.1}$ Minimizes total cost: $TC_{2.1}(Q)$ provided by following

$$\frac{d^2Tc_{2.1}(Q)}{dQ^3} = \frac{2SD}{Q^3} - \frac{pIeD^2M^2}{Q^3} > 0, \text{ for all } Q \quad (15)$$

Sub-case 2.2 $PDM(1 + IeM/2) < cQ$

In this case, the supplier receives the interest from the retailer on the balance amount $U_1 = cQ - [PDM + PIeDM22$ with rate $Ic1$ at time M. Thereafter, the retailer regularly reduces the finance amount of the loan due to constant sales and revenue received. Then, the interest payable per year is as follows

$$IC_{2.2} = Ic_1U_1[U_1/PD]/(2\,Q/D) = \frac{Ic_1}{2PQ}\left[cQ - PDM\left(1 + I_e\frac{M}{2}\right)\right]^2 \quad (16)$$

The interest earned per year is

$$IE_{2.2} = \frac{IE_2}{Q/D} \quad (17)$$

Using eq $3, 4, 5, 16,$ and 17 therefore, the total relevant cost per year is as follows

$$TC_{2.2}(Q) = cD + \frac{SD}{Q} + \frac{hQ}{2} - \frac{PI_eD^2M^2}{2Q} + \frac{Ic_1}{2PQ}[cQ - PDM(1 + I_eM)]^2 \quad (18)$$

The optimal value of $Q = Q_{2.1}$ is the solution of equation

$$\frac{dTC_{2.2}}{dQ} = -\frac{SD}{Q^2} + \frac{h}{2} + \frac{PI_eD^2M^2}{2Q^2} + \frac{Ic_1c^2}{2P} - \frac{Ic_1PD^2M^2(1 + I_eM)^2}{2Q^2}$$

$$Q_{2.2} = \sqrt{\frac{2SD - PI_eD^2M^2 + Ic_1PD^2M^2(1 + I_eM)^2}{h + \frac{Ic_1c^2}{P}}} \quad (19)$$

$Q = Q_{2.2}$ Minimizes total cost; $Tc_{2.2}(Q)$ provided by the following

$$\frac{d^2Tc_{2.2}(Q)}{dQ^2} = \frac{2SD}{Q^3} - \frac{PIeD^2M^2}{Q^3} + \frac{Ic_1PD^2M^2(1 + IeM)^2}{Q^3} > 0$$

for all Q (20)

Case 3 $Q/D \ge M$

This case is similar to case 2. Based on the total purchase cost cQ, the total balance of money in the account at M, $PDM + PI_eD\,M^2/2$, and the total amount of money in the account at N, $PDN + PI_eD\,N^2/2$, there are three possible sub-cases as follows.

Sub-Case 3.1 $PDM + PI_eD\,M^2/2 \ge cQ$

This sub-case is the same as case 2.1

Sub-Case 3.2 $PDM + PI_eD\,M^2/2 < cQ$**,**
But

$$[PD(N - M) + PI_eD\,(N - M)^2/2] \ge [cQ - PDM - PI_eD\,M^2/2]$$

This sub-case is the same as sub-case 2.2

Sub-Case 3.3$PDN + PI_eD\,N^2/2 < cQ$**,** and

$$[PD(N - M) + PI_eD\,(N - M)^2/2] < [cQ - PDM - PI_eD\,M^2/2]$$

In this case, retailer's account has not sufficient balance to pay total amount at time N. He pays $[PDM + PIeDM22$ at M and $PDN{-}M{+}PIeDN{-}M22$ at N. Thus, the supplier receives the interest on balance amount $U_1 = cQ - [PDM + PI_eD\,M^2/2]$ at M with interest rate Ic_1 during the period $[M, N]$ and

$$U_2 = cQ - [PDM + PI_eD\,M^2/2] - [PD(N - M) + PI_eD\,(N - M)^2/2]$$

at time N with interest rate Ic_2. Therefore, the interest charges $Ic_{3.3}$ per time unit is as follows.

$$IC_{3.3} = Ic_1[cQ - PDM - PI_eD\,M^2/2]\frac{(N - M)}{Q/D} + Ic_2U_2\,[U_2/(PD)]/2\,Q/D$$

$$= \frac{Ic_1(N-M)D}{Q}[cQ - PDM(1 + I_e M/2)] + \frac{Ic_2D^2}{2PQ}\left[c\frac{Q}{D} - PN - \frac{PI_e}{2}\{M^2 + (N-M)^2\}\right]^2 \quad (21)$$

And total interest earned per time unit is

$$IE_{3.3} = \frac{IE_2}{Q/D} \quad (22)$$

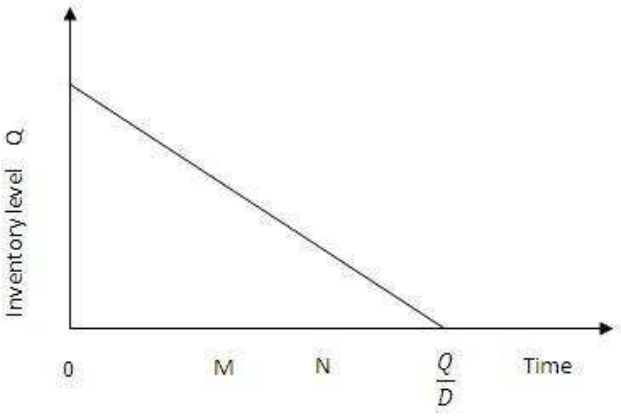

Fig .3 $T \geq N$

Using 3, 4, 5,21 and 22 therefore, total relevant cost is as follows

$$TC_{3.3}(Q) = cD + \frac{SD}{Q} + \frac{hQ}{2} - \frac{PI_eD^2M^2}{2Q} + \frac{Ic_1(N-M)D^2}{Q}\left[\frac{cQ}{D} - PM\left(1 + \frac{IeM}{2}\right)\right] + \frac{Ic_2D^2}{2PQ}\left[\frac{cQ}{D} - PN - \frac{PIe}{2}\{M^2 + (N-M)^2\}\right]^2 \quad (23)$$

The optimal value of $Q = Q_{3.3}$ is the solution of equation

$$\frac{dTc_{3.3}}{dQ} = -\frac{SD}{Q^2} + \frac{h}{2} + \frac{PI_eD^2M^2}{2Q^2} + \frac{Ic_1(N-M)D^2PM\left(1 + \frac{IeM}{2}\right)}{Q^2} + \frac{Ic_2c^2}{2P} - \frac{Ic_2PD^2N^2}{2Q^2} - \frac{Ic_2PD^2\frac{Ie^2}{4}\{M^2 + (N-M)^2\}^2}{2Q^2} - \frac{Ic_2PD^2NI_e\{M^2 + (N-M)^2\}}{2Q^2}$$

$$Q_{3.3} = \sqrt{\frac{2SD - PI_eD^2M^2 + Ic_2PD^2\left[N + \frac{Ie}{2}\{M^2 + (N-M)^2\}\right]}{h + \frac{Ic_2c^2}{P}}} \quad (24)$$

$Q = Q_{3.3}$ Minimizes total cost; $Tc_{3.3}(Q)$ provided by following

$$\frac{d^2Tc_{3.3}(Q)}{dQ^2} = \frac{2SD}{Q^3} - \frac{PIeD^2M^2}{Q^3} - \frac{2Ic_1(N-M)D^2PM(1 + IeM)}{Q^3} + \frac{Ic_2PD^2N^2}{Q^3} + \frac{Ic_2PD^2\frac{Ie^2}{4}\{M^2 + (N-M)^2\}^2}{Q^3} + \frac{Ic_2PD^2NI_e\{M^2 + (N-M)^2\}}{Q^3} > 0 \quad (25)$$

4. Computational Algorithm:

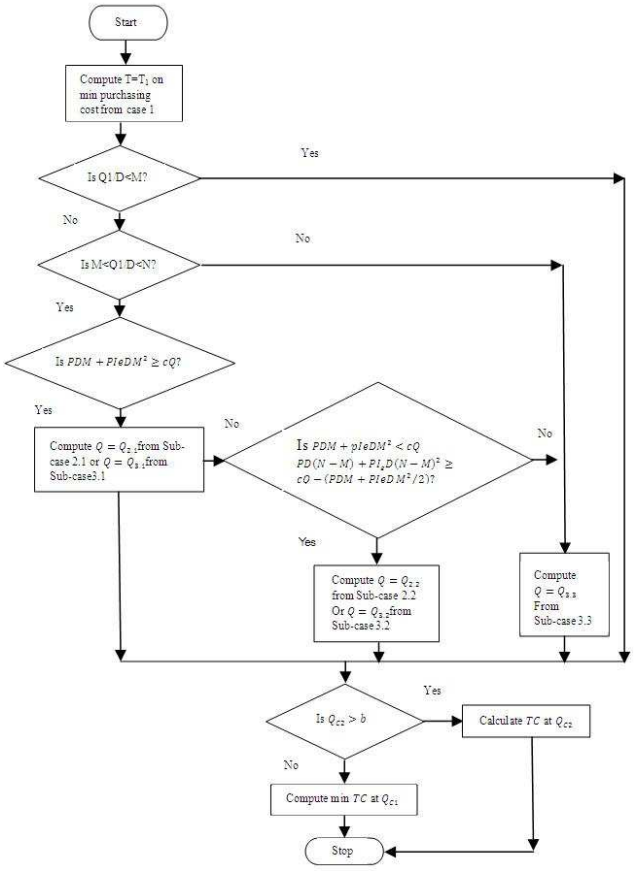

5. Numerical Example:

$Ic_1 = .06/year$, $Ic_2 = .09/year$, $Ie = .04/year$, $P = \$50 per\ unit$, $D = 1200 units/year$
$M = \frac{20}{365} days$, $N = \frac{40}{365} days$, $h = Ic$, $I = \$.2/units/year$, $c = \$30, 35 per\ unit$, $b = 600$
$S = 10, 20, 30, 40, 50, 60, 70, 80, 1200$

Where b is that quantity at and beyond which the quantity discount applies

$0 \le Q_{C1} < 600$ 35
$600 \le Q_{C2}$ 30

Table 1

Ordering Cost (S)	Optimal Cycle Time Q/D	Optimal Order Quantity Q	Total Relevant Cost $TR(Q)$
10	**0.0465**	**55.83**	**37531.33**
20	**0.0682**	**81.83**	**37707.33**
30	**0.0857**	**102.80**	**37837.33**
40	**0.0984**	**118.11**	**37945.78**
50	**0.1093**	**131.20**	**38042.06**
60	**0.1288**	**154.59**	**38180.95**
70	**0.5000**	**600.00**	**38226.90**
80	**0.5000**	**600.00**	**38246.90**
1200	**0.5164**	**619.62**	**41684.46**

Increase in ordering cost result increase in order quantity, increase in replenishment cycle and increase in total relevant cost.

6. Concluding Remark:

In this paper, we developed an EOQ model to determine retailer's optimal order quantity under the conditions of permissible delay in payment and quantity discount. The supplier provides to his/her customer two permissible delay periods for settling the account and one price break in quantity discount scheme to buy more quantity of goods. The computational algorithm is provided to easily and rapidly determine the retailer's optimal order quantity.

References:

[1] P. L. Abad, "Joint price and lot-size deterioration when supplier offers incremental quantity discounts" Journal of Operational Research Society, Vol. 39, 1988, pp. 603-607.
[2] S. P. Aggarwal, C. K. Jaggi, "Ordering policies of deteriorating items under permissible delay in payments" Journal of the Operational Research Society, Vol. 46, 1995, pp 658-662.
[3] T. H. Burwell, D. S. Dave, K. E. Fitzpatrick and M.R. Roy, "An inventory model with planned shortages and price-dependent demand" Decision Science, Vol. 27, 1991, pp. 1188-1191.
[4] S. Chand, J. Ward, "A note on economic order quantity under conditions of permissible delay in payments" Journal of Operational Research Society, Vol. 38, 1987, pp. 83-84.
[5] H. J. Chang, C. Y. Dye, "An inventory model for deteriorating items with partial backlogging and permissible delay in payments", International Journal of Systems Science, Vol. 32, 2001, pp. 345-352.
[6] H. J. Chang, C. H. Huang and C. Y. Dye, "An inventory model for deteriorating items with linear trend demand under the condition of permissible delay in payments", Production Planning and Control, Vol. 12, 2001, pp. 274-282.
[7] M. S. Chen, C. C. Chuang, "An analysis of light buyer's economic order model under trade credit", Asia-Pacific Journal of Operational Research, Vol. 16, 1999, pp. 23-24.
[8] P. Chu, K. J. Chung and S. P. Lan, "Economic order quantity of deteriorating items under permissible delay in payments", Computers and Operations Research, Vol. 25, 1998 pp. 817-824.
[9] H. J. Chung, C. Y. Dye, "An inventory model for deteriorating items under the condition of permissible delay in payments", Yugoslav Journal of Operational Research, Vol. 1, 2002, pp. 73-84.
[10] K. J. Chung, 1998a "A theorem on the determination of economic orders quantity under condition of permissible delay in payments", Computers and Operations Research, Vol. 25, 2002, pp. 49-52.
[11] K. J. Chung, "The inventory replenishment policy for deteriorating items under permissible delay in payments", Opsearch, Vol. 37, 2000, pp.267-281.
[12] K. J. Chung, Y. F. Huang, "The optimal cycle time for EPQ inventory model permissible delay in payments", International Journal of Production Economics, Vol. 84, 2003, pp. 307-318.
[13] K. J. Chung, J. J. Liao, "Lot-sizing decisions under trade credit depending on the order quantity", Computers and Operations Research, Vol. 3, 2004, pp. 909-928.
[14] K. J. Chung, "Economic Order quantity model when delay in payments is permissible", Journal of Information and Optimization Science, Vol. 19, 1998_b, pp. 411-416.
[15] K. J. Chung, S. K. Goyal and Y. F. Huang, "The Optimal inventory policies under permissible delay in payments depending on the ordering quantity", International Journal of Production Economics, Vol. 95, 2005, pp. 303-213
[16] K. J. Chung, J. J. Liao, "The Optimal Ordering policy in a DCF analysis for deteriorating items when trade credit depends on the order quantity", International Journal of Production Economics, Vol. 100, 2006, pp. 116-130.
[17] R. A. Davis, N. Gaither, "Optimal ordering policies under conditions of extended payment privileges", Management Science, Vol. 31, 1985. pp. 499-509.
[18] S. K. Goyal, O. K. Gupta, "A simple approach to the discount purchase problem", Journal of Operational Research Society, Vol. 41, 12, 1990, pp. 1169-1170.
[19] S. K. Goyal, "Economic order quantity under conditions of permissible delay in payments", Journal of Operational Research Society, Vol. 36, 1985, pp. 335-338.
[20] S. K. Goyal, J. T. Teng and C. T. Chang, "Optimal ordering policies when the supplier provides a progressive interest scheme", European Journal of Operational Research, Vol. 179, 2007, pp. 404-413.

[21] Y. F. Huang, "Economic order quantity under conditionally permissible delay in Payments", European Journal of Operational Research, Vol. 176, 2007, pp. 911-924.
[22] Y. F. Huyang, "Optimal retailer's ordering policies in the EOQ model under trade credit financing", Journal of the Operational Research Society, Vol. 54, 2003, pp. 1011-1015.
[23] H. Hwang, D. H. Moon and S. W. Shinn, "An EOQ model with quantity discounts for both purchasing price and freight cost", Computers and Operations Research, Vol. 17, 1990, pp. 73-78.
[24] H. Hwang, S. W. Shinn, "Retailer's pricing and lot sizing policy for exponentially deteriorating product under the condition of permissible delay in payments", Computers and Operations Research, Vol. 24, 1997, pp. 539-547.
[25] A. M. M. Jamal, B. R. Sarker and S. Wang, "An ordering policy for deteriorating items with allowable shortage and permissible delay in payment", Journal of the Operational Research Society, Vol. 48, 1997, pp. 826-833.
[26] A. M. M. Jamal, B. R. Sarker and S. Wang, "Optimal payment time for a retailer's under permitted delay of payment by the wholesaler", International Journal of Production Economics, Vol. 66, 2000, pp. 59-66.
[27] K. H. Kim, H. Hwang, "An incremental discount pricing schedules with multiple customers and single price break", European Journal of Operational Research, Vol. 35, 1988, pp. 71-79.
[28] K. H. Kim, H. Hwang, "Simultaneous improvement of supplier's profit and buyer's cost by utilizing quantity discount", Journal of the Operational Research Society, Vol. 40, No. 3, 1989, pp. 55-265.
[29] T. D. Klastorin, K. Moinjadea and J. Son, "Coordinating orders in supply chain through price discount", IIE Transactions, Vol. 34, 2002, pp. 676-689.
[30] H. L. Lee, M. J. Rosenblatt, "A generalized quantity discount pricing model to increase supplier's profit", Management Science, Vol. 30, No. 9, 1986, pp. 1177-1185.
[31] H. C. Liao, C. H. Tsai and C. T. Su, "An inventory model with deteriorating items under inflation when a delay in payment is permissible", International Journal of Production Economics, Vol. 63, 2000, pp. 207-214.
[32] J. J. Liao, K. J. Chung, "An EOQ model for deterioration items under trade credit policy in a supply chain system", Journal of Operation Research Society of Japan, Vol. 52, 2009, pp. 46-57.
[33] J. P. Monahan, "A quantity discount pricing model to increase vendor profits", Management Science, Vol. 30, No. 6, 1984, pp. 720-726.
[34] B. N. Mondal, S. Phaujdar, "Some EOQ models under permissible delay in payments", International Journal of Management Science, Vol. 5, 1989_c, pp. 99-108.
[35] M. J. Rosenblatt, H. L. Lee, "Improving profitability with quantity discounts under fixed demand", IIE Transactions, Vol. 17, 1985. pp. 388-395.
[36] P. A. Rubin, W. C. Benton, "A generalized framework for quantity discount pricing schedules", Decision Science, Vol. 34, No. 1, 2003, pp. 173-188.
[37] M. K. Salameh, N. E. Abbound, A. N. Ei-Kassar and R. E. Ghattas, "Continuous review inventory model with delay in payment", International Journal of Production Economics, Vol. 85, 2003, pp. 91-95.
[38] B. R. Sarker, A. M. M. Jamal and S. Wang, "Optimal payment time under permissible delay for products with deterioration Production Planning and Control", Vol. 11, 2001, pp. 380-390.
[39] B. R. Sarker, M. A. Kindi, "Optimal ordering policies in response to a discount offer", International Journal of Production Economics, Vol. 100, No. 2 2006, pp. 195-211.
[40] N. H. Shah, "Probabilistic time-scheduling model for an exponentially decaying inventory when delay in payments is permissible", International Journal of Production Economics, Vol. 32, 1993a, pp. 77-82.
[41] N. H. Shah, "A lot size model for exponentially decaying inventory when delay in payment is permissible", Cahiers du CERO, Vol. 35, 1993_b, pp. 115-123
[42] V. R. Shah, N. C. Patel and D. K. Shah, "Economic ordering quantity when delay in payments of order and shortages are permitted", Gujarat Statistical Review, Vol. 15, No. 2, pp. 1988 52-56.
[43] V. R. Shah, M. Sreehari, "An inventory model for a system with multiple storage facility", Opsearch, Vol. 33, No. 2, 1996, pp. 96-106.
[44] H. Shin, W. C. Benton, "A quantity discount approach to supply chain coordination", European Journal of Operational Research, Vol. 180, 2007, pp. 601-616.
[45] H. Shin, W. C. Benton, "Quantity discount-based inventory coordination: Effectivess and Critical environmental factor", Production and Operations Management, Vol. 13, No. 1, 2004, pp. 63-76.
[46] J. T. Teng, "On the economic order quantity under conditions of permissible delay in payments", Journal of the Operational Research Society, Vol. 53, 2002, pp. 915-918.
[47] Z. K. Weng, "Channel coordination and quantity discounts", Management Science, Vol. 41, No. 9,, 1995, pp. 1509-1522.
[48] Z. K. Weng, R. T. Wong, "Generals models of the supplier's all-units quantity discount policy", Naval Research Logistic, Vol. 40, 1993. pp. 971-980.
[49] C. A. Yano, S. M. Gilbert, "Coordinated pricing and production/procurement decisions: A Review, In: Chakravarty, A., Eliashberg J. (Eds), Managing Business Interfaces. Marketing Engineering and Manufacturing Perspectives, Kluwer Academic Publishers, 2004

Integral of Bijective Function in a Bounded Region

Chandan kumar

[1]**Department of Civil Engineering, Delhi Technological University, Formerly: Delhi College of Engineering, Delhi University, Bawana Road, Delhi-42, India.**

Abstract - In the present paper, we will find the relationship between bijective function, inverse of the function and Identity function, their integral values and behavior in a bounded region, for a certain condition we will obtain some standard results.

Key words: *Mean value Theorem, Bounded Inverse theorem, Definite Integral, Continuity, Differentiability and Monotonic function.*

1. Introduction

An identity function is a function that always returns the same value that was used as its argument. In terms of equation, the function by f(x) = x. If the function is one-one and onto then it is bijective function and its inverse exists. If two function f(x) and g(x) are defined so that fog(x) and gof(x) we say that f(x) and g(x) are inverse function of each other. Function f(x) and g(x) are inverse of each other if the operations f(x) reverse all the operation of g(x) in the reverse order and the operation of g(x) reverse all the operations of f(x) in the reverse order. All the points for f(x) are identical to those of g(x) except x is switched with y. The graphs of f(x) and g(x) are mirror images across the line y=x. Let the function f(x) is strictly decreasing then function g(x) will also be strictly increasing. Bijective function plays a fundamental role in many areas of mathematics, for instance in the definition of isomorphism, permutation group, project map and many others. Let f be a function whose domain is the set X, and whose co-domain is the set Y. Then if it exists, the inverse of function f is the function $\mathbf{f}^{-1}$ with domain Y and co-domain X defined by: f(x) = y and $\mathbf{f}^{-1}$(y) = x. In this paper we study the relationship between bijective function, inverse of the function, identity function and finite integral in a definite interval.

2. Theorem.

Let there be any function say f : [a,b] → [d,e]

Then If:
(1) - The function is continuous between [a,b]
(2) - The function f(x) is differentiable in (a,b)
(3)- The function f(x) is bijective in [a,b]
(4)- The sign of both a , b and f(a) , f(b) are opposite
(5)- Either: |f(a)| < |a| and |f(b)| < |b| or |f(a)| > |a| and |f(b)| > |b|

Let $\mathbf{f}^{-1}$(x) = g(x)
so, f(c) = g(c) = c, f' (c) × g' (c) = 1 for f'(c) = g'(c) = 0

(6)- If c=0, |a| = |b| and |d| = |e|

Then there exists at least one point c such that:

$$\left|\int_a^c f(x)dx\right| + \left|\int_d^c g(x)dx\right| = \left|\int_c^b f(x)dx\right| + \left|\int_c^e g(x)dx\right|$$

Where c is the point of intersection of function f(x), g(x) and y=x, and g : [a,b] → [d,e]

Proof: 1- when function is strictly increasing. Case (1)- For a < b , f(a) < f(b) , |f(a)| < |a| and |f(b)| < |b|. The co-ordinate [a,f(a)] will lie between negative of x-axis and line y=x and point [b,f(b)] will lie between positive of x-axis and line y=x, so there must exist at least a single point say [k,f(k)] at the intersection of line y=x. Hence k=f(x).

Case (2)- For d < e, g(d) < g(e) , |g(d)| > |d| and |g(e)| > |e|. The co-ordinate [d,g(d)] will lie between negative of y-axis and line y=x and point [e,g(e)] will lie between positive of y-axis and line y=x. so there must exist at least a single point say [l,g(l)] at the intersection of g(x) and line y=x. Hence l=g(l).

Case (3)- Let [m,f(m)] be any arbitrary point nearest to the line y=x on the curve of the function f(x) then its corresponding nearest point on the curve of the function g(x) will be (f(m),m). If the curve of the function f(x) intersect the line y=x at any point then the inverse g(x) of the function will also intersect at the same point. So m = f (m) = g (m). From cases (1), (2) and (3) we get f(c) = g(c) = c.

Case (4) - For a < b, $\mathbf{f}$(a) < $\mathbf{f}$(b), |$\mathbf{f}$(a)| > |a| and |$\mathbf{f}$(b)| > |b|. The co-ordinate [a,f(a)] will lie between negative of y axis and line y=x axis and point [b,f(b)] will lie between positive of y axis and line y=x. So there must exist at least a single point say [n,f(n)] at the intersection of curve f(x) and line y=x. Hence n=f(n).

Manuscript received ××× ××, 2010.

Manuscript revised ××× ×× , 201×.

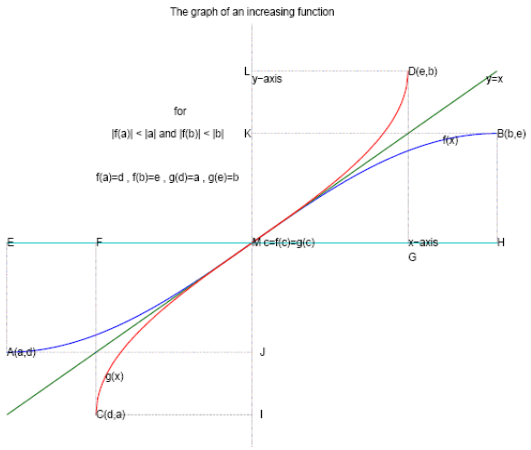

Case (5) - For d < e, g(d) < g(e) , $|g(d)| < |d|$ and $|g(e)| < |e|$. The co-ordinate [d,g(d)] will lie between negative of x-axis and line y=x and point [e,g(e)] will lie between positive of X-axis and line y=x. So there must exist at least a single point say (o,g(o)) at the intersection of curve g(x) and line y=x. So, o=g(o). From cases (3), (4) and (5) we f(c) = g(c) = c.

Case (6) - Since $\left|\int_a^c f(x)dx\right|$ = Area (AEM), $\left|\int_d^c g(x)dx\right|$ = Area (CFM). Since f(x) and g(x) is symmetric about line y=x, So Area (CFM) = Area (AMJ).

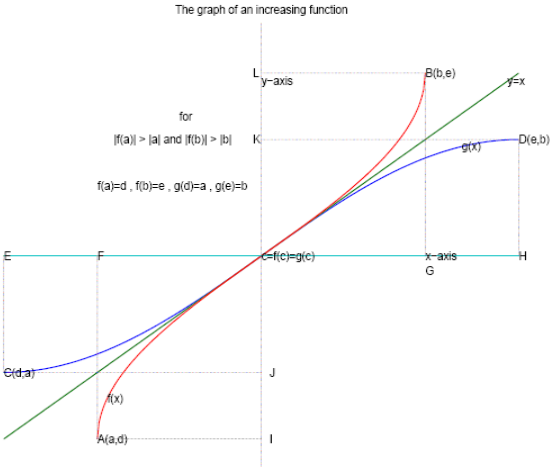

Hence $\left|\int_a^c f(x)dx\right| + \left|\int_d^c g(x)dx\right|$ = Area (AEMJ)

Case (7) - Since $\left|\int_c^b f(x)dx\right|$ = Area (BMH), $\left|\int_c^e g(x)dx\right|$ = Area (MDG). Since f(x) and g(x) are symmetric about line y=x so Area (MDG) = Area (MBK).

Hence $\left|\int_c^b f(x)dx\right| + \left|\int_c^e g(x)dx\right|$ = Area (MHBK).

Since $|a| = |b|$ and $|d| = |e|$, So Area (AEMJ) = Area (MBHK). Hence

$$\left|\int_a^c f(x)dx\right| + \left|\int_d^c g(x)dx\right| = \left|\int_c^b f(x)dx\right| + \left|\int_c^e g(x)dx\right|$$

When function is strictly decreasing:

Case (8)- For a < b , f(a) > f(b) the co-ordinate [a,f(a)] and [b,f(b)] lie on the opposite side of line y=x. So there must exist at least one single point say [p,f(p)] at the intersection of curve f(x) and line y=x. Hence p = f(p).

Case (9)- For e < d , g(e) > g(d) the co-ordinate [d,g(d)] and [e,g(e)] lie on the opposite side of line y=x. So there must exist at least one single point say [q,f(q)] at the intersection of curve g(x) and line y=x. Hence q=g(q). From cases (3), (6) and (7) we get f(c) = g(c) = c.

Case (10)-Since $\left|\int_a^c f(x)dx\right|$ =Area (AEM), $\left|\int_c^d g(x)dx\right|$ = Area (MGD). Since f(x) and g(x) is symmetric about line y=x, So Area (AMK) = Area (MGD). Hence

$$\left|\int_a^c f(x)dx\right| + \left|\int_c^d g(x)dx\right| = \text{Area (AEMK)}.$$

Case (11)-Since $\left|\int_c^b f(x)dx\right|$ =Area (BMH), $\left|\int_c^e g(x)dx\right|$ = Area (MCF). Since f(x) and g(x) are symmetric about line y=x, So Area (MCF) = Area (MBJ). Hence

$$\left|\int_c^b f(x)dx\right| + \left|\int_c^e g(x)dx\right| = \text{Area (MHBJ)}.$$

Since $|a| = |b|$ and $|d| = |e|$. So, Area (AEMK) = Area (MHBK). Hence

$$\left|\int_a^c f(x)dx\right| + \left|\int_d^c g(x)dx\right| = \left|\int_c^b f(x)dx\right| + \left|\int_c^e g(x)dx\right|$$

Proof: 2- Since c=0 the equation of the tangent on the curve of function f(x) and g(x) will be:

$$f'(c) = \frac{y}{x} \text{ and } g'(c) = \frac{y}{x}$$

On solving both equations we get:

$$y - x \times f'(c) = 0 \text{ and } y - x \times g'(c) = 0$$

Then the equation of bisector of both the tangents is given by:

$$\frac{y - x \times f'(c)}{\sqrt{1+[f'(c)]^2}} = + \frac{y - x \times g'(c)}{\sqrt{1+[g'(c)]^2}} \quad \text{and}$$

$$\frac{y - x \times f'(c)}{\sqrt{1+[f'(c)]^2}} = - \frac{y - x \times g'(c)}{\sqrt{1+[g'(c)]^2}}$$

On differentiating both these equation with respect to x, we get:

$$\frac{y' - f'(c)}{\sqrt{1+[f'(c)]^2}} = + \frac{y' - g'(c)}{\sqrt{1+[g'(c)]^2}} \quad \text{and}$$

$$\frac{y' - f'(c)}{\sqrt{1+[f'(c)]^2}} = + \frac{y' - g'(c)}{\sqrt{1+[g'(c)]^2}}$$

Case (1) - Since the graph of f(x) and g(x) are reflection image about line y=x, hence one the angle bisectors of both the tangents gives the equation of line y=x, and the slope of line y=x is given by $y'=1$. Substituting $y'=1$ in the above equation we get:

$$\frac{1 - f'(c)}{\sqrt{1+[f'(c)]^2}} = + \frac{1 - g'(c)}{\sqrt{1+[g'(c)]^2}} \text{ and}$$

$$\frac{1 - f'(c)}{\sqrt{1+[f'(c)]^2}} = - \frac{1 - g'(c)}{\sqrt{1+[g'(c)]^2}}$$

On squaring both sides we get:

$$\frac{[1 - f'(c)]^2}{1+[f'(c)]^2} = \frac{[1 - g'(c)]^2}{1+[g'(c)]^2}$$

On solving and simplifying we get:

$$[1+\{f'(c)\}^2 - 2f'(c)] \times [1+\{g'(c)\}^2] = [1+\{g'(c)\}^2 - 2g'(c)] \times [1+\{f'(c)\}^2]$$

$$f'(c) + f'(c) \times \{g'(c)\}^2 = g'(c) + g'(c) \times \{f'(c)\}^2$$

$$f'(c) \times g'(c)[f'(c) - g'(c)] - [f'(c) - g'(c)] = 0$$

$$[f'(c) \times g'(c) - 1] \times [f'(c) - g'(c)] = 0$$

Hence $f'(c) \times g'(c) = 1$ for $f'(c) = g'(c) \neq 0$

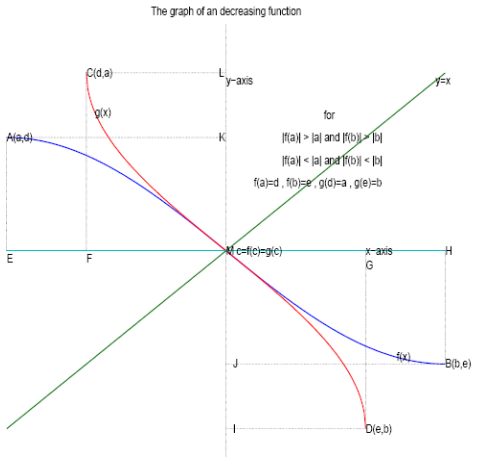

Case (2) - Since one of the angle bisector of both the tangents gives the equation of line y=x, so the other angle bisector of the tangents will be perpendicular to line y=x. Since the product of slope of two lines perpendicular to each other is equal to '-1', so the slope of second bisector is given by $y'=-1$.
Substituting $y'=-1$ in the previous equation in place of $y'=1$, we get:

$$\frac{-1 - f'(c)}{\sqrt{1+[f'(c)]^2}} = + \frac{-1 - g'(c)}{\sqrt{1+[g'(c)]^2}} \quad \text{and}$$

$$\frac{-1 - f'(c)}{\sqrt{1+[f'(c)]^2}} = - \frac{-1 - g'(c)}{\sqrt{1+[g'(c)]^2}}$$

On squaring both sides we get:

$$\frac{[1+f'(c)]^2}{1+[f'(c)]^2} = \frac{[1+g'(c)]^2}{1+[g'(c)]^2}$$

On solving and simplifying we get:

Hence $f'(c) \times g'(c) = 1$ for $f'(c) = g'(c) \neq 0$

We conclude from all the above cases that: $f(c) = g(c) = c$ and $f'(c) \times g'(c) = 1$ for $f'(c) = g'(c) \neq 0$ also

$$\left| \int_a^c f(x)dx \right| + \left| \int_d^c g(x)dx \right| = \left| \int_c^b f(x)dx \right| + \left| \int_c^e g(x)dx \right|$$

3. Conclusion:

We have studied the relationship between bijective function, Inverse of function and Identity function in a definite. We have derived some standard results on definite Integral which will be useful in all branch of science.

Three particles (heavenly bodies, vehicle and satellites) are moving in a plane with their respective path equations y=x, y=f(x) and y=g(x), If they satisfy the above stated theorem, then they can meet at a common point and the products of their velocities will be equal to one. This theorem is first of its kind which combines three functions and gives standard results in a bounded region.

Acknowledgments

I would like to heartly dedicate this paper to my father Late Shri. Mangal Das, mother Bibbo Devi and Brother Mr. Manish Kumar who always encouraged me in the field of research. My thanks go to Honorable Vice Chancellor Prof. P B Sharma, Delhi Technological University and Dr. K. Jayakumar, Joint Secretary of Council of Scientific and Industrial Research Government of India for their insightful suggestions. At last I would like to thanks my friends Mr. Thanvendra Singh and Mr. Rakesh Yadav for their help and moral support.

References

[1]. Sundaram Balchandram, K.P and Makki "On generalized continuous maps in topological spaces", Kochi University 12: 513, (H1991).

[2]. L.E. Boisad, D.O Regan and W.D Royalty "Existence and non existence for a singular boundary value problem", Applicable Analysis28: 245-246,(1988).

Utilization of Energy from Waste for Sustainable Development in Kaduna State, Nigeria

Yusuf Saleh
Department of Geography, Faculty of Science,
Kaduna State University, Kaduna, Nigeria

Abstract-This paper examines how waste can be utilized to produce energy for sustainable development. It analyses the problem using strength, weaknesses, opportunities and threats (SWOT) strategy. The result establishes that with adequate use of science and technology, waste can be utilized as a source of energy. It is recommended that there should be policy proposal and implementation to encourage public, private and individuals to utilize waste through availability of loans, tax holiday, man power training. Awareness campaign should be carried out by both government and NGOs to enlighten people on the benefit of utilizing waste as a source of energy.

Key words: Waste, Energy, Resources, Recycling, Sustainable Development

Introduction

The idea of utilizing energy from waste as a renewable source of energy in Nigeria is one whose time has come. Renewable source can serve as an alternative to some non renewable sources of energy particularly in Kaduna state. Various ways of converting waste to resources, particularly to energy have been documented from various part of the world by [1], [2], [3], [4], [5], [6], [7]and [8].

Thus the concern for production of energy from waste has become an important issue today and is very central to a sustainable use of the natural resource of a place.

In Kaduna state domestic wastes, agricultural bye products and to an extent institutional wastes are the main types of wastes generated in rural areas. Most of the agricultural bye products are used as sources of fuel for cooking. In urban and peri-urban areas the types of wastes found comprises of domestic, industrial, institutional commercial and agricultural. Industrial and commercial wastes are utilized, most especially at the Kaduna Petrochemical and Refining Company Limited (KRPC), Kaduna.

This paper examines how waste can be utilized to produce energy for sustainable development. It analyses the problem by using Strength, Weakness, Opportunity and Threats (SWOT) strategy. In doing this, information was gathered from literature only.

Conceptual Framework and Literature Review

The phenomenon of waste been utilized as sources of energy is being practiced in both the developed and developing countries. However, the degree to which waste is converted to energy varies markedly between the two worlds. In the developed countries the degree is much higher due to their vibrant economy, high level of technology, and the commitment by both public and private sectors of the economy. This is motivated by the urge to diversify their energy sources, thus they generate a lot of energy and revenue from wastes. In developing countries due to low technology, both the private and public sectors are not committed in recycling waste to

energy policy most especially with the availability of crude oil in Nigeria.

Wastes are unwanted materials or substances generated in the process of production and consumption of goods [9]. Waste can be categorized into solid, liquid and gaseous. While solid can be technically regarded as refuse, liquids are effluents while gaseous are in form of emissions, mostly from industries. Based on biological composition solid waste can be classified into the following three main types:

1. Biodegradable (composed of garbage and trash that can be degraded biologically overtime)
2. Semi biodegradable (partially biodegradable)
3. Non biodegradable (comprising of metal scraps and polythene/plastic waste)

Based on the chemical composition the liquid substances (effluents) are categorized into two types: toxic and non toxic.

Just as there are different composition and types, wastes are generated in different ways. However, in general and irrespective of composition, wastes are generated from five main sources in Kaduna state.

(1) Agricultural
(2) Industrial
(3) Domestic
(4) Commercial
(5) Institutional

As Burrow observed, cities generate large quantities of refuse; in the developed countries this can be 500 to 800 tones per day per million people. In the less developed countries refuse is likely to contain less packaging and more organic waste matter and may thus be easier to compost or generate methane from, but difficult to compress or incinerate. Per capital waste generation varies very widely. In industrialized countries, the amount of waste generated is estimated at 1.80kg/person/day [8]. While in developing countries represented by Nigeria the estimate is 1 kg/person/day [6].

Energy derived from waste can be in various forms viz electricity and or heat. Waste conversion to energy processes involves several processes i.e physical, biological, chemical and thermal processes. Electricity can be obtained directly through combustion or to produce combustible fuel such as methane, ethanol, synthetic gas (Syngas) and several others. Waste materials are now been recycled especially metals, paper, plastic, bottles and so on which gives the following:

(i) **Refuse derived fuel (RDF)**: This is the fuel that is derived by shredding and steaming municipal waste i.e steaming under pressure in an Autoclave. RDF is based on organic components of municipal waste especially organic biodegradable waste etc. RDF processing facilities are normally located near waste sources.The product of RDF is used to produce electricity by feeding into gasification or pyrolysis plant.

(ii) **Biogas**: This is the extraction of energy from biomass using anaerobic digestion to produce biogas. In this process animal and human wastes are fed into a closed digesting chamber where they are broken down anaerobically to produce a gas which is a mixture of methane and carbon dioxide. It can be used for cooking or generation of electric power [7]. In countries such as Switzerland, Germany, Sweden etc the methane in the biogas may be concentrated in order to use it as vehicle fuel or as direct input into the gas mains [6].

(iii) **Landfill Gas**: In a well managed landfill, when the biodegradable materials decay, gas especially methane, carbon dioxide with

traces of nitrogen, hydrogen, oxygen, hydrogen sulphide and a range of trace organic compounds are produced. These are extracted or pumped out of the land fill using perforated pipes, the gas may be flared off or burnt in a gas engine to generate electricity or it may be piped into homes to be used for domestic purposes.

(iv) **Synthetic gas (Syngas)**: This is obtained through the process of gasification and the process is characterized by the partial combustion of municipal waste at a high temperature in a reactor, with combustion facilitated through the application of air, oxygen or steam. The resulting chemical reactions produce Syngas. It can be used in gas engine and turbines for the production of electricity [3].

(v) **Ethanol**: This is also obtained from waste through many processes. First, is from the bye product of agricultural produce such as corncobs, straw, rice hulls, saw dust and sugar cane bagasse among others. Cellulose is produced from these materials which are converted to sugar, sugar is then later fermented to produce ethanol. General motors on January 14, 2008 announced a partnership with Coskata Inc the goal of which is to produce cellulose ethanol cheaply, with an eventual goal of $1 per gallon for fuel [10]. Secondly, ethanol can be produced from the bye product of petroleum refining and recently from commercial chicken waste. Ethanol is used largely as motor fuel and fuel additive mostly in Brazil, Canada and the United States.

(vi) **Energy from incineration**: Incineration is a process that involves the complete degradation and combustion of carbon based material in municipal waste through the application of heat in an oxygen rich environment. The excess heat produced is recovered during combustion to produce steam or converted into electricity by means of steam turbine generators. It can be done on a small scale by individual or on a large scale by industries. This is commonly practiced in countries such as Japan, UK, Germany, USA and Canada among others.

(vii) **Energy from used oil**: This process involves refining and the removal of waste, insoluble dirt, heavy metals, nitrogen, chlorine and oxygenated compounds from oil drained, from automobiles or other machines. The resulting product is called Re-Refine oil. Extensive laboratory analyses and field studies have shown that re-refine oil is equivalent to virgin oil. As observed by American Petroleum Institute, recycling just two gallons of used oil can generate electricity to an average house hold for 24 hours and it takes 42 gallons of crude oil, but only one gallon of used oil to produce 2.5 quarts of high quality lubricants.

Energy from Waste as a Tool for Achieving Sustainable Development:

As a result of the need for man to seek for growth and development which encourages him to exploit the environmental resources, this has resulted in generation of enormous amount of waste. This has prompted the

need to protect, safeguard, manage and conserve the natural resources. This is the main reason why the concept of sustainable waste management was established. In the context of global development, there is a general concern that if the present rate of human induced depletion of ecosystem resources continues unchanged, the limits to growth on earth could be reached in less than one hundred years [11]. In other words, the current pattern of development may not be sustainable, and sustainable development must therefore balance the needs of society, the economy and the environment [12]. The concept of sustainable development explains that with proper development strategies, environmental resources can be exploited (or developed) gainfully for the well being of the present generation and still be available in good condition for generations yet unborn [13].

The Swot Analysis

S- **Strength**: The urban, peri urban and the rural areas of Kaduna state generate large volumes of waste. Kaduna city alone is projected to generate 1,058,500 tonnes of waste in 1996 [14]. The major types of wastes are biodegradable which can be composted while the rest can be incinerated to produce electricity if adequately generated. This project can be spearheaded by the state government and supported by the private sector. Others are:-

Agricultural bye products such as corncobs and straws which are used for cooking purposes in rural areas and used to provide light in Koranic Schools at night in the Northern part of the state. The stems of fell trees are utilized to produce charcoal.

Commercial Wastes include those generated from carpentry and or tailoring activities among others. They are used as fuel additives in homes, popularly known as “kashin Tela” or “kashin Kafinta”.

Industrial Waste are utilized at the Kaduna Petrochemical and Refining Company Limited (K.R.P.C), here oil waste obtained during refining process are reused as oil or as fuel in some machines, also cabon monoxide (CO) is utilized for steaming purposes.

These various wastes can be used as raw materials for small scale industries which may be supported by the state government and the private sector.

W- **Weaknesses**: The major weaknesses are inefficiency in the methods of waste collection, lack of waste sorting at household level, lack of depot where waste sorting can be actually done, in availability of capital and poor technological knowledge in Kaduna state. All these slow down the whole process of recycling wastes to energy; so also the low level of awareness and literacy vis-à-vis the cultural settings and political instability among others.

O- **Opportunity**: This is an important sector on its own and a lot could be achieved if it is wisely utilized. It creates substantial employment opportunities and generates a lot of income or revenue to its practitioners. There would be better sanitation, reduction of the amount of waste that will be physically disposed, reduction of air pollution, elimination of the breeding ground of disease vectors e.g mosquitoes, rodents etc while the contamination of underground water through leachate from the dumps or land fill sites would be minimized. The use of waste as a source of energy would lead to preservation of natural resources for generations yet unborn for sustainable development. An example is that the effluents

from both domestic and industrial areas can be diverted using canals to a reservoir to serve as Boiler water. Energy would be utilized from RDF/ Incinerators to process it to generate electricity apart from the energy obtained from the RDF or Incineration.

The processes of waste to energy are as illustrated below:-

Biomass Gas collector → Biogas → Fuel + Electricity

Waste → Autoclave → RDF → Pyrolysis/gasification → Electricity

Waste → Landfill → Methane/gas → Landfill gas → Electricity+Gas

Waste → Reactor → Syngas → Electricity

Waste → Cellulose → Ethanol → Fuel

Waste → Incinerator → Stem turbine generators → Electricity

Used Oil → Laboratory → Re-refine Oil + Electricity

Waste→ Household Burning → Energy

T- **Threats**: The contemporary ways of processing waste to energy is not currently used due to the heterogeneous nature of the waste which make it difficult to handle; workers' health risk; lack of finance; as some of the methods are expensive; difficulty of locating waste processing near the sources of waste; low quantity of waste available; ignorance because as it needs to be practiced by everyone even at the grassroots so as to maximize energy utilization; maintenance culture and so on.

Conclusion

The paper has reviewed the current nature of how energy can be utilized from waste. Although this may not give an accurate reflection of what is on ground, however it has to be noted that the practice of utilizing energy from waste is technical and costly but will save a lot of natural resources in Kaduna State from been exploited and reduce the amount of waste that will be physically available. Finally, various ways of converting waste to energy are now widely practiced in developed countries and there is need to emulate them in this country as it can help to improve the local economy. These may be encouraged through appropriate policy formulation and implementation, provision of loans, tax holidays, man power training etc to public, private and individuals. Awareness campaign should be carried out by both government and NGOs to enlightened people on the benefit of utilizing waste as source of energy. These will reduce the threat to public health and aid in conserving natural resources, most especially the non renewable resources.

Thus, the paper has shown that with adequate use of science and technology, waste can be utilized as a source of energy, much in the way the KRPC utilizes its carbon monoxide (C0) in steaming. But the practice is very low in the state, much the same as in other states of Northern Nigeria.

References

[1]American Petroleum Institute. www.wikipaedia.org/wiki/waste as of April, 02, 2008.

[2] Burrow C. J. **Developing the Environment: Problems and Management**, Longman. 1993

[3] Gartner Lee Limited, **New and emerging residual waste management technologies**, Paper for Regional District of Nanaimo (RDN) and Cowichan Valley Regional District (CURD), Canada. 2005

[4] R. M. Harrison, In C.J. Burrow, **Developing the Environment; Problem and Management,** Longman. 1993

[5] New Scientist, In C. J. Burrow, **Developing the Environment: Problems and Management**, Longman. 11/12/1993

[6] Y. Saleh, "The Management of Waste As A Resource"**, Paper Presented at the Nigerian Institute of Management Monthly Meeting**, Kaduna. 2008

[7] A. Strahler, and A. Strahler, **Physical geography; Science and systems of the human environment**, India: John Wiley and Son (Second Edition), 2007

[8] S. N. Uchegbu, **Environmental Management and Protection,** Enugu, Nigeria: Precision Printers and Publishers, 1998

[9]A. M. Ibrahim, **Introduction to environmental problems and management**, Kano Wa'adallah Environmental Consults (WADEC). 2002

[10] Wikipedia. www.wikipaedia.org/wiki/waste as of April, 02, 2008

[11] Oladipo. In F. A. M Ivbijaro, F. Akintola, and Okechukwu, R.U: **Sustainable Environmental Management in Nigeria.** Ibadan, Nigeria: Mattiu Production, 2006.

[12] F. A. M Ivbijaro, F. Akintola, and R. U Okechukwu, **Sustainable Environmental Management in Nigeria.** Ibadan, Nigeria Mattiu Production. 2006.

[13] E. A. Olofin, "The Meaning, Concept and Application of E.I.A in Planning**", Workshop in Futy**, Yola, Nigeria. 2001

[14] Federal Ministry Of Housing and Environment (1990): In A.N. Sankey, An Evaluation of Kaduna Environmental Protection Authority (KEPA) Solid Waste Management Practice in Kaduna Town from 1980 to 1996. MSc Thesis, Department of Geography and Planning, University of Jos, Nigeria, 1999.

Selection of Insert to Reduce Tooling Cost of Bar Peeling Machine

Ravi K. Patel[1] and Bhaveshkumar P. Patel[2]
[1,2] Assistant Professor, Mechanical Engineering Department,
U. V. Patel College of Engineering, Kherva-382711, Gujarat, India

Abstract - Industries around the world continually strive for lower cost solutions with improved quality and reliability in order to maintain their competitiveness. Even though the machine tool industry in India has made tremendous progress, the metal cutting industries continue to suffer from a major drawback of not running the machine tools at their optimum operating conditions as well as not getting the desired quality of the product with economical cost. In this work, three different inserts were utilized to get the different surface qualities of the bright bar. Out of three inserts, one RNGH 2509 MOS50-R50 is selected based on the experimental data, in which it provides better surface quality compared to existing insert and it saves the tooling cost up to 41.66 % for the bright bar batch size of 500. By selecting the new insert, one pass of grinding is eliminated entirely from peeling process. So it reduces the production time as well as the cost.

Key words: *Bar peeling machine, Bright bar, Insert, Surface finish.*

1. Introduction

Bar peeling is a method, which is used to remove oxide scale, mill scale, surface cracks, etc. from hot-rolled and forged blanks. The size of blank can vary from 4 mm to over 400 mm in diameter. Compared with conventional turning, bar peeling is a method of machining which provides high productivity and low production costs due to the shorter throughput times. The surface quality and dimensional tolerances are also high, which in turn leads to less machining at succeeding stages. [1]

Fig. 1 Peeling Machine

During the peeling operation the bar is moved through a rotating peeling head, with a radial direction of cut. The peeling head in this case has four cartridges; each with one to three inserts which are all in contact with the bar. The inserts serve for roughing and finishing.

Stainless steel bright bars have a very wide application from small fasteners to a very critical mechanical shaft. Stainless Steel Bright Bars are being used because of its high tensile properties as well as anti corrosiveness. Stainless steel bright bars are being used in fastener industry, shafts for ships, chemical pump industry, manufacturing stainless steel valves, manufacturing precision machined components in stainless steel, window grills, stainless steel decorative hardware's and many more. Bar peeling is also applied to thick walled tubes. The most common materials which are peeled are carbon steel, spring steel and stainless steels. Bar peeling is also applied to other materials, such as high-temperature steel, titanium, aluminum and uranium. Application areas vary, but bar peeled blanks are often used as an intermediate stage in the production of products, which are to be processed further. Examples of these are extrusion blanks for tube manufacturing and axle components for the automobile industry. [1]

2. Problem Formulation

The experimental work carried out on bright bars. The bright bars are produced by two processes, (1) Cold Drawing and (2) Peeling. In cold drawing process, the material being drawn is at room temperature (i.e. Cold-Drawn). The pointed/reduced end of the bar or coil, which is smaller than the die opening, is passed through the die where it enters a gripping device of the drawing machine. The drawing machine pulls or draws the remaining unreduced section of the bar or coil through the die. The die reduces the cross section of the original bar or coil, shapes the profile of the product and increases the length of the original product. In Cold Drawing process the bars which are drawn ranges from 14 to 40 mm. And on the bar peeling machine the bars are produced in range of 20 to 75 mm. In peeling machine, the black bars are passed through the rotating cutter head containing cutting inserts. Due to the relative motion between the bar and insert, the bar material is removed from periphery and thus we get required size of bright bar. In peeling machine the black

bars are peeled off to get the bright bars of the required size. During the peeling operation the bars are getting a helical pattern, 'ringing', as shown in figure 1, on their surface. So, more tolerance is to be provided on the peeled bars (around 0.1 – 0.5 mm).

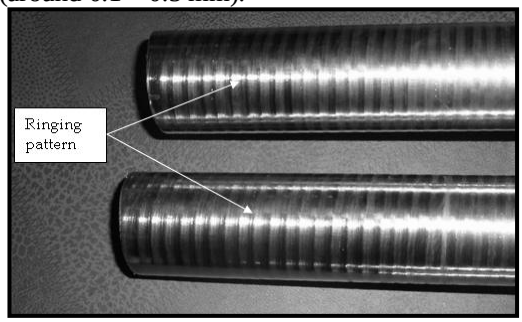

Fig. 2 Ringing pattern on bright bar

After peeling operation, the bars are taken on the center less grinding machines, at where the grinding is done on the bars to achieve the required size. This is done with the help of 3-4 grinding passes as shown in figure 2. So, the operation cost increases.

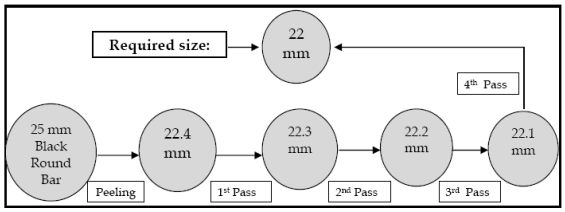

Fig. 3 Bar peeling process steps

The bar is passed through grinding machine and so there are some losses which are adding the cost of final product. The losses like material loss, consumable loss, time loss, electricity loss, labor loss are the main losses which increases the process cost and ultimately the product cost. Figure 4 indicates different losses.

Fig. 4 Losses due to more grinding passes

So, it is required to reduce the losses and the cost of bright bar by reducing/eliminating the problem of 'ringing' pattern on bright bar. The specification of machine which was used for experimental work as given below:

Available Data:

Machine No. : P-3
Machine type : Peeling machine
Supplier : Gajanan ISPAT Pvt. Ltd.
Capacity : 20 mm to 75 mm.
Depth of cut : 1 to 3 mm
Tool: TC tool : Dia.-25mm and 32 mm
Burnishing Roller : Material – HcHcr
: Hardness – 64 HRC
: Qty. – 3 Nos.
Pinch Roll : EN-24
(Feed Roll) : Hardness – 60 HRC

Peeling machine feed and speed: The peeling machine can achieve different speed and feed combinations by different combinations of gears. Table 1 shows different speed and feed for respective gear.

Table – 1 : Speed and Feed of peeling machine - 3

Gear No.	***Feed (mm/rev)***	***Cutter head speed (rpm)***
1	3.296	228
2	5.341	318
3	7.0986	772
4	8.6201	852

Bright Bar Material: For the experimental work, we have chosen the material of bar as SS-202. Chemical composition and mechanical properties of SS-202 are shown in table 2.

Table 2 : Chemical composition and Mechanical properties of SS-202[2]

Material	***Compositions***	***Mechanical properties***
SS-202	C – 0.15% Max.	Tensile Strength 515 Mpa
	Mn – 8-10%	
	Cr – 17-19%	Yield Strength (Mpa) 275 Mpa
	Ni – 1% Max.	
	P – 0.080%	Elongation (%) 40
	S – 0.03% Max.	Elastic Modulus 190-210 Gpa
	Si – 1% Max.	
	Cu – 1.5% Max.	Density 7.8 (×1000 kg/m^3)

3. Insert Selection

Insert selection is very important for bar peeling operation. The insert RCMT 2507 MOS50 – R50 (Round Insert) was used as in existing practice. The bars, which are produced with this insert, are having ringing pattern.

Precision Rolled Products Inc. (PRP), a company of Krupp VDM GmbH, with cutting-tool supplier Sandvik Coromant (Fair Lawn, NJ), helped PRP achieve a 70% improvement in surface-finish quality for bars peeled using the new bar turner, which uses Sandvik inserts. The change enabled PRP to eliminate centerless grinding for a significant portion of the company's Ti6AL-4V bar production, saving time, labor, and materials. They eliminated the ringing problem by changing the tool inserts.[2] So with reference to that we also tried to improve the surface quality by changing the inserts. There are different types of inserts available in market with different shapes. But we have selected only round inserts because existing setup of cutter head was with reference to round insert, which is used right now. If other shape of insert was selected then the whole setup should be changed and that will cost more and other complications may arise due to change in shape. So we have selected different round inserts with different grades.

Using existing insert we are getting ringing pattern as shown in fig. 5.

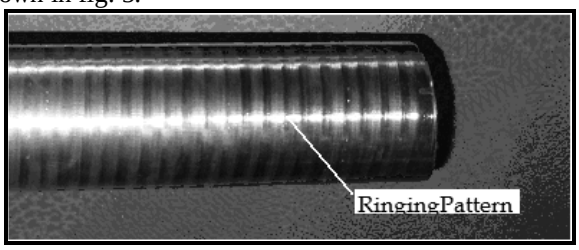

Fig. 5 Ringing pattern on bright bar (For insert RCMT 2507 MOS50 – R 50)

Other inserts, used for experiments, are shown in table 3:

Table 3 Selected Inserts for Experimental Work

Sr. No.	***Insert***	***Shape***
1	RNMG 2509 MO-MR	ROUND
2	RCMX 2507 MOS50-R50	ROUND
3	RNGH 2509 MOS50-R50	ROUND

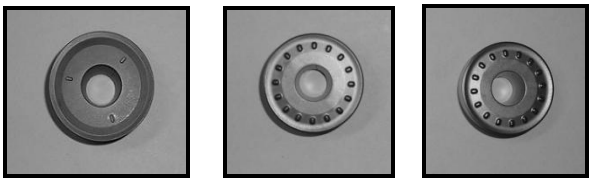

Insert-1 Insert-2 Insert-3

Fig. 6 Selected inserts

3.1 Cutting parameters for experimental work

Material : Stainless steel Grade SS 202
Batch size : 500 Bars
No. of batches : 3
Cutting Speed (rpm) : 772,
Bar length : 4 m,
Feed : 7.0986 mm/rev.

Tool changes, cost of tool and cost saving is considered for selected batch size. The experimental work is carried out for 3 batches of each 500 bars for individual inserts and following tables shows the average of result.

(1) Insert RNMG 2509 MO-MR

Table 4 shows comparison between existing insert and insert 1 taken for experiment.

Table 4 Existing Insert and Insert 1

	Present situation	***Experiment***
Insert	RCMT 25 07 MOS50 – R 50	RNMG 2509 MO-MR
Grade	-	2135
Cost for insert	800 RS.	800 RS.

Table 5 shows results obtained after replacing existing insert with insert 1.

Table 5 Result of Existing Insert and Insert 1

Tool changes	12	10
Cost of tool (Rs.)	9600	8000
Cost saving	1600 Rs. (16%)	

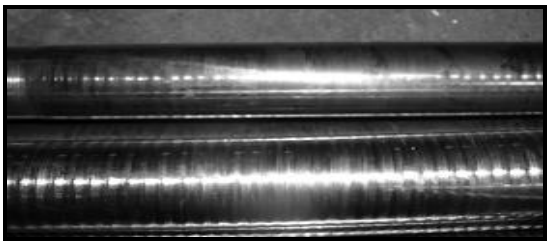

Fig. 7 Ringing pattern on bright bar (For insert RNMG 2509 MO-MR)

Figure 7 shows the ringing pattern on the bright bar by using the insert RNMG 2509 MO-MR, in which we are getting comparatively less ringing effect on it. Here tool changes are reduced.

(2) Insert RCMX 2507 MOS50-R50

Table 6 shows comparison between existing insert and insert 1 taken for experiment.

Table 6 Existing Insert and Insert 2

	Present situation	***Experiment***
Insert	RCMT 25 07 MOS50 – R 50	RCMX 2507 MOS50 - R50
Grade	-	1635

Cost for insert	800 RS.	800 RS.

Table 7 shows results obtained after replacing existing insert with insert 1.

Table 7 Result of Existing Insert and Insert 2

Tool changes	12	9
Cost of tool (Rs.)	9600	7200
Cost saving	2400Rs. (25%)	

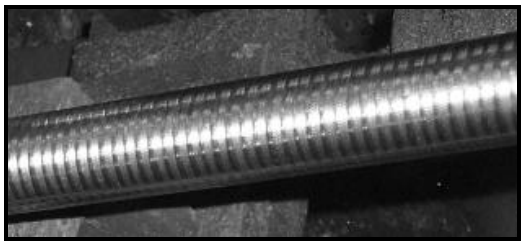

Fig. 8 Ringing pattern on bright bar (RCMX 2507 MOS50-R50)

Above figure 8 shows, the ringing pattern on the bright bar by using the insert RCMX 2507 MOS50-R50, in which we are getting comparatively same as the existing ringing effect on it. But here tool changes are reduced.

(3) Insert RNGH 2509 MOS50-R50

Table 8 shows comparison between existing insert and insert 1 taken for experiment.

Table 8 Existing Insert and Insert 3

	Present situation	***Experiment***
Insert	RCMT 25 07 MOS50 – R 50	RNGH 2509 MOS50 - R50
Grade	-	2025
Cost for insert	800 Rs.	800 RS.

Table 9 shows results obtained after replacing existing insert with insert 1.

Table 9 Result of Existing Insert and Insert 3

Tool changes	12	7
Cost of tool (Rs.)	9600	5600
Cost saving	4000 Rs. (41.66%)	

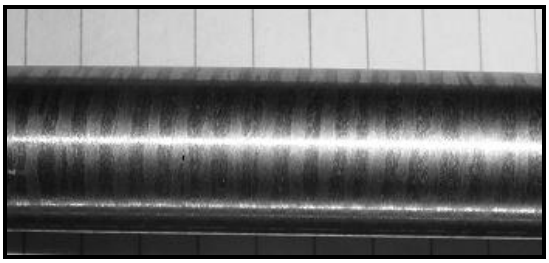

Fig. 9 Ringing pattern on bright bar (RNGH 2509 MOS50-R50)

Above figure shows the ringing pattern on the bright bar by using the insert RNGH 2509 MOS50-R50, in which we are getting comparatively very less ringing effect on it. Also here tool changes are reduced for selected batch size.

4. Results and discussion

We have carried out experiments with 3 selected inserts and the results obtained are shown in table 10.

Table 10 Selection of Insert with Cost Saving

Sr. No.	***Insert***	***Cost saving in Rs. Per batch size***
1	RNMG 2509 MO-MR	1600 (16%)
2	RCMX 2507 MOS50-R50	2400 (25%)
3	RNGH 2509 MOS50-R50	4000 (41.66%)

Based on experimental work, insert 1(RNMG 2509 MO-MR) saves around 16% of tooling cost per batch of 500 bars. Insert 2 (RCMX 2507 MOS50-R50) saves around 25% of tooling cost for same batch size. And Insert 3 (RNGH 2509 MOS50-R50) saves around 41.66% of tooling cost for same batch size. So comparing all the three inserts, we have selected insert 3 (RNGH 2509 MOS50-R50) in place of existing insert (RCMT 25 07 MOS50 – R 50) for bar peeling operation. Also the third insert gives smoother surface as compared to existing insert. So one pass of grinding is removed which reduces overall operational cost and also saves time.

5. Conclusion

Three inserts were used for the experimental work to reduce the ringing pattern and to improve surface finish of the bright bar. Out of three inserts, one RNGH 2509 MOS50-R50 is selected based on the experimental work, in which it provides better surface quality compared to existing insert and it saves the tooling cost up to 41.66 % for the bright bar batch size of 500. By selecting the new insert, one pass of grinding is eliminated entirely from peeling process. So it reduces the production time as well as the production cost.

References

[1] www.bhambraindia.com/index.php
[2] www.industrialnews.com/Precision rolled industries

Harnessing the Potentials of Wireless Sensor Networks in the Context of Developing Countries: A Theoretical Perspective

D. O. Ayanda[1], A. I. Oluwaranti[2], S. I. Eludiora[3], O. M. Alimi[4]

[1,2,3,4]Department of Computer Science and Engineering,

Obafemi Awolowo University, Ile-Ife, Nigeria.

Abstract - Wireless Sensor Network (WSN) is an emerging technology that has the potential of transforming human life in the future. These sensor nodes can operate without any attendance in an environment and location including those where human presence is risky or not possible and therefore they can be deployed in a countless number of applications ranging from military to civilian purposes.

This paper examines the various applications of WSNs and how real-life deployment can form the bedrock of development towards achieving the Millenium Development Goals (MDGs) and the much awaited Vision 20:2020 in Nigeria. The study also attemps to establish a synergy between reviving the economic growth as evidenced from government efforts through various initiatives and science and technology through adoption of the potentials of WSNs. The paper concludes by recommending practical approach that can be taken by the Nigerian government towards actualizing the evolving technology.

Key words: *Wireless sensor networks, sensor nodes, applications, science and technology, government*.

1. Introduction

Developing countries especially Nigeria are faced with myriad of challenges on their way to industrialization and economic well-being. There is growing tension between short-term economic development goals and a long-term sustainable policy as exemplified by the eight Millennium Development Goals [29]. Endorsed by 189 United Nations member states in 2000, the Millennium Declaration lists the eight following goals as the primary targets for an equitable and sustainable human development:

1. Eradicate extreme poverty and hunger.
2. Achieve universal primary education.
3. Promote gender equality and empower women
4. Reduce child mortality
5. Improve maternal health
6. Combat HIV/AIDS, malaria, and other diseases.
7. Ensure environmental sustainability
8. Develop a global partnership for development

Millennium Development Goals (MDGs) analytically anchored in the human development paradigm, representing a set of time-bound quantitative targets to reduce human poverty in its basic dimensions [14]. They also represent a global commitment, a shared responsibility for both the developed and the developing world and provide a platform for addressing all challenges, especially human development challenges around the globe.

Consequently, efforts have been geared towards achieving this initiative by Nigerian government most especially during the beginning of civil rule of Obasanjo's regime in 1999. Ilori *et al*. [14] further recognized the efforts of Nigerian governments at the three levels of government in the process of transformation of its political, economic and social systems. These efforts include the launching of "Economic Empowerment and Development Strategy" a document known as 'National Economic Empowerment and Development Strategy' (NEEDS) at the national level; 'State Economic Empowerment and Development Strategy ' (SEEDS) at the state level; and 'Local Economic and Development Strategy' at the local governments level. These documents provide a framework for a nationally coordinated programme of action by the federal, state and local governments; and focus on four key strategies of re-orienting values, reducing poverty, creating wealth, and generating employment [21]

In the same vein, transitioning from civil rule to another civil rule produced Yar'adua's Seven-Point Agenda in 2007 as a result of his election covenant with the people of Nigeria. Since then, the Agenda have been properly conceptualized and comprehensively articulated and the implementation strategies adequately laid out, to ensure the realization of Vision 20:2020. As spelled out by the Information Section, Nigeria High Commission in UK [15], this Agenda include:

1 Critical Infrastructure - This sector has been seen as the bane of under-industrialization in Nigeria. Failure to provide adequate and reliable electricity, telecommunication, and transportation among others justifies the evolution of initiatives to transform the industry. The thrust of the transport policy, for instance, is the attainment of efficient inter-modal system that would effectively link the different means of transportation. Not only would this bring down the cost of doing business, it will also enhance the growth of Gross Domestic Product (GDP) of the country.

2 Food Security – Agriculture is constrained by various challenges and is characterized by low output, inefficient and antiquated production tools and infrastructure. The technological inadequacies in standardization and quality control have stunted natural farm produce, rendering it uncompetitive in local and international markets.

3 National Security and Intelligence – The success of any Government is measured by its ability in providing security of life and property. The primary challenges, therefore, revolve around the ability of the Government to discharge its constitutional duties to the governed. Lack of security portends a great danger to the polity and to the safety of economic and social sectors of the society.

4 The Niger Delta – There are currently four identifiable challenges, among others, facing the region – economic, environmental, infrastructure and socio-political challenges. Efforts have been geared since Obasanjo's Administration in 1999 till date towards meeting these challenges and improving the general well-being of the people in the region. Failure to fundamentally address these issues would undermine efforts to promote inward investments and economic development since this region is the backbone of oil production in the country.

5 Human Capital Development – The provision of health, education and functional social safety nets are absolutely essential to achieving desirable human capital outcomes. This also requires improving human resources for tackling maternal and child mortality while mobilizing additional resources to address funding gaps for health sector programmes and other related multi-layered activities across the country.

6 Land Tenure Changes and Ownership – The paucity of long term funds is considered to be a barrier towards financing housing in Nigeria. More so, the banking sector has consistently demonstrated its aversion to financing home ownership. This has attracted urgent reforms through a legal and regulatory framework including laws inhibiting efficient land transaction while ensuring a more conducive monetary and fiscal measure to sustainable housing finance.

7 Wealth Creation – There is no gainsaying that there has been an increased incidence of poverty in Nigeria since independence as a result of her undue reliance on revenue accrued from non-renewable sources such as oil. This has also led to the poor performance of the industry. There is therefore need geared towards wealth creation through diversified production especially in allied sector and solid minerals sector. Figure 1 below illustrates the strategic model description of the Seven-Point Agenda.

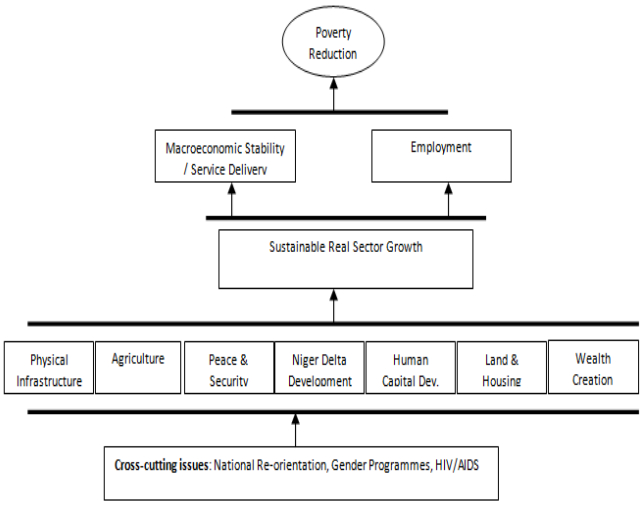

Fig. 1 Strategic Framework for Achieving Vision 20:2020

All the highlighted initiatives are responses at meeting the MDG goals. However, while the revival of economic growth in Nigeria has evidenced from the government efforts is a welcome development, there is a need to recognize the fact that the bane of any economic growth lies in science and technology.

Consequent on the above, this paper examines the emerging potentials of Wireless Sensor Networks and its various applications and how they can be relevant towards achieving the much awaiting Vision 20:2020 in Nigeria. The remaining parts of this paper will be divided into four sections. Section two discusses the emergence of WSNs based on the empirical evidence and characteristics. Section three brings to the fore the various applications in which WSNs lend themselves to while section four projects into the future of WSN. Section five concludes the study and recommends policy towards harnessing the potentials of WSNs.

2.0 Emergence of Wireless Sensor Networks

2.1 Empirical Evidence

The convergence of Internet, communications, and information technologies, coupled with recent engineering advances in low-power wireless communications, Micro Electro-Mechanical Systems (MEMS) and nanotechnology [8], is paving way for a new generation of inexpensive sensors and actuators, capable of achieving a high order of spatial and temporal resolution and accuracy. Wireless Sensor Networks (WSNs) are composed of sensor nodes which are tiny autonomous devices that combine sensing, computing and wireless communication capabilities.

The wireless sensor nodes are deeply embedded into the physical surroundings, and gather and process information such as temperature, humidity, light characteristics, seismic activities or images and sound samples from the physical worlds. Networked systems of such sensors are expected to be used in a variety of applications including habitat monitoring, precision agriculture, disaster recovery operations, health care and supply chain management [3][16].

In an article written by Kris Pister [22], he described his vision of sensor networks in 2010, "*…in 2010 your house and office will be aware of your presence, and even orientation, in a given room. Lighting, heating, and other comforts will be adjusted accordingly…in 2010 a speck of dust on each of your fingernails will continuously transmit fingertip motion to your computer. Your computer will understand when you type, point, click, gesture, sculpt, or play air guitar…".* There is no doubt that researchers are making progress in realizing this vision come true. In the recent time, several real-life implementation of sensor networks are commonplace: CodeBlue, an infrastructure designed to support wireless medical sensors, PDAs and other devices which may be used to monitor and treat patients in various medical scenarios was developed by joint effort of Harvard University with the School of Medicine, Boston, USA [11]; SmartDust Project [23] at Berkeley pushes the size limit of sensors to an extreme – a cubic millimeter, such that these sensors can float in the air like dust; WINS (Wireless Integrated Wireless Sensors) project at University of California, Los Angeles (UCLA) [24] and WSN (Wireless Sensing Network) project at Rockwell Science Centre [26] integrate multi-modality sensing devices and low-level signal processor on the microsensor, making it more intelligent and powerful.
Indeed, there is currently extensive interest in this discipline not only from academia and government but also from developers, manufacturers, startup companies, investors and original equipment manufacturers. According to industry observers, the wireless sensors market has since taken off commercially [12]. And advances in the areas of sensor design and materials that have taken place in the recent past has led, almost assuredly, to significantly reductions in the size, weight, power consumption, and cost of sensors and sensor arrays [1].

The essential function of a sensor network is to identify the state of an environment using multiple sensors. Other aspects of sensor network design, such as the communication, power, and computational resources, are evaluated by their ability to facilitate this function as shown in Figure 2.

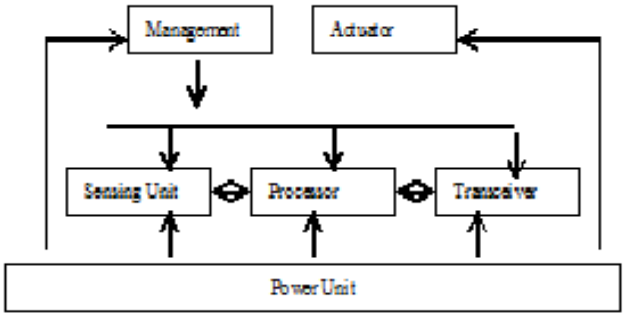

Fig. 2 Basic Architecture of a Sensor Node

Also, in most applications, the use of battery-powered devices is very convenient to make the deployment of such nodes easier. To let the network work under specified performance requirements for a sufficient time (denoted as network lifetime), the nodes must be capable of playing their role for a sufficiently long period using the energy provided by their battery, which in many applications should not be renewed for a long time. Thus, energy efficiency of all tasks performed by a node is a must for the WSN design.

2.2 Characteristics of Wireless Sensor Networks

Wireless sensor nodes have distinguishing features that allow the nodes to self-organize into a non-infrastructure network with dynamic topology. Typically, the number of nodes in a sensor network is much higher than in an ad hoc network, and dense deployments are often desired to ensure coverage and connectivity [24]. Hence, the sensor network hardware should be relatively cheap.
Sensor network hardware should be power-efficient, small, inexpensive and reliable in order to maximize network lifetime, add flexibility, facilitate data collection and minimize the need for maintenance.

3.0 Application of Wireless Sensor Networks

The technology for sensing and control now has the potential for significant advances, not only in science and engineering, but equally important, on a broad range of applications relating to critical infrastructure protection and security, health care, environment, energy, food safety, production processing, quality of life, and the economy. Subsequently, some of the areas of applications are highlighted.

3.1 Environmental monitoring

Wireless sensor networks are intended to be deployed for several types of applications, an example is environmental

monitoring. In this case, each node may be endowed with a temperature sensor, and the goal may be to monitor temperature over the domain. On the other hand, the maximum temperature over the domain could be monitored, which may in turn, be used to flag an alarm when it exceeds a certain critical threshold value. A distinguished node in the sensor network may be dubbed a 'collector node', and it is the goal of the information processing within the network to deliver the desired statistic, say, the mean temperature or the maximum temperature, to this collector node, from where this desired information may be filtered out of the network. Thus the collector node may be regarded as an 'output unit'. The 'input units' are the measurements taken at the sensing nodes in the network. Everything else that comes in between, that is, the entire network itself, is the information processing system. Wireless sensor networks thus combine three aspects – sensing by nodes, computational capabilities at nodes, and wireless information transfer between nodes.

3.2 Security & Intelligence

WSNs are widely used in military applications such as surveillance and communication from intractable areas to the base stations. Since these sensors are inexpensive and deployed in large numbers, loss of sensors would not affect the purpose for which they are deployed. An intriguing example is DARPA's self healing minefield where a self – organizing sensor networks with a peer-to-peer communication between anti-tank mines has been used to respond to attacks and redistribute the mines in order to heal breaches while complicating the progress of enemy troops [13].

Another military application is urban warfare whereby sensor nodes could be deployed in urban landscape to detect chemical attacks or track enemy movements. In the study conducted by [19], an ad hoc acoustic sensor network for sniper localization named 'PinPtr' was developed to detect the muzzle blast and acoustic shock wave that originated from the sound of gunfire. The arrival times of the acoustic events at different sensor nodes were used to estimate the position of the sniper and send it to the base station based on the data-centric nature of the sensor nodes and the routing activities.

3.3 Medical & Biomedical Application

WSNs can also be deployed according to a designed topology such as in health care application. In this area, each sensor node has its own identity and their locations are known before hand. The possibility of unexpected node-death rate is comparatively much lower than those in the harsh environment setting.

These applications include telemonitoring of human physiological data, tracking and monitoring of doctors and patients inside an hospital, drug administration in hospitals and lots more [28]. Medical research and healthcare can greatly benefit from sensor networks. Merging wireless sensor technology into health and medicine applications will make life easier for doctors and patients where diagnosis and consultancy processes are transitioned automatically from one network in a clinic to the other installed in patient's body. As a result, sensors can be used to capture vital signs from patients in real-time and relay the data to handheld computers carried by medical personnel, and wearable sensor nodes can store patient data such as identification, history and treatments.

An interesting example of real-life application of sensor networks to medicine is CodeBlue [11]. This is an infrastructure designed by Harvard University in conjunction with School of Medicine, Boston University, USA to support wireless medical sensors, PDAs, PCs and other devices that may be used to monitor and treat patients in various medical scenarios. The research study went further to create Vita Dust, a set of devices based on the mica sensor node hardware platform. Vita Dust has the capacity to collect heart rate, oxygen saturation and EKG (Electrocardiography) data and relay them over a medium-range wireless network to a PDA [20].

Schwiebert *et al.*, [27] described a biomedical application in the Smart Sensors and Integrated Microsystems (SSIM) project where retina prosthesis chip that consisting of 100 microsensors were built and implanted within human eye. This allows patients with no vision or limited vision to see at an acceptable level. Research is still ongoing on the possible use of radio-frequency biomedical sensors inside the human body whose intended application is accessing the medical records of a patient in an emergency. Promising as the system seems, there are potential challenges associated with the technology: the system must be safe and reliable; require minimal maintenance and energy-harnessing from body heat. With more researches in this field of medicine, improved quality of life can be achieved and the medical cost can be considerably reduced.

3.4 Agriculture

In the study conducted by [4], WSNs were deployed to monitor humidity and temperature in a potato field. The purpose of the deployment is to fight phytophtora – a fungal disease which its development and attack of the crop is aided by the climatological conditions based on humidity and temperature. The goal of the WSN deployment is to predict the emergence of the disease and to schedule fungicide treatment only when needed.

Other researchers have reported the use of sensor networks for the integrated management of a vineyard [5] [7]. The study was motivated by the primary importance of temperature in the development of grapes to ensure wine quality. Other possible applications include field monitoring whereby the agricultural monitoring systems would need enhanced capabilities such as wireless broadband communication and high-resolution image-

monitoring technology; and monitoring the emergence of certain diseases in a greenhouse effect whereby the potential of WSNs can be deployed to control and maintain the temperature, relative humidity and carbon dioxide concentrations within the optimal limits.

3.5 Engineering & Infrastructure Monitoring

WSNs can be deployed in structure monitoring systems to detect, localize and estimate the extent of damage. This can allow civil engineers to test for the soundness of the structures. Also wireless sensor and actuator networks integrated within the buildings could allow distributed monitoring and control, improving living conditions and reducing the energy consumption, for instance by controlling temperature and air flow.

The supply network consisting of pipelines conveying water, oil, and gas are to be considered for structure health monitoring. They require a reliable sensing system since they transport risky and expensive materials over long distances without human attendance. In case of potential leakages or breakdowns due to thunderstorms, floods, encroachment, misuse, etc., problem areas should be immediately discovered and arrested. Wireless sensor networks can be deployed to pipelines on-demand. For example, in very hot areas the rise of a pipe's temperature above a certain threshold can be monitored by temporarily mounting sensor modules on the outer surface. Permanent deployments are relevant for controlling and managing the pipeline from remote. Adjusting the flow and checking the chemical composition are two possible operations.

3.6 Wealth Creation

Consumer applications include, but are not limited to, critical infrastructure protection and security, health care, the environment, energy, food safety, production processing, and quality-of-life support [12]. WSNs are expected to afford consumers a new set of conveniences, including remote-controlled home heating and lighting, personal health diagnosis, and automated automobile maintenance telemetry, to list just a few.

Near-term commercial applications include, but are not limited to, industrial and building monitoring, appliance control (lighting and HVAC), automotive sensors and actuators, home automation, automatic meter reading, electricity load management, consumer electronics and entertainment, and asset management.

3.7 Underwater Sensor Applications

Underwater Sensor Networks are presently being considered as an enabling technology for various aapplications ranging from oceanographic data collection, pollution monitoring, offshore exploration, disaster prevention, assisted navigation and tactical surveillance to exploration of natural undersea resources and gathering of scientific data in collaborative monitoring missions [2]. To make these applications viable, there is a need to enable underwater communications among underwater devices. Wireless underwater acoustic networking provides the enabling technology for these applications.

Underwater acoustic sensor networks consist of a variable number of sensors and unmanned or autonomous underwater vehicles that are deployed to perform collaborative monitoring tasks over a given area.

4.0 Future Research Directions and Projects

Basically, the research in the field of WSNs started very recently with respect to other areas of the wireless communication society, as examples like broadcasting or cellular networks [6]. The authors stated further that the first IEEE papers on WSNs were published after the turn of the Millennium. The first European projects on WSNs were financed after year 2001: During the sixth and seventh Framework Programmes, some Projects were financed by the EC, with explicit activities dedicated to communication protocols, architectural and technological solutions for embedded systems: among them, the first to be launched were WISENTS [17], e-SENSE [10], CRUISE [9] and CONET [18]. In the US the research on WSNs was boosted few years before and in Nigeria, the potentials of this field have not been explored both in academia and in the industry.

5.0 Conclusion

Sensor nodes are capable to form an autonomous intelligent network which does the unattended mmanagement and therefore can be deployed in a countless number of applications. Some of these applications of WSN are critical priority areas towards achieving the Vision 20:2020 by placing Nigeria among the twenty largest economies in the world, consolidating her leadership role in Africa and establishing herself as a significant player in global economy and political arena.

The paper examines and motivates the use of WSNs to interface the physical world with computers thereby creating bedrock for development towards achieving Vision 20:2020 in Nigeria. The MDG goals are clearly spelt out in the study coupled with the seven-point Agenda of the Yar'adua's administration. All these initiatives are aimed at transforming the Nigeria economy into a global competitive one.

It is our belief that science and technology forms the fundamental basis of societal transformation and the deployments of WSNs, if well harnessed, has the potential of transforming the country's economy positively and meet the target come year 2020. The government through the Federal Ministry of Science and technology should collaborate with various research agencies and academia in the development of sensor networks and consequently their deployments into various areas of necessities.

References

[1] A. Akhtar, A. A. Minhas, and S. Jabbar, "Energy Aware Intra Cluster Routing for Wireless Sensor Networks" **International Journal of Hybrid Information Technology**, Vol. 3, No. 1, 2010.

[2] I. F. Akyildiz, D. Pompili, and T. Melodia," Underwater acoustic sensor networks: research challenges" **Published by Elsevier B.V.**, Ad Hoc Networks 3, 2005, pp. 257–279.

[3] I. F. Akyildiz, W. Su, Y. Sankarasubramaniam, and E. Cayirci, ''A Survey of Sensor Networks,'' **IEEE Communications**, 2002, pp. 102-114.

[4] A. Baggio, "Wireless sensor networks in precision agriculture". *In* **The REALWSN'05 Workshop on Real-World Wireless Sensor Networks, IVA, Stockholm**, 2005.

[5] R. Beckwith, D. Teibel, and P. Bowen, "Unwired wine: Sensor Networks in Vineyards". In **IEEE International Conference on Sensors**, 2004.

[6] C. Buratti, A. Conti, D. Dardari, and R. Verdone," An Overview on Wireless Sensor Networks Technology and Evolution" **Journal of Scientific Research** (www.mdpi.com/journal/sensors), 2009, ISSN 1424-8220.

[7] J. Burrell, T. Brooke, and R. Beckwith, "Vineyard Computing: Sensor Networks in Agricultural Production". **IEEE Pervasive Computing**, 2004.

[8] C. Y. Chong, and S. P. Kumar, ''Sensor Networks: Evolution, Opportunities, and Challenges,'' **Proceedings of the IEEE**, Vol. 91, No. 8, 2003, pp. 1247-1254.

[9] EC Project CRUISE, FP6. Available Online: http://www.ist-cruise.eu (accessed on August 25, 2009).

[10] EC Project e-SENSE, FP6. Available Online: http://www.ist-esense.org (accessed on August 25, 2009).

[11] T. Fulford-Jones, D. Malan, M. Welsh, and S. Moulton, "CodeBlue: An ad hoc sensor network infrastructure for emergency medical care," *In* **International Workshop on Wearable and Implantation Body Sensor Networks, London, UK**, 2004.

[12] M. Hatler, Wireless **Sensor Networks: Mass Market Opportunities**, ONWorld, Inc., San Diego, CA, Feb. 22, 2004.

[13] Http://www.darpa.mil/ato/programs/SHM/ (accessed on August 25, 2009).

[14] M. O. Ilori, I. O. Abereijo, and A. A. Adeniyi, "Repositioning Tertiary Institutions within the Nigerian Innovation System for the Achievement of the Vision 20:2020 Millennium Development Goals" **Proceedings of the Faculty of Technology First National Conference on – The Role of Engineering and Technology in Achieving Vision 20:2020**, Obafemi Awolowo University, Ile-Ife, 2009, pp. 119-128.

[15] Information Section, Nigeria High Commission, 9 Northumberland Avenue, London Wc2n 5bx, UK. 24 February, 2009**. Courtesy of www.nigeriafirst.org** (accessed on February 24, 2009)

[16] P. Kamal, Y. Zhang, W. Trappe, and C. Ozturk, "Enhancing Source-Location Privacy in Sensor Network Routing" In **Proceeding of the 25th IEEE Int. Conference on Distributed Computing Systems (ICDCS05)**, 2005, pp. 599-608.

[17] P. J. Marron, D. Minder, and E. W. Consortium, **Embedded WiseNets Research Roadmap,** Information Society Technologies: Berlin, Germany, 2006.

[18] P. J. Marron, **Cooperating Objects NETwork of Excellence**, University of Bonn: Zentrum, Germany.

[19] M. Maroti, G. Simon, A. Ledeczi, and J. Sztipanovits, "Shooter localization in Urban terrain," **IEEE Computer**, vol. 37, 2004, pp. 60–61.

[20] D. Myung, B. Duncan, D. Malan, M. Welsh, M.Gaynor, and S. Moulton, "Vital dust: Wireless sensors and a sensor network for real-time patient monitoring," in **8th Annual New England Regional Trauma Conf., Burlington, MA**, 2002.

[21] Nigerian National Planning Commission, **Meeting Everyone's Needs: National Economic Empowerment Development Strategy**. Nigeria NEEDS Document published by Nigerian National Planning Commission, Abuja, 2004. http://www.nigerianeconomy.com/downloads/part1.pdf.

[22] K. Pister, **My view of sensor networks in 2010**. http://www.eecs.berkeley.edu/~pister/SmartDust/in2010

[23] K. Pister, **Smart Dust: Autonomous Sensing and Communication in a Cubic Millimeter**, http://robotics.eecs.berkeley.edu/~pister/SmartDust/

[24] G. J. Pottie, and W. J. Kaiser, "Wireless integrated network sensors". **Communications of the ACM,** *43(5)*, 2000, pp. 51-58.

[25] D. Puccinelle, M. Haenggi, "Wireless Sensor Networks: Applications and Challenges of Ubiquitous Sensing", **IEEE Circuits and Systems Magazine**, Third Quarter 2005.

[26] Rockwell, **Wireless Sensing Network (WSN)**, http://wins.rsc.rockwell.com/

[27] L. Schwiebert, S. K. S. Gupta, and J. Weinmann, "Research challenges in wireless networks of biomedical sensors". **Mobile Computing and Networking**, 2001, pp. 151-165.

[28] J. A. Stankovic, Q. Cao, T. Doan, L. Fang, Z. He, R. Kiran, S. Lin, S. Son, R. Stoleru, and A. Wood, "Wireless sensor networks for in-home healthcare: Potential and Challenges" **Proceedings of High Confidence Medical Device Software and Systems (HCMDSS) Workshop, Philadelphia, PA**, 2005.

[29] UN General Assembly. **United Nations Millennium Declaration**, 2002. http://www.un.org.millennium/declaration/ares552e.

Influence of process parameters during Ytterbium Fiber laser cutting of Mild steel using O_2 assist Gas

Dhaval M. Patel[1], Dr. J. L. Juneja[2] and Dr. K. Babapai[3]
[1] Research Scholar, Mechanical Engineering Department, [2]Principal and [3]Dean and Head of Department
U. V. Patel College of Engineering, Ganpat University, Kherva, Dist-Mehsana, Gujarat, India,
Ahmedabad Institute of Technology, Ahmedabad, Gujarat, India,
Faculty of Engineering and Technology, M.S. University, Vadodara, Gujarat, India[3]

Abstract - There are many non-linear interaction factors responsible for the performance of the laser cutting process. Identification of the dominant factors that significantly affect the cut quality is important. The present research aims to evaluate the effect of Ytterbium Fiber laser cutting parameters (gas pressure, laser power, and cutting speed) on 5 mm thick MS sheet cut quality. In this paper experimental investigation carried out on cut quality attributes like Surface roughness, Kerf width and Perpendicularity. Results revealed that good quality cuts can be produced in MS sheets at a set of laser cutting speed 1400 mm/min and at a power input of 1000 W under an assisting O_2 gas pressure of 0.7 bar with accepted cut quality like Surface roughness is 7.28 µm, Kerf width is 0.236 mm & Perpendicularity is 0.0222 radian.

Key words: *Ytterbium fiber laser cutting, Oxygen assist gas, Surface roughness*.

1. Introduction

The emergence of CO_2 and Nd: YAG lasers for material processing in the early 1970's have made a major impact on industrial cutting applications. Laser cutting have many principles as same as the conventional fusion cutting methods. But the laser cutting excels in applications requiring high productivity, a high edge quality and a minimum waste, due to the fast and precise cutting process. Mild steel is a daily used material and dominantly used in the laser cutting industry. In the last few years, the rapid development of high power fiber lasers provides more efficient, robust new technologies for materials process. These modern solid-state lasers operate offer multitude of advantages over conventional lasers and shows great promise to open up new applications [1, 2].

2. Laser Cutting Principal

Laser cutting is a thermal cutting process. The principle components includes the lasers power source with some shutter control, beam guidance train, focusing optics and a means of moving the beam or work piece relative to each other. When the beam is required, the shutter mirror is rapidly removed by a solenoid or pneumatic piston. And the beam generated with the laser power source passes to the beam guidance which directs the beam to the focusing optic. The focusing optic can be either transmissive or reflective. The reflective optics consists of parabolic off-axis mirrors. The focused beam then passes through and melts the material throughout the material thickness and a pressurized gas jet. The gas jet is needed both to aid the cutting operation and to protect the optic from spatter [3].

2.1 Laser oxygen cutting

In this process, the laser beam heats the material in an oxidizing atmosphere into the melting point of the material. Therefore an additional source of energy is obtained from the exothermic oxidation reaction of the oxygen with the material. And the molten material is rapidly removed away by the assist gas as shown in figure 1.The laser oxygen cutting is mainly used for steel and low-alloyed steel. Compared to the vaporized cutting method, about one twentieth of the energy is required with a very high processing speed. However, the cut edge is oxidized [4, 5].

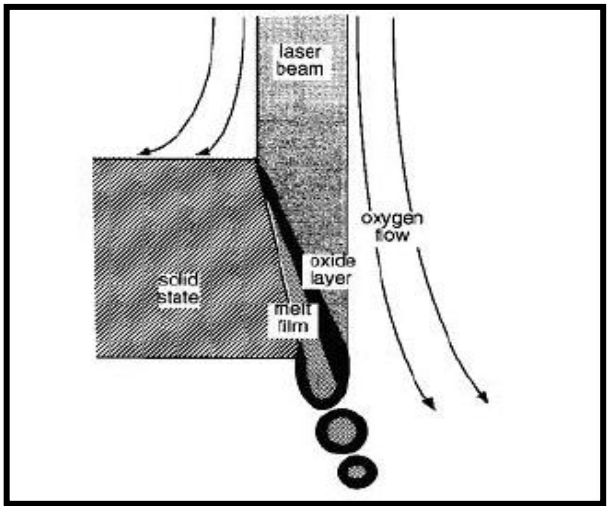

Fig. 1 Basic Principle of laser oxygen cutting

Manuscript revised March 15, 2011.

3. Experimental Procedures

The experiments were performed on as-received 5mm thickness sheets of mild steel. Experiments were conducted using a continuous-wave IPG YLR- 1000-SM ytterbium single-mode fiber laser with the following specifications: 1 kW maximum output power, 1.07 μm wavelength, 14 μm output fiber core diameter, mode TEM00 and M^2 =1.1. The laser beam was focused using a 125 mm focal length lens, which achieved a beam diameter of nominally 50 μm. General surface roughness was inspected using Mitutoyo SJ-201 surface roughness measuring instrument, Kerf width and perpendicularity measured with the help of UTHSCSA Image Tool program. Machine used in this experimental work is shown in figure 2 and ranges of parameters are mention in table 1.

Fig. 2 Laser cutting machine (YLR-1000)

Table 1: Parameter of laser cutting machine

Parameter	***Range***
Laser Type	Ytterbium fiber
Mode of operation	CW
Polarization	Random
Nominal output power	1000 Watt
Emission Wave length	1070-1080 nm
Switching ON/OFF	80 μsec
Output fiber core diameter	150 μm
Fiber length	10 m
Frequency	50-60 Hz
Laser source weight	330 kg
Laser cooling flow rate	6 Lit/min
Laser cooling water Temp.	18-26 C
Operation Voltage 3 phase	400-460 volt
Operating Current	8 A
Starting current	18 A
Work Table	3000 X 1500 mm

4. Material Composition (IS-2062 Grade: A)

Widely used material of above mention grade is used for experimentation and composition of elements of base material is mention in table 2.

Table:-2 Composition of element

Element	***% Composition***
Carbon	0.140
Sulphur	0.010
Phosphorous	0.025
Silicon	0.110
Manganese	0.850
Chromium	0.010
Nickel	0.004
Moly	Nil
Copper	0.004
Aluminum	0.020

5. Experimental Parameters

To perform set of experiments, known effective parameters are considered as input parameters from table 1 and is mention with available range in table 3 following with output parameters considered as cutting quality parameters.

Table 3: Input parameter of experiment

Parameter	***Range Available***	***Variable***
Laser power	900 to 1000 W	√
Cutting Speed	1.3 to 1.5 m/min	√
Gas Pressure	0.7 to 0.9 bar	√
Focal Length	125mm	X
Focus Point position	-1 mm	X
Nozzle Size	1.5 mm	X

Output Parameter: -

1. Surface Roughness (Ra in μ): The surface roughness for all trial runs is measured with profile meter named as SJ-201 (Surface Roughness Tester) as shown in figure 3.

Fig. 3 Measuring surface roughness of sample

2. kerf width (mm): The kerf is the slot that is formed during the laser cutting by removing the material and kerf width is defined as the width of the cutting slot, which is typical a bit larger than the focused laser beam diameter. It is desirable to keep the kerf width to a minimum. Measurement of kerf width is shown in figure 4.

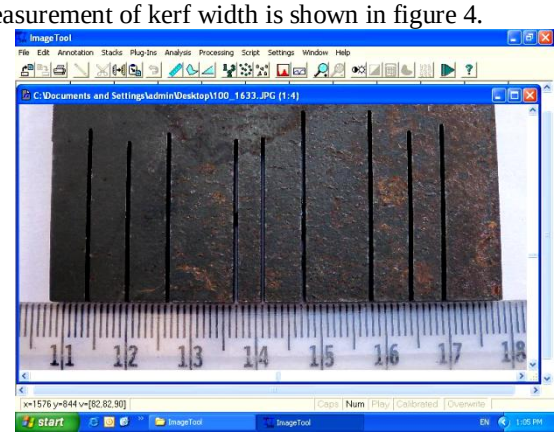

Fig. 4 Print screen of image tool software measuring Kerf width

3. Perpendicularity (radian): The perpendicularity includes not only the perpendicularity but also the flatness deviation for the bevel cut. The perpendicularity and inclination tolerance is the greatest perpendicular between the actual surface and intended surface. Measurement of perpendicularity is shown in figure 5.

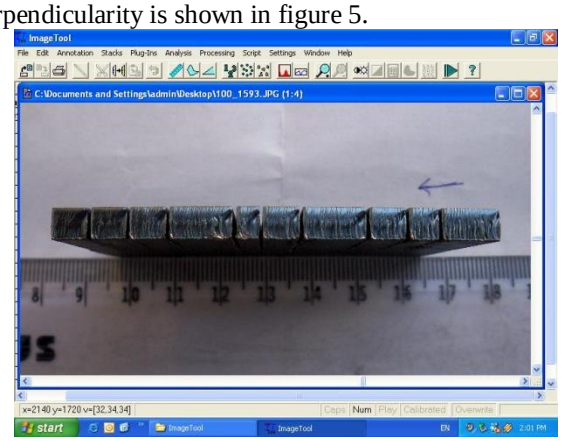

Fig. 5 Print screen of image tool software measuring Perpendicularity

6. Result and Analyses

We have varied input parameter mention in Table.3 and surface roughness, kerf width & perpendicularity measured for all set of parameters and documented. Table.4 indicates surface roughness at different input parameters.

Table 4: Experiments at different parameters

Trial No	*I/P*			*O/P*
	Laser power, watts	*Cutting speed (mm/min)*	*Gas pr. (bar)*	*SR, Ra in μ*
1	1000	1500	0.9	10.1
2	1000	1500	0.8	7.9
3	1000	1500	0.7	8.2
4	1000	1400	0.9	10.6
5	1000	1400	0.8	8.32
6	1000	1400	0.7	7.28
7	1000	1300	0.9	11.7
8	1000	1300	0.8	10.5
9	1000	1300	0.7	8.8
10	950	1500	0.9	10.3
11	950	1500	0.8	7.97
12	950	1500	0.7	8.3
13	950	1400	0.9	10.7
14	950	1400	0.8	8.4
15	950	1400	0.7	7.38
16	950	1300	0.9	11.72
17	950	1300	0.8	10.61
18	950	1300	0.7	8.9
19	900	1500	0.9	11.7
20	900	1500	0.8	12.6
21	900	1500	0.7	13.9
22	900	1400	0.9	12.5
23	900	1400	0.8	11.5
24	900	1400	0.7	13.94
25	900	1300	0.9	13.99
26	900	1300	0.8	12.8
27	900	1300	0.7	11.73

Figure 5 indicates graph of gas pressure and cutting speed vs. surface roughness at 1KW.

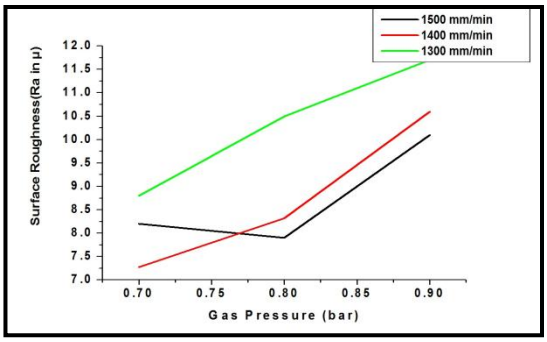

Fig. 5 Power 1KW, Gas Pressure and cutting speed versus surface roughness

Whereas figure 6 indicates graph of gas pressure and cutting speed vs. surface roughness at 0.95KW.

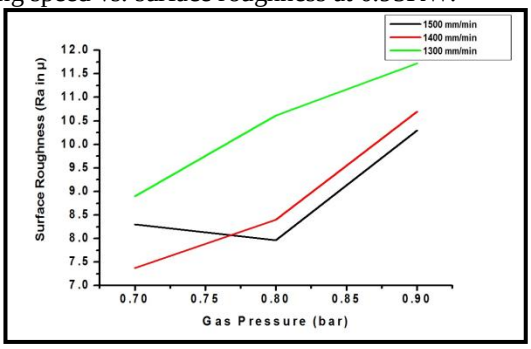

Fig. 6 Power 0.95W, Gas Pressure and cutting speed versus surface roughness

Whereas figure 7 indicates graph of gas pressure and cutting speed vs. surface roughness at 0.9KW.

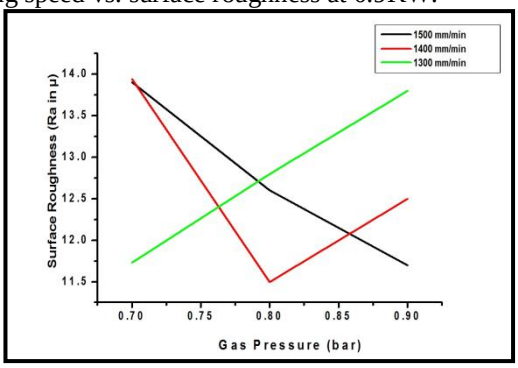

Fig. 7 Power 0.9W, Gas Pressure and cutting speed versus surface roughness.

Same way table.5 indicates kerf width at different parameters and figure 8 indicates graph of cutting speed vs. kerf width.

Table 5: Experiments for Ker width

Laser Power	*Cutting Speed*	*Kerf Width(mm)*
1000	1500	0.251
1000	1400	0.236
1000	1300	0.266
950	1500	0.261
950	1400	0.246
950	1300	0.276
900	1500	0.291
900	1400	0.286
900	1300	0.296

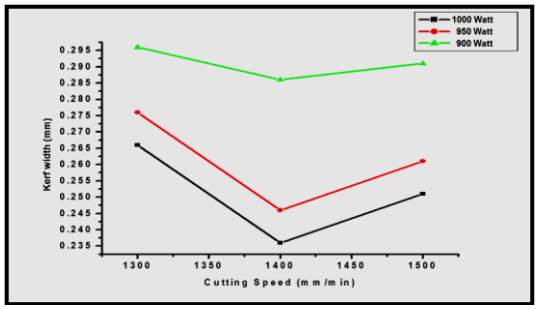

Fig. 8 Cutting speed vs. kerf width at different laser power

Whereas table.6 indicates perpendicularity at different parameters and figure 9 indicates graph of cutting speed vs. perpendicularity.

Table 6: Experiments for Perpendicularity

Laser power, (watts)	**Cutting Speed (mm/min)**	**Perpendicularity (Radian)**
1000	1500	0.0240
1000	1400	0.0222
1000	1300	0.0256
950	1500	0.0248
950	1400	0.0231
950	1300	0.0265
900	1500	0.0276
900	1400	0.0270
900	1300	0.0281

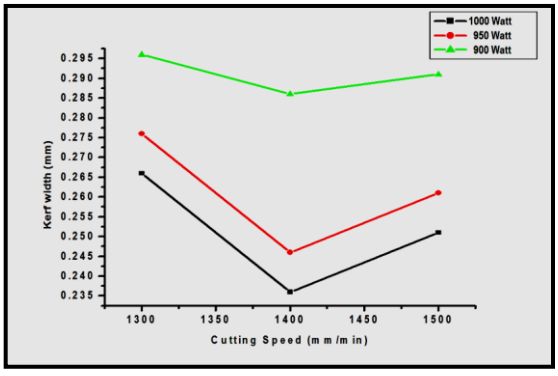

Fig. 9 Cutting speed vs. perpendicularity at different laser power

7. Parametric Contribution

MINITAB is a powerful, easy-to-use, statistical software package that provides a wide range of basic, advanced data analysis capabilities and find out the percentage contribution process parameter. MINITAB's straightforward command structure makes it accessible to users with a great variety of background and experience. To find out percentage contribution of each input parameter using MINITAB 15 software for surface roughness, kerf width and perpendicularity results are tabulated below.

Table: - 7 Percentage Contribution of Parameters for Surface Roughness

Sr No.	***Input Parameter***	***Percentage contribution***
Surface Roughness		
1	Laser Power (Watt)	61.50
2	Cutting speed (mm/min)	7
3	Gas Pressure (bar)	12.50
Kerf Width		
1	Laser Power (Watt)	78
2	Cutting speed (mm/min)	13
3	Gas Pressure (bar)	1
Perpendicularity		
1	Laser Power (Watt)	63.90
2	Cutting speed (mm/min)	30.90
3	Gas Pressure (bar)	0.98

8. Conclusion

Through this experimental result measurement and analysis one can conclude that the effect of cutting speed, gas pressure, and laser power on the quality characteristics of laser cut on 5 mm thick MS sheet.

Minimum surface roughness is achieved at a set of parameters; applied Power 1KW, cutting speed 1400 mm/min. and gas pressure 0.7 bars with 7.28 µm**.** Minimum kerf width was achieved at applied Power 1KW, cutting speed 1400 mm/min is 0.236 µm**.**

After experimental work it can be notice that the perpendicularity increased linearly as power increases and cutting speed decreases. Minimum perpendicularity achieved at Power 1KW, cutting speed 1400 mm/min is 0.0222 radian**.**

The Optimum cutting is achieved at a set of parameters, applied Power 1000 watt, cutting speed 1400 mm/min. and gas pressure 0.7 bars with 7.28 µm surface roughness, 0.236mm kerf and 0.0222 radian perpendicularity**.**

Contribution of each input parameters is determined by MINITAB software version 15 during cutting operation, clearly indicated in table 7. It can surely helpful to select the proper Laser power, Cutting speed, Gas pressure for required surface roughness, kerf width & perpendicularity.

Acknowledgments

The authors gratefully acknowledge the technological support of M/s Sahajanand Laser Technology Limited for experimental guidance and useful discussions at their, Ministry of Science and Technology (Government of India), recognize In – House R & D Unit. The authors would like to express their thanks to the authority & staff for both their invaluable contribution to the work detailed in this paper.

References

[1]. **P. K. Mishra**, Non-conventional machining processes, 3rd reprint 2005, Published by N. K. Mehra (Naroja publishing house).

[2]. **Avinash dubey, Vinod yadav,** 2008, "Laser beam machining –A review", Journal of machine tools & manufacturing technology, 48, pp.609-628.

[3]. **M.Sobih, P.L.Crouse L.LI,** 2008, "Striation free fiber laser cutting of mild steel sheets "Journal of material science processing, applied physics A 90, pp. 171-174.

[4]. **H.Golnabi, M.Bahar,** 2009, "Investigation of optimum condition in oxygen gas assisted laser cutting" Journal of optics & laser technology, 41, pp.454-460.

[5]. **R.Neimeyer, R.N.Smith,** 1993, "Effect of operating parameter on CO_2 laser cutting on M.S" Journal of engineering for industries, 115, pp. 359-362.

Safety and Steadiness in Advance database Systems: A Massive Confront

[1]Gyanendra Kumar Gupta, A K Sharma[2] and Vishnu Swaroop[3]
[1] Computer Science & Engineering Department, [2&3]Computer Science & Engineering Department
[1] Kanpur Institute of Technology, Kanpur, [2&3]M.M.M. Engineering College, Gorakhpur

Abstract - Numerous type of Information System is broadly used in various fields. Safety is mainly concern with that the data must secure in any form for correct transactions. Where Steadiness is the key of database, it must be consistence after every transaction. Collectively Safety i.e. security and Steadiness i.e. consistency is key factor of any database. In this paper we focus on these two important features of database and review the database system. Advance database are in many forms like traditional centralized or local from of database, advance database are very frequently changes in other forms as real time database, distributed database, mobile database and Grid database. With the fast development of computer network, information system users think about more data sharing in networks. In traditional relational database, data consistency was controlled by consistency control mechanism when a data object is locked in a sharing mode, other transactions can only read it, but can not update it. If the traditional consistency control method has been used yet, the system's concurrency will be inadequately influenced. So there are many new necessities for the consistency control and security in Mobile, Distributed, Real Time Databases. The problem not limited only to kind of data (e.g. mobile or real-time databases). There are many aspects of data consistency tribulations in advance databases, such as inconsistency between attribute and type of data; the inconsistency of topological relations after objects has been modified. In this paper, many cases of consistency are discussed. As the mobile computing becomes well-liked and the database grows with information sharing security is a big issue for researchers. Consistency and Security of data is a big confront for researchers because whenever the data is not consistent and secure no maneuver on the data (e.g. transaction) is productive. It becomes more and more crucial when the transactions are used in non-traditional environment like Mobile, Distributed, Real Time and Multimedia databases. In this paper we raise the different aspects and analyze the available solution for consistency and security of databases. Traditional Database Security has focused primarily on creating user accounts and managing user privileges to database objects. But in real time, distributed and mobile database uses different way in multi-user environment and most effectively is wireless medium. The mobility and nomadic computing uses these database creating a new opportunities for research. The wide spread use of databases over the web, heterogeneous client-server architectures, application servers, and networks creates a critical need to magnify this center.

Key words: *Data sharing, Data Consistency, Concurrency Control & Recovery, Mobile Distributed Real Time Database, security.*

1. Introduction

The growing capability to interconnect computers through internetworking, wireless network, high bandwidth satellite and cable network has spawned a new class of information centered applications based on data dissemination. In contrast to traditional, where data are delivered from servers to clients on demand, a wide range of emerging database applications benefit from a broadcasts mode for data dissemination. In such applications, the server repetitively broadcasts data to a client population without a specific request. Clients monitor the broadcast channel and retrieve the data items they need as they arrive on the broadcast channel. As the data dissemination systems continue to involve, more and more sophisticated client applications will require reading current and consistence data despite updates at the server. Since many data item in mobile computing systems are used to record the real time information. Trough this paper we review the problem of disseminating consistent data item to mobile transactions while allowing update to be executed concurrently on the database server. Consistent data items are provided to mobile transactions by requiring the mobile transactions to read data items committed at the same point of time.

The comprehensive correctness of a database is a definitive goal and cannot be guaranteed. Only a lower level of database consistency can be enforced in practice. We discuss the issue of database consistency beginning with identification of correctness criteria for database systems. Arrangement of methods for verification and restoration of database consistency is used to identify classes of methods with a practical significance. We discuss how fault tolerance (using both general and application-specific system properties) allows us to maintain database consistency in the presence of faults and errors in a database system and how database consistency can be restored after site crashes and network partitioning. A database system can ensure the semantic integrity of a database via verification of a set of integrity assertions. We show how to efficiently verify the integrity of a database state. Finally, batch verification of integrity assertions is presented as one of the promising approaches that use parallelism to speed up the verification.

In a single-user database, the user can modify data in the database without unease for other users modifying the same data at the same time. However, in a multi-user

Manuscript received March 25, 2011.

database, the statements within multiple simultaneous transactions can update the same data. Transactions executing at the same time need to produce meaningful and consistent consequences. Therefore, control of data concurrency and data consistency is crucial in a multi-user database.

- Data concurrency means that many users can access data at the same time.
- Data consistency means that each user sees a consistent view of the data, including evident changes made by the user's own transactions and transactions of other users.

2. Databases Steadiness

Data steadiness summarizes the validity, accuracy, usability and integrity of related data between applications and across the IT enterprise. This ensures that each user observes a consistent view of the data, including visible changes made by the user's own transactions and transactions of other users or processes. Data Consistency problems may arise at any time but are frequently introduced during or following recovery situations when backup copies of the data are used in place of the original data [1].

To illustrate consistent transaction activities when transactions execute at the same time, database researchers have defined a transaction isolation form called serializability. The serializable mode of transaction behavior tries to make sure that transactions execute in such a way that they appear to be executed one at a time, or serially, rather than concurrently.
While this degree of isolation between transactions is generally enviable, running many applications in this mode can dangerously negotiation application throughput. Complete isolation of concurrently running transactions could mean that one transaction cannot perform an insert into a table being queried by another transaction. In short, real-world considerations usually require a compromise between perfect transaction isolation and performance.
Various kinds of data consistency have been identified they are:

2.1 Consistency - Point in Time

Data is said to be Point in Time consistent if all of the interrelated data components are as they were at any single instant in time. This type of consistency can be visualized by picturing a data center that has experienced a power failure. Before the lights come back on and processing resumes, the data is considered time consistent, due to the fact that the entire processing environment failed at the same instant of time. Different types of failures may create a situation where Point in Time consistency is not maintained.

Mobile database are a tiny track database which is installed on mobile devices. Most commonly it is a replica of a piece of a central and distributed database that is save on database servers. In a mobile database application a part or a replica of the database is locally installed on the mobile devices. It differs from traditional database client – server application in which all data is stored on a central server. The advancement with a mobile database provides the necessary independence to the mobile device to work independently from the central server database. The client application can work with the mobile database asynchronously, and needs to connect to the central database server only when it is necessary to synchronize where the clients do not use local storage.

2.1 Consistence Point in Time

Data is said to be Point in Time consistent if all of the interrelated data components are as they were at any single instant in time. This type of consistency can be visualized by picturing a data center that has experienced a power failure. Before the lights come back on and processing resumes, the data is considered time consistent, due to the fact that the entire processing environment failed at the same instant of time. Different types of failures may create a situation where Point in Time consistency is not maintained.
Mobile database are a tiny track database which is installed on mobile devices. Most commonly it is a replica of a piece of a central and distributed database that is save on database servers. In a mobile database application a part or a replica of the database is locally installed on the mobile devices. It differs from traditional database client – server application in which all data is stored on a central server. The advancement with a mobile database provides the necessary independence to the mobile device to work independently from the central server database. The client application can work with the mobile database asynchronously, and needs to connect to the central database server only when it is necessary to synchronize where the clients do not use local storage.

2.2 Consistence in Transaction

A transaction is a transformation of state which has the properties of atomicity (all or nothing), durability (effects survive failures) and consistency (a correct transformation). The transaction concept is a key to the structuring of data management applications. The concept seems to have applicability to programming systems in general [2]. In some kinds of failure, the data will not be transaction consistent. In most cases what occurs is that once the application or database is restarted, the incomplete

transactions are identified and the updates relating to these transactions are either "backed-out" or processing resumes with the next dependant write [3].

A transaction is a group of actions such as insert, update, and delete performed on the database to change the state of a database. After a transaction is performed successfully, the database changes to a new state from its existing state.

The databases that support transaction are known as transactional databases. Most of the modern day relational databases support transaction.

A single transaction may require many SQL queries to execute to change the current state of the database. It is also important that all the queries be executed. For example, if money is transferred from one account to another, then in this scenario, the account from which the money is taken out should be debited and the account to which the money is deposited should be credited.

A transaction is issued to the database using SQL (structured query language) and has the following stages:

A transaction begins.

Execution of queries to change the current state of the database. After the successful execution of all the queries, a transaction is committed, i.e. the changes are saved permanently.

A database transaction has the following properties:

- Atomicity
- Consistency
- Isolation
- Durability

2.3 Consistence in Application

Application Consistency is similar to Transaction consistency. Instead of data consistency within the scope of a single transaction, data must be consistent within the confines of many different transaction streams from one or more applications. An application may be made up of many different types of data, such as multiple database components, various types of files, and data feeds from other applications. Application consistency is the state in which all related files and databases are in-synch and represent the true status of the application.

2.4 Steadiness in Data

Data Steadiness refers to the usability of data and is often taken for granted in the single site environment. Data Consistency problems may arise even in a single-site environment during recovery situations when backup copies of the production data are used in place of the original data.

For a set of backup data to be of any value it needs to be consistent in some fashion; Time, Transaction or Application consistency is required. For an individual data set, one with no dependencies on any other data, this can be accomplished by creating a simple Point in Time copy of the data and ensuring that the data is not updated during the backup process.

In fact, there are three different possible outcomes, should this fuzzy backup be restored:

The data is accidentally consistent and useable. This is a happy circumstance that may or may not be repeatable.

The data is not consistent and not useable. A subsequent attempt to use the data detects the errors and abnormal end subsequent processing.

The data is NOT consistent, but does not cause an ABEND and happens to be useable to the application. It is used by subsequent processing and any data errors go undetected and uncorrected. This is the worst possible outcome.

In this greater context, simple data consistency within individual data sets is no longer sufficient. What is required is time consistency across all of the interdependent data. As it is impossible to achieve this with the traditional backup methodologies, newer technologies are required to support time consistent data?

To guarantee the correct results and consistency of databases, the conflicts between transactions can be either avoided, or detected and then resolved. Most of the existing mobile database CC techniques use the (conflict) serializability as the correctness criterion. They are either pessimistic if they avoid conflicts at the beginning of transactions, or optimistic if they detect and resolve conflicts right before the commit time, or hybrid if they are mixed. To fulfill this goal, locking, timestamp ordering (TO) and serialization graph testing can be used as either a pessimistic or optimistic algorithm.

3. Database Safety

Database Safety is the system, processes, and procedures that protect a database from unintended activity. Unintended activity can be categorized as authenticated misuse, malicious attacks or inadvertent mistakes made by authorized individuals or processes. Traditionally databases have been protected from external connections by firewalls or routers on the network perimeter with the database environment existing on the internal network opposed to being located within a demilitarized zone.

Additional network security devices that detect and alert on malicious database protocol traffic include network intrusion detection systems along with host-based intrusion detection systems.

One of the main issues faced by database security professionals is avoiding inference capabilities. Basically, inference occurs when users are able to piece together information at one security level to determine a fact that should be protected at a higher security level. Database security is more critical as networks have become more open [4]. Databases provide many layers and types of information security, typically specified in the data dictionary, including:

Access control

Auditing

Authentication

Encryption

Integrity controls

Database safety can begin with the process of creation and publishing of suitable security standards for the database location. The standards may include specific controls for the various relevant database platforms; a set of best practices that cross over the platforms; and linkages of the standards to higher level polices and governmental regulations. Nowadays, almost every computer user has a firewall or antivirus is running on every computer, a popup blocker and many other programs. All of these are with access control functions. All of these programs guard us from intruders of sorts. They inspect everything trying to enter the computer and let it in or leave it out. Computers have complicated access control abilities. They ask for authentication and search for the digital signatures. Also, there are different types of keypads and access control systems. In today's world the keys and locks are beginning to look different. With the passage of time, the key locks also got smarter. They can identify the patterns of your physical features, your voice, and fingerprint locks can read your fingerprints [5].

Access control is a rapidly growing market and soon may manifest itself in such ways we cannot even imagine. Nowadays, security access control is a necessary component for businesses [6]. There are many ways to create this security. Some companies hire a security guard to stand in the gateway. There are many security devices that prevent or permit access such as a turnstile. The best most effective access control systems are operated by computers.

Auditing is a computer security audit is a manual or systematic measurable technical assessment of a system or application. Systems can include personal computers, servers, mainframes, network routers, switches. Applications can include Web Services, Databases [7].

Authentication is the process of confirming a user or computer's identity. The process normally consists of four steps:

1. The user makes a claim of identity, usually by providing a username. For example, It might make this claim by telling a database that my username is something.

2. The system confronts the user to prove his or her identity. The most common confront is a request for a password.

3. The user responds to confront by providing the requested proof. In this example, it would provide the database with my password.

4. The system verifies that the user has provided acceptable proof by, for example, checking the password against a local password database or using a centralized authentication server

The database security is of great importance and a major concern for any organization. Securing the data from people of malicious intent, accidental damage, catastrophic damage is a great challenge for a Database Administrator. The Database Administrator decides the level of security keeping in view the sensitivity of data. There are different levels of security.

At the lowest level of security, there is no restriction, i.e. everybody has full access to the database. This level of security is implemented where there is already network security through which access can be restricted. In such type of scenario, there is no need to duplicate the security scheme.

The subsequently level of security is share level security. At this level, the Database Administrator assigns a password to the whole database and the users who know the password can access the full database. This level of security is easy to implement and administer because it requires changing only one password periodically. This type of security is sufficient in situations where the organization wants to provide full access to the database to its employees. For example, a database that stores annual holiday list or database regarding news, which the organization publishes from time to time.

After this level comes user level security. At this level, each user is assigned some particular privileges by the Database Administrator. For example, it is the prerogative of the Database Administrator to assign different rights to different users so that each user can be restricted to use the database. He can assign various rights such as some users are entitled to only view the data, some can modify by adding or deleting entries from the database, etc. This level of security is a bit difficult to implement and administer,

but it provides a higher degree of security to the data. This level of security can be implemented on individual users as well as a group of users. To implement on a group of users, each group should be identified first such as system administrators, order-entry clerks, salespeople, and so forth-and then determine the security privileges that each role has for each object in the system.

4. Database Security Troubles and Evade

Database security managers play a vital role in any organization and are required to multitask and juggle a variety of headaches that accompany the maintenance of a secure database. Once it is understood that how, where, and why database security can prevent [10, 11].

Daily Maintenance: Database audit logs require daily review to make certain that there has been no data misuse. This requires overseeing database privileges and then consistently updating user access accounts.

Varied Security Methods for Applications: More often it can create difficulty with creating policies for accessing the applications. The database must also possess the proper access controls for regulating the varying methods of security otherwise sensitive data is at risk.

Post-Upgrade Evaluation: When a database is upgraded it is necessary for the administrator to perform a post-upgrade evaluation to ensure that security is consistent across all programs. Failure to perform this operation opens up the database to attack.

Split the Position: Sometimes organizations fail to split the duties between the IT administrator and the database security manager. Instead the company tries to cut costs by having the IT administrator do everything.

Application Spoofing: Hackers are capable of creating applications that resemble the existing applications connected to the database. These unauthorized applications are often difficult to identify and allow hackers access to the database via the application in disguise.

Manage User Passwords: Password rules and maintenance needs to be strictly enforced to avoid opening up the database to unauthorized users.

Windows OS Flaws: Windows operating systems are not effective when it comes to database security. Often theft of passwords is prevalent as well as denial of service issues. We discuss recent confronts for database security and some preliminary approaches that address some of these confronts.

Security Awareness and End-users

Standard Compliance & Regulations Updates

Vulnerability Management

Frequently Change of Management and Lack of Co-ordination in Management

One of the most important issues of recent computing systems is the condition of sufficient security and privacy guarantees for the user data. Security issues of mobile devices are discussed in recent works like [12]. In the field of databases and database management systems, security is a well studied subject. See for example [13] and the related chapters in [14, 15]. More recently, issues about privacy in databases are discussed for example in [16]. However in the case of a mobile database application there are additional security challenges due to the distributed nature of the application and the hardware constraints of mobile devices. Achieving a sufficient level of security for such a platform is an important problem which has to be addressed. For example, data privacy and confidentiality is identified in [17] as one of the critical open issues and research directions in mobile databases.

5. Steadiness Issues in Advance Databases

A real-time database system (RTDBS) is a transaction processing system that is designed to handle workloads where transactions have completion deadlines. The objective is of the system is to meet these deadlines, that is to complete processing transactions before their deadline expires [18]. In real-time database system (RTDBS), transactions have to be completed before their deadlines and all the accessed temporal data objects have to be valid. Besides meeting these timing constraints, a RTDBS needs to observe data consistency constraints as well [19]. Different transactions scheduling algorithms and concurrency control protocols have been proposed to satisfy these constraints [20, 21]. The problems become more complicated in a distributed real-time database system (DRTDSB) where a database is partitioned into a number of smaller local databases residing at different sites. The communication network, which is an essential component in a DRTDBS, is another important performance issue [22]. A Mobile transaction is distinguished by the features that the operations of it can be submitted by a portable (in small size, less memory and limited power backup) to the data servers from different locations [23].

The Sharing concepts of loading the database by more than one user for any network system are the big issues in MDRTDB system. The rapid growth of mobile computing technology provides a new, alternative platform for mobile distributed real-time database applications [24, 25]. With increasing uses of portable and mobile computers, mobile real-time database applications become more and more popular. We call the new systems as mobile distributed real-time database systems (MDRTDBS). Processing time-constrained transactions in MDRTDBS is a very new area

and a lot of design issues still remain unresolved. Mobile transactions are largely limited to soft or firm deadlines because of the execution delays due to the system constraints [26].

The predictability of a advance database is affected by a number of factors such as concurrency control, priority scheduling, commitment and mobile wireless communication. In a mobile environment, the behavior of the underlying wireless network is highly unpredictable. Certain behavior of the mobile computing system creates an additional burden on the system performance and increases the unpredictability of the system. In particular, the narrow wireless bandwidth and the limitation of processing power in the mobile clients may be bottlenecks to the performance [27]. Mobile clients (MCs) face wide variance in network quality including unpredictable call setup probability. There are several factors which may affect a call to setup such as the availability of the receiver in the cell site and the utilization of the channel in the Main Terminal Switching Office (MTSO). Even when a call can be set up, the setup time is also fluctuating. Furthermore, MCs always prefer a light, compact, and power-saving units. Methods have to be designed to save power in the MCs. Also, the mobility of the MCs affects the distribution of workload on different cells and thus the system predictability. Failures are not fully avoided in Mobile computing as well as mobility also raises the database dependency on servers moving across one geographical area to another.

Another source of problem is the cost in resolving data conflicts. In advance database, different real-time concurrency control protocols have been proposed. One of the commonest methods to resolve data conflict between transactions with different priorities is by restarting transactions. However, this will be very expensive under a mobile environment. The restarted transaction will have a very probability of deadline missing. Methods have to be designed to reduce the cost in resolving the conflict. One of the possible solutions to reduce the number of restarts is to adopt less restrictive correctness criteria for database consistency such as using the concept of similarity or epsilon serializability. Similar problem will occur when a committing transaction has a data conflict with an executing transaction. Up to now, very little of work has been done on the design of real-time commitment protocol which is required to reduce the impact of transaction commitment on the system predictability. Some proposals are based on the optimistic method. Serializibility is widely accepted correctness criteria for controlling concurrent execution of transactions in database systems. Serializable schedules provide correct results and leave the database consistence. However serialzibilty can be restrictive for some mobile applications because of the limitation of concurrency allowed by serialzible executions.

Consistency guarantee for data processed by mobile clients are an important area of research. These guarantees provide the basis for any collaborative work and transaction processing done with these systems [28]. The mechanism to provide individual applications with a view of the database that is consistence with their own actions. This is important since in their environment, clients can read or write data from any one of the available server and these servers can contain in consistence views of the database [29].

In the two phase commit protocol, the coordinator decides to commit the distributed transaction if all its sub-transactions are in a state called the “prepared state”. We have increased the semantics of the two phase commit protocols by replacing the prepared state by more restrictive states called the “source state” and the “serializable state”. The source state ensures that the execution of committed distributed transactions is not only atomic but also serializable. It also ensures that distributed transactions cannot interfere with other distributed transactions through local transactions, but it does not ensure a serializable view of the distributed database if local transactions are taken into account. The serializable state ensures that the execution is serializable also if local transactions are taken into account. Which of the two correctness criteria is appropriate for global concurrency control depends on the distributed applications of the system. In the proposed mechanism, each interconnected site supports the source state or the serializable state. Various methods of supporting these states are presented. Which method is appropriate for a site depends on the concurrency control method and the autonomy requirements of the site.[30] High performance Mobile computing provides an infrastructure for access and processing of large volume, terabyte or even pet-bytes, of distributed data. Research in Mobile distributed data has focused on security issues, resource ownership, infrastructure development and replication issues assuming presence of single transaction in the system.

4. Conclusions

Advance databases uses mobile distributed real-time information through a database system that requires the integration of concepts from both real-time systems and mobile distributed database systems. Some new criteria need to be developed to involve timing constraints of real-time applications in many database systems design issues, such as transaction/query processing, data buffering, CPU, and IO scheduling. In this paper, a basic understanding of the issues in real-time database systems is provided and the research efforts in this area are introduced. Different

approaches to various problems of real-time database systems are briefly described, and possible future research directions are discussed.[31]

Concurrency raises the complication of consistency and sharing grows the security issues in any environments. There are several technique and protocol have been built for maintaining the consistency and security of database systems like Data Consistency. Two-Process Mutual Exclusion: Dekker's- and Peterson's Algorithms, N-Process Mutual Exclusion using Hardware, N-Reader, 1-Writer Mutual Exclusion using Head/Tail Flags. But the available techniques are not sufficient for the different database environment where the data is huge and complex for transactions including security system. Security is more than Just Good Crypto – The point here is not that encryption is worthless. The point is that encryption by itself is not helpful. The endpoints need to be secure, passwords need to be difficult to crack, and those who do have access to the system need to be trustworthy. System call traces can be used on any kind of process such as e-mail daemons, web servers, or encrypted chat programs. A new protocol must be needed to control both the situation for consistency and security in Advance datbase. In order for any security tool to be effective, it needs to be layered with other strong security tools, starting with a security policy. No one tool, by itself, can ever prevent information theft or attacks, but several layers of security provide the most solid defense against would-be hackers.[32, 33]. Encryption needs to be accompanied by server hardening, intrusion detection, firewalls, and auditing. Without it, encryption is easily compromised [34]. Increase in quantity of data stored and requirement of quick response time has motivated the research in Parallel Database Systems (PDS). Requirement for correctness of data still remains one of the major issues. Concurrency control algorithms used by PDS uses single scheduler approach. Single scheduler approach has some inherent weaknesses such as – very big lock tables, overloaded centralized scheduler and more number of messages in the system. In this paper we investigate the possibility of multiple schedulers and conclude that single scheduler algorithms cannot be migrated in the present form to multi-scheduler environment. [35] Efficient database management algorithms for accessing and manipulating data are required to satisfy timing constraints of supported applications. Mobile Distributed Real-time database systems involve a new research area investigating possible ways of applying database systems technology for safety and steadiness.

References

[1] Joann J Ordille, Barton P Miller, Database confronts in Global Information System", **International Conf. on Management of Data Processing, ACM SIGMOD**, Washington,DC,US, 1993, pp. 403-407, 1993.

[2] Jim Gray, "The Transaction Concept: Virtues and Limitations" , **7th International Conference, Cannes, France, Proceedings, IEEE Computer Society**, 1981, pp. 144-54.

[3] Song X, Liu W. S., "Maintaining Temporal Consistency: Pessimistic vs Optimistic concurrency control", **IEEE Transactions on Knowledge Engineering**, 7(5):786-796, Oct 1995.

[4] Srinivasan, Anup Kumar, "Database security curriculum in InfoSec program", **Proceedings of the 2nd annual conference on Information security curriculum development**, Kennesaw, Georgia, Sep. 23-24, 2005.

[5] E. Bertino D. Leggieri and E. Terzi, "Securing DBMS: Characterizing and Detecting Query Flood", **Proc. Ninth Information Security Conf.** (ISC '04), Sept. 2004.

[6] Elisa Bertino , Barbara Catania , Elena Ferrari, "A nested transaction model for multilevel secure database management systems", **ACM Transactions on Information and System Security** (TISSEC), v.4 n.4, p.321-370, November 2001.

[7] B. Thuraisingham, "Database and Applications Security: Integrating Databases and Applications Security", **CRC Press**, Dec. 2004.

[8] A Kush, "Security Aspects in Adhoc Routing", **CSI of India Communication**, Vol No 32 Issue 11, pp. 21-33, March 2009.

[9] Walid Rjaibi, "An introduction to multilevel secure relational database management systems", **Proceedings of the 2004 conference of the Centre for Advanced Studies on Collaborative research**, Markham, Ontario, Canada, p.232-241, October 04-07, 2004.

[10] Elisa Bertino , Laura M. Haas, "Views and Security in Distributed Database Management Systems", **Proceedings of the International Conference on Extending Database Technology: Advances in Database Technology**, p.155-169, March 14-18, 1988.

[11] Elisa Bertino , Sushil Jajodia , Pierangela Samarati, "Database security: research and practice", **Information Systems**, v.20 n.7, p.537-556, Nov. 1995.

[12] Benjamin Halpert., "Mobile device security", **Proceedings of the 1st annual conference on Information security curriculum development**, pages 99–101, New York, NY, USA, 2004. ACM Press.

[13] Sushil Jajodia, "Database security and privacy", **ACM Comput. Surv**., 28(1):129–131, 1996

[14] Ramez Elmasri and Shamkant B. Navathe., Fundamentals of Database Systems, **4th Edition. Addison-Wesley**, 2004.

[15] Thomas Connolly and Carolyn E. Begg., "Database Systems: A Practical Approach to Design, Implementation and Management", **4th Ed. Addison-Wesley**, 2005.

[16] Rakesh Agrawal, Jerry Kiernan, Ramakrishnan Srikant, and Yirong Xu., "Hippocratic databases", i**In 28th Int'l Conf. on Very Large Databases** (VLDB), Hong Kong, 2002.

[17] Guy Bernard, Jalel Ben-Othman, Luc Bouganim, G´erˆome Canals, Sophie Chabridon, Bruno Defude, Jean Ferri´e, St´ephane Gan¸carski, Rachid Guerraoui, Pascal Molli,

Philippe Pucheral, Claudia Roncancio, Patricia Serrano-Alvarado, and Patrick Valduriez, "Mobile databases: a selection of open issues and research directions", **SIGMOD Record**, 33(2):78–83, 2004.

[18] Jayant R Haritsa, "Data Access Sceduling in Firm Real time Database Systems", **The Journal of Real Time Systems**, Vol 4, pp 203-241, 1992.

[19] O. Ulusoy, "Processing Real-Time Transactions in a Replicated database System", **International Conf. on Distributed and parallel Databases**, 2(4),pp. 405-436, 1994.

[20] P.S. Yu, K.L. Wu, K.L. Lin, and, S.H. Son, "On Real-time Databases: Concurrency Control and Scheduling", **Proceedings of the IEEE**, vol. 82, no. 1, pp. 140-157, 1994.

[21] Kin, L, Reoat, G, "Consistency issues of Real Time Systems", **In proceeding of International Symposium on system Science and Technology**, pp. 118-129, 1999.

[22] O. Ulusoy, "Real-time Data Management for Mobile Computing", **International Workshop on Issues and Application of Database Technolgy**, pp. 223-240, 1998.

[23] A. Elmagaemid J. Jing, O Bukhers, "An efficient and reliable reservation algorithm for mobile transactions", International Conf. on Information and Knowledge Management(CIKM), 1995.

[24] Evaggelia Pitoura and Bharat Bhargava, "Dealing with Mobility: Issues and Re-search Challenges", **Technical Report, Purdue Univ**., Nov. 1993.

[25] Tomasz Imielinski and B. R. Badrinath, "Mobile Wireless Computing: Challenges in Data Management", **Communications of the ACM**, vol. 37, no. 10, Oct. 1994.

[26] Kayan, E, Ulusoy, O, "An evaluation of Real Time transaction management issues in Mobile Database Systems", **The Computer Journa**l, Vol 42, pp. 501-510, 1999.

[27] Panos K. Chrysanthis, "Transaction Processing in Mobile Computing Environment", **in Proceeding of IEEE Workshop on Advances in Parallel and Distributed Systems**,pp. 77-82, USA, 1993.

[28] Dainel Barbara, "Mobile computing and Databases-A Survey", **IEEE Transactions on Knowledge and data Engineering**, Volume 11 No. 1 Jan-Feb,1999.

[29] D Terry, A J Demers, K Peterson, et al, "Session Guarantee for weakly consistent replicated data", **Proc. Conf. Parallel and Distributed Computing**, Austin, Texsas, Oct 1994.

[30] Juha Puustjavi, "Distributed management of transactions in heterogeneous distributed database system",**ACM**, Vol 31, 3, 06-420, Nov. 2003.

[31] O. Ulusoy, G. G. Belford, "A Performance Evaluation Model for Distributed Real-Time Database Systems", **International Journal of Modelling and Simulation**, vol.15, no.2, April 1995.

[32] Mario Guimaraes , Meg Murray , Richard Austin, "Incorporating database security courseware into a database security class", **Proceedings of the 4th annual conference on Information security curriculum development**, Kennesaw, Georgia, Sep. 28, 2007.

[33] Norjihan Abdul Ghani , Zailani Mohamed Sidek, "Personal information and privacy in E-commerce application", **Proceedings of the 7th WSEAS international conference on Information security and privacy**, Cairo, Egypt, p.28-32, December 29-31, 2008,

[34] Charles P. Pfleeger , Shari Lawrence Pfleeger, "Security in Computing", **Prentice Hall Professional Technical Reference**, 2002.

[35] Sushant Goel, Hema Sharda et al, "Transaction Management in Distributed scheduling Environemnt for high performance database Applications", **ACM**, Vol 2918/2003, 837, 2003.

Long term endurance testing of indirect injection diesel engines fueled with diesel, neat jatropha oil and their blends

P. K. Sahoo, R. K. Tripathi & A. K. Sharma
University of Petroleum & Energy Studies, Dehradun, India 248007

Abstract - The use of straight vegetable oils (SVOs) as a fuel substitute for diesel engines for rural sector is currently being debated upon the country. Keeping in view this fact, investigations is being carried out on the use of SVOs in diesel engines at Biofuels Research Laboratory, University of Petroleum & Energy Studies, Dehradun. This paper is aimed at investigating the technical feasibility of using straight vegetable oils (Jatropha) and its blend in various proportions into five numbers of constant (slow) speed indirect injection (IDI) diesel engines widely used for irrigation pump sets in the country. Diesel and jatropha oil fuel blends (Diesel, 10%, 20%, 50% and 100% jatropha oil) were used to conduct long term engine endurance test as per IS:10000 on five numbers of IDI diesel engines. The performance & emission characteristics were compared vis-à-vis fossil diesel as base line in each cycle throughout the endurance test. Engine performance parameters such as fuel consumption, thermal efficiency, exhaust gas temperature and exhaust emissions (Smoke, CO, CO_2, HC, NOx and O_2) were recorded. Tribological analysis (wear and tear) revealed that engine fuelled with 100% jatropha oil showed comparatively less wear and tear over the entire range of endurance test. The bake specific energy consumption was observed minimum in case of neat diesel. The overall emission characteristics were found to be best for the case of engine fuelled with diesel over the entire range of long term endurance test.

Key Words: *Jatropha Oil, Endurance Test, Engine Tribological Analysis*

1. Introduction

Various sources of origin of biofuels used in developed countries include rapeseed, soybean, sunflower etc [1, 2]. All these are edible oil sources in India. Further, the country is having a deficit supply in the country of these oils and is dependent on imports to a substantial extent. Thus, utilizing non-edible seeds from oil bearing trees is the only option for the country. This development also provides much needed ecological balance and is advantageous in many aspects [3-6]. Biofuels from non-edible sources are important for the country to raise energy security and environment protection of the country. Apart from objectives of energy security and environmental protection, rural economic growth, agricultural diversification and income generation are also relevant for Biofuels program in India. One of the deliverable targets of biofuels programme in the country is employment generation at grass root level for involvement in energy crop cultivation as well as utilization of fallow land for economic purpose [7, 8].

The high viscosity and low volatility of vegetable oils are generally considered to be the major drawbacks for their utilization as a fuel in diesel engines. The high viscosity of vegetable oils causes problems in the injection process, leading to an increase in smoke levels, and the low volatility of the vegetable oils results in oil sticking on the injector or cylinder walls, causing the deposit formation which interferes with the combustion process [9]. Preheating of vegetable oils in order to equalize their viscosity to that of pure diesel may ease the problem of injection process. Increased injection pressure may also result in efficient combustion in the CI engine.

There are a number of fuel properties that are essential to the proper operation of a diesel engine. The addition of biodiesel to diesel fuel affects certain key properties with particular reference to blend stability, relative density, viscosity and lubricity, energy content, cloud point, pour point and cetane number. Material compatibility and corrosiveness are also important factors that need to be considered [10, 11].

Thus there is need to focus research and development on obtaining bio fuel from non-edible seeds oil bearing trees. The research work carried out at various research institutions over last decade has resulted in standardization of production technologies for production of biodiesel from oilseeds of Jatropha and Karanja [12]. This is achieved through the process of trans-esterification which involves the reaction of vegetable oils with alcohol in presence of a catalyst to form mono alkyl esters, glycerol and fertilizer [13, 14]. In this process, acid value of the oil is substantially reduced. Also, the properties of the fuel so obtained are quite similar to mineral diesel which implies that the fuel could be used as a diesel substitute in compression-ignition engines. But there

is a little work on utilization of SVO on Direct and Indirect Injection Diesel Engine. Due to the extreme physico-chemical properties of SVO, the use of Indirect Injection Diesel Engines may contribute significant results to the fleet of Biofuel Research. The engines proposed for this study are generally used for agricultural applications such as Gen set and Irrigation pump sets. In an internal combustion engine, the term indirect injection refers to a fuel injection method which does not inject fuel directly into the combustion chamber. Diesel engines are usually equipped with indirect injection systems, where a fuel injector delivers fuel at some point before the intake valve [15].

While application of bio-diesel so derived from non-edible oilseeds has been proven technically feasible in compression ignition engines, the utilization of Straight Vegetable Oils (SVOs) has not founded favour due to various technical limitations imposed primarily because of its high viscosity. However, SVOs could be advantageous in certain specific application areas such as remote village electrification and pump-set energization for rural irrigation needs due to lower cost and simpler production technology. Some research work is in progress in our country by using SVOs, Biodiesel and their blends utilization on Direct Injection (DI) diesel engine and the results are not up to the mark due to high viscosity leading to improper combustion of SVOs in the combustion chamber. Therefore the proposed studies are aimed at effective utilization of SVOs and their blends with diesel in single cylinder Indirect Injection (IDI) Diesel Engine in which the fuel is processed in the pre-combustion chamber in order to bring the desired quality of fuel grade to be injected to the combustion chamber.

An indirect injection diesel engine delivers fuel into a chamber off the combustion chamber, called a pre-chamber, where combustion begins and then spreads into the main combustion chamber. The pre-chamber is carefully designed to ensure adequate mixing of the atomized fuel with the compression-heated air. This has the effect of slowing the rate of combustion, which tends to reduce audible noise. It also softens the shock of combustion and produces lower stresses on the engine components [16]. The addition of a pre-chamber, however, increases heat loss to the cooling system and thereby lowers engine efficiency. Aside from the above advantages, early diesels often employed in indirect injection in order to use simple, flat-top pistons and made the positioning of the early bulky diesel injectors easier. The present project aims to identify key characteristics of the fuel that affect the performance of engine running on these fuels.

This project was aimed at investigating the technical feasibility of using straight vegetable oils (Jatropha) and its blend in various proportions into a constant (slow) speed Indirect Injection Diesel Engine (Fieldmarshal make) widely used for irrigation pump sets in the country. After identifying performance and emission parameters, the fuel obtained by SVOs and their blends with Diesel in a pre-defined volumetric percentage were characterized and its performance & emission characteristics were compared vis-à-vis fossil diesel as base line. Long term endurance test as per IS 10000 helped us for analyzing wear and tear (tribological studies) in the research engines used for this study. A detailed maintenance protocol was developed as per the data generated for the use of SVO in engines at different blends.

2. Methodology

2.1. Procurement of non-edible oils

In the present study, 15MT of jatropha seeds were procured from Udaipur, Rajasthan and expelled in two mechanical oil expeller of capacity 50 kg/hr each with an oil recovery of 33% for jatropha seed. The oil cake produced was used for biogas production and the slurry is being used for organic farming.

2.2. Analysis of straight vegetable oil (Jatropha)

Vegetable oils are water insoluble, hydrophobic substances of plant and animal origin, which are primarily composed of the fatty esters of glycerol, so called triglycerides. The chemical structure of vegetable oils, in general, is shown in Figure 1. R_1, R_2 and R_3 represent the hydrocarbon chain of fatty acids. The R_1, R_2 and R_3 may be the same, depending upon the particular oil, but ordinarily are different in chain length and number of double bonds. Free fatty acids play vital role during the biodiesel production process which lead to formation of soap and water. The types and percentage of fatty acids contained in vegetable oils, depends on the plant species and on the growth conditions of the tree.

Acid value of vegetable oil is defined as the number of milligrams of potassium hydroxide required to neutralize the free acid present in 1 gm of the oil sample. Acid value of these oils was determined by a standard titration method. For determination of acid value, specified amount of the test sample was titrated with aqueous solution of the

KOH of known normality (N). 5 gm of the oil under test was mixed with 50 ml of neutral alcohol (propanol) in a 250 ml conical flask and heated over a water bath for 30 minutes. The flask was cooled to room temperature and few drops of phenolphthalein indicator was added. Titration was carried out with the standard N/10 KOH solution until a faint permanent pink colour appeared at the end point. The acid value of the sample in terms of mg of KOH/gm was computed by using the following expression.

Acid value = ml of KOH x N x 56.11/weight of sample (gm)

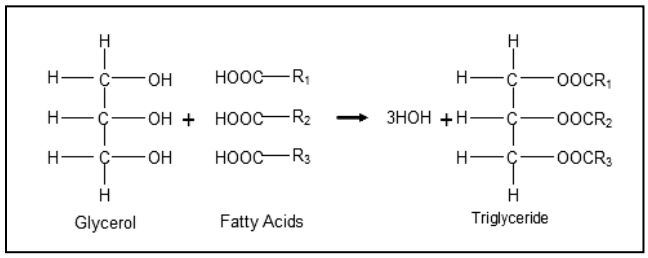

Figure 1: Chemical structure of a typical triglyceride (Vegetable oil)

2.3. Refining of Jatropha oil

After oil expelling, the crude vegetable oils contain some of the impurities such as uncrushed seed cake and other particulates. Therefore it was essential to refine the crude vegetable oils. The crude non-edible oils such as jatropha oil were refined in the laboratory through simple filtration methods. These were filtered by using 4 micron filter paper under vacuum condition. These filtered oils were dried in a vacuum drier at a constant temperature of 60^0C for 4 hours to remove the traces of moisture. The dried oils were stored in the air tight dry PVC cans. The oils were filled up to the brim of the can to avoid any chances of oxidation. These cans were stored in a room at ambient temperature.

2.4. Test Fuel Characterization

The physico-chemical properties of the jatropha oil and their various blends with diesel were evaluated as per the ASTM standards and the experimental procedures for evaluating physico-chemical properties were followed.

2.5. Experimental set up for engine testing

2.5.1. Engine

Five engines were provided with suitable arrangement, which permitted wide variation of controlling parameters and the experimental set up is shown in Figure 2. These engines, manufactured by Fieldmarshal Diesel Engines Pvt. Ltd. India, are indirect injection (IDI) low speed coupled with 7.5 kVA alternators run by diesel fuel. It is widely used mostly for agricultural irrigation purposes and in many small and medium scale commercial applications. This is a single cylinder, four stroke, vertical, water cooled system having a bore of 120 mm and stroke of 139.7 mm. At the rated speed of 1000 rpm, the engine develops 7.35 kW power output in pure diesel mode. The engine can be started by hand cranking, using decompression lever. The engine is provided with a centrifugal speed governor. Other detail specifications of the test engine are presented in Table 1

Sl.No.	Particulars	Specifications
1	Make	Fieldmarshal Diesel Engines
2	Model	FM-4
3	Rated brake power (bhp/kW)	10 /7.35110
4	Rated speed (rpm)	1000
5	Number of cylinder	One
6	Bore x Stroke (mm)	120 x 139.7
7	Compression ratio	17:1
8	Cooling system	Water Cooled
9	Lubrication system	Forced Feed
10	Cubic capacity	1580 cc
11	Nozzle	DL30S1202MICO
12	Nozzle Holder	9430031264MICO
13	Fuel pump	9410032034
14	Fuel pump plunger	9.03/323 MICO
15	Injection pressure	145 kg/cm^2
16	Specific fuel consumption	265g/kW hr or195g/bhp/hr
17	Sump capacity	4.5 ltr
18	Lubricating oil consumption	15g/hr
19	Net Weight	355 kg
20	Gross Weight	490 kg

Table 1: Specifications of Fieldmarshal make single cylinder IDI diesel engine

The test engines are directly coupled to a 230 V single phase AC generator of 7.5 kVA capacities to absorb the maximum power produced by the engine. The alternators are used for loading

the engine. When the load bank is switched on, the electricity generated by alternator is consumed. Alternator converts mechanical power produced by the engine to electricity and provides it to the load bank. The specifications of the alternator are given in Table 2.

Sl.No.	Particulars	Specifications
1	Make	Fieldmarshal
2	Alternator type	Single phase, 50 Hz, AC
3	Rated output	7.5 KVA at 1500 rpm, PF=0.8
4	Rated speed (rpm)	1500
5	Rated voltage (Volts)	230 V
6	Rated currents (Amps)	32 A

Table 2: Specifications of the alternator coupled with single cylinder diesel engine

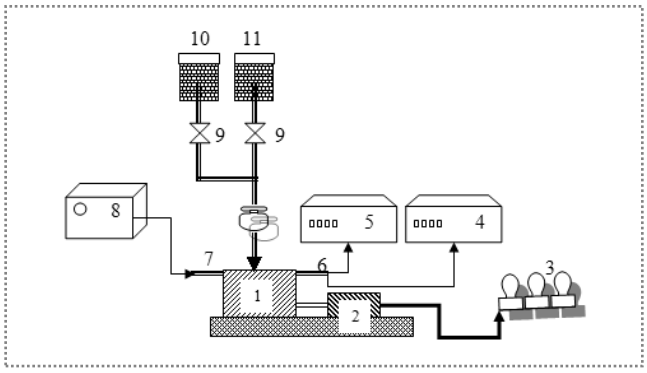

1. Single cylinder 4-stroke diesel engine, 7.35 kW
2. Alternator
3. AC shunt lamp load
4. Gas Analyzer
5. Smokemeter
6. Exhaust manifold
7. Intake manifold
8. Air drum
9. Control valve
10. Fuel tank for neat diesel
11. Fuel tank for blends of diesel and JSVO

Figure 2: Schematic diagram of test set up for single cylinder IDI diesel engine

2.5.2. Engine loading system

Load banks (AC shunt lamp load) were fabricated for the present investigations. The engine-alternator system was connected to load bank. The load bank consists of six heating coils (1000 Watts each) and nine filament lamp (200 W & 100 W). The engine/alternator was loaded up to 100% load using these load banks.

2.5.3. Engine control panel

Five set of engine control panel were built up for test purposes which were equipped with fuel supply system, measurement of output system and various temperature indicators for analyzing the engine performance and emission parameters.

2.5.4. Fuel supply system

A burette was placed on the control panel to measure the volumetric fuel consumption of the engine. The fuel flow was measured by noting the time taken for 50 cc of fuel consumed by the engine. Two fuel tanks were used for each experimental set up to carry out the performance and emission characteristics of the engine with neat diesel and various blends with JSVO. The fuel system was modified by adding an additional filter and three-way hand operated two position directional control valve which allowed rapid switching between the diesel fuel used as a standard and the test fuels. Fuel was fed to the injector pump under gravity and the volumetric flow rate was measured by the use of a 50 cc graduated burette & stopwatch.

2.5.5. Measurement of power

Voltmeter and ammeter were also mounted on the control panel. Voltmeter and ammeter were used to measure the voltage and current consumed by the load in the load bank. The product of voltage and current gives the actual load on engine-alternator system.

2.5.6. Measurement of temperature

Chromel/alumel thermocouples were installed to monitor gas temperatures at inlet and outlet ducts, the exhaust gas and lubricating oil as well as cylinder wall temperatures. Digital temperature indicators were used to measure the temperature of these parameters by using these thermocouples.

2.5.7. Measurement of speed and air flow rate

The speed was also checked with an infrared type digital tachometer. The speed of the engine was sensed by pointing the laser beam of digital tachometer to a sensor mark at the flywheel of the engine and indicated by digital display of the tachometer.

Pressure difference in the inlet manifold was measured by a normal U-tube manometer. Airflow was measured by taking the difference in heights of water column in the two legs of the manometer and area of orifice of the surge tank.

2.5.8. Exhaust gas analyzer and Smoke Opacity

The exhaust gas composition was measured using exhaust gas analyzer (AVL DIGAS – 4000 model). It measures NO_x, CO_2, CO, HC and O_2 in the exhaust gases. The basic principle for measurement of NO_x, CO_2, CO and HC emissions is a non-diffractive infrared radiation (NDIR) and an electrochemical method for oxygen measurement. Measurement range and resolution for different gases by the exhaust gas analyzer used are given in Table 3.

Exhaust gas	Measurement range	Resolution
NO_x	0-4000 ppm	1 ppm
CO	0-10 vol. %	0.01 vol. %
CO_2	0-20 vol. %	0.1 vol. %
HC	0-20000 ppm	1 ppm
O_2	0-22 vol. %	0.01 vol. %

Table 3: Exhaust gas analyzer specifications

The opacity of the exhaust gases was measured by smoke meter (AVL Austria, 437). The exhaust opacity is defined as the extinction of light between the light source and receiver in a pipe filled with exhaust gases. The smoke opacity is usually measured to quantify the amount of particulate matter present in the engine exhaust. In the smoke meter, exhaust gases flow through a chamber having non-reflective inner surfaces. The light is passed through this chamber. The light source is an incandescent bulb with a temperature between 2800K and 3250K. The light travels through the chamber and falls on a photocell placed at the other end of chamber. The current delivered by the photocell is a linear function of the intensity received by it. When the light is passed through the chamber with exhaust smoke, the particulate matters present in the smoke, hinders the path of light. Thus only a fraction of light reaches the photoelectric cell and generates a voltage signal. The voltage signal is reciprocal to the opacity of the exhaust gases.

AVL 437 smoke meter measures the opacity of the polluted exhaust, in a particular diesel exhaust gases (in a measurement chamber of a defined measurement length). The effective length of the measurement chamber was 0.430 ± 0.005 m. The temperature of the exhaust gas to be measured was kept between 70^0C and 130^0C as per recommendations of the manufacturer.

2.5.9. Engine testing

The short-term performance and emission characteristics were evaluated by testing the engine fueled with prepared test fuels to determine how each fuel would perform under identical engine and load conditions. The variables involved in the short-term engine testing are listed in the test matrix shown in Table 4.

Types of variables studied	Details of variables studied
Fuels used	Diesel, Jatropha Oil (JSVO100), Jatropha Diesel Oil (JSVO50), Jatropha Diesel Oil (JSVO20), Jatropha Diesel Oil (JSVO10)
Load, %	0% , 20%, 40%, 60%, 80%, 100%
BSEC	At 0% , 20%, 40%, 60%, 80%, 100% load
BTE	At 0% , 20%, 40%, 60%, 80%, 100% load
Engine Exhaust Emissions	Carbon monoxide (CO), Carbon dioxide (CO_2), Hydrocarbon (HC), Nitrogen oxides (NOx), Smoke (Opacity %)

Table 4: Test matrix for short term engine testing on single cylinder diesel engine

2.5.10. Test conditions

In the present test matrix, a total of five fuels were tested during the investigation keeping all the independent variables same. The experiments were carried out by using Diesel, Jatropha Oil (JSVO100),

Jatropha Diesel Oil (JSVO50), Jatropha Diesel Oil (JSVO20), and Jatropha Diesel Oil (JSVO10) at different load condition on the engine from 0 % to 100 % in steps of 20 per cent. The objective of such a study was to compare the suitability of these fuels for engine application and to determine the optimum fuel blend for recommendation.

To evaluate the performance parameters, some of the observations like engine speed, generator output, fuel consumption rate, airflow rate and temperature of engine exhaust gases were measured. The performance parameters were calculated from their fundamental relations while varying the load on the engine from 0% to 100% in steps of 20 per cent.

The engine emissions like carbon monoxide, carbon dioxide, nitrogen oxides, unburned hydrocarbon and smoke were measured with an AVL five gas analyzer and a smoke-meter. The sensor of the analyzer was exposed to the exhaust gas and the observations were recorded.

2.5.11. Engine test procedure

i. The engine was started by setting the load bank switches closed. The fuel control lever was set towards higher fuel rate. The speed was adjusted exactly to 1000 rpm through fuel control lever.
ii. Before starting of the test, the engine was run for 30 minutes to get stabilization and thereafter stabilization period of 10 minutes was allowed in subsequent testing. At first, the tests were conducted using neat diesel as fuel by varying the load from 0% (idle load) to 100% and engine speed was kept constant.
iii. The load on the engine was applied by closing the load switch. The load was increased by increasing the current and voltage. The engine was loaded continuously till the dense black smoke appeared from exhaust pipe and further loading was not possible.
iv. At each operating condition; load on control panel, engine speed, time for 50 cc fuel consumption, lubricating temperature, difference in U-tube manometer, air inlet temperature, exhaust temperature and readings of exhaust emissions (CO, CO_2, NO_x, HC, O_2 and Opacity) were recorded.
v. The same procedure was repeated for testing the prepared fuel blends for all the experimental set up. After completion of the testing of one prepared fuel blend, the engine was run up to 15 minutes duration with diesel for its stabilization and combustion of remaining fuel in the pipe line as well as in the injection systems.
vi. The experiments were conducted for each blend and three replications were made on each setting of independent variables. The results of the engine performance and emission characteristics were compared with that of neat diesel.

2.5.12. Engine performance indices

The data collected on response variables with three replications for each setting of independent variables were averaged for calculation of BSFC, BSEC and BTE.

2.5.13. Long term endurance test

IS: 10000 (part IX) – 1980 specifies the method of conducting endurance test on constant speed internal combustion engines. These tests were performed after the initial performance test specified in IS: 10000 (part VIII) – 1980. After completion of the initial performance test the engines were run for 32 cycles (each of 16 hours continuous running) at rated speed. Test cycle for the endurance test is given in Table 5. At the end of each cycle, the engines were stopped and necessary servicing and minor adjustment were carried out in accordance with the manufactures schedule. Before starting the next cycle, the temperature of the engine sump oil was checked and had reached within the room temperature. The engines were topped up with engine oil. The oil was changed according to the manufacturer's recommended schedule. The amounts of makeup oil used during the tests were used to establish the lubricating oil consumption rate.

When, engines needs to be stopped during any cycle for any minor attention, the running time of that cycle was not counted as part of the test and the cycle was recommenced. During the endurance tests, periodic checks were made of the fuel and oil and they were confirmed to the specifications of the manufacturer.

Load (Percent of rated Load)	Running Time (Hours)
100	4 (including warm up period 0.5 h)
50	4
100	1
No Load	0.5
100	3
50	3.5

Table 5: Test cycle for endurance test

The long-term performance and emission characteristics were evaluated by testing the engine fueled with prepared test fuels to determine how each fuel would perform under identical engine and load conditions. In the present test matrix, a total of five fuels were tested during the investigation keeping all the independent variables same. The experiments were carried out by using Diesel, Jatropha Oil (JSVO100), Jatropha Diesel Oil (JSVO50), Jatropha Diesel Oil (JSVO20), and Jatropha Diesel Oil (JSVO10) at different load condition on the engine from 0 % to 100 % in steps of 20 per cent. To evaluate the performance parameters, some of the observations like engine speed, generator output, fuel consumption rate, airflow rate and temperature of engine exhaust gases were measured. The performance parameters were calculated from their fundamental relations while varying the load on the engine from 0% to 100% in steps of 20 per cent.

The engine emissions like carbon monoxide, carbon dioxide, nitrogen oxides, unburned hydrocarbon and smoke were measured with an AVL five gas analyzer and a smoke-meter. The sensor of the analyzer was exposed to the exhaust gas and the observations were recorded. The objective of such a study was to compare the suitability of these fuels for engine application and to determine the optimum fuel blend for recommendation.

2.5.14. Measurement of wear

The tribological analysis of lubricating oil is very much essential to adopt any alternate fuel for the existing engines. The engines used for endurance test were from the regular production line of the manufacturer. Prior to the endurance test, the five engines were completely dismantled and examined physically so that design features and also the conditions of the various parts noted before tests were commenced. After the physical examination, the dimensions of the main working parts such as cylinder head, bore/liner, piston, piston rings, gudgeon pin, valves, valve seats, valve guide, connecting rod etc were checked and recorded.

The engines were re-assembled under the supervision of the manufacturer, mounted on a suitable test bed. The engine was operated for the entire period of endurance test. Lubricating oil samples were drawn after regular intervals of 64 hours for all the five engines. A number of tests were conducted on lubricating oil samples for comparison with base line diesel engine. After the completion of tests, the engines were dismantled. Its conditions were noted and the dimensions of the critical parts were recorded to find out the wear of the engines.

3. Results & Discussions

3.1. Test Fuel Characterization

The important physico-chemical properties of jatropha oil and their blends with diesel were determined by standard methods and compared with diesel. The analytical results are shown in Table 6.

Properties	Diesel	JSVO10	JSVO20	JSVO50	JSVO100
Density (gm/cc at 30^0 C)	0.816	0.842	0.845	0.870	0.910
Kinematic Viscosity (cSt at 30^0 C)	4.3	6.7	13.1	28.1	51.4
Calorific Value (kJ/kg)	45022	44185	43225	40793	39935
Flash Point (^{0}C)	86	98	107	176	211
Pour Point (^{0}C)	-15	-13	-11	-8	-3
Total acid number (mgKOH/g)	0.17	0.21	0.26	0.53	0.92
Cetane Index	46	46	44	41	38
API gravity	31.7	29.8	28.6	26.5	22.7
Carbon residue (%,w/w)	0.1	0.16	0.19	0.39	0.64

Table 6: Physico-chemical properties of diesel and jatropha oil blend

The results show that the heating value of the vegetable oil is comparable to the diesel oil and the cetane index is slightly lower than the diesel fuel. However, the kinematic viscosity and the flash point of jatropha oil are several times higher than the diesel oil.

3.1.1. Effect of blending Jatropha oil with diesel on viscosity of the test fuel

The viscosity of the vegetable oil was decreased on increasing the diesel content in the blend (Table 6). Though a substantial decrease in viscosity and density was observed with JSVO50 and JSVO20, still the viscosity and density are higher than that of diesel. A reduction of viscosity of 45.33%, 74.51% and 86.96% was obtained with JSVO50, JSVO20 and JSVO10 respectively. The viscosity and density of jatropha curcas oil were reduced from 51.4 and 0.910 to 28.1 cSt and 0.870 g/cc, respectively, with JSVO50. The viscosity of the JSVO10 was slightly higher than diesel oil. In this case the viscosity of JSVO10 was found to be close

to that of diesel oil. Therefore, 80–90% of diesel may be added to jatropha oil to bring the viscosity close to diesel fuel and thus blends containing 10–30% of jatropha oil can be used as engine fuel without preheating.

3.1.2. Effect of temperature on viscosity of jatropha oil, diesel and their blends

It has been found that heating the fuel makes its spray characteristics more like those of diesel oil, which is the direct result of viscosity reduction. In the present study, efforts have been made to reduce the viscosity by pre-heating the vegetable oils, prior to injection in the in the pre-combustion chamber of the engine. Therefore, the viscosities of these blends were measured at different temperature ranging from 30-100^{0}C. It was observed from the Figure 3 that viscosity of vegetable oil decreased remarkably with increasing temperature and became close to diesel at temperature above 80^{0}C. Therefore, the blends of JSVO10 and JSVO20 may be used with slight heating or even without heating, particularly in summer season (within ASTM limit).

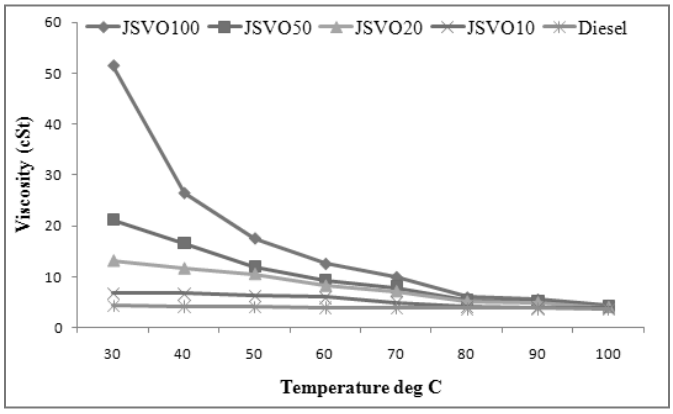

Figure 3: Effect of temperature on viscosity of jatropha oil and various blends.

3.2. Performance study

3.2.1. Effect of load and blend on brake specific energy consumption (BSEC)

When corresponding observations of brake specific fuel consumption (BSFC) at different loads were evaluated, the trends of the BSFC increased slightly for all blends as compared to neat petro-diesel. This may be due to the low calorific value of JSVO and its blends with diesel. However, BSFC is not a very reliable parameter to compare fuel blends as the calorific value and the density of the blends follow a slightly different trend. Hence BSEC is a more reliable parameter for comparison. Therefore, this parameter is used in this study to compare volumetric consumption of all of the test fuels.

Fig 4 compares the specific energy consumption of diesel, JSVO10, JSVO20, JSVO50 and neat jatropha oil at varying brake loads in the range 0–6kW over the entire period of long term endurance test. It was observed that the specific energy consumptions of the neat diesel oil as well as the blends were decreased with increasing load. The energy consumptions were also found to increase with a higher proportion of jatropha curcas oil in the blend. Though the blends as well as the jatropha curcas oil maintained a similar trend to that of diesel, the BSEC in the case of the blends were higher compared to diesel oil in the entire load range throughout the long term endurance test. This is mainly due to the combined effects of the relative fuel density, viscosity and heating value of the blends. However, JSVO10 and JSVO20 have BSEC very close to that of diesel oil. The BSEC values were found minimum in case of diesel over the entire range of long term endurance test cycle. The specific energy consumption of 15223kJ/kWh was observed using JSVO10 at 100% load which is comparable to the BSEC obtained with diesel oil under the same load. The higher density of blends containing a higher percentage of jatropha curcas oil has led to more discharge of fuel for the same displacement of the plunger in the fuel injection pump, thereby increasing the BSEC.

3.2.2. Effect of load and blend on brake thermal efficiency (BTE)

The variation of brake thermal efficiency of the engine with various blends and jatropha oil is shown in Fig. 5 and compared with the brake thermal efficiency obtained with diesel in each cycle during the long term endurance test. From the test results it was observed that initially with increasing load the brake thermal efficiencies of the vegetable oil, diesel and the blends were increased and the maximum thermal efficiencies were obtained at 100% load in case of JSVO50. There was a considerable increase in efficiencies with the blends compared to the efficiency of jatropha oil alone, but the brake thermal efficiencies of the blends and the jatropha curcas oil were higher than that with diesel fuel throughout the entire range. The maximum values of thermal efficiencies with JSVO50, JSVO20 and JSVO10 were observed as 25.02%, 22.01% and 21.53%, respectively. Among the blends tested, in the case of JSVO100, the thermal efficiency and maximum power output were close to the diesel values.

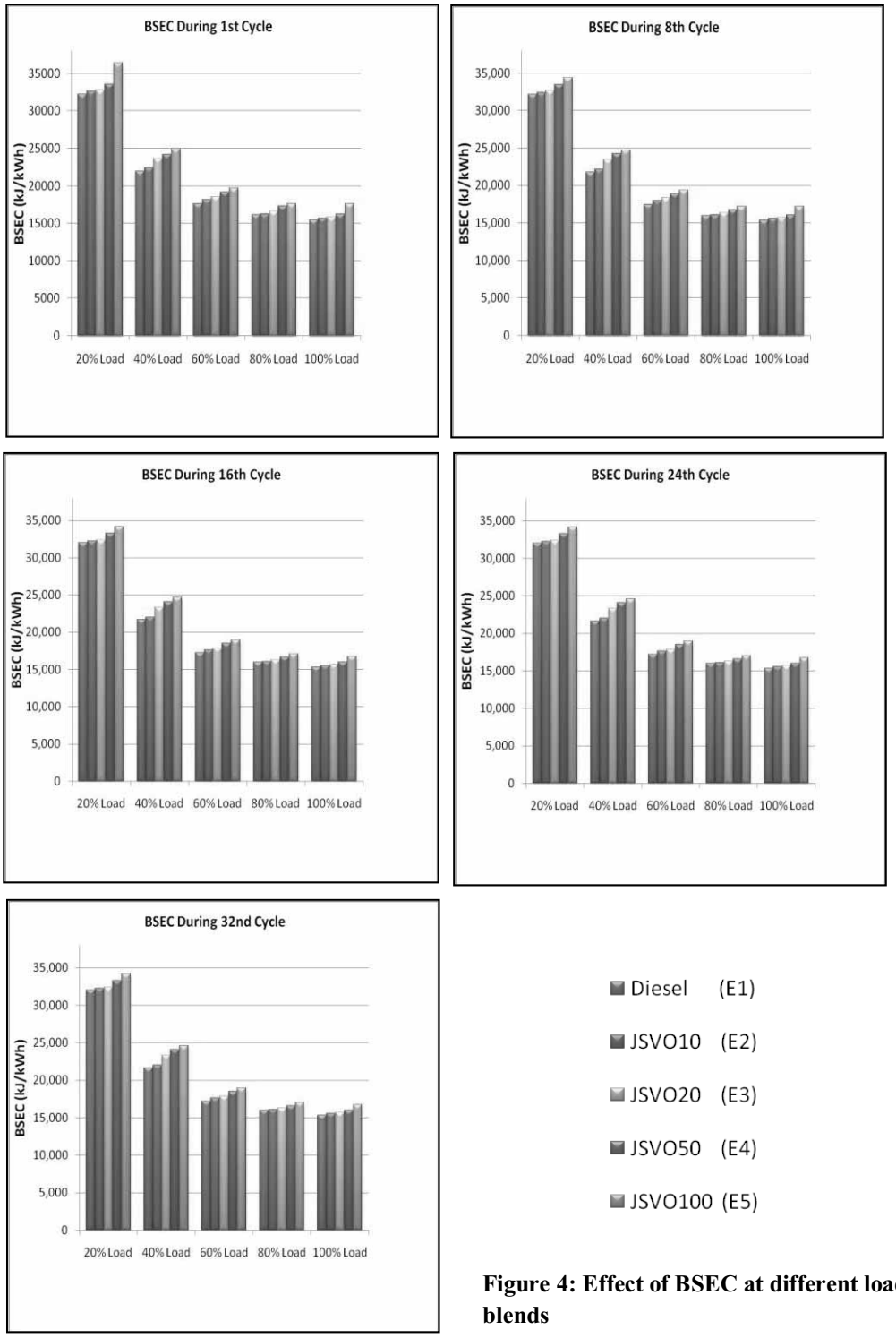

Figure 4: Effect of BSEC at different loads and blends

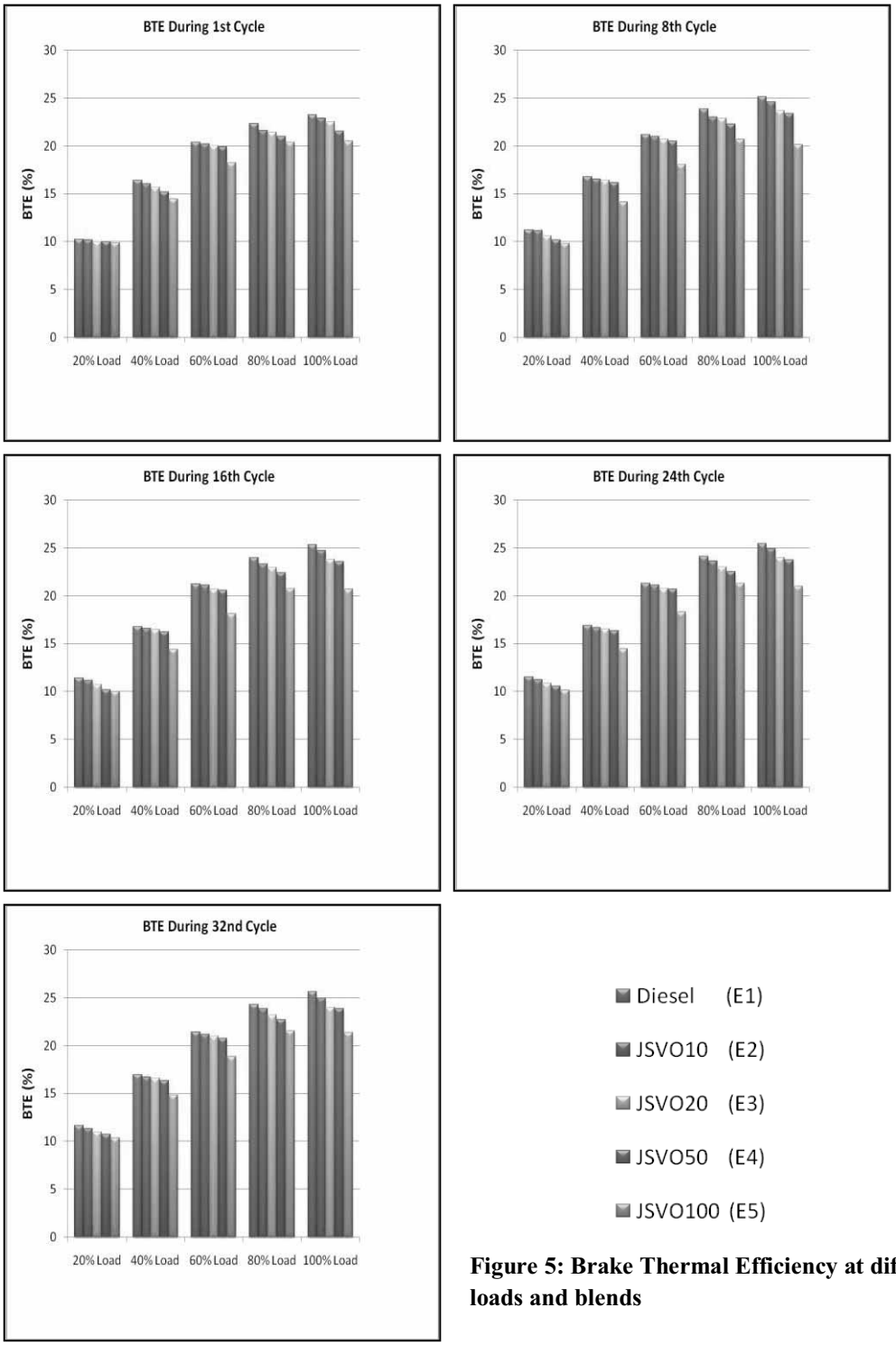

Figure 5: Brake Thermal Efficiency at different loads and blends

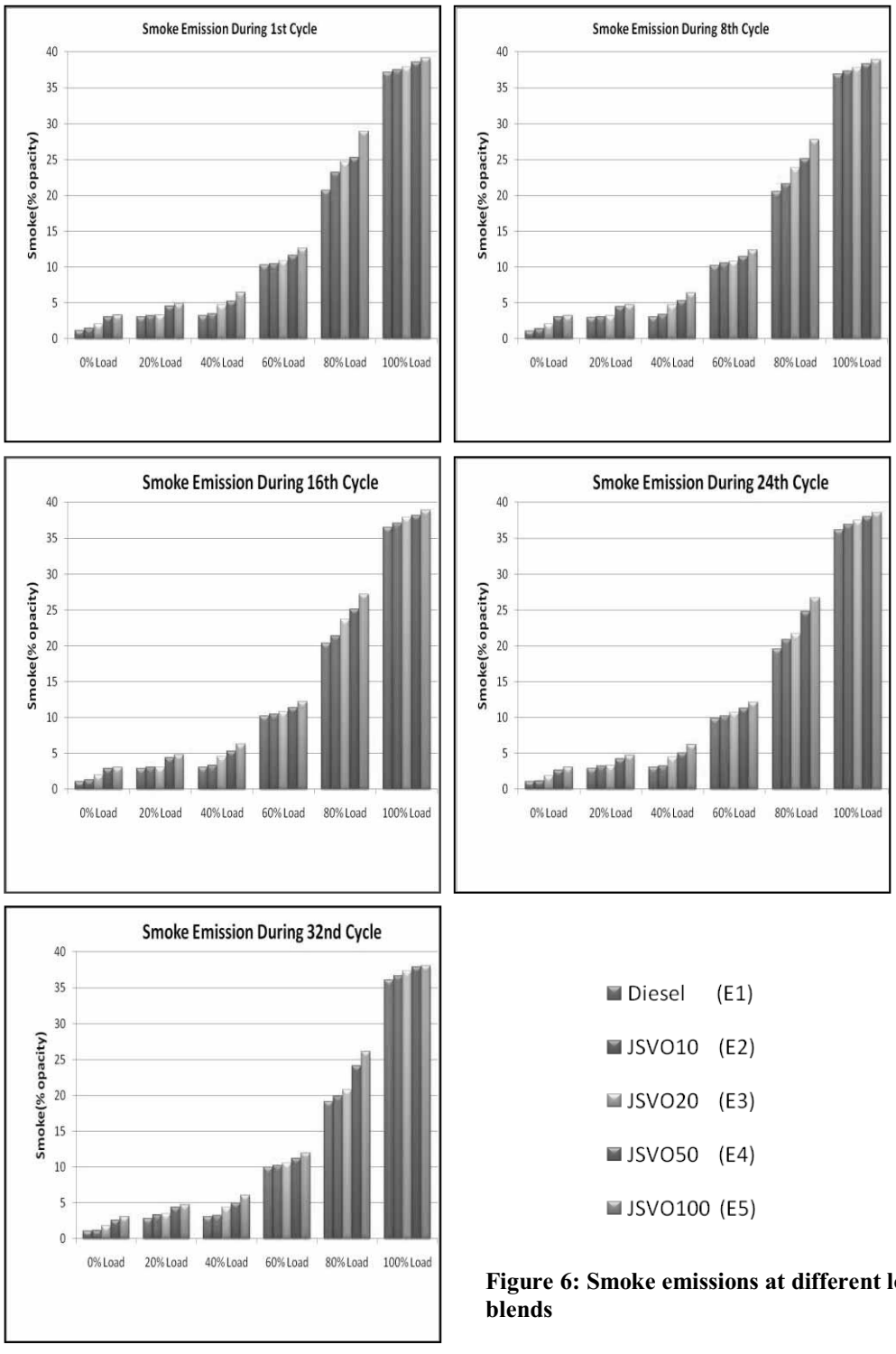

Figure 6: Smoke emissions at different loads and blends

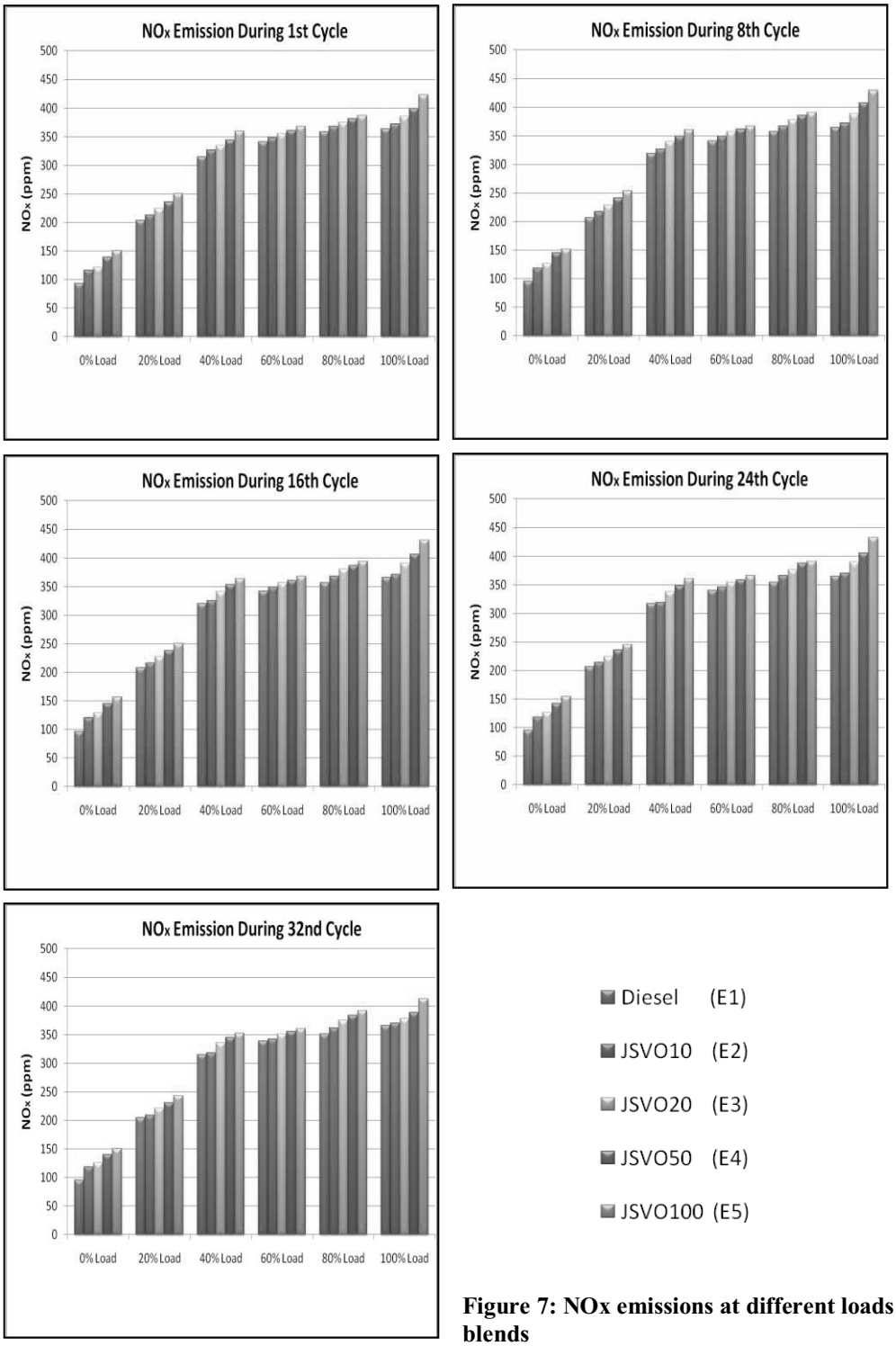

Figure 7: NOx emissions at different loads and blends

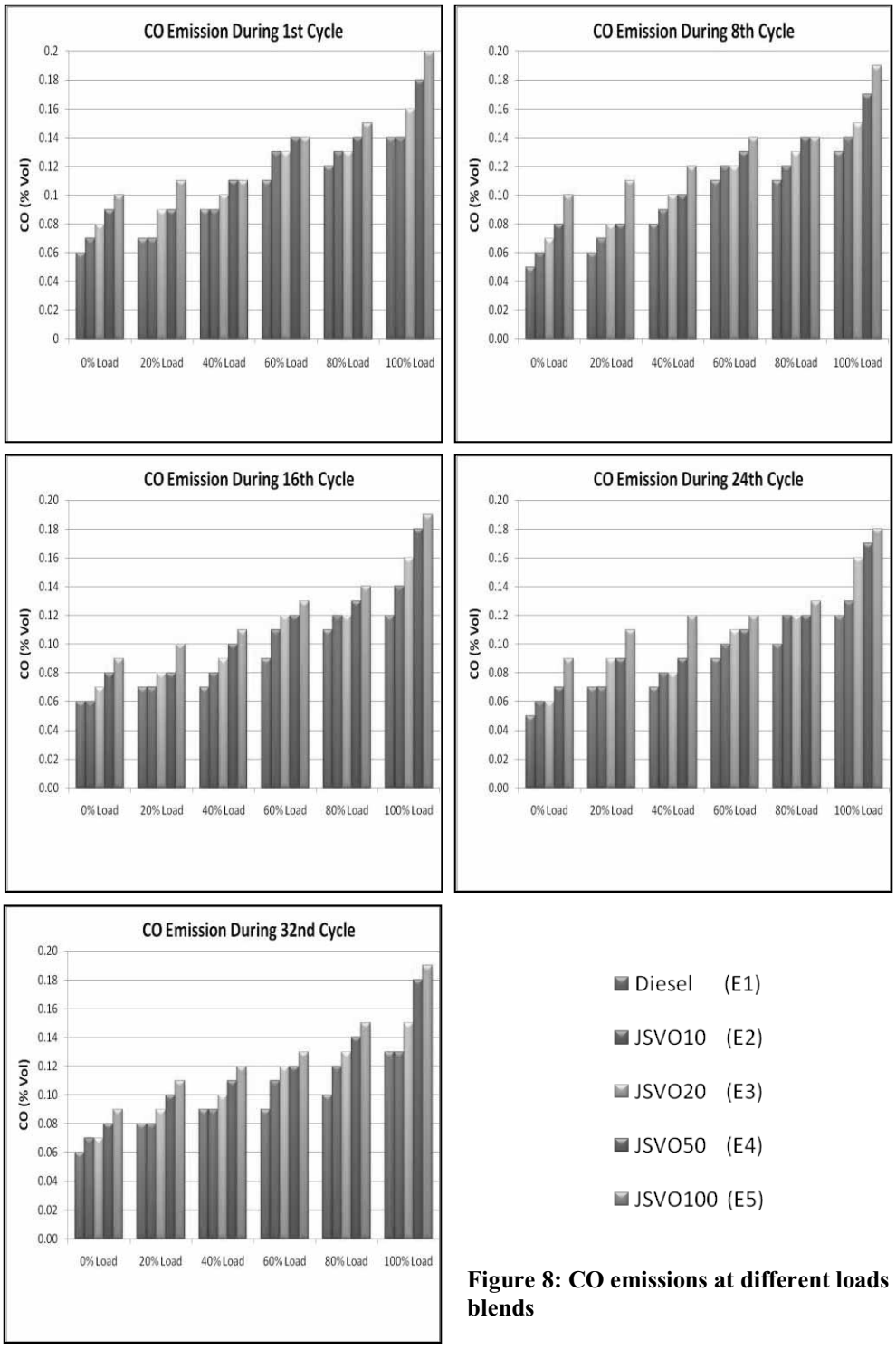

Figure 8: CO emissions at different loads and blends

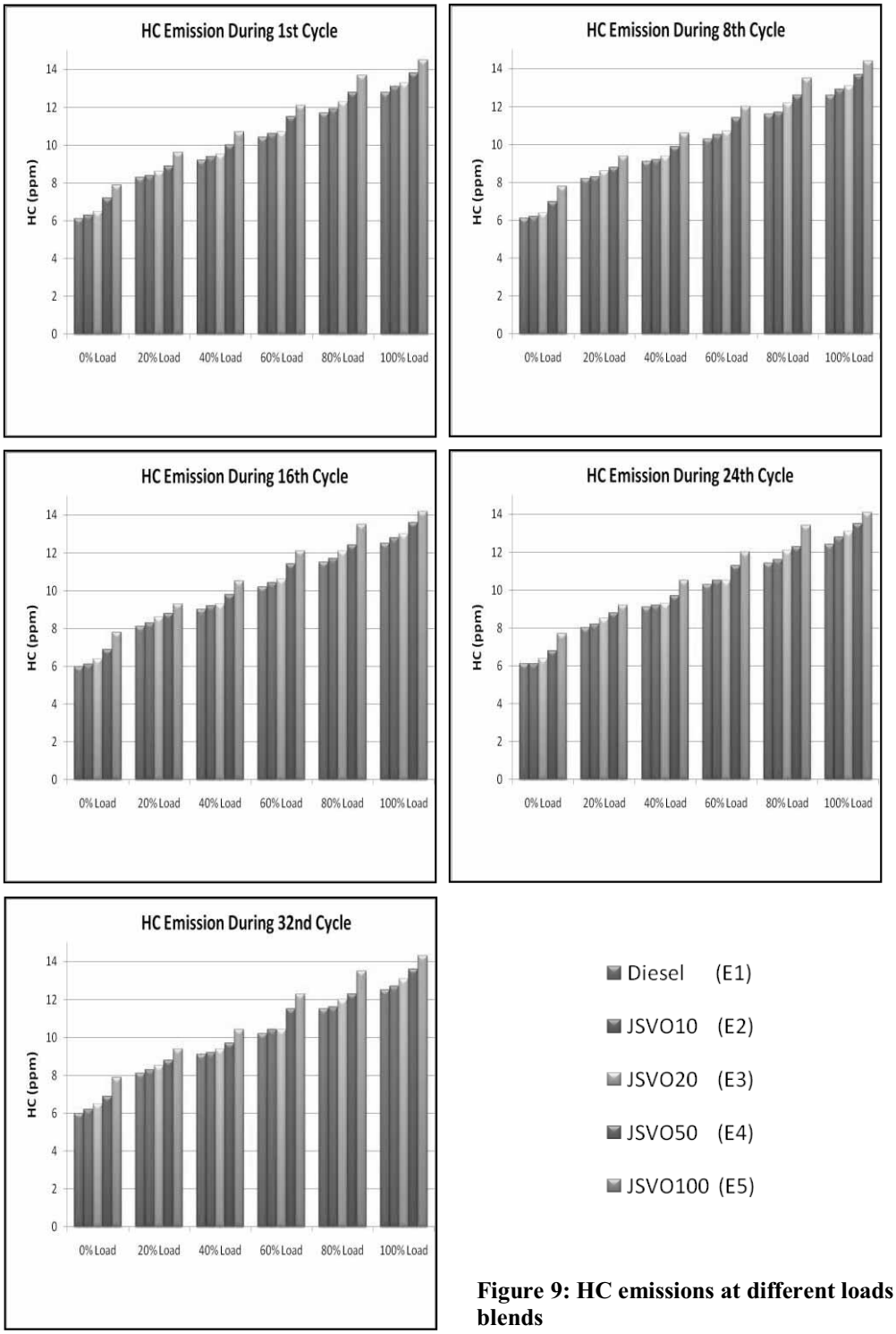

Figure 9: HC emissions at different loads and blends

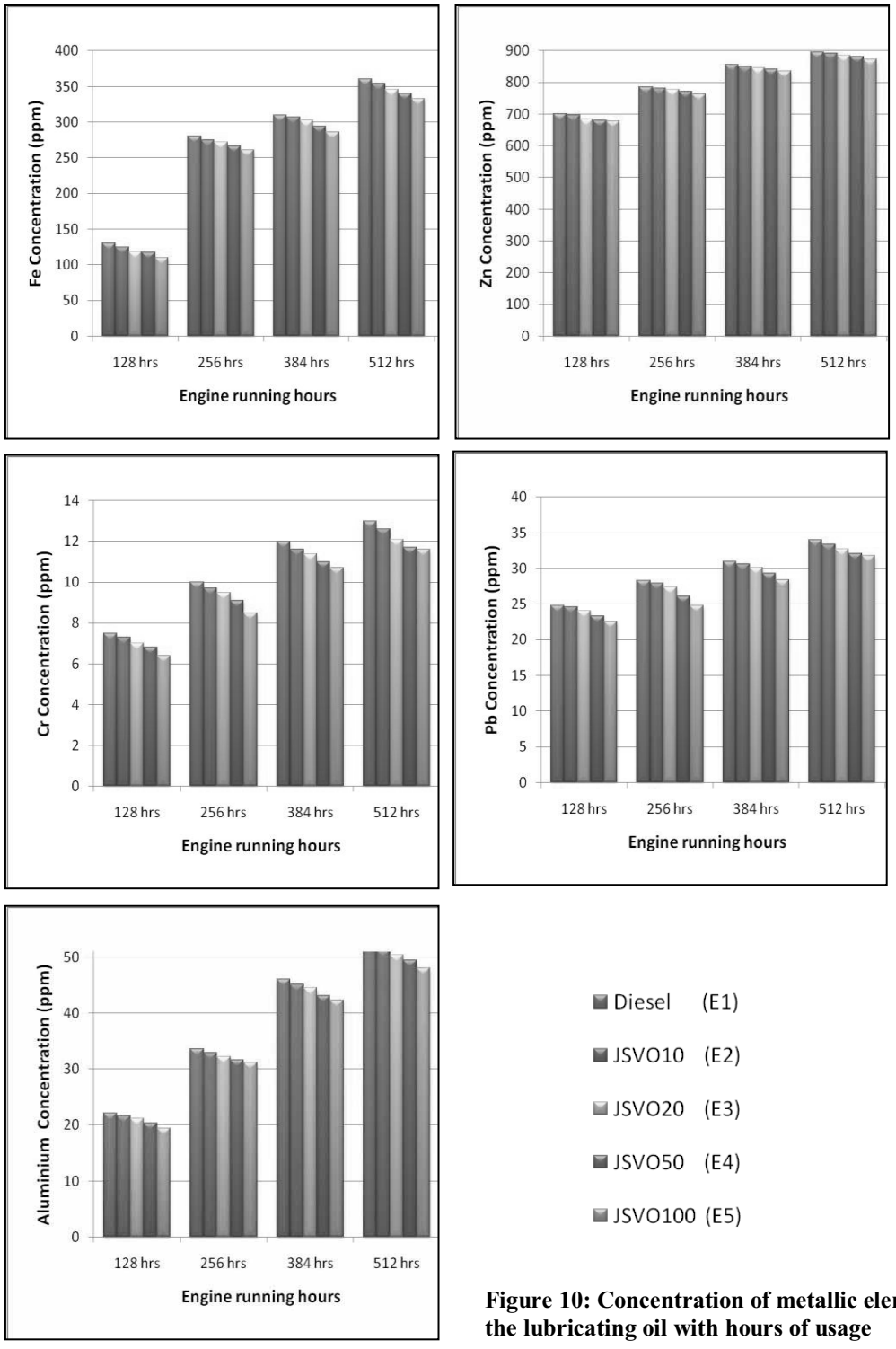

Figure 10: Concentration of metallic elements in the lubricating oil with hours of usage

A reasonably good thermal efficiency of 25.02% was also observed with the JSVO50. The increase in thermal efficiency with increase in proportion of vegetable oil must be attributed to the pre-combustion characteristics of the vegetable oils in the pre-chamber in case of IDI diesel engines.

3.3. Emission study

The engine emissions were measured with an AVL-5 gas analyzer (for NOx, HC, CO, CO2, and O2) and a smoke-meter. The measured emissions are shown graphically in Figs. 6-9. The smoke was slightly increased for all test fuels as compared to neat petroleum based diesel fuel (Fig. 6) over the entire period of endurance test. This was due to the high viscosity and incomplete combustion of the blend. The opacity was least for the case of diesel at up to 80% load. It can be found that smoke opacity increased more at higher loads than at lower loads for blended fuel. The smoke emission is the higher for JSVO100. This is reasonable since more fuels are supplied for the higher load and short time is available for preparation of the air/fuel mixture at high speeds. This factor leads to the reduction of combustion quality for blends when compared to diesel fuels. Therefore, diesel is the optimum fuel when smoke opacity is taken into consideration. Here also, it is possible that the smoke emissions can be reduced further through optimized injection timing.

The influence of load per cent and SVO blends on NOx emissions is shown in Fig 7. The NOx emissions depend on the engine type, engine operating conditions and fuel properties. The diesel engines produce lower NOx emissions because of their lower combustion temperature. It can be seen from Fig 7 that raising the SVO from 10 to 100 per cent increased the exhaust NOx level from 100 ppm to 200 ppm for jatropha oil at 0% load. Similarly, there was substantial increase in NOx for JSVO10, JSVO20 and JSVO50 over the entire range of engine operation. It can be noted that lean fuel with a high cylinder temperature may generate higher NOx emission level that may possible for SVO blends because of higher heat release rate at the premix or slow combustion phase. Another reason may be due to the maximum temperature, high temperature duration and oxygen concentration in the mixture has a dominant effect on NOx emission. It is clearly observed from the figure that diesel is the optimum fuel blend which gives less NOx emissions over the entire range of engine operations.

Fig 8 shows the relationships between CO emission and load per cent at different fuel blends. It is seen from the figure that, CO emission increases remarkably at higher loads. The increase in CO levels at lower load is a result of incomplete combustion of the test fuels. Factors causing combustion deterioration (such as high latent heat of evaporation) could be responsible for the increased CO emission. Another reason for the increase of CO emission is the increase in ignition delay. This leads to a lower combustion temperature at lower and medium loads. On the other hand the CO emissions decrease for the blended fuel at higher loads. This can be explained by the enrichment of oxygen owing to SVO addition, as increasing the proportion of oxygen will promote further oxidation of CO during the engine exhaust process. It is also found from the figure that CO emission increases gradually with blending of higher concentration of JSVO to diesel. This may be due to increase in viscosity with blending leading to less homogenous mixtures. It is observed from the graph that the emission of CO is least in case of diesel at 80 and 100 per cent load. Therefore, diesel is the optimum fuel blend for CO emission at 80% and 100% load followed by JSVO10.

It is seen from the Fig 9 that increasing load per cent and JSVO blends has a adverse effect in increasing HC emissions. It is interesting to note that the increase in HC is primarily due to the result of incomplete combustion of JSVO blends within the combustion period. As the load and blend on the engine was increased, the percentage of CO_2 also increased gradually and reached a maximum value of 8.49% for pure jatropha oil, 7.7% at 50% JSVO blend, 7.5% at 20% JSVO blend, 7.3% at 10% JSVO blend and 6.4% for diesel at full load for all the fuel blends as shown in Fig 10. Higher percentage of CO_2 in the exhaust indicated higher oxidation of fuel at the constant engine speed and release of more heat for power conversion. It also indicated better combustion as more fuel was converted from CO to CO_2.This trend was because the engine attained optimum operation of CO_2 at the rated load conditions and as such the highest percentage of CO_2 was observed at rated load value. Results described that CO_2 emissions increased as load and blends on the engine was increased.

3.4. Tribological study

3.4.1. Effect of JSVO on lubricating oil

The viscosity of JSVO fuelled engine first decreases and then increases slightly. The decrease in viscosity due to fuel dilution could have slowed down in case of JSVO100 fueled engine. It may be due to the formation of thin lubricating oil film inside the cylinder liner preventing the fuel dilution through the piston rings and cylinder liner. The density of lubricating oil from all five engines showed an

increasing trend with usage. It was observed that the density of lubricating oil from diesel fuelled engine increased mainly due to addition of wear debris, fuel dilution and increase in moisture content. It was also observed that the ash content decreases for JSVO fuelled engines suggesting lesser amount of fuel dilution, moisture addition and wear debris. The flash point for lubricating oil samples with usage were reduced considerably and maximum of 233^0C was observed in case of JSVO100 engine. The flash point of JSVO100 fueled engine lubricating oil increased possibly due to oxidation of base lubricating oil. Interestingly, the carbon residue of the diesel fueled engine was increased up to 1.9% followed by 1.2%, 1.1% and 0.9% for JSVO50, JSVO20 and JSVO10 fueled engine respectively. It was observed that the carbon residue of lubricating oil from JSVO fueled engines is generally lower than that of diesel fueled engine.

3.4.2. Effect of JSVO on engine wear

The quantity of various metals present in the lubricating oil samples from five engines was evaluated to study the wear of different parts and material compatibility of the test fuels with the existing engines. The change in internal dimensions of the sliding components of the engine, confirmed the lubricating oils atomic absorption spectroscopy analysis. It was found that iron wear in case of JSVO100 fueled engine was lowest followed by JSVO50, JSVO20, JSVO10 and Diesel (Fig 10). It was confirmed by measuring the dimensions of cylinder liner, piston rings, valves, gears, shafts, bearing and crankshaft after endurance test responsible for iron wear. Similar trend was observed in case of other metals wear such as zinc, chromium, magnesium, lead and aluminum. Copper corrosiveness of all the lubricating oils was evaluated and was of grade1a. Hence, it can be concluded that JSVO fueled engines are as safe for engines as diesel fueled engine from copper corrosion point of view.

3.5. Maintenance Schedule

Lubricating oil consumption was observed in the range of 14 to17 gm/hr and engine fueled with JSVO100 consumed maximum lubricating oil (17.1 gm/hr) as compared to 15 gm/hr as recommended by the manufacture. The air filters of all the engines were cleaned after 100 hours of running as per the manufacture's maintenance schedule. The physical conditions of various vital engine parts were compared for the engines before and after endurance test. Auxiliary machineries such as governor linkage, fuel pump side window and radiator fan were lubricated after 100 hours of engine running by visual observations instead of 250 hours as mentioned in manufacturer's schedule. Fuel injectors were cleaned after 256 hours of engine running in order to analyze the carbon deposits in two phase i.e. half of 512 hours (Endurance test hours) instead of 250 hours. An important observation during this test was that the injector tip of all the engines were not choked during the total duration 256 hours. It was clearly observed that the carbon deposit on diesel fuelled engine injector tip was close to that of JSVO10 and JSVO20 fuelled engine. There was a slight increase in carbon deposits in case of JSVO50 and JSVO100 when compared with diesel fuelled engine injector tip. This is due to the presence of higher percentage of unsaturated fatty acid in JSVO50 and JSVO100 which leads to polymerization and incomplete combustion. The engines are running successfully with JSVO100 for standby power generation after modification of the maintenance schedule.

4. Conclusions

The main aim of the present investigation was to carry out long term endurance analysis of IDI diesel engine fueled with jatropha straight vegetable oil to make it suitable for use in a C.I. engine and to evaluate the performance and emission characteristics of the engine with the modified oils. Significant reduction in viscosity was achieved by dilution of vegetable oil with diesel in varying proportions. Among the various blends, the blends containing up to 20% (v/v) jatropha oil have viscosity values close to that of diesel fuel. The blend containing 50% (v/v) vegetable oil has a viscosity slightly higher than that of diesel. The viscosity was further reduced by heating the blends. Acceptable brake thermal efficiencies and brake specific energy consumption were achieved with the blends containing up to 50% jatropha oil. The bake specific energy consumption was observed minimum in case of neat diesel. The overall emission characteristics were found to be best for the case of engine fuelled with diesel over the entire range of long term endurance test. Blends with a lower percentage of vegetable oils showed slightly higher emission when compared to an engine running with diesel but they were much lower than the jatropha oil in all cases. Therefore, from the engine test results, it has been established that up to 50% jatropha oil can be substituted for diesel for use in a C.I. engine without any major operational difficulties. Tribological analysis (wear and tear) revealed that engine fuelled with 100% jatropha oil showed comparatively less wear and tear over the entire range of endurance test.

Acknowledgement

The author is thankful to the Department of Science & Technology, New Delhi for sanctioning and providing the funds under a R&D project titled "Feasibility of blending of straight vegetable oil (SVO) in petro-diesel and its utilization in IDI diesel engine", sanction letter no. 100/IFD/7010/2006-2007 dated 05.01.2007.

References

[1] A. C. Hansen, P. W. L. Lyne, Q Zhang, "Ethanol-diesel blends: A step towards a bio-based fuel for diesel engines", ASAE Paper No. 02-6048, 2001

[2] D.N. Tewari, "Report of the committee on development of Bio-fuel", Planning commission, Government of India, New Delhi, 2003

[3] A.S. Ramadhas, C. Muraleedharan, S. Jayaraj, "Performance and emission evaluation of a diesel engine fueled with methyl esters of rubber seed oil", Renewable Energy, Vol. 20:1-12, 2005

[4] S. Bari, W.C. Yu, T.H. Lim, "Performance deterioration and durability issues while running a diesel engine with crude palm oil", Proc. Instn Mech. Engrs. Part D: J. Automobile Engineering, Vol. 216(D1), 785-792, 2002

[5] H.H. Masjuki, M.A. Kalam, M.A. Maleque, A. Kubo, T. Nonaka, "Performance, emissions and wear characteristics of an indirect injection diesel engine using coconut oil blended fuel." Proc. Instn Mech. Engrs. Vol. 215, Part D, 393-404, 2000

[6] C. M. V. Prasad, M. V. S. M. Krishna, C.P. Reddy, K. R. Mohan, "Performance evaluation of non-edible vegetable oils as substitute fuels in low heat rejection diesel engines", J. Instn. Mech. Engrs., Vol. 214, 181-187, 2000

[7] Yi-Hisu Ju, S. R. Vali, "Rice bran oil as a potential resource for biodiesel: a review", Journal of Scientific & Industrial Research, Vol.64:866-882, 2005

[8] N. Kumar, P. B. Sharma, "Jatropha curcas – a sustainable source for production of biodiesel", Journal of Scientific & Industrial Research, Vol.64:883-889, 2005

[9] P.K. Sahoo, S. N. Naik, M.K.G. Babu, L.M. Das, "Biodiesel Development from High Acid Value Polanga Seed Oil & It's performance in a CI Engine" Proceeding of 3rd International Biofuels Conference organized by Winrock International India, Page 463-478, Jan,18-19, 2006

[10] M. Subramanian, R. K. Malhotra, P.C. Kanal, "Performance evaluation of biodiesel- diesel blends in passenger car", SAE paper no. 280088, 2004

[11] A. K. Agarwal, L.M. Das, "Biodiesel development and characterization for use as a fuel in compression ignition engines.", American Society of Mechanical Engineers Journal Engineering, Gas turbines power, Vol.123, pp 440-447, 2000

[12] T. K. Bhattacharya, S. Chatterjee, T. N. Mishra, "Studies on suitability of lower ethanol proofs for alcohol-diesel microemulsions", Agricultural mechanization in Asia, Africa and Latin America, Vol. 34, No. 1, 2003

[13] L. C. Meher, S. N. Naik, L. M. Das, "Methanolysis of Pongamia pinnata (Karanja) oil for production of biodiesel", Journal of Scientific & Industrial Research, Vol.63:913-918, 2004

[14] D. Kusdiana, S. Saka, "Kinetics of transesterification in rapeseed oil to biodiesel fuel as treated in supercritical methanol", Fuel, Vol.80:693-698, 2001

[15] P. K. Sahoo, S. N. Naik, L. M. Das, "Studies on Biodiesel Production Technology from Jatropha curcas and its Performance in a CI Engine", Journal of Agricultural Engineering, Indian Society of Agricultural Engineering (ISAE), Vol. 42(2):14-20, 2005

[16] Y. Ali, M. A. Hanna, "Durability testing of a diesel fuel, methyl tallowate, and ethanol blend in a Cummins N14-410 diesel engine", Transactions of the ASAE. Vol. 39(03), 793-797, 2001

Fabrication of Aluminum AA6061 Metal Matrix Nano composites

Govind.Nandipati[a,*], Nageswara Rao.Damera[b], Ramanaiah.Nallu[c], Ravindra kommineni[d]

[a]*Asst.Professor, Department of Mechanical Engineering , R.V.R&J.C college of Engineering ,Guntur,*
[b] *Professor, Department of Mechanical Engineering, AUCE, Andhra University, Visakhapatnam,*
[c] *Asssociate Professor, Department of Mechanical Engineering, AUCE, Andhra University, Visakhapatnam,*
[d] *Professor ,Department of Mechanical Engineering, R.V.R&J.C college of Engineering ,Guntur,*

Abstract: Aluminum alloy composites are having significance in structural applications for automobile, aerospace, marine and numerous other light weight applications. Light weight Aluminum alloy composites are prepared by the addition of different % by weights of nano SiC particles. These alloy composites with Nano particulate are called as metal matrix nano composites (MMNCs).Mechanical stirring and Ultrasonic dispersion methods are used for reinforcing nano particulate. The composites are heat treated and aged. These composites are tested for hardness and tensile properties apart from the dispersion of nano particles in the matrix. Mechanical properties of MMNCs are found to be better with a 0.5 weight percentage of nano SiC particles compared to base metal AA6061 and the dispersion of nano particles is observed to be uniform.

Key words: *Metal matrix composites (MMC), Metal matrix Nano composites (MMNC), Nano SiC.*

1. Introduction:

Metal matrix composites (MMCs) have superior mechanical properties like specific modulus, creep, thermal stability and thermal expansion. S.Gustafsson et.al,[1]reports that mullite/5vol.% nano SiC composite has anincreased creep resistance which is caused by grain boundary pinning by intergranular SiC particles and a reduced matrix grain size. C.P You et.al [2] conducted SEM examination on tensile fractured surfaces revealed that larger voids (5-10 μm) associated with SiC particles and smaller voids (<1 μm) associated with ductile failure. In a study Y. Flom et.al [3] reported that, voids are formed at the location of particles inclusion and extend to few times the distances of the size of the particles. The fracture toughness depends on the spacing between larger particles and size of the particles. H.J.Kim,et.al [4],on examining the fracture surface, the size and distribution of the SiC particles, have concluded that particles larger than the calculated critical diameter occupied the main portion of the fractured surface. The plastic zone size decreased as the volume fraction of SiC particles increased. . For the aluminum alloys the fracture toughness decreases as the volume fraction of large inclusions increase, since these inclusions are locations of crack initiation, resulting in low fracture toughness value. Aluminum matrix composites when reinforced with hard ceramic particles have emerged as a potential material especially for wear resistant and weight critical applications P.Gyftou et.al.[5] studied wear properties by co-depositing the micro sized and nano sized SiC particles on the Nickel matrix. The results showed an improvement. The hard dispersoids make the matrix alloy plastically constrained and improves the high temperature strength of the alloy. These hard dispersoids present on the surface of the composite as protrusions, protect the matrix from the severe contact with the counter surfaces [6-7], resulting in lower wear and coefficient of friction. The effect of matrix alloy and sliding wear characteristics of high strength aluminum alloys with silicon carbide particulate was examined by Rao.R.N et.al. [8],under varying applied pressures and fixed sliding speeds and found that, sliding wear behavior of composites varies as a function of reinforcement volume fraction. Further wear resistance of the alloy was improved significantly due to particle reinforcement.

Discontinuously reinforced aluminum alloy metal matrix composites are preferred choice for several critical applications due to the advantages of increase in strength, increase in stiffness and superior wear resistance, improved creep rupture properties, good corrosion resistance, fatigue crack initiation resistance compared to unreinforced aluminum alloys and thermal conductivity [9-12]. The studies on tensile properties and fracture behavior of a silicon carbide particle reinforced aluminum alloy metal matrix composite at ambient and elevated temperature [13] revealed that increase in test temperature decreases the elastic modulus and strength of 2009/SiC_p composite while ductility increases. The presence of the hard, brittle and

elastically deforming SiC particles in soft, ductile and plastically deforming alloy metal matrix causes fine microscopic cracks to initiate at low values of applied stress. Norika Bamba et.al.[15] fabricated Silicon carbide nano composites by hot pressing technique.Fine SiC particulate inhibited the densification and abnormal grain growth, resulting in increased thermal conductivity.

C.F.Deng et. al [16], reinforced the aluminum alloy matrix with Carbon nano tubes(CNT) by iso-static pressing followed by hot extrusion techniques. Carbon nano tubes react with aluminum and forms Al_4C_3phases at 656.3^oC.The nano tube content effects significantly mechanical properties. At 1.0%wt of CNT content the mechanical properties increased while these decline at higher %weight**.** The more percentage of Si constrains the reaction between the SiC and Al in the matrix. It is observed that viscosity of the molten metal increase due to the addition of the nano sized SiC particles [18]

2. Experimental procedure:

The base material used in this study is AA6061alumunium alloy having the following chemical composition is solutionised and aged**.**

Table.1 Chemical composition of AA6061

Alloy element	Al	Mg	Si	Fe	Cu	Mg	Cr	Ti
%by weight	97.768	0.825	0.711	0.342	0.152	0.023	0.017	0.083

SiC nano particulate of size 100nm are used in the study. SiC is selected as its density is close to the Al, and thus there will not be any agglomeration of the particulate during the process. The experimental setup consists of an electrical resistance heating unit for melting the AA6061 aluminum alloy in a EN-8 steel crucible at 710^{0}C. A Sonicator consists of ultrasonic transducer probe is dipped into the melt for ultrasonic processing. Nano sized SiC particles are added at 0.1%,o.2%,0.3%,0.4%,0.5% to the melt during the cavitation process. The molten metal is protected from atmospheric air by Argon gas during melting. The molten metal is poured into a Die of size 200x130x8mm^3 and plates are casted. The as cast plates are heat treated, (solutionised at 560^{0}c for 1hr) and ageing is done at 160^{0}c for12hrs. Tensile specimens are prepared as per the ASTM-E8 standards from these plates. For Microstructural analysis MMNC cast plates are cut to size of 10x10x5mm^3 ground and polished. The samples are etched with Keller's reagent (composed of 2ml HF, 3mlHcl, 5ml HNO^3 and 190ml water). Optical images and SEM images are taken to study the grain refinement and grain structures.

3. Results and discussion

The mechanical properties and microstructures are studied on the parent metal and on the fabricated composites. The results are presented below**.**

3.1. Hardness Tests

The SiC particles are added to the molten metal. During the addition the particulate tend to float on the surface of the melt. The SiC particles have a slightly larger specific density than that of the molten aluminum alloy [18].The reasons for this are high surface tension of the melt and poor wetting between SiC particulate and the melt. Due to the application of high intensity ultrasonic waves the acoustic streaming traps the nano particles into the melt effectively.

Hardness of the composites is measured at different locations on the samples. The hardness increased nearly linear with various weight percentages of the nano SiC particulate. The hardness of the aluminum AA6061 alloy is found to be Hv-106.The hardness values of the MMNC are plotted in the fig-1.

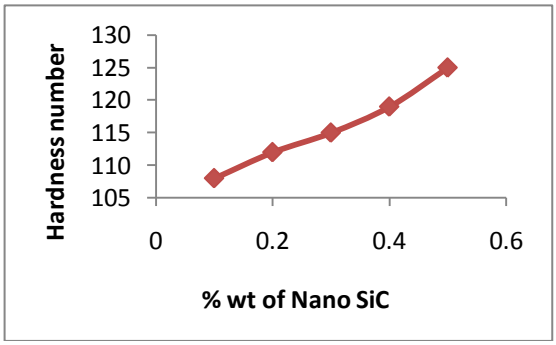

Fig-1 showing the hardness profile of MMNC

3.2. Tensile Tests*:*

The tensile specimens are prepared with gauge length 28mm and cross sectional area as 5x6mm^2.The tests are conducted on 2Tonn extensometer. The ultimate tensile strength and yield strength of the base metal AA6061 are found to be306MPa and 282MPa respectively. The tensile tests are also conducted on metal matrix nano composites and are presented in table-2. With only 0.5%by weight of nano SiC particles the ultimate tensile strength has been increased by 31% and reads 452MPa.The higher dislocation density in the MMNC is responsible for strengthening mechanism. This dislocation phenomenon is due to the difference in thermal expansion coefficients between matrix and uniformly dispersed nano SiC particulate, which act as barriers for dislocation movements. The coefficient of thermal expansion mismatch the strain between the aluminum alloy metal matrix and the reinforcing SiC particulate. The plastic deformation of the ductile aluminum alloy metal matrix in the presence discontinuous SiC reinforcements, is non uniform. This is due to the hard, brittle and elastically deforming particles **resisting** the plastic flow of the soft, ductile and plastically deforming aluminum alloy metal matrix [13].

Tables.2 Mechanical properties of Aluminum MMNC

% by weight of nano Sic particulate	Yield strength(MPa)	Ultimate Tensile strength [MPa]	Elongation (%)
0.1	320	336	39
0.2	335	355	35
0.3	360	390	30
0.4	386	425	28
0.5	402	452	24

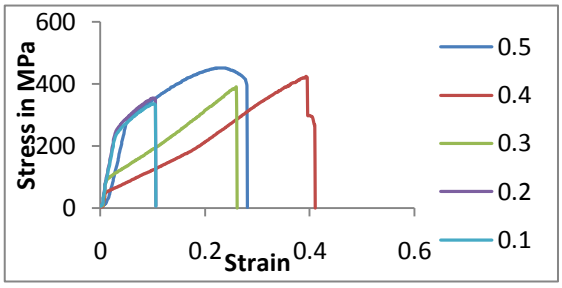

Fig-2.Stress Strain Diagram for MMNC

The fig-2 shows the stress-strain relationship for various percentages of nano SiC particles. The plastic deformation induced dislocations, or slip dislocations become dominant when the plastic strain exceeds the thermal mismatch strain and the two effects eventually act in combination. The increased yield strength of the MMNC is due to dislocation generation and accumulation and assuming the dislocations to be uniformly dispersed in the metal matrix. The residual dislocations are likely to be trapped at the reinforcing SiC_p. This results in local regions of high dislocation density; i.e. the density is highest near the reinforcing SiC_p or at the reinforcement matrix interfaces.

3.2.1 .Damage during tensile deformation: Due to the influence of tensile load fine microscopic voids appear to have undergone limited growth confirming a possible contribution from particle constraint-induced triaxiality on failure of composite matrix. Failure of the reinforcing particles is governed by combined effect of local plastic constraints, particle size and agglomeration. The fracture is highly localized at the discontinuous SiC_p reinforcement with the formation of voids away from fractured SiC particulate.

Fracture occurred in the regions of particle clustering due to the enhanced local stresses resulting from restriction of plastic deformation. The stress immediately adjacent to a reinforcing nano SiC particle is a combination of stress components imposed by the macroscopic applied stress and the stress component that develop on a microscopic scale. The microscopic scale components arise as a result of conjoint influence of strain incompatibility between the reinforcing particle and deforming matrix, individual stresses arising from thermal expansion mismatch between the second phase inclusion and the matrix and load sharing by the reinforcing particulates. A combination of thermally

induced stress, local stress concentration and macroscopic applied stress and intrinsic brittle nature of reinforcing particle is responsible for cracking. Furthermore, assuming that the aluminum alloy metal matrix-SiC particle interfaces are strong, the triaxial stresses generated during far field tensile loading favors limited growth of microscopic voids in the matrix of the composite. The limited growth of voids during far field tensile loading coupled with lack of their coalescence and thus inhibiting the dominant fracture mode to be ductile failure.

4. Microstructures

The various properties of the metal matrix nano composites depend on distribution of the reinforcing particles and interface bonding between metal matrix and the dispersed particles. The properties vary with the reinforcing particles. The optical micrograph and SEM images of MMNC reinforced with 0.5wt% of nano SiC_p are presented in figures below. The optical images of the base metal in fig-3 show the grain boundaries clearly. With the optical microscopy no pores are observed. The grains in fig 3(a) are larger in size and that of MMNC's are smaller as seen in fig-3(b). The fig-4 shows images at higher magnification the grain boundaries are seen clearly.

The SEM images reveal that, there is uniform distribution of the nano SiC particles in the matrix (fig-5,6) and also small agglomerates of the powders and voids are seen at higher magnification fig-5. The overall microscopic analysis shows that there is good bonding between the matrix and the ceramic particulate, indicating uniform distribution of particles due to ultrasonic cavitation and grain boundaries are seen distinctly in fig-6 at lower magnification.

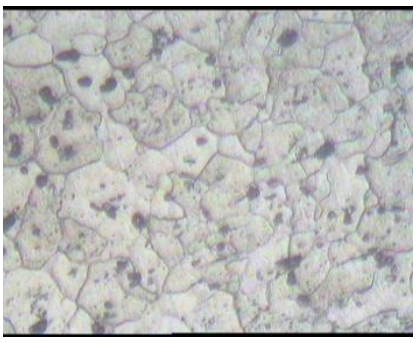

(a)

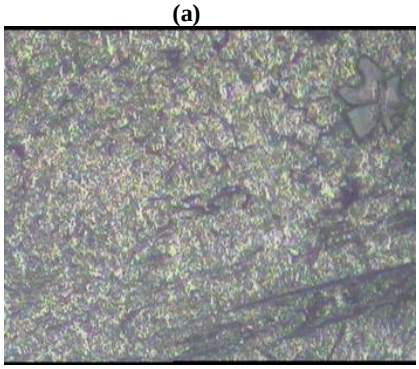

(b)

Fig.3-optical images of (a) base metal-200x (b) MMNC-200x

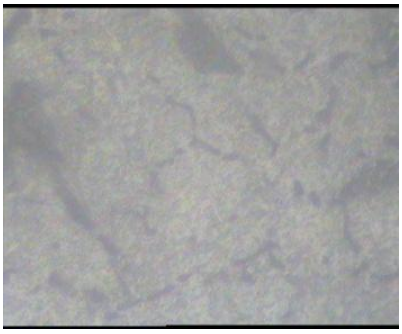

(a)

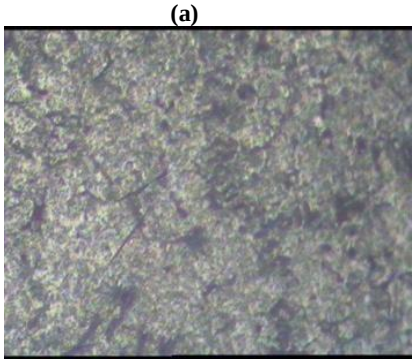

(b)

Fig.4-optical images of (a) base metal-400x b) MMNC-400x

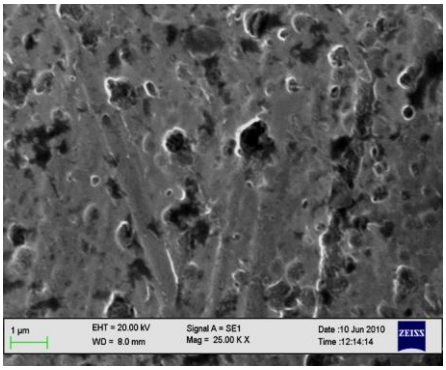

(a)

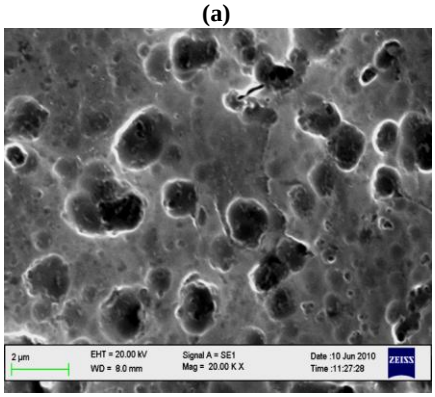

(b)

Fig-5-SEM images of (a) 0.5wt% nanoSiC-25kx (b) 0.5wt% nano SiC-20kx

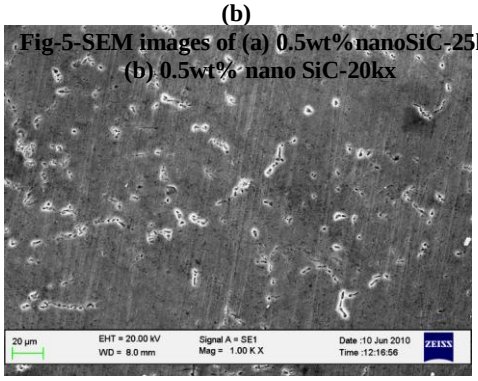

(a)

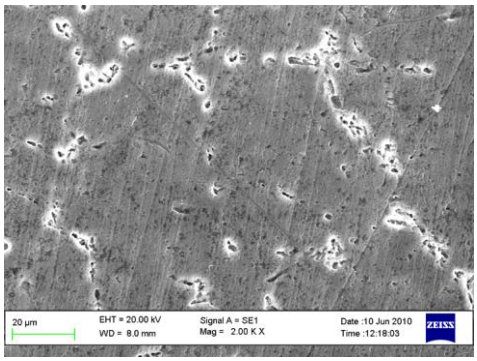

(b)

Fig-6-SEM images of (a)-0.5wt% nanoSiC-1000x (b)-0.5wt% nano SiC-2000x

4. Conclusions

The metal matrix nano composites are fabricated using mechanical stirring and ultrasonic cavitation methods. The effects of nano SiC dispersion on microstructure and mechanical properties are investigated.

i The metal matrix nano composites have fine and more homogeneous microstructure with the increase of % wt of nano SiC content.

ii. The hardness of the aluminum MMNC improved significantly by the addition of SiC particles into it.

iii. The ultimate tensile strength, yield strength are increased with the increase of SiC content. The hardness, UTS, Y.S increased by 15%, 28%, 29% respectively.

iv. Ultrasonic nonlinear affects efficiently disperse nano particles into molten alloy by enhancing their wettability.

Acknowledgments: The authors wish to thank Mechanical department- Andhra University,Metals joining laboratory- IIT Madras and Central Research Facility-IIT Kharagpur for providing the Machinery for conducting Experiments.

References:

[1] S.Gustafsson et.al2009,*Development of microstructure during creep of poly crystalline mullite and a nano composite mullite/5vol.%SiC*,Journal of Europian Ceramic society vol29,pp539-550.

[2] C.P.You et.al.1987, *Proposed failure mechanism in a discontinuously reinforced aluminum alloy,*Scripta metallurgica,vol.21,pp181-185.

[3] Y.Flom and R.J.Arsenault, 1989, *Effect of particle size on fracture toughness of SiC/Al composite materials,* Acta Metall.,37 ,pp2413.

[4] H.J.Kim,et al. 1992, *Micro-mechanical fracture process of SiC particle reinforced aluminium alloy 6061-T6 metal matrix composites*,

Material science and Engineering ,A 154 ,pp 35-41.

[5] P.Gyftou et.al, 2005,*Tribological study of Ni-matrix coatings containing Nano and Micro SiC particles*, Electrochimica Acta 50, 4544-4550.

[6] Sannino A P, Rack H J. 1995, *Dry sliding wear of discontinuously reinforced aluminum composites:* review and discussion. 'Wear'; 189:pp1-19.

[7] Sharma S.C. 2001,*The sliding wear behavior of Al6061-garnet particulate composites*, 'Wear', 249: pp1036-45.

[8] Rao.R.N. and Das.S,'2010,*' Effect of matrix alloy and influence of SiC particle on the sliding wear characteristics of aluminum alloy composites*, Materials and Design 31,pp 1200-1207.

[9] G U Wan-Li, 2006, *Bulk Al/SiC nano composite prepared by ball milling and hot pressing method*, Transactions of Non ferrous metals Society of China vol.16,pp398-401.

[10] Zhiwu Xu et.al. 2008, *Floating of SiC particles in a Zn-Al filler metal*, Material Science and EngineeringA 474 pp157-164.

[11] T.C.Willis, 1988, *Spray deposition process for metal matrix composite manufacture*, Metals and Materials, August, pp 485-488.

[12] Tianle Zhou et.al, 2008, *Study of the thermal conduction mechanism of nano-SiC/DGEBA/EMI-2,4 composites*, Polymer 49, pp4666-4672.

[13] T.S.Srivastan et.al, 2003,*The tensile response and fracture behavior of 2009 aluminum alloy metal matrix composite* ,Material Science and Engineering A346 ,pp 91-100.

[14] Ch.Vives et.al, 1993, *Fabrication of metal matrix composites using helical induction stirrer*, Material Science and Engineering, A173, pp 239-242.

[!5] C.F.Deng et.al, 2007, *Processing and properties of carbon nano tubes reinforced aluminum composites*, Material Science and Engineering A 444 pp138-145.

[16] Norika Bamba, et.al. 1998, *Effect of nano sized silicon carbide particulate on microstructure and ionic conductivity for 8 mol%Yttria stabilized zirconia based nano composites,Solid state Ionics* 111,pp171-179.

[17] K.M. Mussert, et.al,2002, *A nano indentation study on the mechanical behavior of the matrix material in an AA6061-Al_2o_3 MMC*, Journal of Material Science.37 pp789-794.

[18] Y.Yang et.al, 2004, *Study on bulk aluminum matrix nano composite fabricated by ultrasonic dispersion of nano sized SiC particles in molten Aluminum alloy*, Material Science and Engineering A380,pp 378-383.

[19] Y.Sahin, 2003, *Preparation and some properties of SiC particle reinforced aluminum alloy composites*, Materials and design 24,pp 671-679.

[20] Akio K., Atsushi O., Toshiro K. and Hiroyuki T., 1999, *Fabrication Process of Metal Matrix Composite with Nano-size SiC Particle Produced by Vortex Method*, Journal of Japan Institute of Light Metals, 49:149–154.

Short Term Load Forecasting Using Artificial Neural Network in a North Area of Bangladesh

Kamol K. Das[1], Md M. Biswas[2], Md A. Muztoba[3], S. M. F. Rabbi[4], and Sams S. Farhana[5]
[1,3,4,5]Department of Electrical and Electronic Engineering, Rajshahi University of Engineering and Technology (RUET), Rajshahi-6204, Bangladesh
[2]Department of Electrical and Electronic Engineering, Bangladesh University of Engineering and Technology (BUET), Dhaka-1200, Bangladesh

Abstract - This paper presents artificial neural network (ANN) for the electric energy demand forecasting of a north area in Bangladesh with a prediction time of one week. The actual forecast is obtained by using artificial neural network trained with the back propagation of momentum learning algorithm. The neural network is trained using historical load data available for a part of the electric grid in Rajshahi region. The model validation is performed by comparing model predictions with load data that were not used for the network's training. The main stages are the pre-processing of the data sets, network training, and forecasting. The inputs used for the neural network are the previous hour load, previous day load, previous week load, day of the week, and hour of the day. The neural network used has three layers: an input, a hidden, and an output layer. The input layer has five neurons, the number of hidden layer neurons can be varied for the different performances of the network, while the output layer has a single neuron. An absolute mean error of 2.54% was estimated when the trained network was tested on one week's data. This represents, on average, a high degree of accuracy in the load forecast.

Key words: *Load Forecasting, Short-Term Load Forecasting (STLF), Electricity Generation, Electric Power System, Artificial Neural Network (ANN).*

1. Introduction

Load forecasting is very important for the power system planning and security. The main problem for the planning is the determination of load demand in the future. Because electrical energy cannot be stored appropriately, correct load forecasting is very important for the correct investments. There are three types of load forecasting: Short-term, middle-term and long-term load forecasting. Short-term load forecasting (STLF) is to predict the hourly loads, one day or even one week. Short-term load forecaster calculates the estimated load for each hours of the day, the daily peak load, or the daily or weekly energy generation. Short term load forecasting is important for the economic and secure operation of power systems [1].

Many algorithms have been developed in the last few decades for performing accurate load forecasting. They are based on various statistical methods such as regression [2], Box Jenkins model [3], exponential smoothing [4] and Kalman filters [5]. Many electric power companies have adopted conventional prediction methods for load forecasting. However, these methods cannot properly represent the complex nonlinear relationships that exist between the load, and series of factors that influence it [6]. Recently, artificial neural networks (ANN) have been successfully applied to short term load forecasting [7]-[9]. Artificial neural networks (ANNs) make a reference to a class of models inspired by the biological nervous system. The models are composed of many computing elements, usually denoted neurons; each neuron has a number of inputs and one output [10]. It also has a set of nodes called synapses that connect to the inputs, output, or other neurons.

A linear combiner is used to produce a single value from all the inputs [11]. The single value is the weighted sum of the inputs from which the threshold value associated with the neurons is subtracted to compose the activation of the neuron. The activation signal is passed through an activation function to produce the output of the neuron. The chosen activation function is normally a non-linear function (e.g. a sigmoid function), a feature that allows the ANN to represent more complex problems [12]. A supervised ANN has been used in this research. Here, the neural network is trained on input data as well as the associated target values. The trained network can then make predictions based on the relationships learned during training.

This paper is organized as follows: First, a detail discussion on the load forecasting problem has been carried out in Section 2 to initiate the necessary idea throughout this paper. This is followed by an introduction on the concept of ANN in Section 3. Section 4 covers potential applications of neural network in load forecasting. The pre-processing of the data series that were used in this study of a north region (Rajshahi) of Bangladesh is addressed in Section 5. Finally, in Section 6, the required computer simulation and results of the forecasting has been presented, which is followed by a concluding remarks in Section 7.

Manuscript revised April 4, 2011.

2. The Load Forecasting Problem

When the power industry undergoes various structural and organizational changes, the load forecasting becomes a problem. Various generation companies, transmission and system operation companies, as well as distribution companies want to take their rightful place in power industry through load forecasting. All the developments can only translate to better and efficient services if, among other vital factors, there is a good and accurate system in place for forecasting the load that would be in demand by electricity customers. Such forecasts are highly useful in proper system planning and operations.

3. Artificial Neural Network (ANN)

The most popular artificial neural network architecture for electric load forecasting is back propagation. Back propagation neural networks use continuously valued functions and supervised learning. That is, under supervised learning, the actual numerical weights assigned to element inputs are determined by matching historical data (such as time and weather) to desired outputs (such as historical electric loads) in a pre-operational "training session". Artificial neural networks with unsupervised learning do not require pre-operational training [13]. Many published studies use artificial neural networks in conjunction with other forecasting techniques.

Fig. 1 shows a sort of a human neuron. The artificial neuron shown in Fig. 2 is equivalent to that of a human neuron as shown in Fig. 1. So, the idea of neural network comes from the human neuron. This network can make decision while getting trained up.

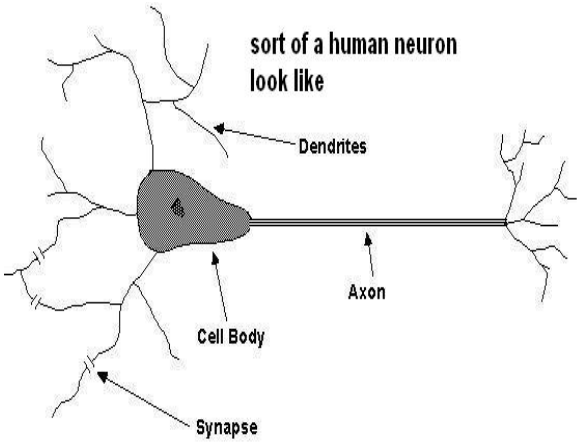

Fig. 1. Sort of a human neuron

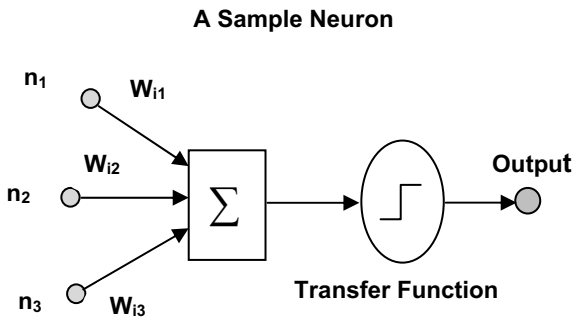

Fig. 2. A sample neuron.

4. Load Forecasting Using Neural Network

The back-propagation algorithm is a supervised learning algorithm used to change or adjust the weights of the neural network. In back-propagation, the gradient vector of the error surface is calculated. This vector points along the direction of steepest descent from the current point, so that a movement over a short distance along it decreases the error. A sequence of such moves will eventually find a minimum error point [14]. The following data were selected as network inputs:

1) The load of the previous hour,
2) The load of the previous day,
3) The load of the previous week,
4) The day of the week, and
5) The hour of the day.

This results in a total of five ANN input values. The neural network architecture used has only two hidden layers. The number of neurons in the hidden layers must be carefully chosen; too many neurons make the network overspecialized, leading to loss of generalizing capability. If there are not enough hidden layer neurons, the network may find it difficult to learn the behavior of the series. In this present work, varying number of hidden layer neurons was experimented with, the number ranging from five to eleven [15]. Eleven neurons were finally utilized because it offered a better model characteristic.

In Bangladesh Friday and Saturday are weekends. An analysis of the load series data for the month of January 2009 shows that basically two load patterns were observable: one for weekends (Friday and Saturday) and another for week days (Sunday through Thursday). Fig. 3 shows that the load demand is lowest on Friday, there is little variation in the load for Sunday through Wednesday and the peak load demand was recorded on Thursday. The load on Saturday was lower than that recorded on any weekday.

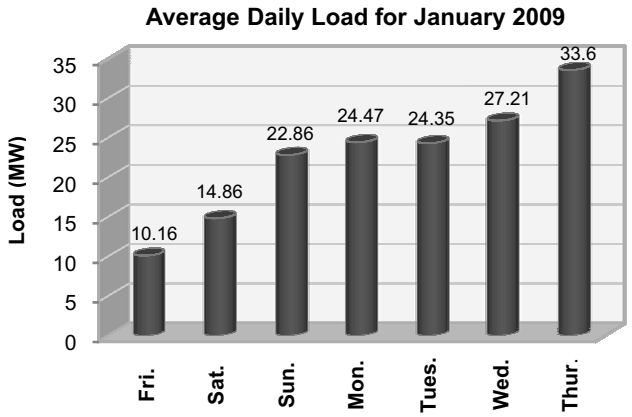

Fig. 3. Average Daily Load for January 2009.

The different load patterns could be due to the high industrial load demand during the week (which is greatly reduced over the weekend), the peak recorded on Thursday can easily be attributed to the social and cultural activities that peaks up on Thursday evenings.

5. Training of Neural Network

In training, at first all weights and biases are initialized. Then from inputs and targets, the outputs are calculated and compared with the targets. Thus errors are found. Now back-propagation is started. Delta vectors are calculated from error vectors. From delta vectors the amount of change required for weights and biases are calculated. This process is looped until the error is less than the reference [16] - [17]. The flowchart for training is shown in Fig. 4. After the neural network is trained on the input data set, a new data set is presented at its input, and the network provides a forecast of the load for the next one hour.

Once the series had been corrected, the data were normalized so that their values would be between the values 0 and 1, this was achieved by using the sigmoid function and the effect of this is to avoid a saturation of the neural network. The sigmoid function acts as an output gate that can be opened (1) or closed (0). Since the function is continuous it is possible for the gate to be partially opened (i.e. somewhere between 0 and 1). Models incorporating the sigmoid transfer function show well generalized learning characteristics and yield models with excellent accuracy.

Other transfer functions that can be used include the hyperbolic tangent and the hyperbolic secant functions. These functions exhibit different learning dynamics during training but may not achieve the same accuracy as sigmoid-based models.

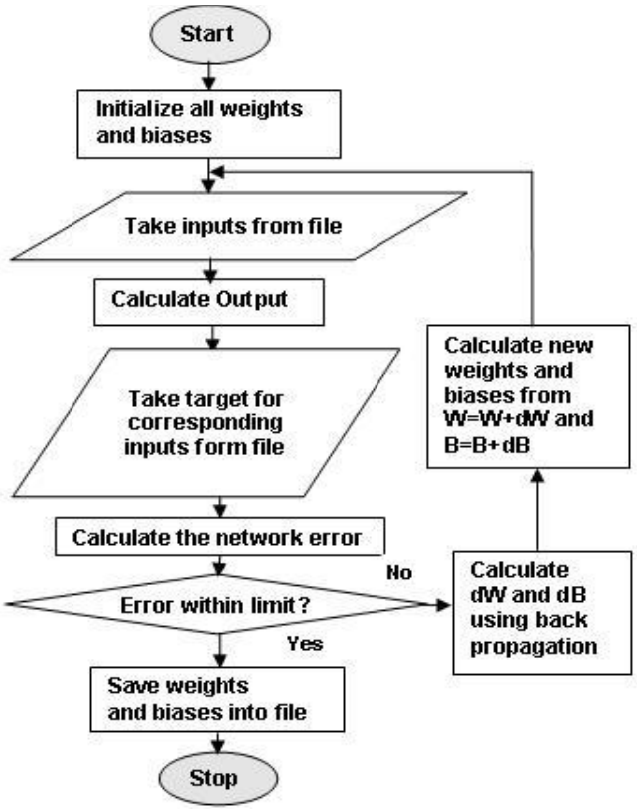

lowchart of training process.

6. Computer Simulation and Results

A back-propagation network with momentum and with an adaptive learning rate was trained and the neural network can forecast future load one hour ahead given the various inputs to the network. A sigmoid transfer function was used in the hidden layer while a linear transfer function was used in the output layer. The Fig. 5 is a bock-diagram showing entire process to find the forecasted load.

The experimental result for a one week session is shown in Fig. 6. In Fig. 6, the solid line represents the forecasted load curve and the cross marked line represents the actual load curve. Here we can see that most of the points of the forecasted load curve lay on the actual load curve. This ensures the accuracy of the neural network.

In Fig. 7 the percentage network errors for different hours are shown. Here we can see that the maximum error occurred in a one week session is about 6.3 %. The average error was calculated as 2.7%. So the efficiency of the network is about 97.3 %.

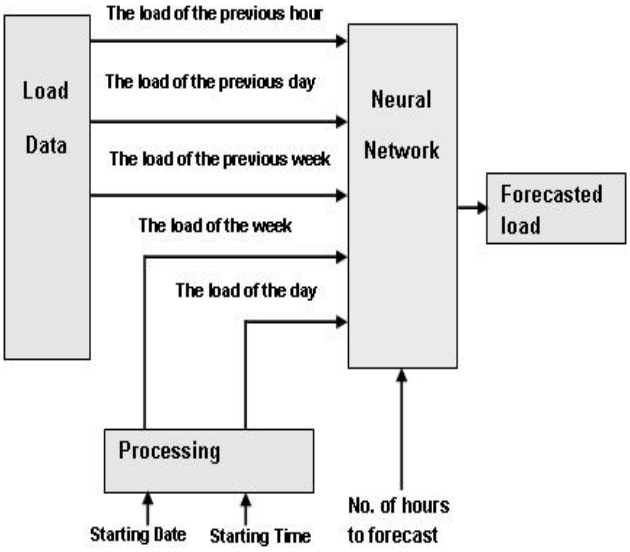

Fig. 5. Taking the output.

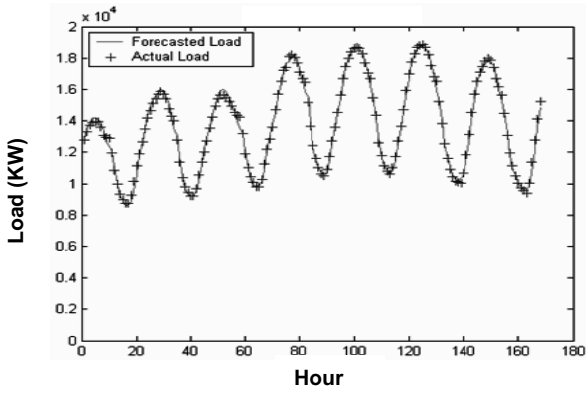

Fig. 6. Comparison between actual load curve and forecasted load curve.

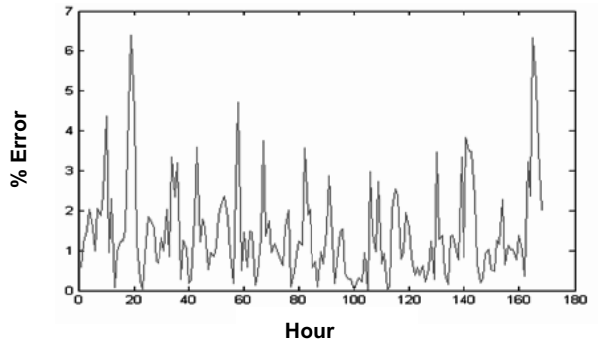

Fig. 7. Network percentage error.

The results obtained from testing the trained neural network on new data for 24 hours of a day over a one-week period are presented in Fig. 8. In each graph the solid line represents the forecasted load and the cross marked line represents the target load in Megawatt (MW) values against the hour of the day. The absolute mean error AME (%) between the 'forecast' and 'target' loads has been

Table 1: The absolute mean error AME (%) between the 'forecast' and 'target' loads

Sam-ple	Current Hour	Next Hour	Predicted Load (MW)	Actual Load (MW)	Error
1	2	3	10.325	10.101	2.22%
2	9	10	12.125	12.512	3.09%
3	16	17	14.141	13.997	1.03%
4	20	21	15.977	16.181	1.26%

calculated and presented in the Table 1. The highest AME (%) values were recorded for Saturday. This is due to the greater deviation about the minimum demand point in addition to errors in the forecast for the peak demand periods. Overall, the above error values translate to an absolute mean error of 2.54% for the network. This represents a high degree of accuracy in the ability of neural networks to forecast electric load.

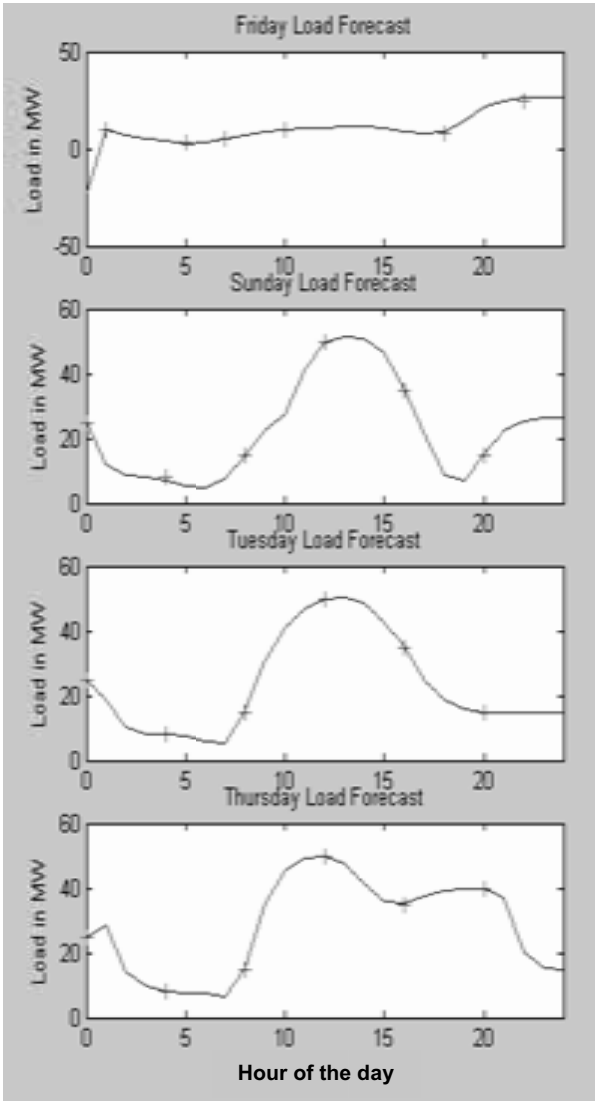

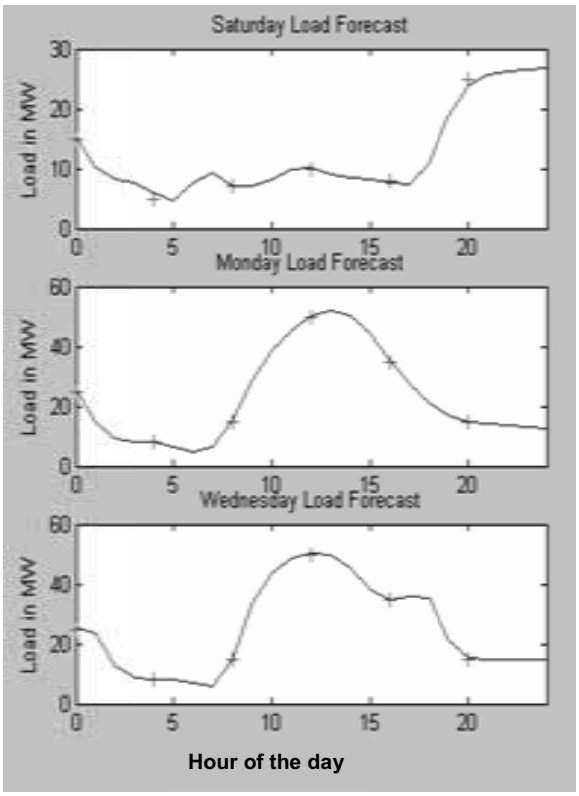

Fig. 8. Network performances for different weekdays

6. Conclusion

The results obtained in this work confirm the applicability as well as the efficiency of neural networks in short-term load forecasting. The neural network was able to determine the nonlinear relationship that exists between the historical load data supplied to it during the training phase and on that basis, and make a prediction of what the load would be in the next one hour. It must, however, be ensured that the network is not over-trained as this will lead to a loss of its generalizing capability. Accurate load forecasting is very important for electric utilities in a competitive environment created by the electric industry deregulation.

References

[1] G. Gross and F.D. Galiana, "Short term load forecasting", **IEEE Proceedings**., Vol. 75, No. 12, Dec. 1987, pp. 1558-1573.

[2] A.D. Papalexopoulos and T.C.Hesterberg, "A regression based approach to short-term system load forecasting", **IEEE PICA Conference Proceedings**, 1989, pp. 414-423.

[3] T. Hill, M. O'Connor, and W. Remus, "Neural networks models for time series forecasts", **Management Science**, Vol. 42, No. 7, July 1996, pp. 1082-1092.

[4] H. C. Huang, R. C. Hwang, and J. G. Hsieh, "A new artificial intelligent peak power load forecaster based on non-fixed neural **ternational Journal of Electrical Power and Energy Systems**, Vol. 24, No. 3, March 2002, pp. 245-250.

[5] G.D. Irisarri, S.E. Widergren, and P.D. Yehsakul, "Online load forecasting for energy control center application", **IEEE Trans. Power Apparatus and Systems**, Vol. PAS-101, No. 1, Jan. 1982, pp. 71-78.

[6] W. R. Christiaanse, "Short-term load forecasting using general exponential smoothing", **IEEE Trans. Power Apparatus and Systems**, Vol. PAS-90, No. 2, March 1971, pp. 900- 911.

[7] C. N. Lu, H.T. Wu, and S. Vemuri, "Neural network based short term load forecasting", **IEEE Trans. Power Systems**, Vol. 8, No. 1, Feb. 1993, pp. 336-342.

[8] T.M. Peng, N.F. Hubele, and G.G Karady, "An adaptive neural network approach to one-week ahead load forecasting", **IEEE Trans. Power Systems**, Vol. 8, No. 3, Aug. 1993, pp. 1195-1203.

[9] T. Senjyu, P. Mandal, K. Uezato, and T. Funabashi, "Next day load curve forecasting using recurrent neural network structure", **IEEE Proc. Generation, Transmission and Distribution**, Vol. 151, No. 3, May 2004, pp. 388 – 394.

[10] A.G. Bakirtzis, V. Petridis, S.J. Kiartzis, M.C. Alexiadis, and A.H. Maissis, "A neural network short term load forecasting model for the Greek power system", **IEEE Trans. Power Systems**, Vol. 11, No. 2, May 1996, pp. 858-863.

[11] H. Chen, C. A. Canizares, and A. Singh, "ANN-based short term load forecasting in electricity markets", **IEEE Power Engineering Society Proceeding**, Vol. 2, 2001 pp. 411 – 415.

[12] R.F. Engle, C. Mustafa, and J. Rice, "Modeling peak electricity demand", **Journal of Forecasting**, Vol. 11, 1992, pp. 241-251.

[13] T. Senjyu, H. Takara, K. Uezato, and T. Funabashi, "One hour ahead load forecasting using neural network", **IEEE Trans. Power Systems,** Vol. 17, No. 1, Feb. 2002, pp. 113-118.

[14] M. James. (2002, August). Back propagation for the uninitiated. [Online]. Available: **http://www.generation5.org/content/2002/bp.asp.**

[15] K.Y. Lee, Y.T. Cha, and J.H. Park, "Short term load forecasting using an artificial neural network", **IEEE Trans. Power Systems**, Vol. 7, No. 1, Feb. 1992, pp. 124-132.

[16] L.S. Neto, K.T. Figueirido, M.M.B.R Vellasco, and M. Pacheco, "Modelling neural networks to very short term load forecasting", **Proceedings of Nineteenth Annual International Symposium on Forecasting**, 1999.

[17] T. Senjyu, H. Sakihara, Y. Tamaki, and K. Uezato, "Next Day Peak Load Forecasting using Neural Network with Adaptive Learning Algorithm Based on Similarity", **Electric Machines and Power Systems**, Vol. 28, No. 7, 200

Improvised Sorting Algorithm Visualization Application on Students Comprehension of Core Sorting Algorithm Performance Concepts

Opani Aweh[1] and Christopher Brambraifa [2]
Department of Computer Science and I T [1]
College of Natural and Applied Sciences
Igbinedion University, Okada. Edo State
Nigeria

Department of Computer Science and I T [2]
College of Natural and Applied Sciences,
Igbinedion University, Okada. Edo State
Nigeria

Abstract - This empirical study was conducted to ascertain how visualization tools impact on the rate or pace of comprehension of concrete and abstract concepts by students. The study was undertaken for a period spanning four successive sessions using a suitable course (design and analysis of sorting algorithms) as our case study. In the first session (2006/2007) no visualization tool was used and the level of performance was dismal. Some existing visualization tools augmented with series of life programming samples were employed in the 2007/2008 session and a remarkable level of performance resulted. 2008/2009 session did not witness any new ideas but a minimal level of improved performance still resulted. A more remarkable level in performance was however recorded in the 2009/2010 session when we implemented our improvised application in addition to all our existing tools. Our findings are presented in a raw, simple and straight forward manner using percentages to depict observed performances.

KEYWORDS: Algorithms, Comprehension, Improvised, Performance, Sorting, Visualization.

1. INTRODUCTION

Empirical evidence indicates that learning and teaching aids impacts heavily on the depth of comprehension of concepts being conveyed from teachers or lecturers to their pupil. They also impact positively on the extent of assimilation of these concepts by these teachers or lecturers in their bid to understand same prior to preparing lecture notes and delivering such lectures. And more importantly they ease the onerous tasks of traditional verbose descriptions and illustrating incidental to teaching some courses like Design and Analysis of Sorting Algorithms that contains substantial abstract contents. Prior to this time this course was taught using a multiplicity of approaches ranging from verbose descriptions and explanations augmented with graphical illustrations on chalk or marker boards, through prepared charts using cardboard papers to more sophisticated computer animations, simulations or visualizations.

In all of these, majority of students still found it very difficult to get a proper understanding of the ideas that the course lecturers try to convey. And the major reason for this development as observed in the course of this study was because a complete mind picture was never readily gleaned from the explanations and the demonstrations proffered. While we agree completely that some of the existing sorting algorithms teaching and illustrative aids covering simulations, animations and visualizations provided a monumental leap, we still wish to observe that a reasonable number of students could not be carried along. For example, in spite of our elaborate explanation of the fact that besides the size of the input data, concepts such as the number of passes and data exchanges a sorting algorithm has to make to sort a given

array has a direct consequence on running time, majority still failed to comprehend it. This was presumably due to their inability to grasp the internal workings of these algorithms as it relates to the number of passes and swap they have to undergo to complete a circle of sorting based on the initial ordering and of course the size of the input data. This fact was gleaned from their responses of matching the wrong sorting algorithms or algorithm to a given problem scenarios and of course the illogicality of their explanations for such choices.

It was against this backdrop that we undertook to illustrate how the running time of any given sorting algorithm on a given set of data is largely dependent on the number of passes and data swaps it has to make to sort that array. We accomplished this by designing an application that implemented different sorting algorithms on the same user interface. On these user interface, the pupil could input a set of data and invoke any algorithm of choice or invoke all of them one after the other and then observe the sequence of passes and swaps physically. The application had features that could be used to vary the speed of execution by selecting various time delays so he or she could observe passes and data swaps in slow motion.

2. RELATED STUDIES

A lot of studies have been undertaken in the area of algorithm visualization, simulation, or animations with the objective of enhancing the teaching and learning of algorithm analysis and design, with sorting algorithms receiving a lot of attention. In the session following, we will undertake a cursory evaluation of some of these studies and tools in chronological sequence.

We commence with Brown and Sedgewick (1984) who outlined the conceptual framework they developed for animating algorithms. In it they described a software environment that provided facilities at a variety of levels for animating algorithms. This environment essentially helps to illustrate the properties of programs by displaying multiple dynamic views of the program and associated data structures. Records showed that the system was used successfully in several applications for teaching and research in computer science and mathematics. As far back as 1987 Barnes and Gary already developed a microcomputer based software package for the graphic simulation of fundamental binary search tree algorithms to augment instructional aides available to the instructor during classroom lecture. In another study, Matsaggouras (1997) noted that understanding sorting algorithms requires students' higher mental functions because the procedures involved were based on a number of different layers of abstraction that they do not grasp easily. In their own study, Dios and Geller, (1998) examined some instructional methods that couled enhance the learning and comprehension of sorting algorithms by pupils. In their discussion of some problems associated with learning sorting algorithms, they stressed the need to identify the educational effects of "activity oriented" instructional techniques to ease the learning process. Du Feu (1999) believes that providing secondary level education students with opportunities to sort measurable entities using hands-on experience was essential to their conceptualization of sorting algorithms. While Lauer et al (2001) observed that it was quite common to promote algorithm animation base on the argument that an animation is the best way to explain a dynamic, i.e., a time varying, phenomenon. They argued that instead of drawing series of pictures of the various stages of a running algorithm by hand, it was certainly more

convenient to run the algorithm on a computer and have an animation system generate the series of figures. They concluded that this approach has worked very well for illustrating and teaching of sorting and searching algorithms, graph algorithms, algorithms for processing text, and many others usually employed in teaching courses on algorithms and data structures. Another study by Karavirta et al (2004) noted that algorithm animation has been researched since the early 1980s. They were however quick to add that many different visualization systems that have been developed have persisted as mere research prototypes which have failed to gain wide acceptance by teachers as classroom demonstration tools. The argument they advanced for this trend was that preparing animations was a laborious task. They then proceeded to demonstrate a new tool dubbed MatrixPro, in which animations are generated in terms of visual algorithm simulation by simply invoking ready-made operations available in the application library to simulate the working of real algorithms. A comparative analysis of current Algorithm Visualization Systems (AVS) was conducted by Naser and Samy (2007). They observed that visualization tools helped students to overcome their difficulties with understanding of Artificial Intelligent Searching Algorithms because of the improvement in performance arising from the use of these tools compared to traditional method. In another study, Myller et al (2007) observed that more collaborative use of visualizations is taking place in the classrooms due to the introduction of pair programming and collaborative learning as teaching and learning methods. They presented an empirical study in which the learning outcomes of students were compared when students were learning in collaboration and using materials which contained visualizations on different engagement levels. Their results indicated that the level of engagement has an effect on students' learning results even though the difference was not statistically significant. They noted that students without previous knowledge seem to gain more from using visualizations on higher engagement level.

At a more practical level, Ashraf and Boris (2008) motivated by their observation concerning the decreasing interest in algorithm improvisations over the last few years, developed and implemented a generic architecture. Emond et al (2008) as part of their own contribution developed visualization tools to aid the teaching of Computer Architecture, Algorithms and Data Structures courses at the University of Victoria.

A word of caution however came from Naps et al (2009) who though agrees that visualization technology can be used to graphically illustrate various concepts in computer science. But they argue that such technology, no matter how well it is designed, is of little educational value unless it engages learners in an active learning activity. They reviewed experimental studies of visualization effectiveness against the backdrop of current attitudes and best practices and suggested a new taxonomy of learner engagement with visualization technology. And based on Bloom's well-recognized taxonomy of understanding, they suggested a metrics for assessing the learning outcomes to which such engagement may lead. They then presented a framework for experimental studies of visualization effectiveness based on these taxonomies of engagement and effectiveness metrics, and called on interested computer science educators to collaborate with them in carrying out studies within this framework.

3. RESEARCH METHODOLOGY

The focus of this study was essentially finding a means of easing the teaching, learning and comprehension of sorting algorithms processes to pupils. The methodology employed in this study can rightly be categorized to comprise of interviews or group interviews, written test and observation. Each of these processes is briefly explained next.

(1) Interviews: We will describe our interview process to comprise of both personal and group interview. We fielded specific questions to test individual students understanding of basic concepts. In the same token, we entertained questions from them to enable them clear some areas where they had scruples relating to asked questions or other closely related questions. In some other instances, designated questions are thrown to the entire class and different responses are collated and conversely, questions were entertained from the class. This latter case is what we have described as group interview in this study.

(2) Written Tests: In specific terms, we designed some set of questions comprising the painting of different varying case scenarios covering sundry volume of input data, sundry initial ordering of these data, available hardware and software requirements, programming expertise level and contextual questions requiring logical explanations. And the pupils were made to attempt all these questions in writing. And the scores from these tests we duly graded.

(3) Observation: Our observation methodology is intricately linked to our interview and tests. It afforded us the opportunity to garner first hand experiences pertaining to the taught patterns and mind pictures of the pupils.

These above methodologies were replicated for a period of four years covering four successive sessions: 2006/2007, 2007/2008, 2008/2009 and 2009/2010. The 2006/2007 session was our base year for this study. Personal experiences in the course of this study and the evolution of techniques to facilitate the creation of a very good teaching and learning environment are discussed next.

At the beginning I had great hassles explaining basic concepts of passes and data exchanges impact on performance to majority of the pupil. In spite of the series of real life illustrations with Pascal and Java program samples coupled with my drawing of illustrative schemas the level of understanding of the core concepts by majority of the pupil was still vague. In the 2007/2008 succeeding session I employed some already existing visualization/animation tools in addition to the code samples/schemas used previously, but the core concepts could still not be grasped by many. This prompted my rethink of strategy to develop an application that will enable us to run a combination of sorting algorithms on the same data set and on the same graphical user interface such that the process of passing and data exchanges or swaps would be visible to the pupil.

This application came to fruition at the end of 2008/2009 session as a student project. See appendix 1 for screen shots of our executed application. It was design with the facility to input or to select/generate a required ordering of data from a pool or to enter it directly in the provided text area. It also has a feature to adjust the sequence of

execution by selecting appropriate time delays so the pupil could observe the processes of passes and swapping in slow motion.

This application was put to use in the 2009/2010 session. And it proved to be an invaluable means of conveying the core concepts of some sorting algorithms to pupils with ease. Also, the formation of a veritable mind picture germane to the understanding of these concepts became apparent. The increasing level of pupils performances in response to our set of interviews and questions are as set out below in our findings.

We wish to stress that because our procedure was straight forward and our results distinct, we did not find it expedient to compute some statistics. Rather, we employed simple percentages to depict our rising levels of observed performance. We computed our percentages based on score of fifty percent (50%) and above relative to the total number of pupils involved in each of the academic sessions involved.

4. PRESENTATION OF FINDING

Our findings are as presented in table 1 below.

SESSION	TEACHING APPROACH	AVERAGE PERFORMANCE (%)
2006/2007	Verbose descriptions/Drawing of schemas	45 %
2007/2008	Verbose descriptions/Drawing of schemas/Running sample programs/Use of some existing visualization or animations tools	62 %
2008/2009	Same as above	67 %
2009/2010	Use of developed application in addition to the approaches above	91 %

Table 1 Table Showing Average Performance Based on Teaching Approach Employed in Each Session

5 DISCUSSIONS

Our discussion is based on the table above and our observations in the course of this study. In the 2006/2007 session the performance with respect to the questions asked was a paltry 45%. This means that less than half of the class understood the concepts that have been explained and illustrated with schemas on marker board. But it can be argued also that since this was the first time I was teaching the course, my low level of proficiency might have contributed to the poor performance. There was a remarkable increase in performance in the succeeding 2007/2008 session and this is substantially attributable to the introduction of aids such as program samples and visualization/simulation illustrations. But let us note also that the teacher's rising level of proficiency and confidence may have been contributory as well. And another important factor that cannot be discounted is the possibility of a prior knowledge of the questions from previous sessions even though the questions were not officially handed to the students. The 2008/2009 performance level was negligible compared to that of 2007/2008 session. Although exactly the same approach was used but there was still a minimal increase in performance. As have been argued previously, the lecturer's proficiency and rising confidence and the possibility of prior

knowledge of the questions may have played out. But going by the minimal observed increase in performance, the issue of prior knowledge seems to have been less of a factor even in the preceding year. We wish to mention also that this application was actually realized at the end of this same session. We had even a more remarkable performance level in the 2009/2010 session relative to the other sessions. And the reasons for this are not farfetched. First, the process of conveying the core concept to the pupil became very easy as the illustrations from the application provided an explicit means. On the part of the pupils, the visible illustrations translated into an appropriate mind picture that facilitated their comprehension of the entire process.

6. CRITICISM

We have already acknowledged the fact that the teachers rising level of proficiency and confidence may have impacted on the rising level of performance. We also cited the issue of the possibility of prior knowledge of the questions as another factor. There is still another major factor that we could not evaluate. And that is the level of intelligence of the pupils used for the study during the periods covered. This is because it can be argued that the level of performance might have been influenced also by the caliber of the students in the designated sessions of study. We could not adjust for these factors in our report.

7. CONCLUSION

This study supports existing facts that visualization, animation or simulation tools impact positively on the pace and level of comprehension of abstract concepts by teachers and pupils. This it does by facilitating the process of explanation and demonstration by teachers or lecturers and formation of appropriate mind pictures by pupils. For most teaching and learning situations, especially in some core courses (data structures and algorithms for instance) in computer science discipline, verbose explanations or illustrations are never enough except we augment them with veritable teaching and learning aids such as visualizations, animations and simulations.

The major contribution of this study can be gleaned from the fact that we no doubt, have a multiplicity of these tools in abundance especially in disciplines like Computer Science. But while we subscribe to the exploitation of some of these existing tools rather than reinventing them, studies such as this, that will help adapt them to peculiar environments and situations are quite germane.

This will not only help to extend or expand their functionalities but will in addition help to popularize their usage and further encourage studies that will help extend them to other fields where they are currently not been deployed.

REFERENCES

[1] Ashraf Abu Baker and Boris Milanovic (2008) A Universal Extensible Architecture for Algorithm Visualisation Systems 2008 International Conference on Computer Science and Software Engineering, DOI Bookmark: http://doi.ieeecomputersociety.org/10.1109/CSSE.2008.509

[2] Barnes, G. M., and Gary, A (1987) Visual simulations of data structures during lecture, Technical Symposium on Computer Science Education, Proceedings of the eighteenth SIGCSE technical symposium on Computer science education, Pages: 267 – 276, St. Louis, Missouri, United States

[3] Brown, H. M. and Sedgewick, R. (1984) A system for algorithm animation ACM SIGGRAPH Computer Graphics, Volume 18 , Issue 3, Pages: 177 – 186, ACM New

York, NY, USA. DOI http://doi.acm.org/10.1145/964965.808596
[4]Du Feau, C. (1999). A Sort for Statistics Lesson. *Teaching Statistics*, Vol. 21, No. 1, pp. 8-10.
Karavirta, V., Korhonen, A., Malmi, L. and Stâlnacke, K. (2004) MatrixPro - A Tool for Demonstrating Data Structures and Algorithms Ex Tempore, Fourth IEEE International Conference on Advanced Learning Technologies (ICALT'04) Joensuu, Finland. DOI http://doi.ieeecomputersociety.org/10.1109/ICALT.2004.1357707
[5] Lauer, T., Müller, R. and Ottmann, T (2001) Animations for Teaching Purposes: Now and Tomorrow, Computing Milieux Computers and Education Computer Uses in Education, Volume 7 / Issue 5 / Abstract, Pages 420-432 DOI 10.3217/jucs-007-05-0420
[6] Matsaggouras, E. (1997). Teaching Strategies. Gutenberg, Athens.
[7] Myller Niko, Laakso, Mikko and Korhonen, Ari (2007) Analyzing engagement taxonomy in collaborative algorithm visualization, Annual Joint Conference Integrating Technology into Computer Science Education Proceedings of the 12th annual SIGCSE conference on Innovation and technology in computer science education Dundee, Scotland, Pages: 251 – 255, ACM New York, NY, USA
[8] Naps, L. T., Roblin, G., Almstrum, V., Dann, W. Fleischer, R., Hundhausen, C., Korhonen, A., Malmi, L., McNally, M., Roger, S. and Velazquez-Iturbide, J. A. (2003) Exploring the Role of Visualization and Engagement in Computer Science Education, ACM SIGCSE Bulletin, Volume 35 , Issue 2, Pages: 131 – 152, ACM New York, NY, USA. DOI http://doi.acm.org/10.1145/782941.782998

APPENDIX: SAMPLE SCREEN SHOTS OF RUNNING APPLICATIONS

(1) BUBBLE SORT EXECUTED

(2) SELECTION SORT EXECUTED

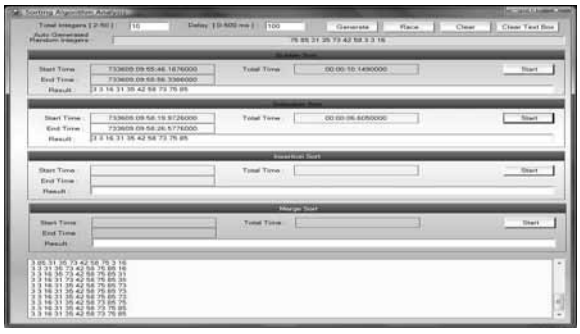

(3) INSERTION SORT EXECUTED

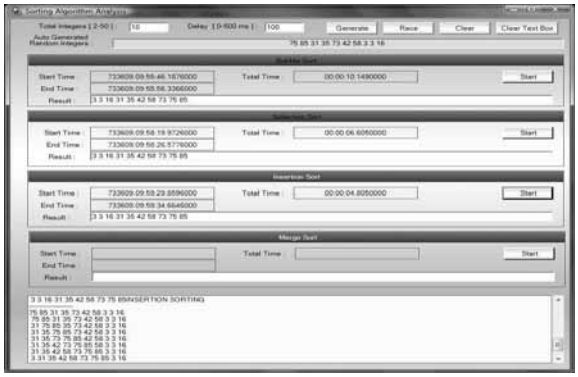

(4) MERGE SORT EXECUTED